



Marjenberg, Zoe R. (2016) *New prophylactic and therapeutic treatments to combat pathogenic Enterohaemorrhagic Escherichia coli*. PhD thesis.

<http://theses.gla.ac.uk/7689/>

Copyright and moral rights for this work are retained by the author

A copy can be downloaded for personal non-commercial research or study, without prior permission or charge

This work cannot be reproduced or quoted extensively from without first obtaining permission in writing from the author

The content must not be changed in any way or sold commercially in any format or medium without the formal permission of the author

When referring to this work, full bibliographic details including the author, title, awarding institution and date of the thesis must be given

Glasgow Theses Service
<http://theses.gla.ac.uk/>
theses@gla.ac.uk



University
of Glasgow

**New prophylactic and therapeutic treatments
to combat pathogenic Enterohaemorrhagic
*Escherichia coli***

A thesis submitted to the University of Glasgow for the degree of
Doctor of Philosophy

Zoe R. Marjenberg BSc (Hons), MPhil

Submitted October 2016

Institute of Infection, Immunity and Inflammation
College of Medical, Veterinary and Life Sciences
University of Glasgow

Acknowledgements

I would firstly like to thank my supervisors Dr. Andrew Roe and Dr. Gillian Douce, whose guidance, patience, advice and positivity have been an invaluable source of encouragement over the last four years. I will always be appreciative of the support they have both provided, and for how much I have learned under their supervision. Thank you also to Novartis Vaccines and the University of Glasgow for funding my PhD.

I am extremely grateful to all the members of the Roe lab, past and present, for all the support, assistance, and incredibly useful discussions they have provided. Particular thanks go to Kate Beckham and James Connolly for their advice and help in the earlier stages of my PhD, and to Alejandro Huerta Uribe for all the hard work he contributed to our collaboration. Thank you also to Tom Parker, Riccardo Zambelloni, Liyana Binti Azmi and Claire McQuitty: you have made the last few years really enjoyable, and I will miss you all very much.

I would like to thank Dr. Olwyn Byron and Dr. Shana Coley for their invaluable assistance and their generosity with their time. Thank you to my assessors, Prof. Mark Roberts and Prof. Robert Nibbs, whose advice and encouragement have been truly appreciated. I am also very grateful to the staff of the animal house, especially Colin, who were always extremely kind and helpful to me.

Thank you to my parents who have always been incredibly encouraging of anything I do, and to Louisa, Shona and Emma for their valued friendship over the last few years. Finally, thank you to Darren for being the most patient, understanding and supportive partner I could ever ask for.

Author's Declaration

I declare that, except where explicit reference is made to the contribution of others, this dissertation is the result of my own work and has not been submitted for any other degree at the University of Glasgow or at any other institution.

Zoe Marjenberg

October 2016

Summary

Bacterial diarrhoeal diseases have significant influence on global human health, and are a leading cause of preventable death in the developing world. Enterohaemorrhagic *Escherichia coli* (EHEC), pathogenic strains of *E. coli* that carry potent toxins, have been associated with a high number of large-scale outbreaks caused by contaminated food and water sources. This pathotype produces diarrhoea and haemorrhagic colitis in infected humans, and in some patients leads to the development of haemolytic uremic syndrome (HUS), which can result in mortality and chronic kidney disease. A major obstacle to the treatment of EHEC infections is the increased risk of HUS development that is associated with antibiotic treatment, and rehydration and renal support are often the only options available. New treatments designed to prevent or clear *E. coli* infections and reduce symptoms of illness would therefore have large public health and economic impacts.

The three main aims of this thesis were: to explore mouse models for pre-clinical evaluation *in vivo* of small compounds that inhibit a major EHEC colonisation factor, to assess the production and role of two proteins considered promising candidates for a broad-spectrum vaccine against pathogenic *E. coli*, and to investigate a novel compound that has recently been identified as a potential inhibitor of EHEC toxin production.

As EHEC cannot be safely tested in humans due to the risk of HUS development, appropriate small animal models are required for *in vivo* testing of new drugs. A number of different mouse models have been developed to replicate different features of EHEC pathogenesis, several of which we investigated with a focus on colonisation mediated by the Type III Secretion System (T3SS), a needle-like structure that translocates bacterial proteins into host cells, resulting in a tight, intimate attachment between pathogen and host, aiding colonisation of the gastrointestinal tract. As *E. coli* models were found not to depend significantly on the T3SS for colonisation, the *Citrobacter rodentium* model, a natural mouse pathogen closely related to *E. coli*, was deemed the most suitable mouse model currently available for *in vivo* testing of T3SS-targeting compounds.

Two bacterial proteins, EaeH (an outer membrane adhesin) and YghJ (a putative secreted lipoprotein), highly conserved surface-associated proteins recently identified as

protective antigens against *E. coli* infection of mice, were explored in order to determine their suitability as candidates for a human vaccine against pathogenic *E. coli*. We focused on the expression and function of these proteins in the EHEC O157:H7 EDL933 strain and the adherent-invasive *E. coli* (AIEC) LF82 strain. Although expression of EaeH by other *E. coli* pathotypes has recently been shown to be upregulated upon contact with host intestinal cells, no evidence of this upregulation could be demonstrated in our strains. Additionally, while YghJ was produced by the AIEC strain, it was not secreted by bacteria under conditions that other YghJ-expressing *E. coli* pathotypes do, despite the AIEC strain carrying all the genes required to encode the secretion system it is associated with. While our findings indicate that a vaccine that raises antibodies against EaeH and YghJ may have limited effect on the EHEC and AIEC strains we used, recent studies into these proteins in different *E. coli* pathogens have suggested they are still excellent candidates for a broadly effective vaccine against *E. coli*.

Finally, we characterised a small lead compound, identified by high-throughput screening as a possible inhibitor of Shiga toxin expression. Shiga toxin production causes both the symptoms of illness and development of HUS, and thus reduction of toxin production, release, or binding to host receptors could therefore be an effective way to treat infections and decrease the risk of HUS. Inhibition of Shiga toxin production by this compound was confirmed, and was shown to be caused by an inhibitory effect on activation of the bacterial SOS response rather than on the Shiga toxin genes themselves. The bacterial target of this compound was identified as RecA, a major regulator of the SOS response, and we hypothesise that the compound binds covalently to its target, preventing oligomerisation of RecA into an activated filament.

Altogether, the results presented here provide an improved understanding of these different approaches to combating EHEC infection, which will aid the development of safe and effective vaccines and anti-virulence treatments against EHEC.

Table of Contents

ACKNOWLEDGEMENTS	I
AUTHOR'S DECLARATION.....	II
SUMMARY	III
TABLE OF CONTENTS.....	V
LIST OF FIGURES.....	XIV
LIST OF TABLES	XVII
ABBREVIATIONS	XVIII
CHAPTER 1: INTRODUCTION	1
1.1 Pathogenic <i>Escherichia coli</i>	2
1.1.1 <i>E. coli</i> pathotypes, classification and identification	2
1.1.2 Diarrhoeagenic <i>E. coli</i> pathotypes	4
1.1.3 Uropathogenic and neonatal meningitis-causing <i>E. coli</i>	6
1.1.4 Pathogenic animal <i>E. coli</i>	7
1.2 Enterohaemorrhagic O157:H7 <i>E. coli</i>	8
1.2.1 Sources and transmission of O157:H7	8
1.2.2 O157:H7 and human disease	10
1.2.3 O157:H7 virulence factors	12
1.3 Shiga toxin	13
1.3.1 Stx structure and mechanism of action	13
1.3.2 Stx variants.....	14
1.3.3 Shiga toxin-encoding bacteriophages.....	15

1.3.4 Horizontal gene transfer of <i>stx</i> and its contribution to new EHEC outbreak strains	16
1.3.5 Regulation, activation and expression of the bacterial SOS response	18
1.3.6 Regulation of Stx expression	20
1.3.7 The role of Stx in bacterial colonisation and the immune response	20
1.3.8 The significance of Stx outside of the human host	23
1.4 The Type 3 Secretion System and the attaching/effacing lesion	24
1.4.1 Structure of the T3SS	25
1.4.2 Protein translocation by the T3SS	26
1.4.3 T3SS-mediated formation of the attaching/effacing lesion	27
1.5 Animal models of O157:H7	28
1.5.1 The infant rabbit O157:H7 model	28
1.5.2 O157:H7 mouse models	29
1.5.3 <i>Citrobacter rodentium</i> as an O157:H7 surrogate model of infection	30
1.6 Development of a human vaccine to prevent O157:H7 infections	32
1.6.1 The case for a broad-spectrum <i>E. coli</i> vaccine	33
1.6.2 EHEC vaccine development: Stx vaccines	34
1.6.3 EHEC vaccine development: reverse vaccinology	35
1.6.4 Animal vaccines against O157:H7	36
1.7 Development of a therapeutic treatments for O157:H7 infections	36
1.7.1 Inhibition of Stx expression and binding to host receptors	37
1.7.2 Modified bacteriocins	39
1.7 Project aims	41
CHAPTER 2: MATERIALS & METHODS	43
2.1 Chemicals, growth media and buffers	44
2.1.1 Chemicals	44
2.1.2 Bacterial growth media	44
2.1.3 Growth media supplements	45
2.1.4 Buffers	45

2.2 Bacterial strains and plasmids	46
2.2.1 Bacterial strains	46
2.2.2 Storage of bacterial strains	47
2.2.3 Bacterial growth conditions	47
2.2.4 Bacterial growth curves and calculation of colony-forming units	47
2.2.5 Plasmids	47
2.3 Eukaryotic cell lines and growth conditions	48
2.3.1 Eukaryotic growth media	48
2.3.2 Eukaryotic cell lines	48
2.3.3 Eukaryotic growth conditions and passage	49
2.4 Molecular techniques	49
2.4.1 Preparation of genomic DNA	49
2.4.2 Oligonucleotide primers	49
2.4.3 Polymerase chain reaction (PCR)	50
2.4.4 Agarose gel electrophoresis	51
2.5 Molecular cloning	51
2.5.1 Restriction enzyme digests	51
2.5.2 DNA gel purification	52
2.5.3 DNA ligation	52
2.5.4 Production of electrocompetent <i>E. coli</i>	53
2.5.5 Electroporation transformation	53
2.5.6 Heat-shock transformation	53
2.5.7 p16 <i>Slux</i> integration	54
2.5.8 Creation of <i>eaeH</i> and <i>yghJ</i> deletion mutants by lambda red phage mutagenesis	54
2.5.9 Creation of spontaneous streptomycin-resistant mutants	55
2.6 Protein overexpression and purification	56
2.6.1 Protein overexpression	56
2.6.2 Protein purification	56
2.7 Phenotypic characterisation of strains	57
2.7.1 Secretion assays	57

2.7.2 SDS-PAGE	57
2.7.3 Western blotting	58
2.7.4 Motility assay	59
2.7.5 Bacterial adhesion assay	59
2.7.6 Immunofluorescence microscopy.....	60
2.7.7 GFP reporter fusion assays	61
2.7.8 Mitomycin C (MMC)-induced Stx-GFP reporter fusion assay	61
2.7.9 Phage transduction assays.....	61
2.8 Biophysical techniques.....	62
2.8.1 Microscale thermophoresis	62
2.8.2 Analytical ultracentrifugation	62
2.8.3 ATPase assays	63
2.8.4 AHU cytotoxicity testing	64
2.9 Animal experiments	65
2.9.1 Home Office animal licence	65
2.9.2 Mouse maintenance	65
2.9.3 Bacterial infection of mice	65
2.9.4 Live imaging of infected mice	66
2.9.5 Faecal shedding counts of infected mice.....	66
2.9.6 Tissue collection and histology	66
2.10 Analysis of data.....	67
 CHAPTER 3: DEVELOPMENT AND CHARACTERISATION OF MOUSE MODELS OF <i>E. COLI</i>	
INFECTION	68
3.1 Introduction.....	69
3.1.1 Aims of this chapter	70
3.2 Bioluminescent labelling of bacterial strains	72
3.3 Colonisation of BALB/c, C57 and C3H/HeJ mouse strains by TUV93-0.....	73
3.4 Colonisation of dextran sodium sulfate-treated BALB/c mice by TUV93-0 and LF82	74

3.5 Colonisation of streptomycin-treated ICR mice by <i>E. coli</i>	77
3.5.1 Colonisation of streptomycin-treated ICR mice by TUV93-0 carrying plasmid-borne Str ^R	77
3.5.2 Generation of Str ^R bacterial strains	80
3.5.3 Colonisation of streptomycin-treated ICR mice by Str ^R TUV93-0 and OI-148A	81
3.5.4 Colonisation of streptomycin-treated ICR mice by Str ^R LF82	84
3.6 Stx-producing <i>Citrobacter rodentium</i>	87
3.6.1 Colonisation and pathogenesis of Stx-producing <i>C. rodentium</i>	87
3.6.2 Colonisation and production of disease by <i>C. rodentium</i> (λ stx _{2dact}) is dependent on the T3SS	92
3.7 Discussion	94
3.7.1 Streptomycin treatment of mice lowers colonisation resistance to <i>E. coli</i>	94
3.7.2 The Str-treated TUV93-0 mouse model is not T3SS-dependent	95
3.7.3 The Stx-expressing <i>Citrobacter rodentium</i> mouse model is a strong replicator of T3SS-mediated adhesion and Stx-mediated kidney damage	98
CHAPTER 4: EVALUATION OF EAEH AND YGHJ AS POTENTIAL VACCINE CANDIDATES	100
4.1 Introduction	101
4.1.1 EaeH as a vaccine candidate	101
4.1.2 YghJ as a vaccine candidate	102
4.1.3 Aims of this chapter	103
4.2 Bacterial carriage of <i>eaeH</i> and <i>yghJ</i>	104
4.3 Overexpression of His-tagged EaeH and YghJ	105
4.4 Construction of <i>eaeH</i> and <i>yghJ</i> deletion mutants	106
4.5 Reporter fusion analysis of <i>eaeH</i> and <i>yghJ</i> expression	107
4.5.1 Construction of GFP reporter fusions	107
4.5.2 GFP reporter fusion assays	109
4.5.3 Expression of ETEC <i>eaeH</i> is upregulated by interaction with host cells	110
4.5.4 Expression of GFP reporters upon contact with Caco-2 cells	110

4.6 Western blot analysis of EaeH and YghJ expression.....	114
4.6.1 Expression and detection of EaeH and YghJ	114
4.6.2 Expression of EaeH upon contact with Caco-2 cells	115
4.6.3 Expression of EaeH in Caco-2-conditioned MEM media.....	116
4.7 Secretion of YghJ by LF82	118
4.8 Discussion	120
4.8.1 Expression of EaeH by TUV93-0 and LF82.....	120
4.8.2 The function of EaeH in <i>E. coli</i>	121
4.8.3 Expression and secretion of YghJ by LF82.....	122
4.8.4 The function of YghJ.....	124
4.8.5 YghJ function in LF82	126
4.8.6 YghJ and EaeH as vaccine candidates	127
4.8.7 LF82 <i>yghJ</i> and <i>eaeH</i> deletion mutants <i>in vivo</i>	128
CHAPTER 5: DEVELOPMENT OF NOVEL INHIBITORS OF THE <i>E. COLI</i> SHIGA TOXIN.....	129
5.1 Introduction.....	130
5.1.1 Aims of this chapter	131
5.2 Modification of the hit compound 5324836 (AHU1)	132
5.3 Stx2 reporter-fusion assays	133
5.3.1 Inhibition of bacterial lysis and <i>pstx2</i> :GFP expression by AHU1.....	133
5.3.2 Inhibition of bacterial lysis and <i>stx2</i> :GFP expression by AHU2 and AHU3.....	135
5.3.3 Inhibition of bacterial lysis and <i>stx2</i> :GFP expression by AHU4.....	138
5.3.4 The maleimide group on its own can inhibit lysis and Stx expression	139
5.3.5 AHU3 does not inhibit expression of <i>rpsM</i> and <i>tir</i>	140
5.4 AHU3 inhibits phage production	141
5.4.1 Inhibition of Stx phage production by AHU3	141
5.4.2 Inhibition of Gram-positive phage production by AHU3	142
5.5 AHU3 does not target mitomycin C	144
5.6 Identifying the possible target of AHU3.....	146

5.7 Microscale thermophoresis of AHU3 and RecA.....	148
5.8 AHU3 inhibits the ATPase activity of RecA.....	149
5.9 AHU3 inhibits RecA oligomerisation	151
5.10 Cytotoxicity of the AHU compounds.....	154
5.11 Discussion	155
5.11.1 The AHU compounds target the SOS response protein RecA.....	155
5.11.2 The maleimide moiety of the AHU compounds inhibits bacterial RecA	156
5.11.3 Antimicrobial properties of maleimide compounds	160
5.11.4 RecA as a target of anti-virulence therapies.....	162
5.11.5 The future of AHU3 as an anti-virulence therapy	163
 CHAPTER 6: EVALUATION OF ALTERNATIVE THERAPEUTIC TREATMENTS WITHIN MOUSE MODELS OF INFECTION.....	 164
6.1 Introduction.....	165
6.1.1 Aims of this chapter	165
6.2 The effect of disulfiram on <i>C. rodentium</i> colonisation	167
6.2.1 Salicylidene acylhydrazides, AdhE and the T3SS.....	167
6.2.2 Disulfiram as a potential inhibitor of AdhE.....	169
6.2.3 Effect of disulfiram on <i>C. rodentium</i> colonisation <i>in vivo</i>	169
6.3 The effect of RCZ20 on <i>C. rodentium</i> colonisation	171
6.3.1 RCZ20 is a derivative of the salicylidene acylhydrazide ME0055.....	171
6.3.2 Effect of RCZ20 on <i>C. rodentium</i> colonisation <i>in vivo</i>	172
6.4 The effect of D-serine on <i>Citrobacter rodentium</i> colonisation and microflora short-chain fatty acid (SCFA) production	173
6.4.1 D-serine metabolism by <i>E. coli</i>	173
6.4.2 D-serine represses the T3SS and induces the SOS response	174
6.4.3 Effect of D-serine on <i>C. rodentium</i> colonisation of mice	175
6.4.4 Effect of D-serine on SCFA production.....	176

6.4.5 D-serine concentration in urine is higher in mice treated with D-serine in drinking water.....	178
6.5 The effect of colicin E1 on LF82 colonisation.....	179
6.5.1 Colicin E1 is an antimicrobial against AIEC LF82	179
6.5.2 Effect of encapsulated colicin E1 on LF82 colonisation <i>in vivo</i>	180
6.6 Discussion	182
6.6.1 Disulfiram does not reduce <i>Citrobacter rodentium</i> colonisation of mice.....	182
6.6.2 The RCZ20 compound does not reduce colonisation <i>in vivo</i>	184
6.6.3 D-serine does not affect <i>C. rodentium</i> colonisation or SCFA metabolism by the gut microflora	184
6.6.4 Colicin treatment does not affect LF82 colonisation <i>in vivo</i>	186
CHAPTER 7: FINAL DISCUSSION	188
7.1 Mouse models of EHEC infection.....	189
7.1.1 <i>C. rodentium</i> and <i>C. rodentium</i> (λ Stx _{2dact}) as <i>in vivo</i> EHEC surrogates	189
7.1.2 The importance of the T3SS in human pathogenesis	190
7.2 Candidates for a broadly protective vaccine against <i>E. coli</i>.....	191
7.2.1 Expression of EaeH and YghJ in <i>E. coli</i> strains.....	191
7.2.2 Recent insights into the other identified ExPEC vaccine candidates	192
7.3 Inhibitors of Shiga toxin production and the bacterial SOS response	193
7.3.1 The AHU compounds prevent Stx expression by inhibiting RecA.....	193
7.3.2 Covalent binding as a mode of action for therapeutic drugs.....	194
7.3.3 The AHU compounds are toxic to mammalian cells	194
7.4 Future directions.....	194
7.5 Concluding remarks	196
CHAPTER 8: REFERENCES	197
CHAPTER 9: APPENDICES	215

9.1 Characterisation of <i>E. coli</i> Str^R mutants	216
9.1.1 Bacterial growth in LB, MEM and M9 media	216
9.1.2 Bacterial motility	217
9.1.3 Bacterial adherence to Caco-2 cells	217
9.2 The T3SS in O157:H7 colonisation of streptomycin-treated ICR mice	218
9.3 Comparison of pET-21b <i>eaeH</i> and <i>yghJ</i> to chromosomal sequences	221

List of Figures

Figure 1-1: Phylogenic tree of intestinal pathogenic <i>E. coli</i>	3
Figure 1-2: Transmission routes of O157:H7	10
Figure 1-3: Annual reported O157:H7, <i>Campylobacter</i> and <i>Salmonella</i> cases in England, Scotland, and Wales.....	12
Figure 1-4: Mechanism of action of Stx	14
Figure 1-5: The lytic and lysogenic cycles of bacteriophages	17
Figure 1-6: Activation of the SOS response	19
Figure 1-7: Structure of the T3SS apparatus.....	26
Figure 1-8: Basic representation of T3SS-mediated formation of the attaching/effacing lesion.....	27
Figure 1-9: Phylogenetic tree showing the relationship of <i>C. rodentium</i> to <i>E. coli</i> and other enteric bacteria.....	31
Figure 3-1: Integration of the <i>lux</i> operon into <i>E. coli</i> O157:H7 strain TUV93-0 and its luminescence on agar and in mice.....	72
Figure 3-2: Colonisation of inbred mice by <i>E. coli</i> TUV93-0.....	74
Figure 3-3: Effect of DSS pretreatment on <i>E. coli</i> colonisation	76
Figure 3-4: Effect of streptomycin-treated drinking water on faecal shedding of TUV93-0 in ICR mice	78
Figure 3-5: Effect of streptomycin-treated drinking water on TUV93-0 colonisation of ICR mice	79
Figure 3-6: pGB2 plasmid stability	80
Figure 3-7: Colonisation of TUV93-0 and OI-148A.....	82
Figure 3-8: Intestinal bacterial recovery of TUV93-0 and OI-148A.....	83
Figure 3-9: Colonisation of LF82	85
Figure 3-10: Intestinal bacterial recovery of LF82	86
Figure 3-11: Weight changes of <i>C. rodentium</i> and <i>C. rodentium</i> (λ stx _{2dact})-infected mice	88
Figure 3-12: Colonisation of wild type <i>C. rodentium</i> and <i>C. rodentium</i> (λ stx _{2dact}) in BALB/c and C57BL/6.....	89
Figure 3-13: <i>C. rodentium</i> (λ stx _{2dact}) causes tubular injury and interstitial haemorrhage in kidneys of BALB/c and C57BL/6 mice	91

Figure 3-14: Production of Tir is required for colonisation and production of disease by <i>C. rodentium</i> (λ <i>stx</i> _{2<i>dact</i>}).....	93
Figure 4-1: Genomic organisation of <i>eaeH</i> and <i>yghJ</i>	103
Figure 4-2: <i>E. coli</i> carriage of the <i>eaeH</i> and <i>yghJ</i> genes.....	104
Figure 4-3: Expression of His-tagged EaeH and YghJ	106
Figure 4-4: Confirmation of LF82 Δ <i>eaeH</i> and Δ <i>yghJ</i>	107
Figure 4-5: Construction of <i>eaeH</i> and <i>yghJ</i> reporter fusions	108
Figure 4-6: Expression of gene:GFP reporter fusions	109
Figure 4-7: Expression of GFP by <i>eaeH</i> and <i>yghJ</i> reporter fusions in contact with Caco-2 cells	111
Figure 4-8: Expression of <i>eaeH</i> :GFP by TUV93-0 adhered to HeLa cells.....	113
Figure 4-9: EaeH and YghJ expression by TUV93-0 and LF82.....	115
Figure 4-10: Expression of EaeH after host cell contact	116
Figure 4-11: Expression of EaeH after growth in conditioned or unconditioned media ..	117
Figure 4-12: Expression and secretion of YghJ.....	119
Figure 4-13: Comparison of the promoter regions used for <i>eaeH</i> expression reporters ..	121
Figure 4-14: Comparison of the promoter regions used for <i>yghJ</i> expression reporters...	123
Figure 5-1: Structure of AHU1	132
Figure 5-2: Structures of the modified AHU compounds.....	133
Figure 5-3: <i>Stx2</i> :GFP reporter assay.....	134
Figure 5-4: Inhibition of MMC-induced bacterial lysis by AHU1	134
Figure 5-5: Dose-dependent inhibition of MMC-induced <i>stx2</i> :GFP expression by AHU1.	135
Figure 5-6: Effect of AHU2 and AHU3 on bacterial growth, MMC-induced lysis, and MMC-induced <i>stx2</i> :GFP expression	136
Figure 5-7: Inhibition of <i>stx2</i> :GFP expression by 25 and 50 μ M AHU1, AHU2 and AHU3 at 6 hours after addition of AHU1-3 and MMC.....	137
Figure 5-8: Effect of AHU4 on bacterial growth, MMC-induced lysis, and MMC-induced <i>stx2</i> :GFP expression	138
Figure 5-9: Comparison of inhibitory effects of AHU3 and maleimide	139
Figure 5-10: Effect of AHU3 on <i>rpsM</i> :GFP and <i>tir</i> :GFP expression	140
Figure 5-11: Reduction of MMC-induced Stx phage production by 50 μ M AHU3	142
Figure 5-12: Reduction of MMC-induced SLT phage production by AHU3.....	143
Figure 5-13: Effect of AHU3 on MMC-induced bacterial lysis by 80 α	144

Figure 5-14: AHU3 prevents ciprofloxacin-mediated SOS response.....	146
Figure 5-15: Possible stages of SOS response activation that AHU3 may inhibit	148
Figure 5-16: Interaction of RecA with AHU3 and AHU4.....	149
Figure 5-17: AHU3 inhibits RecA-mediated ATP hydrolysis	150
Figure 5-18: AHU4 does not inhibit RecA-mediated ATP hydrolysis.....	151
Figure 5-19: AHU3 decreases RecA oligomerisation.....	153
Figure 5-20: Proposed covalent attachment of AHU3 to RecA.....	157
Figure 5-21: Cysteine residues are not solvent accessible in oligomeric RecA.....	159
Figure 5-22: Structures of natural maleimides	161
Figure 6-1: Proposed model of <i>adhE</i> deletion in <i>E. coli</i> O157:H7	168
Figure 6-2: Effect of disulfiram on colonisation of BALB/c mice by lux-marked <i>C. rodentium</i>	170
Figure 6-3: Structures of ME0055 and RCZ20	171
Figure 6-4: Effect of RCZ20 on colonisation of BALB/c mice by lux-marked <i>C. rodentium</i>	173
Figure 6-5: Effect of D-serine treatment on colonisation of <i>C. rodentium</i>	175
Figure 6-6: SCFA production in mice treated with D-serine and infected with <i>C. rodentium</i>	177
Figure 6-7: Effect of D-serine treatment and <i>C. rodentium</i> infection on faecal SCFA composition	178
Figure 6-8: D-serine treatment increases the relative abundance of urinary D-serine	179
Figure 6-9: Effect of colicin E1 treatment on LF82 colonisation	181
Figure 9-1: Growth curves of <i>E. coli</i> Str ^R mutants.....	216
Figure 9-2: Motility of Str ^R mutants	217
Figure 9-3: Bacterial adherence to Caco-2 cells.....	218
Figure 9-4: Colonisation of pGB2-transformed TUV93-0 and OI-148A.....	219
Figure 9-5: Intestinal bacterial recovery of TUV93-0 and OI-148A.....	220
Figure 9-6: Comparison of pET-21b-EaeH <i>eaeH</i> and TUV93-0 <i>eaeH</i>	224
Figure 9-7: Comparison of pET-21b-YghJ <i>yghJ</i> and LF82 <i>yghJ</i>	227

List of Tables

Table 1-1: Stx types and variants	15
Table 2-1: Bacterial growth media recipes	44
Table 2-2: Antibiotic concentrations for bacterial growth media used in this study.....	45
Table 2-3: Components of phosphate buffered saline (PBS)	45
Table 2-4: Bacterial strains used in this study.....	46
Table 2-5: Plasmids used in this study	48
Table 2-6: Eukaryotic cell lines used in this study.....	48
Table 2-7: Primers used in this study.....	50
Table 2-8: Components of a 25 µl PCR mixture	51
Table 2-9: Standard PCR protocol.....	51
Table 2-10: Components of restriction enzyme digests for a 10 µl reaction.....	52
Table 2-11: Components of DNA ligation mixture for a 10 µl reaction	52
Table 2-12: Components of protein purification buffers.....	57
Table 2-13: Components of SDS-PAGE stains	58
Table 2-14: Antibodies used in this study	58
Table 2-15: Components of adhesion assay buffer	59
Table 2-16: Components of phage buffer	62
Table 2-17: Partial specific volumes of proteins, and densities and intrinsic viscosities of buffers used in analytical ultracentrifugation.....	63
Table 2-18: Volumes of components in a single ATPase assay well	64
Table 5-1: Cytotoxicity of AHU1-3	154

Abbreviations

+ve	positive
-ve	negative
°C	degrees Celsius
Δ	deletion
A ₆₅₀	Absorbance at 650 nm
AcfD	accessory colonisation factor D
AdhE	bifunctional acetaldehyde/alcohol dehydrogenase
A/E	attaching/effacing
AIEC	adherent-invasive <i>E. coli</i>
ANOVA	analysis of variance
APEC	avian pathogenic <i>E. coli</i>
ATP	adenosine triphosphate
ADP	adenosine diphosphate
cAMP	cyclic adenosine monophosphate
Arp2/3	actin-related protein 2/3
amp	ampicillin
BLAST	basic local alignment search tool
BLV	bovine leukemia virus
bp	base pair
CEACAM	carcinoembryonic antigen-related cell adhesion molecule
CFU	colony forming unit
chl	chloramphenicol
cipro	ciprofloxacin
Da	dalton
kDa	kilodalton
DSS	dextran sodium sulphate
DMEM	Dulbecco's Modified Eagle's Medium
DNA	deoxyribonucleic acid
gDNA	genomic DNA
dsDNA	double-stranded DNA
ssDNA	single-stranded DNA

EAEC	enteroaggregative <i>Escherichia coli</i>
EDTA	ethylenediaminetetraacetic acid
EHEC	enterohaemorrhagic <i>Escherichia coli</i>
EPEC	enteropathogenic <i>Escherichia coli</i>
aEPEC	atypical EPEC
ETEC	enterotoxigenic <i>Escherichia coli</i>
ery	erythromycin
FCS	foetal calf serum
Gb3	globotriaosylceramide
GFP	green fluorescent protein
GLM	general linear model
g	gram
mg	milligram
µg	microgram
ng	nanogram
H&E	hematoxylin and eosin
HEPES	4-(2-hydroxyethyl)-1-piperazineethanesulfonic acid
HUS	haemolytic uraemic syndrome
hrs	hours
IC ₅₀	half maximal inhibitory concentration
IL	interleukin
IPTG	isopropyl β-D-1-thiogalactopyranoside
IVIS	<i>in vivo</i> imaging system
kan	kanamycin
kb	kilobase
L	litre
ml	millilitre
µl	microlitre
LB	Luria-Bertani
LEE	locus for enterocyte effacement
Ler	LEE-encoded regulator
LexA	locus for X-ray sensitivity A
LPS	lipopolysaccharide

LT	heat-labile enterotoxin
M	molar
mM	millimolar
μ M	micromolar
nM	nanomolar
MEM	Minimum Essential Medium
MMC	mitomycin C
MOI	multiplicity of infection
MOPS	3-(N-morpholino)propanesulfonic acid
MRSA	multidrug resistant <i>Staphylococcus aureus</i>
MST	microscale thermophoresis
MW	molecular weight
cm	centimeter
mm	millimeter
μ m	micrometer
NO	nitric oxide
N-WASP	neuronal Wiskott-Aldrich syndrome protein
OD	optical density
OMVs	outer membrane vesicles
PAS	periodic acid-Schiff
PBS	phosphate buffered saline
PBST	PBS containing 0.1% Tween
PCR	polymerase chain reaction
PFA	paraformaldehyde
p/s	photons per second
RecA	recombinase A
RFP	red fluorescent protein
RNA	ribonucleic acid
mRNA	messenger RNA
rRNA	ribosomal RNA
tRNA	transfer RNA
rpm	revolutions per minute
SA	salicylidene acylhydrazides

SCFA	short chain fatty acid
SDS-PAGE	sodium dodecyl sulfate polyacrylamide gel electrophoresis
SE-AUC	sedimentation equilibrium-analytical ultracentrifugation
Str	streptomycin
Str ^R	streptomycin-resistant
Stx	Shiga toxin
T2SS	Type 2 Secretion System
T3SS	Type 3 Secretion System
TAE	Tris-acetate-EDTA
TCA	trichloroacetic acid
Tir	translocated intimin receptor
TLR5	Toll-like receptor 5
TNF	tumour necrosis factor
TSB	tryptic soy broth
tet	tetracycline
UK	United Kingdom
UPEC	uropathogenic <i>Escherichia coli</i>
USA	United States of America
UV	ultraviolet
VFA	volatile fatty acid
v/v	volume per volume
w/v	weight per volume
<i>x g</i>	centrifugal force

Chapter 1: Introduction

1. INTRODUCTION

1.1 Pathogenic *Escherichia coli*

Escherichia coli are Gram-negative, facultative anaerobic bacteria commonly found in the lower intestine of warm-blooded organisms, including humans who are colonised shortly after birth. Strains can be classed into a number of phylogenetically distinct groups, with up to 7 phylogroups proposed (A, B1, B2, C, D, E, and F), with the closely related *Shigella* species forming an accessory group (Clermont *et al.*, 2013). The vast majority of *E. coli* strains coexist in a mutually beneficial symbiotic relationship with their human host, rarely causing disease except in immunocompromised hosts or where normal gastrointestinal barriers are breached. *E. coli* strains are also extensively used as a model organism in the laboratory, due to its fast growth and ease of genetic manipulation.

1.1.1 *E. coli* pathotypes, classification and identification

Pathogenic strains of *E. coli* are capable of causing a range of diverse intestinal and extraintestinal diseases, which result in three distinct clinical syndromes: sepsis/meningitis, urinary tract infection, and enteric/diarrhoeal disease. Diarrhoeagenic *E. coli* isolates can be classed into distinct clinical subcategories: enterohaemorrhagic *E. coli* (EHEC), which are the main focus of this thesis, enteropathogenic *E. coli* (EPEC), enterotoxigenic *E. coli* (ETEC), enteroinvasive *E. coli* (EIEC), enteroaggregative *E. coli* (EAEC), adherent-invasive *E. coli* (AIEC), and diffusely adherent *E. coli* (DAEC). Pathotypes do not always group together in the same phylogroup; for example, EHEC strains are found in both phylogroups B1 and E (Figure 1-1).

1. INTRODUCTION

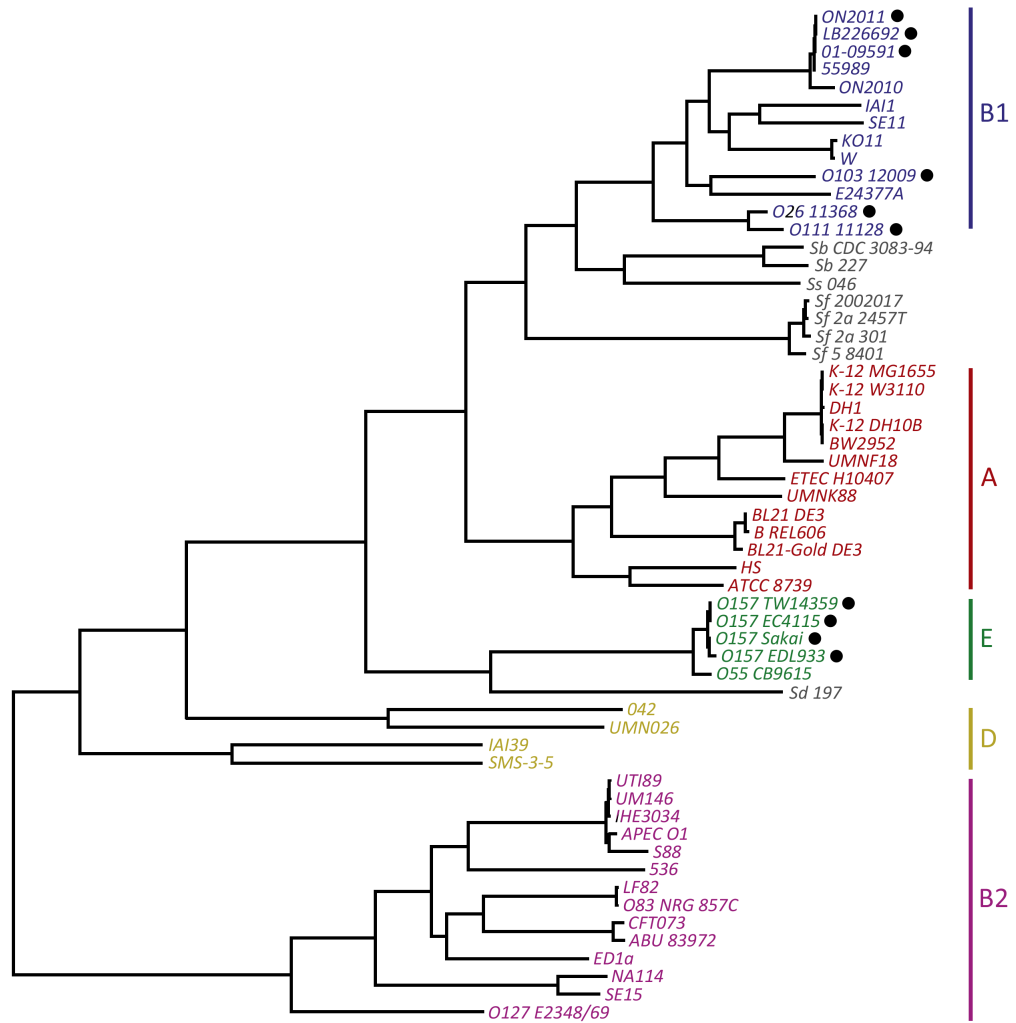


Figure 1-1: Phylogenetic tree of intestinal pathogenic *E. coli*. The 5 main *E. coli* phylogenetic groups are indicated by branch colour coding as follows: Phylogroup B1 = blue; Phylogroup A = red; Phylogroup E = green; Phylogroup D = yellow; Phylogroup B2 = pink. Strains with the enterohaemorrhagic pathotype are denoted by a black circle. Adapted from Hao *et al.* (2012), which was published under a Creative Commons licence.

Classification of pathogenic *E. coli* strains into serotypes is based on particular surface-exposed antigens they express: the O antigen, a polymer present in the lipopolysaccharide layer, and the H antigen, a major component of flagella. Some strains can also be classified by their K antigen, which denotes their capsular polysaccharide group. Laboratory identification of *E. coli* often utilises selective growth media, with MacConkey and eosin methylene blue agar, which select for Gram-negative bacteria and lactose fermentation, commonly used for initial identification. *E. coli* strains are also oxidase negative, produce indole, do not ferment citrate, and demonstrate a negative

1. INTRODUCTION

Voges-Proskauer reaction. Additional determination of particular isolates from the array of virulence genes they carry can be performed by a number of molecular methods, including pulsed field gel electrophoresis (currently considered the gold standard for typing of *E. coli* during outbreak investigations), DNA-DNA hybridisation, PCR and multiplex PCR, and microarray technology.

1.1.2 Diarrhoeagenic *E. coli* pathotypes

The first type of *E. coli* to be associated with human disease, EPEC is a major cause of infantile diarrhoea and infant mortality in developing countries. Transmission of EPEC occurs through the faecal-oral route, with its reservoir believed to be symptomatic or asymptomatic children and asymptomatic adult carriers. The defining characteristic of EPEC is the ability to produce an attaching/effacing (A/E) lesion at the site of bacterial attachment to host cells, which involves major host cytoskeletal changes directly beneath the attached bacteria. Symptomatic infection by EPEC produces watery or bloody diarrhoea, which is achieved without the production of enterotoxins or invasion of host cells. Although there are many EPEC strains that produce disease in animals such as rabbits, dogs and pigs, these strains are not usually associated with human disease.

Members of the EHEC group are classified by their production of Shiga toxin (Stx), also known as Verotoxin, which inhibits protein synthesis in mammalian cells. EHEC are associated with a broad spectrum of disease, ranging from mild diarrhoea to severe haemorrhagic colitis and haemolytic uraemic syndrome (HUS), a serious and life-threatening illness characterised by haemolytic anaemia, acute kidney failure and thrombocytopenia. Cattle, not humans, are the main reservoir of EHEC, with sporadic outbreaks of human disease occurring through contaminated beef and dairy products, as well as through fruits and vegetables that have come into contact with contaminated animal faeces. Despite the isolation of over 380 different EHEC serotypes from humans and animals, only a small number of these have been shown to be responsible for clinical disease (Nguyen & Sperandio, 2012). The most important of these in relation to human health is O157:H7, although other serotypes have been involved in major outbreaks.

1. INTRODUCTION

ETEC strains are classified by their ability to produce at least one member of the heat-labile (LT) or heat-stable (ST) groups of enterotoxins, and the presence of fimbriae for attachment to intestinal host cells. Infection produces watery diarrhea with no blood or abdominal cramping, although, like EPEC, strains can also be carried asymptotically. ETEC infections are a major concern in developing countries, with 840 million cases estimated to occur annually, 280 million of these in children under the age of four (Wennerås & Erling, 2004), and are also the leading cause of traveler's diarrhoea. Illness caused by ETEC infection of young children in developing countries also has been linked to later poor growth and malnourishment, and ETEC have also been implicated in an increased risk of developing post-infectious irritable bowel syndrome following traveler's diarrhoea (reviewed by Croxen *et al.*, 2013).

Infection by EIEC strains produces shigellosis, an illness ranging from mild abdominal discomfort to severe dysentery, which is also caused by *Shigella* species, with whom EIEC shares many genetic and pathogenic features. EIEC are highly invasive, penetrating the epithelial barrier of intestinal cells by transcytosis, and subvert host cell signalling pathways to enable their survival and replication. Although reported EIEC infections are rare compared to other pathotypes, this is likely to be influenced by the lower severity of its clinical manifestations and possible misclassification of EIEC infections as *Shigella*.

EAEC strains are defined by their adherence phenotype, a "stacked brick" adhesion pattern on Hep-2 human epithelial cells, with the genes encoding this phenotype contained in the pAA plasmid, and a lack of LT/ST enterotoxin secretion. This pathotype is increasingly recognised as an emerging enteric pathogen since it was first described in 1987, and causes persistent diarrhea in children and human immunodeficiency virus (HIV)-infected patients. In a large-scale study of bacterial diarrhea of two large US hospitals, EAEC was found to be the most common pathogen in diarrhoeal stool samples (Nataro *et al.*, 2006). In 2011, the causative agent of a major *E. coli* outbreak in Germany that resulted in particularly high levels of HUS was identified as an EAEC strain that had acquired genes encoding an EHEC toxin; as several EAEC has previously been reported to acquire these genes by multiple separate studies (reviewed by Croxen *et al.*, 2013), it is likely that similar outbreaks may occur in the future.

1. INTRODUCTION

E. coli strains belonging to the AIEC group have been implicated in the development of Crohn's disease (CD), a chronic inflammatory disorder of the intestine that occurs due to an aberrant immune response to intestinal bacteria in susceptible hosts. CD causes symptoms such as bloody diarrhoea, abdominal pain, fatigue and weight loss, and recent epidemiological studies have shown a rising prevalence in developed countries, with 1.4 million people in the USA and 2.2 million people in Europe estimated to suffer from CD (Loftus, 2004). No single causative agent of CD has been identified, and it is currently believed that a combination of genetic, environmental, and microbiological factors contribute to disease. AIEC bacteria bind host carcinoembryonic antigen-related cell adhesion molecule 6 (CEACAM6) receptors, antigens upregulated by inflammatory cytokines and possibly AIEC itself, present on M cells overlying Peyer's patches, lymphatic tissue present in the ileum involved in detection of bacterial pathogens and immunological responses. Invasion of bacteria into Peyer's patches is then facilitated by bacterial long polar fimbriae, where they can induce immune responses of patch macrophages, further aggravating inflammation (reviewed by Strober, 2011).

Diarrhoeagenic DAEC strains are a unique group of *E. coli* that adhere to cells in non-classical patterns of attachment (such as attaching and effacing or localised), instead binding diffusely over the entire surface of the host cell in a scattered pattern. This adhesion phenotype is mediated by surface fimbriae, the genes for which are encoded either on the bacterial chromosome or on a plasmid. The epidemiology of DAEC is difficult to assess, due to a lack of a universal method of identifying strains in a clinical setting. However, some studies have identified DAEC isolates from both healthy patients and those with diarrhoea, and have suggested that younger children have a higher risk of DAEC-associated diarrhoea (Levine *et al.*, 1993).

1.1.3 Uropathogenic and neonatal meningitis-causing *E. coli*

Urinary tract infections (UTIs) are primarily caused by uropathogenic *E. coli* (UPEC) strains, which are responsible for 70-95% of community-acquired UTIs and 50% of nosocomial UTIs (Foxman, 2003). UTIs are one of the most common infectious diseases of humans with approximately 150 million annual cases worldwide, while it is estimated that 40-50% of women and 5% of men will develop a UTI in their lifetime (reviewed by Totsika

1. INTRODUCTION

et al., 2012). UPEC are opportunistic pathogens whose reservoir is often the intestinal tract; isolates identified as the cause of an UTI often match faecal isolates from the patient or their sexual partners (Russo *et al.*, 1995; Foxman *et al.*, 2002). Following infiltration of the urinary tract, UPEC preferentially colonise the bladder, causing cystitis, but can also ascend via the ureters to reach the kidneys where they can cause pyelonephritis, a potentially serious and life-threatening inflammation of kidney tissue. A wide array of virulence factors facilitate UPEC infection, including adhesive pili that enable attachment and invasion of epithelial cells in the urinary tract, toxins that allow bacterial dissemination and modulation of host signalling pathways, and siderophores to acquire host iron supplies (reviewed by Wiles *et al.*, 2009).

Neonatal meningitis *E. coli* (NMEC), which belong mainly to the B2 phylogenetic group, are one of the most common causes of bacterial neonatal meningitis, inflammation of the meninges caused by bacterial infection of the blood, which carries a high mortality and morbidity rate as well as severe neurological defects in many survivors. Many NMEC strains produce the K1 capsular polysaccharide which contains sialic acid, a monosaccharide widely distributed in human tissues and not recognised by the innate immune system, thus protecting the bacteria from host responses. This capsule also enables bacteria to breach the blood-brain barrier in order to reach the meninges.

1.1.4 Pathogenic animal *E. coli*

Although some pathotypes of *E. coli* have only been identified in humans, pathogenic EHEC, EPEC and ETEC are responsible for a wide range of diseases in animals, including many domesticated species such as cattle, pigs, goats, and dogs. An additional pathotype, avian pathogenic *E. coli* (APEC), can cause extraintestinal infections exclusively in poultry, producing respiratory infection, pericarditis, and septicaemia. Many APEC strains are present in the intestinal microbiota of healthy animals, and diseases associated with them are considered secondary to environmental and host predisposing factors (reviewed by Dho-Moulin & Fairborther, 1999).

1. INTRODUCTION

1.2 Enterohaemorrhagic O157:H7 *E. coli*

The first recognition of an EHEC strain as a foodborne pathogen occurred in 1982 in Oregon and Michigan, USA, during an investigation into customers of a fast-food restaurant chain who were exhibiting bloody diarrhoea and severe abdominal cramping with no fever. The *E. coli* strain O157:H7, which had not previously been associated with human disease, was isolated from infected individuals and traced to contaminated hamburger meat (Riley *et al.*, 1983). Shortly thereafter, O157:H7 was linked to the development of HUS (Karmali *et al.*, 1983), a disease predominantly affecting children and carrying a 5-10% mortality rate. Since then, EHEC have been recognized as responsible for hundreds of food and waterborne outbreaks, with O157:H7 being the most prevalent serotype and the leading cause of HUS in Europe and the United States (Tarr *et al.*, 2005).

1.2.1 Sources and transmission of O157:H7

The natural reservoir of O157:H7 is the gut of ruminants, particularly domesticated cattle. O157:H7 colonises the recto-anal junction of cattle (Naylor, 2005), in contrast to the colon of humans, and is excreted into the environment. O157:H7 are non-pathogenic in cattle, as the globotriaosylceramide (Gb3) receptor for the Shiga toxin associated with HUS is not present in the bovine gastrointestinal tract. While Gb3 receptors have been identified in the kidney and brain of cattle, lack of vascular Gb3 expression in the gut prevents the toxin from being transported through the endothelium into blood vessels and delivered to those organs (Pruimboom-Brees *et al.*, 2000).

Carriage studies in cattle have shown large variations in the quantity of O157:H7 shed in faeces. Prevalence of colonisation in dairy cattle as measured by faecal shedding ranges from 0.2-48.8%, with carriage by calves with a functioning rumen higher than adult cows, and a higher level of prevalence observed in warmer months compared to colder months (reviewed by Pennington, 2010). Carriage between animals within herds is also highly variable with some individual animals, termed supershedders, responsible for large numbers of excreted O157:H7 compared to the rest of the population. Fitting dynamic

1. INTRODUCTION

epidemiological models to prevalence data from a survey of cattle farms in Scotland found that 80% of transmission arises from just 20% of animals that are most infectious (Matthews *et al.*, 2006). These supershedders, which excrete O157:H7 at a high rate and for a longer period, are associated with bacterial colonisation of a lymphoid follicle-dense mucosal region proximal to the recto-anal junction (Cobbold *et al.*, 2007). However, no genetic marker for supershedders has yet been identified.

The most frequent mode of O157:H7 transmission to humans is through consumption of contaminated food and water (Figure 1-2), a method that is substantially facilitated by its low infectious dose, which has been calculated to be between tens to hundreds of microorganisms based on data from outbreaks. Analysis of the causes of 90 outbreaks from the USA, Japan, and several European countries between 1982 and 2006 found that contaminated food was the most common source of infection, with non-dairy food responsible for 42.2% of outbreaks, dairy products for 12.2%, direct animal contact for 7.8%, water for 6.7%, and environmental for 2.2% (Snedeker *et al.*, 2009). Although cattle are considered the major reservoir of O157:H7 and other EHEC, sheep may also be significant carriers of EHEC; faecal shedding studies claim that high numbers of these animals (65-87%) contained Stx-positive microbes (Cookson *et al.*, 2006; Heuvelink *et al.*, 1998). Stx-carrying *E. coli* have also been identified in many other animal species, including goats, pigs, deer, and wild birds. The use of cattle waste as a fertiliser for crop production can also cause O157:H7 contamination of human food, with many O157 outbreaks associated with produce such as spinach, apple juice, lettuce, and radishes. Other non-fruit/vegetable foods have also been implicated in outbreaks, such as the 2009 outbreak caused by consumption of uncooked cookie dough (Neil *et al.*, 2012). The globalisation of food distribution has helped to facilitate the easy spread of contaminated food and has increased the complexity of identifying the source of an outbreak.

1. INTRODUCTION

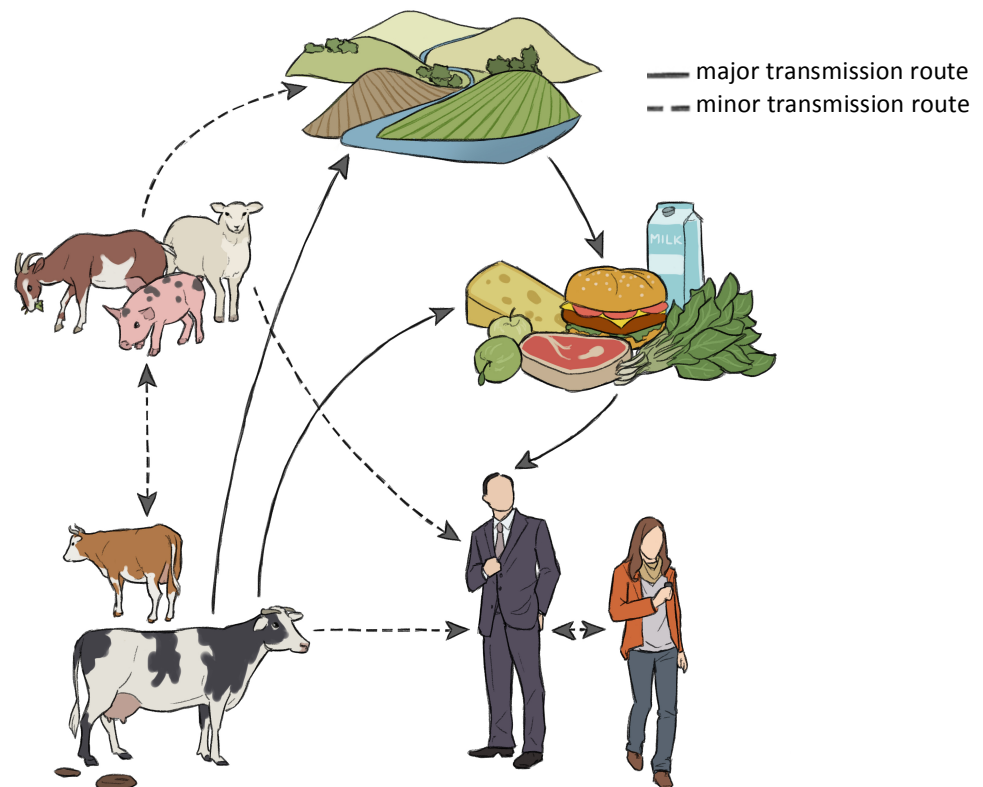


Figure 1-2: Transmission routes of O157:H7. Cattle are the major source of O157:H7, although its high prevalence in other farm animals has been reported. Direct transmission from animals to humans can occur by contact (farms, petting zoos), although the majority of outbreaks have been caused by ingestion of O157:H7-contaminated food, such as meat, dairy products, fruit and vegetables. Contamination of crops occurs through faecal contamination from animals, such as the use of manure in fertiliser.

Human and animal wastewater is thought to be responsible for contamination of aquatic environments, including drinking and recreational water. Detection rates have estimated that one in a thousand faecal coliforms in human sewage carries the *stx* gene, rising to one in a hundred in agricultural animal sewage, and even higher in wastewater from sources such as slaughterhouses and agricultural waste disposal sites (reviewed by Mauro & Koudelka, 2011).

1.2.2 O157:H7 and human disease

Infection by O157:H7 can result in a wide range of effects, from asymptomatic to watery diarrhoea, HUS, and thrombotic thrombocytopenic purpura (TTP). In the majority of clinical manifestations of O157:H7 infection, disease is mild with abdominal pain and watery diarrhoea occurring 3-4 days after infection. In patients with severe symptoms,

1. INTRODUCTION

blood in the faeces can vary from streaked stools to pure (100%) blood, with this symptom more commonly observed in O157:H7 than other EHEC infections. Illness is not accompanied by fever, and usually resolves within a week. Approximately 2-15% of people infected with O157:H7 go on to develop HUS, and children are particularly at risk of this disease, with 15% of children under 10 years of age with an O157:H7 infection developing HUS (Tarr *et al.*, 2005). O157:H7 is the most common cause of HUS, and this disease is responsible for the majority of acute renal failure in children in the Western world (Noris & Remuzzi, 2005). EHEC-associated HUS is caused by bacterial production of the Shiga toxin, which produces widespread thrombotic microvascular lesions in the kidney with subsequent red blood cell destruction and prevention of blood and oxygen supply, eventually resulting in loss of tissue function and organ failure.

The severity of disease varies between O157:H7 outbreaks, due to differences in the virulence of the strains involved. Some particularly severe outbreaks include the 1996 Sakai outbreak in Japan, caused by contamination of radish sprouts which caused 12 deaths and left thousands ill (Michino *et al.*, 1999), and the 2006 North American spinach outbreak which resulted in 3 deaths and hospitalisation of half of the people who reported symptoms (Grant *et al.*, 2008). There is a high economic cost associated with O157:H7 disease; the annual cost in the USA is estimated to be \$405 million, which includes medical care, lost productivity, and premature deaths (Frenzen *et al.*, 2005). The cost of individual outbreaks varies greatly by size, severity, and incidence of HUS. The 1994 West Lothian outbreak in Scotland cost approximately £3 million at the time of the outbreak, but its projected cost as a consequence of long term damage to health was predicted to be over £11 million over the next 30 years (Roberts *et al.*, 2000). Although the yearly number of reported O157:H7 infections is significantly lower than that of other enteric pathogens such as *Salmonella* or *Campylobacter* (Figure 1-3), O157:H7 is treated as a major health concern due to its higher hospitalisation, HUS risk, and mortality rate.

1. INTRODUCTION

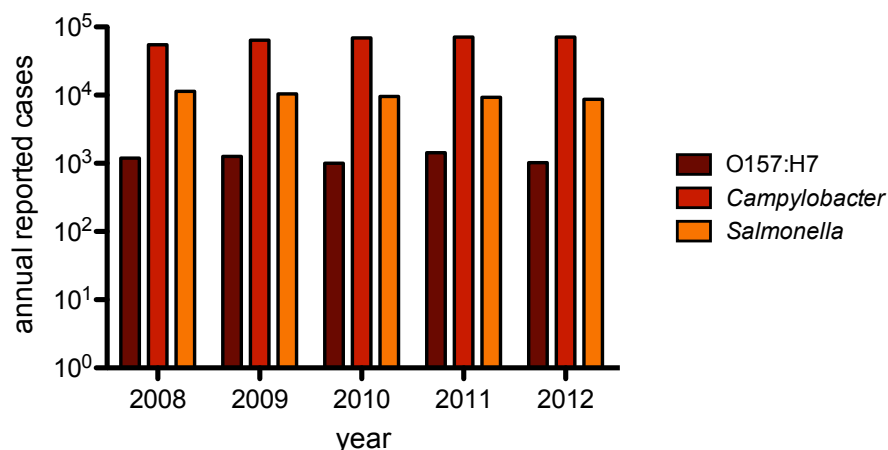


Figure 1-3: Annual reported O157:H7, *Campylobacter* and *Salmonella* cases in England, Scotland, and Wales. The average annual reported cases between 2008-2012 were 1,186 for O157:H7, 66,165 for *Campylobacter*, and 9,882 for *Salmonella*. Data was obtained from Public Health England (<https://www.gov.uk/government/organisations/public-health-england>) and Health Protection Scotland (<http://www.hps.scot.nhs.uk/>).

1.2.3 O157:H7 virulence factors

Pathogenic *E. coli* carry a range of virulence factors that allow them to colonise, survive, and cause disease in their human host. The genes encoding many of these can be transferred horizontally between different strains of *E. coli*, enabling dissemination of virulence factors between different phylogroups. This can result in the acquisition of new virulence properties, potentially leading to the emergence of novel *E. coli* pathotypes, as seen by the O104:H4 strain responsible for the recent 2011 outbreak in Germany.

As in other EHEC strains, the production of Shiga toxin in O157:H7 is associated with the development of HUS. The Type 3 Secretion System (T3SS) is another important virulence factor that mediates intimate attachment of bacteria to enterocytes, and is carried not only by EHEC strains but also by EPEC, *Shigella*, *Salmonella*, and *Yersinia* species. Other virulence factors expressed by O157:H7 include the flagella, long extracellular appendages that provide motility but also have sensory and adherence functions (Girón *et al.*, 2002), and the putative virulence plasmid pO157, carried by all clinical isolates, which contains many different mobile genetic elements such as prophages and transposons. The focus of this thesis, however, will be centered on just two of these virulence factors: the Shiga toxin and the Type 3 Secretion System.

1. INTRODUCTION

1.3 Shiga toxin

The pathogenesis of haemorrhagic colitis and HUS is dependent on the production of Shiga toxin, a family of related toxins essential, though not solely responsible for disease. Stx from *Shigella dysenteriae* was first identified over a hundred years ago by Kiyoshi Shiga, and subsequently found to be expressed by EHEC strains in 1983 (O'Brien *et al.*, 1983).

1.3.1 Stx structure and mechanism of action

Stx belongs to the AB family of toxins, in which one A subunit and five B subunits associate to form an active toxin. Within the AB₅ holotoxin structure, enzymatic activity is located in the single A subunit, while the binding activity is associated with the pentameric B domain. This structure binds to the Gb3 receptor, expressed by Paneth cells in the intestinal mucosa and by kidney epithelial cells, allowing clathrin-dependent endocytosis of the A subunit. The internalised A subunit is then proteolytically cleaved into two parts, A1 (27.5 kDA) and A2 (4.5 kDA), which remain covalently associated by a disulphide bond until the two cysteine residues are reduced (Olsnes *et al.*, 1981). N-glycosidase activity within the A1 subunit enables it to cleave a single adenosine from the 28S ribosomal RNA of the 60S ribosomal subunit, an enzymatic activity shared with the plant lectin ricin (Endo *et al.*, 1988), preventing binding of elongation factor to the ribosome and thus inhibiting protein synthesis, resulting in cell death by apoptosis (Figure 1-4). Stx is also capable of interacting with other non-epithelial cells, and can affect renal tubular cells, mesangial cells, monocytes and platelets.

1. INTRODUCTION

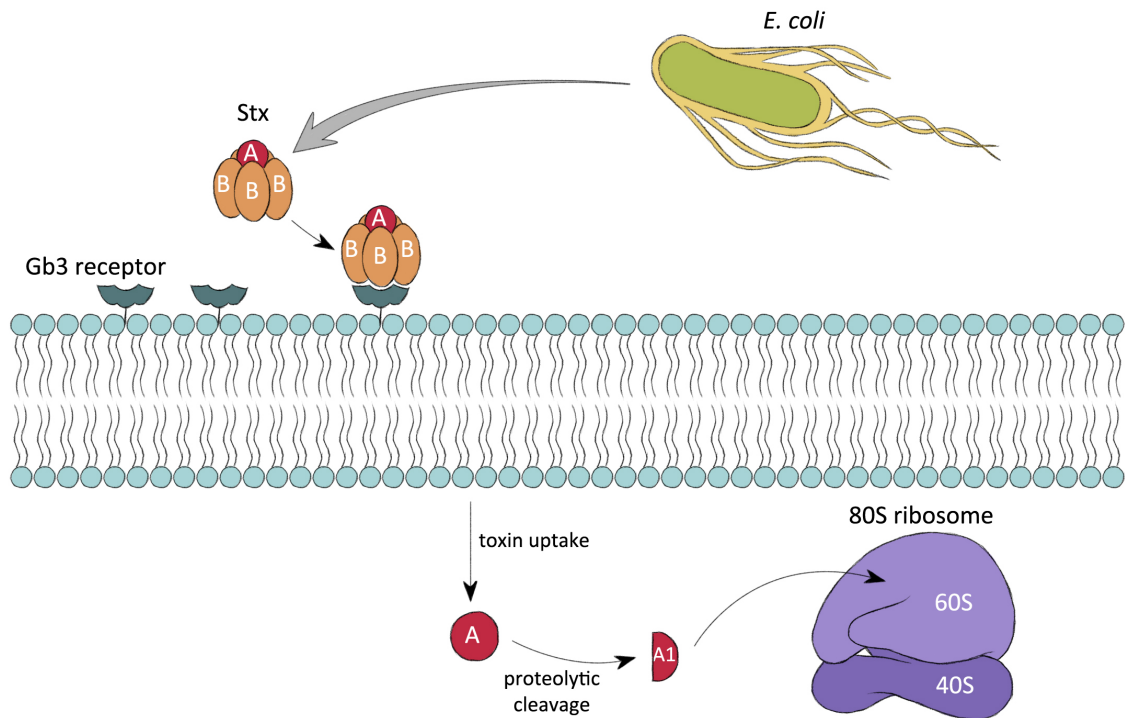


Figure 1-4: Mechanism of action of Stx. The B subunits of Stx bind to the host receptor Gb3 on the cell surface, allowing the A subunit of Stx to be internalised. Inside the host cell, the A subunit is cleaved into two parts, and the A1 component cleaves a specific adenine residue from the ribosome, disrupting protein synthesis and thus leading to cell death.

1.3.2 Stx variants

Stx produced by EHEC strains are differentiated into two types that share 55% sequence homology (Fraser *et al.*, 2004): Stx1, which shares very high homology with *Shigella dysenteriae*, and Stx2, which is structurally similar to Stx1, but antigenically distinct. O157:H7 can carry genes encoding both forms of the toxin, although it is Stx2 whose expression is more strongly associated with the production of bloody diarrhoea and higher risk of HUS. Within each group, Stx is classed into variants (Table 1-1) that differ from each other in biological and immunological reactivity, with the Stx2 group displaying a higher level of heterogeneity compared to the Stx1 group. Only the genes for Stx1a, Stx1d, Stx2a, and Stx2c have been identified in O157:H7 isolates.

1. INTRODUCTION

Table 1-1: Stx types and variants. Stx variants found in O157:H7 are underlined. Adapted from Pacheco and Sperandio (2012) and Scheutz *et al.* (2012).

Stx type	Variants
Stx1	<u>Stx1a</u> , Stx1c, <u>Stx1d</u>
Stx2	<u>Stx2a</u> , <u>Stx2c</u> , Stx2d, Stx2dact, Stx2e, Stx2f, Stx2g

The most virulent Stx2 variants are Stx2c and Stx2dact. Two amino acid changes in the B subunit of Stx2c reduces its potential to generate a significant neutralising antibody response in mice compared to the other Stx2 variants, although it displays equal toxicity (Lindgren *et al.*, 1994). The Stx2dact variant also shows these alterations in the B subunit, along with a further two amino acid changes in the A subunit that allows an additional proteolytic cleavage event by elastase to occur (Kokai-Kun, 2000). This results in a greater capacity for Gb3 binding and thus an enhanced increase in toxicity (Bunger *et al.*, 2013). Consequently, bacteria carrying these toxins are more virulent than any other Stx2-expressing strain in the mouse model of disease (Melton-Celsa *et al.*, 1996). Although Stx2dact has been associated with a severe clinical outcome and high risk of HUS development (Bielaszewska *et al.*, 2006), it has not yet been found in an O157:H7 strain.

1.3.3 Shiga toxin-encoding bacteriophages

The genes for Shiga toxins in *E. coli* are exclusively located on temperate lysogenic phages that integrate into the genome of their host bacterium. The Stx1 bacteriophage genes are integrated into *yehV* (Yokoyama *et al.*, 2000), a gene encoding a positive regulator of curli expression. The Stx2 bacteriophage genes are integrated into the locus for *wrbA* (Makino *et al.*, 1999), which encodes a NAD(P)H:quinone oxidoreductase, with the exception of the Stx2c variant which is found next to *sbcB*, a gene encoding the exonuclease ExoI involved in genetic stability (Eppinger *et al.*, 2011). In the lysogenic state, Stx genes are replicated as an integral part of the bacterial genome. Expression of the phage genes occurs when the phage lytic cycle is activated, allowing the genes encoding Stx to be packaged in phage particles, which are assembled and released through lysis of the cell. The released Stx bacteriophages are then able to infect other non-*stx E. coli*, potentially leading to integration of the Stx genes into the chromosome of the new host and thus

1. INTRODUCTION

dissemination of this virulence phenotype. Lysis of bacteria also allows release of translated Stx protein into the local environment.

1.3.4 Horizontal gene transfer of *stx* and its contribution to new EHEC outbreak strains

Infection of bacteria by bacteriophages can result in integration of the phage genes into the bacterial chromosome as the phage undergoes lysogeny (Figure 1-5). This type of horizontal gene transfer by phage has been associated with acquisition of a number of major virulence factors, such as diphtheria toxin of *Corynebacteria diphtheria*, cholera toxin from *Vibrio cholerae*, and enterotoxin A of *Staphylococcus aureus*. Together, these examples highlight the contribution that phages have played in the evolution of novel pathogens.

1. INTRODUCTION

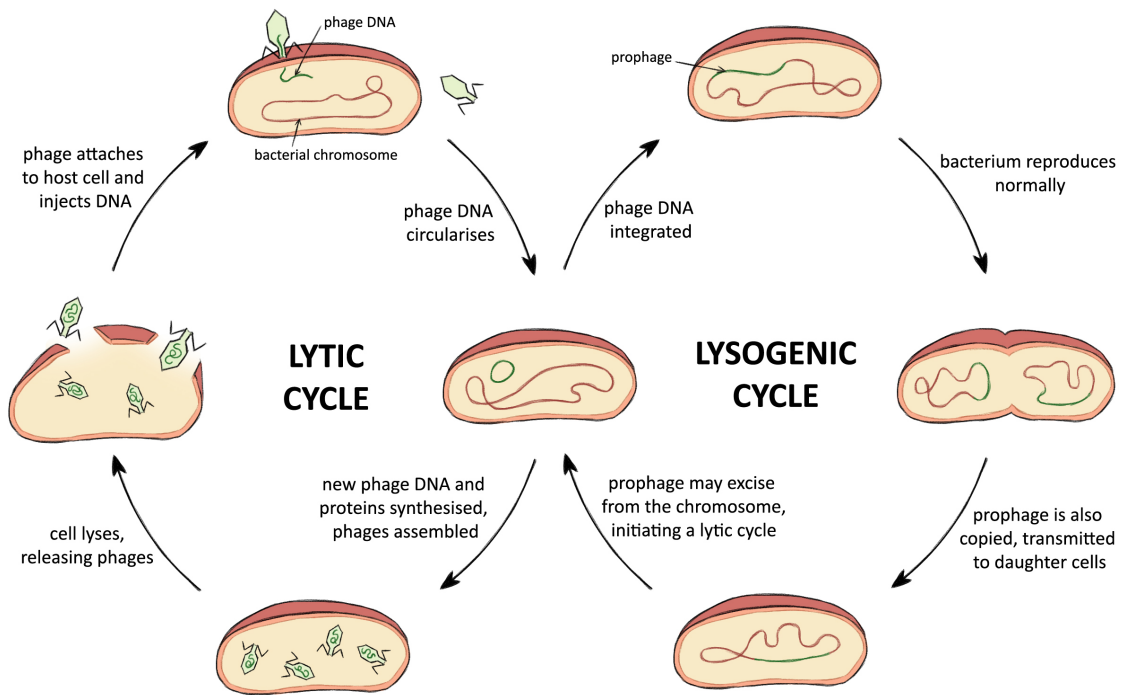


Figure 1-5: The lytic and lysogenic cycles of bacteriophages. When phage DNA is injected into bacterial cells it can enter one of two cycles of reproduction. In the lytic cycle (left) the phage DNA hijacks the cell's replication and translation mechanisms, using them to produce more phage DNA and proteins. Eventually, the assembled phages cause lysis of their host bacterium, releasing progeny phages into the surrounding environment where they can go on to infect other bacteria. In the lysogenic cycle (right) the phage DNA is integrated into the bacterial chromosome, becoming a prophage. The phage DNA continues to reproduce during cell division and is transmitted to daughter cells. Certain conditions can release the prophage from the chromosome, causing it to enter the lytic cycle and produce phages.

A recent and significant example of how Stx acquisition can result in the emergence of a new outbreak strain is provided by the *E. coli* O104:H4 outbreak in Germany in 2011. This incident resulted in over four thousand cases of infection and 852 cases of HUS. This was a much higher rate of HUS (approximately 29% of cases) compared to many other EHEC outbreaks (Buchholz *et al.*, 2011). Although symptoms indicated the infection to be caused by an EHEC strain such as O157 or O111, the actual organism responsible was eventually identified as an EAEC strain which had acquired the *stx* gene. The combination of Stx expression, capacity to adhere using the enteroaggregative phenotype, and the ability to generate biofilms was thought to contribute to the high level of virulence observed in this outbreak (Scheutz *et al.*, 2011).

1. INTRODUCTION

1.3.5 Regulation, activation and expression of the bacterial SOS response

The switch from a lysogenic lifestyle to a lytic cycle by bacteriophages is controlled by the SOS response, a high-activity repair response to damage of DNA. When the cell undergoes stress that results in DNA damage, such as exposure to UV light or certain antibiotics, the SOS response is activated and allows Stx bacteriophage to escape into the surrounding environment, where it may infect other bacteria and enter the lysogenic cycle once more.

At least 43 genes in *E. coli* are activated by the SOS response (Courcelle *et al.*, 2001), and the proteins they encode include those involved in DNA repair, protection of single-stranded DNA (ssDNA) from destruction, DNA mutagenesis, and arrest of the cell cycle. The interplay of two major proteins, RecA (recombinase A) and LexA (locus for X-ray sensitivity A), regulates the SOS response. RecA, a 38 kDa ATP-dependent protein with DNA-binding abilities, is highly conserved in bacteria, with structural and functional homologues present in all organisms, including humans in which it is known as RAD51. LexA is a 27 kDa protein which represses the expression of genes involved in the SOS response, including that of *recA* and *lexA*.

Under non-stressed conditions, LexA binds as a dimer to its cognate LexA box sequence within the promoter for those genes expressed by the SOS regulon, thus inhibiting their production (Thliveris *et al.*, 1991). As a consequence, SOS gene expression is dependent on the affinity of LexA for each promoter. When DNA damage occurs, RecA is recruited to ssDNA by the RecFOR complex, whereupon it oligomerises to form a right-handed helical nucleofilament, with one RecA monomer bound per three base pairs of DNA and a total of six monomers per helical turn. RecA can also form filaments on double-stranded (dsDNA) when recruited by the RecBCD complex, albeit much weaker ones (Arenson *et al.*, 1999). The assembled RecA filaments, known as RecA*, have the ability to catalyse strand exchange and enable homologous recombination to repair DNA. In addition, they have protease activity which allows the facilitation of LexA autocleavage, removing it from the promoter sequence of the SOS genes and allowing their transcription (Figure 1-6). Studies using UV light to damage DNA have shown that after irradiation, the amount

1. INTRODUCTION

of intact LexA within the cell severely decreases within a matter of minutes (Sassanfar & Roberts, 1990).

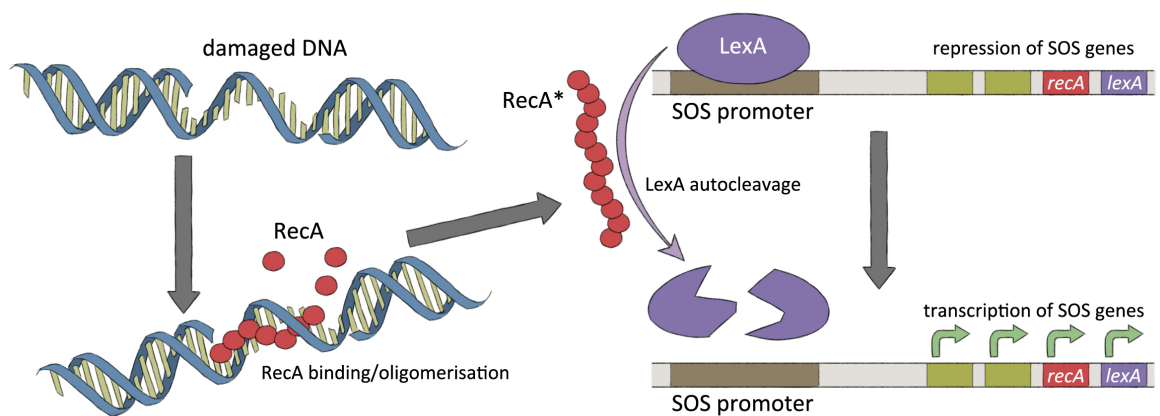


Figure 1-6: Activation of the SOS response. RecA monomers (red) recognise and bind to damaged ssDNA, forming filaments that enable autocleavage of the LexA repressor (purple). Cleavage of LexA results in its removal from promoter regions upstream of genes encoding proteins involved in the SOS response, including those that encode for RecA and LexA.

The first SOS genes to be expressed are *urvA*, *urvB*, and *urvD*, which catalyse nucleotide excision repair, removing damaged nucleotides from DNA. This is followed by expression of *recA* and homologous recombination functions, which result in repair of lesions at replication forks. Cell division is also halted by the production of the inhibitor SfiA. Late expression of *umuC* and *umuD*, approximately 40 minutes after DNA damage, produces the mutagenic DNA repair polymerase Pol V. This is an error-prone polymerase strictly regulated by the cell and only generated when the SOS response is active. As the SOS response risks the introduction of lethal mutations into the genome, strong regulation is required to ensure that these genes are repressed when no longer required. Constitutive expression of *lexA*, allowing LexA re-accumulation as DNA is repaired, results in eventual repression of the SOS response once more.

The SOS response is not considered to be relative to the amount of DNA damage accumulated. Rather, studies investigating the promoter activity of the SOS genes suggest that the SOS response is induced to a level that repairs damage but allows the cell to survive, irrespective of the extent of DNA damage. If this is insufficient to complete the repair, further rounds of SOS induction are initiated. This demonstrates that the SOS

1. INTRODUCTION

response is highly structured, with precise temporal modulation of gene expression levels (Friedman *et al.*, 2005).

1.3.6 Regulation of Stx expression

Expression of *stx* and the other Stx prophage genes are under the control of the λ *ci* repressor, which prevents the phage from entering the lytic cycle when bacteria are growing and persisting without exposure to external stress. The *ci* repressor, like other phage repressors such as the *c2* repressor of P22 and the *ci* repressor of ϕ 80, is a functional homologue of LexA and is able to undergo RecA nucleofilament-mediated self-cleavage (Sauer *et al.*, 1982). Therefore when the SOS response is activated, the *ci* repressor is removed from the prophage promoter region, allowing expression of these genes and a shift from lysogenic to lytic growth. The *stx* genes are located downstream of P_R , a promoter which is only active when the lytic cycle has been initiated. This results in the expression of genes involved in late phage function (Roberts *et al.*, 1998).

Agents that interfere with the SOS response further control regulation of Stx expression. These include the nitric oxide (NO) donor NOR4, which significantly decreases expression of *stx2* and inhibits production of phage particles through its capacity to reduce the expression of *recA*, thus preventing activation of the SOS response (Vareille *et al.*, 2007). In contrast, hydrogen peroxide, produced by human neutrophils, results in increased Stx and phage production due to its upregulation of *recA*, suggesting that oxidative stress may stimulate pathogenicity determinants of EHEC (Imlay & Linn, 1987). Expression of *stx1* is also repressed in a non-SOS-dependent manner by iron, as Stx1 is controlled by the iron-sensitive repressor Fur (Calderwood & Mekalanos, 1987). The promoter sequence to which Fur binds is not found in the Stx2 promoter region and thus its expression is unaffected by the presence of iron.

1.3.7 The role of Stx in bacterial colonisation and the immune response

Shiga toxin may also have a function in the Type 3-mediated attachment of bacteria to human epithelial cells. In order to colonise the intestine, the T3SS facilitates attachment

1. INTRODUCTION

to enterocytes and the formation of an attaching/effacing lesion by translocation of the protein Tir (translocated intimin receptor) into the host cell membrane, where it acts as a receptor for the bacterial adhesin intimin. Intimin can also recognise nucleolin, a eukaryotic protein which, despite being involved in the synthesis and maturation of ribosomes, can also be found on the cell surface of many cell types (Ginisty *et al.*, 1999). *In vitro* infection studies of nucleolin-expressing human epithelial cells with O157:H7 have shown that microcolonies of the organisms associate with regions of surface-expressed nucleolin, and that treatment with anti-nucleolin serum reduces bacterial adherence (Sinclair & O'Brien, 2002). Further work by Robinson *et al.* (2006) observed increased surface expression of nucleolin by epithelial cells following exposure to enzymatically active purified Stx2. Stx2 also significantly enhanced the adherence of O157:H7 to host cells, with the Stx2-expressing wild type strain binding more effectively to epithelial cells in tissue culture than the isogenic *stx2* deletion mutant, and showing higher colonisation of BALB/c mice (Robinson *et al.*, 2006).

The link between the Type 3 Secretion System and Stx is likely to be a complex one. There is evidence that the presence of Stx phages may cause repression of the T3SS at the transcriptional level. In particular, O157:H7 phage type p21/28, which is the most prevalent strain linked with human EHEC infections in the UK, has high carriage rates of both Stx2a and Stx2c (90%), and yet lower median levels of Type 3 secretion compared to O157:H7 strains in which carriage of these phages is lower (28%). Strains that were genetically manipulated to delete Stx2 phages increased Type 3 secretion, and addition of the Stx2 phage to strains that naturally lack this phage resulted in decreased secretion (Xu *et al.*, 2012). This was further confirmed by Xu *et al.* (2012) in an Stx-negative K-12 *E. coli* strain in which the presence of a genome-integrated Stx2 phage was demonstrated to repress induction of Type 3 gene expression. A promoter fusion reporter whose expression of fluorescence was controlled by Ler, the major regulator of Type 3 expression, was transformed into the K12 strains and used to measure Type 3 secretion. Ler was expressed from an IPTG-inducible plasmid, as K12 does not naturally carry the gene encoding this protein. The K12 strain containing the Stx2 phage showed lower levels of fluorescence production, implying that the phage represses Ler-mediated promoter activation. This repression involved the *cil* phage regulator and reduced expression of the *cl* repressor, which had no direct impact on Type 3 secretion in the absence of an

1. INTRODUCTION

integrated Stx prophage. A model based on these findings proposes that colonisation of epithelial cells via regulation of the T3SS is coordinated in part by Stx2-encoding bacteriophages. This regulation could select for co-acquisition of other genes that encode Type 3-secreted proteins and regulators that can overcome this Stx phage-mediated control (Xu *et al.*, 2012).

There is strong evidence that the Stx proteins are involved in the activation of inflammation in the host. This response, which is fundamental to the elimination of invading pathogens, involves the synthesis and release of cytokines and chemokines by immune cells. Studies have reported that interleukin 8 (IL-8), a chemokine and important mediator of the innate immune system response, is upregulated by the presence of Stx. Stx has been proposed to work synergistically with flagellin, the principal component of the bacterial flagella, to produce superinduction of IL-8 that leads to absorption of Stx into systemic circulation (Jandhyala *et al.*, 2010). Other components of the inflammatory response, including interleukin 6 (IL-6), macrophage chemoattractant protein 1 (MCP-1) and macrophage inflammatory protein 1 α/β , have been implicated in the response to Stx (reviewed by Lee *et al.*, 2013). The elicitation of these responses is achieved through the activation of multiple cell signalling pathways, including those initiated through ribosomal stress. This occurs during Stx-mediated depurination of the ribosome, resulting in activation of multiple mitogen-activated protein kinase signalling pathways (Smith *et al.*, 2003). Stx can also stimulate circulating proinflammatory cytokines such as tumour necrosis factor- α (TNF- α) and interleukin 1 β (IL-1 β) by directly acting on monocytes, which results in the further production of the Gb3 receptor, further sensitising epithelial cells to the effects of Stx (van de Kar *et al.*, 1992). However, there is also evidence that EHEC produce an anti-inflammatory molecule that attenuates the inflammatory responses to its own Stx, possibly to limit the host immune response when bacteria are present. In contrast, Stx that have been translocated across the epithelium and away from EHEC can produce unimpaired toxin-mediated inflammatory responses (Bellmeyer *et al.*, 2009).

1. INTRODUCTION

1.3.8 The significance of Stx outside of the human host

Humans are considered an incidental host for O157:H7 as, while human-to-human transmission is possible, spread is frequently limited to outbreak situations and thus humans are considered insufficient hosts for sustainability. In contrast, ruminant animals are the primary host of O157:H7 and other EHEC members. Despite long-term persistence, infection is asymptomatic in ruminants, which is associated with a lack of host Gb3 receptors at sites of bacterial colonisation. This raises a question regarding the function of Stx in O157:H7 given that humans are not considered the intended biological target, especially as Stx phages are found in the genomes of EHEC at high frequency. These phages are lysogenic and their reproduction results in killing of the bacterial host so, while expression of their genes is usually inhibited, their presence in bacteria carries the risk of bacteriophage production and subsequent cell lysis. Therefore, there must be an evolutionary advantage for bacterial carriage of Stx phage in many EHEC strains.

One hypothesis is that the purpose of Stx is to defend bacterial populations from unicellular eukaryotic predators. This is supported by coinfection studies that mixed the grazing protzoa *Tetrahymena pyriformis* with O157:H7 strains positive and negative for Stx phages. The presence of Stx-encoding prophages was found to be advantageous for the bacteria, as it increased the survival rate of O157:H7 following ingestion into the *T. pyriformis* food vacuole (Steinberg & Levin, 2007). Stx has also been shown to provide protection against killing by another protozoan bacterivore, *Tetrahymena thermophila*. Studies by Lainhart *et al.* (2009) found that *T. thermophila* was killed in the presence of both Stx-producing bacteria and purified Stx, while Stx-producing bacterial strains also displayed a growth advantage over Stx-negative strains. This production and release of Stx in response to *T. thermophila* is thought to be triggered by bacterial detection of reactive oxygen species released by the predator. This activates the SOS response, resulting in production of Stx which is released into the surrounding environment following bacterial lysis (Lainhart *et al.*, 2009).

Stx has also shown antiviral activity, with the A subunit of Stx1 found to reduce the production of bovine leukemia virus (BLV) particles *in vitro* (Ferens *et al.*, 2004). Furthermore, rates of BLV viraemia, as assessed by spontaneous lymphocyte

1. INTRODUCTION

proliferation, was significantly lower in sheep given wild type O157:H7 than those treated with an Stx-negative mutant (Ferens *et al.*, 2006). This has been further corroborated by a year-long study assessing animal health and the prevalence of Stx-producing *E. coli* in BLV-infected sheep, which showed a convincing correlation between animals in good health and high levels of Stx-producing *E. coli*. In contrast, poor health and tumour development only occurred in animals with low levels of Stx-producing *E. coli* (Ferens *et al.*, 2008).

These findings may explain the tolerance of EHEC for the carriage of a toxin whose production is strongly associated with cell death, especially if this strategy enables survival of a bacterial population rather than that of individual organisms. If lysis of a small percentage of the bacterial population results in the release of sufficient Stx to ensure the survival of daughter cells, this may be a cost-effective defense strategy for the population. One argument against this altruism hypothesis (reviewed in further detail by Loś *et al.*, 2012) is that a spontaneous induction rate (phages produced in the absence of any inducing agents) of 0.005% cells per generation for Stx prophages, while considered low, is significantly more frequent than any other lambdoid phage (Livny & Friedman, 2004; Shimizu *et al.*, 2009). Similarly, the observation that Stx production and accompanying bacterial lysis occurs in many other situations where the toxin has no discernible purpose, such as induction by high hydrostatic pressure and UV light, rejects this theory. However, current research supports the suggested model of altruism (Loś *et al.*, 2012) and overall, there is a substantial amount of evidence that the Stx toxin has a far broader function than merely causing human disease.

1.4 The Type 3 Secretion System and the attaching/effacing lesion

E. coli contains several virulence factors that facilitate the attachment of bacteria to host cells. The most important one of these, the function of which is central to pathogenesis of EHEC and EPEC, is the Type 3 Secretion System, encoded by the locus of enterocyte effacement (LEE) pathogenicity island. In EHEC, the LEE consists of five major operons containing a total of 41 genes encoding structural proteins, regulators, effector proteins, and chaperone proteins. The major regulator of the LEE is Ler, a transcriptional activator

1. INTRODUCTION

essential for the expression of LEE-encoded genes and therefore attaching/effacing (A/E) lesion formation (Elliott *et al.*, 2000).

The T3SS is a multi-protein complex that spans the inner and outer bacterial membrane of Gram-negative organisms, with a thin needle-like structure protruding outside the bacterium where it can interact with the eukaryotic cell membrane. Bacterial proteins known as effectors are secreted directly by the T3SS into the cytoplasm of eukaryotic cells where they can hijack host signalling pathways, and aid bacterial survival by mechanisms such as promotion of attachment and invasion, immune system subversion, and cellular trafficking interference.

1.4.1 Structure of the T3SS

The T3SS is composed of three main structures: the needle complex, the translocon, and the basal body (Figure 1-7). The needle complex is a cylindrical structure, similar to the flagellar basal body, and is composed of the protein EscF which forms a helical structure. The needle complex extends to approximately 80 nm, although this can vary substantially between bacterial species. At the tip of the needle complex, the hydrophobic membrane-spanning proteins EspB and EspD form the translocon, a proteinaceous pore that is inserted directly into the host cellular membrane. Unique to the EHEC and EPEC T3SS is the tip protein EspA, which forms a highly extended filament at the end of the needle, an adaptation thought to be important for attachment to intestinal cells (Yip *et al.*, 2005). The basal body of the T3SS is made up of a number of different structural proteins, which form ring structures in both bacterial membranes. The inner membrane ring of the basal body is composed of the proteins EscD, EscQ, EscR, EscS, EscT, EscU and EscV, with the ATPase EscN facilitating transport of proteins through the complex, while the outer membrane ring is made up of EscC subunits. In the periplasmic space of the membrane and connecting these two rings is EscJ, a protein that shares sequence similarity with the central pore-forming flagellar protein FliF and is one of the first structural proteins involved in assembly of the T3SS, acting as a platform for the rest of the basal apparatus (Yip & Strynadka, 2006). A large number of chaperone proteins are also involved in T3SS assembly, and have roles such as preventing premature oligomerisation or degradation of the structural proteins.

1. INTRODUCTION

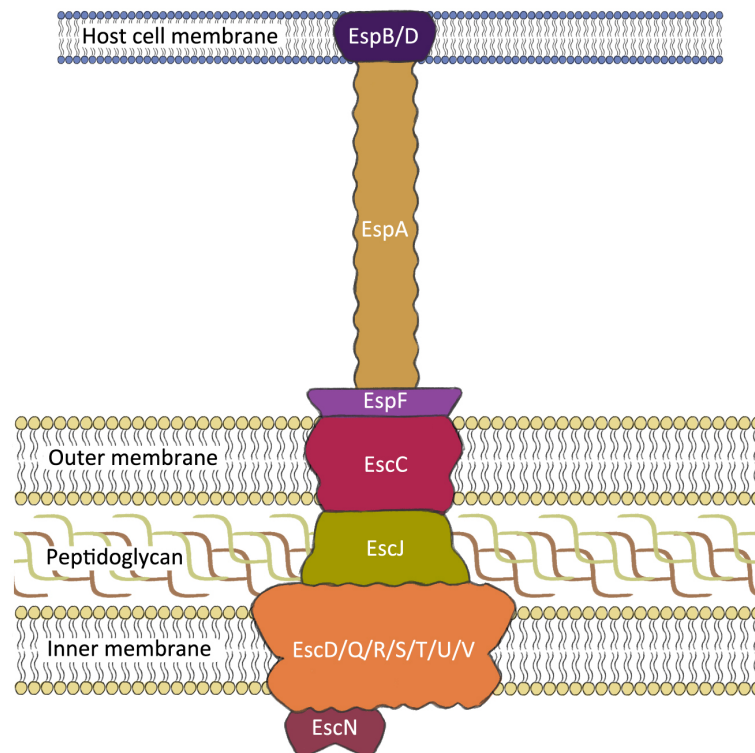


Figure 1-7: Structure of the T3SS apparatus. The basal body of the T3SS spans the bacterial inner and outer membrane and forms a base for the needle filament that comes into contact with and inserts into the host cell membrane.

1.4.2 Protein translocation by the T3SS

Activation of Type 3 secretion is strictly regulated by several influences including environmental factors, global regulators, and LEE-encoded regulators. The inner diameter of the EspA filament has been measured at 2.5 nm (Daniell *et al.*, 2003), too small to allow passage of structurally folded proteins. The effector proteins often have dedicated associated chaperone proteins, which are not exported with the effector. It has been implied that these proteins help target the export of effectors, provide storage of proteins in an appropriate state prior to export, and help mask cellular localisation domains (reviewed by Cornelis, 2006). In *Salmonella* Typhimurium, the ATPase EscN homologue InvC is involved in the unfolding of effector proteins prior to export by removal of the effector's chaperone (Akeda & Galán, 2005).

1. INTRODUCTION

1.4.3 T3SS-mediated formation of the attaching/effacing lesion

All genes required for formation of attaching/effacing lesions, including seven effector proteins, are encoded by the LEE. The first protein involved in T3SS-mediated attachment is Tir which, when injected into the host cytoplasm, is directed toward and inserted into the membrane so that its central domain is surface-exposed. This domain then interacts with the bacterial surface protein intimin, forming a tight attachment between the two cells (Kenny *et al.*, 1997). The intracellular domain of Tir contains several phosphorylation domains that, cooperatively with the secreted non-LEE-encoded effector EspF_U, interact with host proteins in the cytosol such as neuronal Wiskott-Aldrich Syndrome protein (N-WASP). N-WASP recruits the actin-related protein 2/3 (Arp2/3) complex, a major regulator of the actin cytoskeleton, which nucleates actin filaments and results in the accumulation of filamentous actin beneath the attached bacteria. This is accompanied by localised destruction of the intestinal microvilli and the formation of an actin-rich pedestal-like structure, the A/E lesion, which promotes bacterial colonisation (Figure 1-8). Other LEE-encoded effectors such as EspB and EspF are involved in the subversion of the host cytoskeleton, or have roles such as disruption of mitochondrial function (Kodama *et al.*, 2002; Dean *et al.*, 2010).

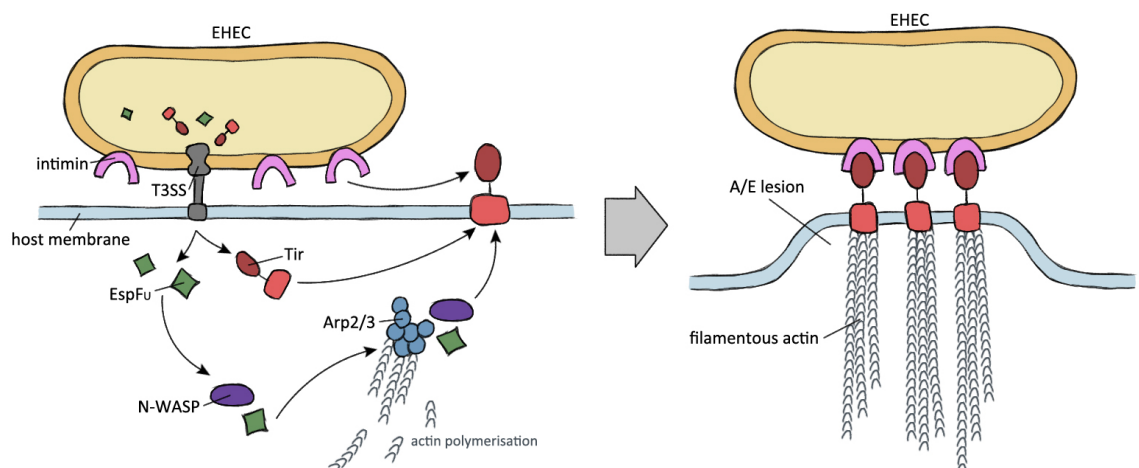


Figure 1-8: Basic representation of T3SS-mediated formation of the attaching/effacing lesion. The effectors Tir and EspF_U are translocated across the bacterial and host cell membrane by the T3SS into the cytosol of the host cell. Tir is inserted into the host cell membrane where it can bind to intimin on the outer surface of the bacteria. EspF_U targets N-WASP, resulting in recruitment of Arp2/3 and polymerisation of actin beneath the bacterium. This creates a tight attachment of bacteria to host cells on a pedestal of actin filaments.

1. INTRODUCTION

Many studies, both *in vitro* and *in vivo*, have implied that the capacity to form A/E lesions is associated with virulence, with bacteria lacking the essential proteins such as Tir and intimin showing a reduced capacity for epithelial cell attachment. In addition, EHEC strains unable to produce crucial components of T3SS-mediated attachment demonstrate reduced faecal shedding and a significant decrease in colonisation in cattle (Dziva, 2004; Naylor, 2005) providing further evidence that the T3SS is vital for successful persistence within its natural host.

1.5 Animal models of O157:H7

Evaluation of the effectiveness of anti-virulence strategies requires the availability of animal models that can recapitulate pathogenesis. Large animal models of EHEC infection include gnotobiotic pigs, cows, sheep, goats, chickens, macaques and baboons, and replicate many features of colonisation and disease (reviewed by Ritchie, 2014). However, smaller models such as mice, rats and rabbits are preferable due to their low costs, ease of breeding, handling, maintenance, and availability of inbred and transgenic strains. Although mice have been used as a small animal model for EHEC, *E. coli* does not naturally colonise the mouse intestine. Consequently, different treatments, including those that modify the local environment within the gut, have been tested in an attempt to provide a model in which EHEC-specific colonisation and disease symptoms can be observed.

1.5.1 The infant rabbit O157:H7 model

The O157:H7 infant (3-day-old) rabbit model, first developed in 1986, produces diarrhoea, histological changes in the colon, and bacterial attachment to epithelial intestinal cells. No additional treatment of the animal is required as EHEC readily colonises very young rabbits, and the production of Shiga toxin is important for the clinical symptoms of disease (Pai *et al.*, 1986). A study by Ritchie *et al.* (2003) using deletion mutants of O157:H7 has identified the roles of Stx2, intimin, and Tir in this model. In particular, Stx increased both the severity and duration of diarrhoea, while Tir and intimin were essential for colonisation and disease (Ritchie *et al.*, 2003). Although

1. INTRODUCTION

some *in vitro* studies have implied a role for Stx in T3SS-mediated attachment, Stx had no effect on intestinal colonisation or inflammation and, contrary to other studies which used this model, O157:H7 did not cause death in any of the animals. Lack of HUS symptoms in this model most likely reflects a lack of Gb3 receptors on kidney cells of rabbits (Zoja *et al.*, 1992). However, the combination of bacterial adhesion and Stx-induced illness make this model particularly valuable for studying O157:H7 pathogen-host interactions.

1.5.2 O157:H7 mouse models

The first mouse model for pathogenesis of O157:H7 was developed by Wadolkowski *et al.* in 1990 and was based on previous models for other *E. coli* strains (Myhal *et al.*, 1982). Within this model, mice were treated with streptomycin in their drinking water prior to infection to reduce the normal gut flora and thus competition for O157:H7 (Wadolkowski *et al.*, 1990). Streptomycin was determined to be a suitable antibiotic as it greatly reduced the number of facultative anaerobic bacteria shed faecally by the mice, and because its activity was directed toward protein synthesis and not cell wall biogenesis. In this respect, any resistance would be less likely to interfere with cell wall components involved in colonisation (Myhal *et al.*, 1982). In the O157:H7 model, 5- to 8-week-old male outbred ICR mice were provided with 5 g/L streptomycin in their drinking water for one day, followed by removal of food and water for 24 hours before oral infection of 10^{10} CFU O157:H7. Bacterial colonisation was monitored by faecal shedding, revealing that the organism was shed at levels of approximately 10^7 CFU/g faeces for a period of 25 days. Lack of symptoms highlighted that this was a strong model of colonisation but not disease. After culling of the animals, O157:H7 was recovered from epithelial cells of the small intestine, caecum, and large intestine, indicating that these are the sites of colonisation in this model (Wadolkowski *et al.*, 1990).

Other O157:H7 mouse models, each with advantages and limitations, have been developed in order to replicate aspects of infection (reviewed by Mohawk & O'Brien, 2011). Diet restriction, as used in the protein-calorie malnutrition model, lowers the infectious dose required for colonisation and disease. This is pertinent as humans are sensitive to low doses of the organism (<100 CFU), unlike the streptomycin-treated model

1. INTRODUCTION

in which relatively high doses are required for effective mouse colonisation ($\sim 10^9$ - 10^{10} CFU). In this model, protein in the diet is restricted to 5% (as opposed to the 25% protein control diet) for two weeks prior to infection. Subsequent intragastric inoculation of 2×10^6 CFU O157:H7 resulted in colonisation and, five days post infection, induction of neurological symptoms, which are considered an important predictive factor for HUS mortality in children. Ten days after infection, 75% of the protein-calorie restricted mice had died from cerebral haemorrhage while the control mice remained healthy, although no significant kidney pathology in infected mice was observed (Kurioka *et al.*, 1998).

Gnotobiotic mice, which lack competitive intestinal flora, have also been used as models. In these mice, infectious doses similar to those used in the streptomycin-treated model have been shown to cause disease and death within 7 days without the need for streptomycin treatment. Studies by Isogai *et al.* (1998) showed that a lower infectious dose (2×10^3 CFU) in the gnotobiotic model could result in colonisation in the absence of disease symptoms. However, when mice were pretreated with TNF- α , a cytokine induced by Stx with renal-damaging properties (Harel *et al.*, 1993), the animals developed severe neurotoxic symptoms and kidney pathology. The mice showed evidence of a strong contribution by cytokines to initiation of damage in the brain and kidney (Isogai *et al.*, 1998).

Models of HUS using C57BL/6 mice have also been developed. The coadministration of LPS and Stx2 has shown reproduction of major HUS symptoms such as thrombocytopenia, haemolytic anemia, and renal failure (Keepers *et al.*, 2006), while outer membrane vesicles of O157:H7 containing LPS and Stx2 produced HUS-like symptoms (Kim *et al.*, 2011). A mouse model that does not require the presence of LPS has also been established, whereby multiple sublethal doses of endotoxin-free Stx2 injected intraperitoneally over 7-8 days produce symptoms similar to that of HUS in humans: increased blood urea nitrogen and serum creatinine levels, proteinuria, glomerular endothelial damage, haemolysis, leukocytopenia, and neutrophilia (Sauter *et al.*, 2008).

1.5.3 *Citrobacter rodentium* as an O157:H7 surrogate model of infection

As O157:H7 and other EHEC are poorly pathogenic in mice, models often require alteration of the 'natural' niche, including disruption of the host microbiota. To avoid such

1. INTRODUCTION

complications, an alternative approach makes use of the natural murine pathogen *Citrobacter rodentium*, which readily colonises the large intestine of the mouse. *C. rodentium* is related to EHEC and EPEC (Figure 1-9) and, like these pathogens, produces a T3SS that is required for the formation of A/E lesions. Oral challenge of mice with 10^8 - 10^9 CFU allows initial colonisation of the lymphoid tissue surface in the caecum (caecal patch) followed by colonisation of the distal colon a few days later, with the bacteria cleared from the host after 3-4 weeks (Wiles *et al.*, 2004). Infection of mice with *C. rodentium* can result in colonic hyperplasia, a thickening of the colonic tissue, although in most mouse strains this does not result in mortality.

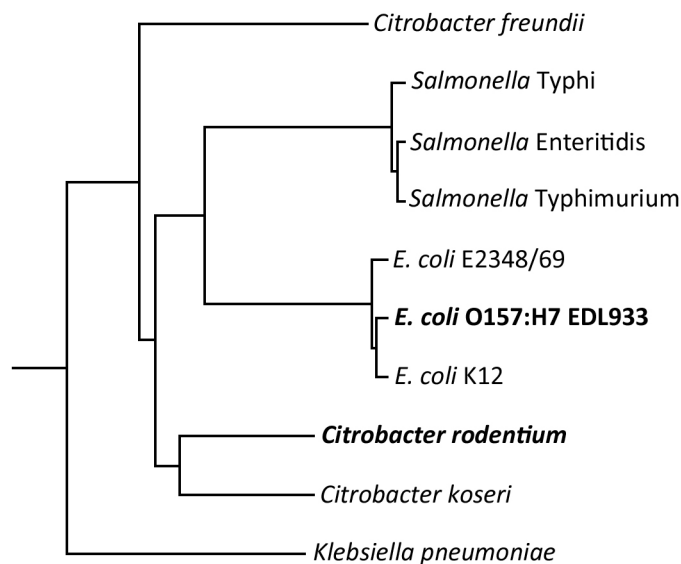


Figure 1-9: Phylogenetic tree showing the relationship of *C. rodentium* to *E. coli* and other enteric bacteria. Phylogenetic relationships were determined from the nucleotide sequences of seven housekeeping genes (Petty *et al.*, 2010).

The *C. rodentium* LEE is closely related to the LEE of EHEC and EPEC (Deng *et al.*, 2001). Genome sequencing has revealed that *C. rodentium* contains a LEE pathogenicity island, along with genes encoding 29 T3SS effectors, 22 of which encode all the core effectors of the EPEC E2348/69 strain. EHEC and *C. rodentium* also share many other virulence factor genes, such as those for fimbriae and adhesins, many of which are located on mobile genetic elements (Petty *et al.*, 2010). The *C. rodentium* T3SS and the effectors involved in A/E lesion formation are required for colonisation, with strains in which genes encoding intimin or EspB have been mutated showing no virulence in mice as a consequence of colonisation failure (Schauer & Falkow, 1993; Newman *et al.*, 1999). While this makes

1. INTRODUCTION

Citrobacter rodentium an excellent model for studying colonisation and A/E lesions *in vivo*, it lacks many other O157:H7 genes, including those encoding Stx, and therefore does not produce symptoms associated with EHEC disease.

A novel *C. rodentium* strain has recently been developed to address the issue of Stx production. Mallick *et al.* (2012) constructed a *C. rodentium* strain capable of producing Stx by inserting the Stx2dact phage genome into the *C. rodentium* chromosome. The resultant strain $\lambda\text{stx}_{2\text{dact}}$ expresses the Stx2dact toxin and lyses bacteria at levels similar to that of O157:H7. When this strain was tested in inbred C57BL/6 mice it produced lethal infection, with all mice succumbing to death after 4-9 days. *Citrobacter* ($\lambda\text{stx}_{2\text{dact}}$)-infected animals displayed significant weight loss (10-20% of starting weight) and increasing faecal water content. While the overall level of colonisation was similar to that of the wild type, the Stx strain produced some pathological changes associated with human EHEC infection. These included increased levels of renal cytokines and Stx-mediated damage as determined by histopathological evaluation of tissue. While the kidneys did not show a strong inflammatory response, there was evidence of proximal tubule injury such as flattened epithelium, loss of luminal brush border, and sloughing of dead cells (Mallick *et al.*, 2012). Although this model may not display all features associated with EHEC disease and HUS, the production of both A/E lesion formation and Stx-mediated tissue damage greatly increases the functionality of *C. rodentium* as an EHEC alternative.

1.6 Development of a human vaccine to prevent O157:H7 infections

The mortality rate of EHEC infections, the risk of severe and long-term HUS sequelae, the limited treatment options available, and the high cost of EHEC outbreaks – not merely that of health care but also the substantial financial impact on the agriculture industry during and after human outbreaks – implies a need for effective vaccines against EHEC. However, given the relatively low incidence of EHEC infection compared to other infectious bacterial species, the high cost of general immunisation may be discouraging to health care providers. Selective immunisation of individuals or groups at high risk of infection is also hindered by the sporadic, unpredictable nature of human EHEC outbreaks and the fact that the vast majority of infections arise from unknowingly ingesting

1. INTRODUCTION

contaminated food rather than by human-human or animal-human contact. A broad-spectrum vaccine against multiple pathotypes of *E. coli* may therefore be a more viable and cost-effective approach to preventing EHEC outbreaks.

1.6.1 The case for a broad-spectrum *E. coli* vaccine

Antibiotic resistance is a growing problem for treatment of bacterial pathogens, including that of *E. coli*. Diarrhoeal infections caused by *E. coli* are often self-limiting and managed by rehydration therapies, but persistent infections by some pathotypes are often treated by antimicrobials. Resistance of *E. coli* has been observed for penicillins, cephalosporins, aminoglycosides and fluoroquinolones, while emerging multi-drug resistance phenotypes, involving coresistance to four or more unrelated families of antibiotics has also been reported (reviewed by Croxen *et al.*, 2013). Recently, a UPEC isolate from a patient in the USA was found to carry a plasmid conferring resistance against colistin, a last-resort antibiotic. This particular phenotype had previously only been reported in China and Europe, and while the strain was still susceptible to other antibiotics there is the concern that this plasmid and the resistance it provides could be transferred to other strains of multi-drug resistant bacteria (McGann *et al.*, 2016).

Prophylactics for management of pathogenic *E. coli* are therefore of significant interest, and vaccines against all pathotypes are currently being developed and evaluated. While an EHEC-specific vaccine may not provide enough economic incentive in order to be widely adopted, a vaccine that protects against major EHEC strains as well as other *E. coli* pathotypes with high clinical importance would be greatly desirable and have a major impact on global human health. This approach has recently been explored in a study that tested *in vivo* a vaccine consisting of a killed whole-cell mixture of EAEC, EPEC, EIEC, EHEC and ETEC pathotypes. When mice were subcutaneously immunised with this combined vaccine candidate, a significant increase in survival compared to non-immunised controls after challenge with a living combination of the five *E. coli* pathotypes was observed, as was a significant increase in immunological responses (Gohar *et al.*, 2016). The authors of this study suggest that this combined vaccine is a cost-effective approach with promise for further testing in humans. Another possible tactic may be development of a multi-subunit vaccine, which presents several bacterial antigens to the immune system. If these

1. INTRODUCTION

selected antigens are highly conserved across *E. coli* strains and pathotypes, this may provide the vaccine with broader coverage across different pathotypes.

1.6.2 EHEC vaccine development: Stx vaccines

Several approaches towards the development of a protective vaccine against EHEC have been undertaken. As Stx1 and Stx2 play a crucial role human disease and risk of HUS, the ability to induce neutralizing antibodies to Stx is attractive. Additionally, targeting this antigen offers the potential to provide an effective vaccine against other non-O157:H7 EHEC strains, an important consideration given that other EHEC strains are responsible for a large number of outbreaks and cases of HUS.

Vaccination with inactive Stx derivatives effectively induces the production of neutralising antibodies and protects against toxemia in mouse models (Ishikawa *et al.*, 2003; Marcato *et al.*, 2005). A live attenuated O157:H7 vaccine constructed by Liu *et al.* (2009) has also shown promise in mouse models. This attenuated vaccine consisted of an O157:H7 *ler stx* deletion mutant transformed with a plasmid containing *stx1* and *stx2* (under the control of their own promoters) with mutations in the active center and membrane-spanning region of the toxin A subunit. This strain significantly reduced toxicity in comparison with wild type O157:H7 with no clinical signs of disease displayed by infected mice. Importantly, mice immunised with this vaccine strain were protected against subsequent challenge with wild type O157:H7 and, when pregnant females were immunised, this protection was shown to be horizontally transmitted to suckling newborns (Liu *et al.*, 2009).

A DNA vaccine based on a non-toxic Stx2 gene consisting of the last 32 amino acids of the A2 subunit sequence and the complete B subunit also generates a systemic Stx-specific antibody response that targets both subunits of native Stx2. Antibodies against Stx2 raised by mice immunised with this vaccine had toxin-neutralising activity *in vitro* and conferred partial protection against Stx2 challenge *in vivo* (Bentancor *et al.*, 2009). Other Stx-based vaccine approaches such as protein-conjugated polysaccharides (Konadu *et al.*, 1999), purified B subunit (Zhu *et al.*, 2008), and synthetic peptides derived from the B subunit (Harari & Arnon, 1990) have exhibited varying degrees of protection and toxin

1. INTRODUCTION

neutralisation. However, these candidate vaccines have not yet proceeded beyond animal tests, partly due to the inherent difficulty of organising human trials, as EHEC outbreaks are sporadic and unpredictable.

1.6.3 EHEC vaccine development: reverse vaccinology

Other conventional approaches to *E. coli* vaccines have relied on surface-expressed proteins, such as the adhesin P fimbriae (Roberts *et al.*, 2004) and type 1 pilus subunits (Langermann *et al.*, 1997). These conferred protection in cynomolgus monkey and mouse models respectively, but failed to show sufficient efficacy in phase II clinical trials (Brumbaugh & Mobley, 2012). However, the availability of genomic sequences from multiple isolates of particular pathogens is providing a rich resource for vaccine candidate identification. Subtractive reverse vaccinology, which employs bioinformatic analysis of genomes to identify potential antigens, was first used in the development of the recently licensed vaccine against *Neisseria meningitidis* Serogroup B (Pizza *et al.*, 2000). This approach has subsequently been applied to other bacterial pathogens including *S. aureus* and *Streptococcus pneumoniae*. Reverse vaccinology offers more rapid progress than conventional vaccinology, and has the advantage of identifying virtually every single antigen in a pathogen (with the exception of non-protein antigens such as polysaccharides and glycolipids), including those that are not intrinsically immunogenic and those whose expression is transient or limited under conditions of *in vitro* cultivation (Rappuoli, 2000).

Reverse vaccinology was recently employed to identify antigen candidates for inclusion in a vaccine against extraintestinal pathogenic *E. coli* (ExPEC) (Moriel *et al.*, 2012). This approach aimed to determine potential targets by comparison of the sequenced genome of the K1 ExPEC strain IHE3034 with other ExPEC and non-pathogenic strains. The K1 strain contained 19 genomic islands that were not present in non-pathogenic strains, accounting for approximately 20% of the total K1 genome. These islands contained genes for 230 unique surface-associated or secreted proteins, 220 of which were successfully purified using His-tag technology. The protective efficacy of these proteins in mice was determined by subcutaneous injection followed by infection with pathogenic *E. coli* strains. Nine of these proteins induced a significant level of protection compared to the

1. INTRODUCTION

control group, with a protective efficacy ranging from 13-82%. These antigens were not only present in ExPEC strains, but conserved in many other pathogenic *E. coli*, including EHEC strains, raising the possibility of their use in a broadly cross-reactive *E. coli* vaccine (Moriel *et al.*, 2010).

1.6.4 Animal vaccines against O157:H7

Prophylactic treatments against O157:H7 are not limited just to humans; animal vaccines that target O157:H7 in its reservoir host are also of interest, as reduction of carriage in cattle may lower the risk of foodborne outbreaks. Two cattle subunit vaccines have been approved for use in Canada and the US: Econiche, which raises antibodies against Type 3-secreted proteins (Potter *et al.*, 2004), and EpiTox SRP, which targets O157:H7 siderophore receptor and porins (Fox *et al.*, 2009). Although their use has been predicted to result in an 85% reduction in human cases (Matthews *et al.*, 2013), uptake by farmers has been low. This is largely because the conditional license restrictions of EpiTox SRP limits purchase to licenced veterinarians, and the production of Econiche has been recently discontinued.

1.7 Development of a therapeutic treatments for O157:H7 infections

The use of antibiotics to treat infections caused by Stx-expressing bacteria is largely avoided to prevent the increase in Stx expression and release caused by the bacterial lysis they stimulate, and the subsequent increased risk of HUS development. Wong *et al.* (2000) assessed the risk of HUS in 71 antibiotic-treated children with O157:H7 infections, finding the relative risk of HUS development to be 17.7 for those administered the antibiotic trimethoprim-sulfamethoxazole, and 13.4 for those administered beta-lactams. *In vitro* studies by McGannon *et al.* (2010) have suggested that the increase of Stx production depends on the class of antibiotic used. Addition of sub-inhibitory concentrations of the DNA synthesis-targeting antibiotics ampicillin, trimethoprim-sulfamethoxazole and ciprofloxacin increased Stx production, while the cell wall, ribosome, or RNA polymerase-targeting antibiotics azithromycin, doxycycline, phosphomycin and gentamycin showed little ability to induce Stx production, with some

1. INTRODUCTION

resulting in decreased Stx production when compared to untreated O157:H7. Additionally, when bacteria were exposed to much higher growth-inhibiting levels of ciprofloxacin, levels of Stx were still very high even when bacterial growth was completely suppressed (McGannon *et al.*, 2010). Other forms of treatment are also discouraged, with anti-motility agents and narcotics associated with increased HUS risk and HUS-induced neurological effects. Non-steroidal anti-inflammatory agents should also be avoided due to their impact on renal blood flow (Tarr *et al.*, 2005). There is therefore a urgent need for alternative therapeutic options that restrict EHEC colonisation or toxin expression, release or binding, without initiating additional Stx production.

Bacterial virulence factors are a promising target for novel inhibitors, as interference with mechanisms essential for bacterial colonisation and disease symptoms, such as adherence to and invasion of host cells, production of toxins, and avoidance of host immune responses, provide an opportunity to prevent disease without modifying the prevalence of these strains. Without the capacity to colonise and cause harm to the host, the bacteria can be rapidly cleared by both the host immune response and by competition from commensal bacteria. Unlike traditional antibiotics which work to either kill or inhibit growth, this strategy is attractive as by inhibiting bacterial functions non-essential for survival, there is potentially less selection pressure to drive the emergence of drug-resistant mutants, which may decrease the rate at which resistance occurs (Allen *et al.*, 2014). Specific targeting of virulence determinants also has the advantage of avoiding alteration of the host microbiota, which could prevent the development of diseases associated with disruption of the gut flora, such *Clostridium difficile* infections.

1.7.1 Inhibition of Stx expression and binding to host receptors

Bacterial toxins such as Stx are an obvious target for anti-virulence-based approaches, given their crucial role in disease symptoms. One strategy that targets Stx currently under investigation is inhibition of quorum sensing, a mechanism used by bacteria in the regulation of gene expression in response to changes in the bacterial population density. This involves the secretion and detection of signalling molecules known as autoinducers by growing bacteria, which regulate many bacterial physiological activities including that of toxin release (Zhu *et al.*, 2002) and other virulence factors such as the T3SS and flagella

1. INTRODUCTION

(Kanamaru *et al.*, 2000; Sperandio *et al.*, 2002). An O157:H7 strain with a mutation in the *luxS* gene, whose product is involved in synthesis of the autoinducers AI-2 and AI-3, produced less Stx2 when compared to the wild type strain (Sperandio *et al.*, 2001), suggesting that inhibition of essential stages of quorum sensing may reduce or prevent production of Shiga toxin.

Virulence gene expression can also be modulated by chemical signals within the host. The adrenergic receptor QseC acts as a receptor for the mammalian stress response hormones epinephrine and norepinephrine, and in EHEC has been shown to activate expression of metabolic, virulence and stress response genes, including that of *stx2* via *recA* (Hughes *et al.*, 2009). When a rabbit model was infected with EHEC strains containing a *qseC* deletion, these strains were attenuated for virulence (Clarke *et al.*, 2006). These findings led to high-throughput screening by Rasko *et al.* (2008) to find inhibitors for QseC, which identified the small molecule LED209. LED209 is highly selective for QseC and prevents its autophosphorylation by allosteric modification of lysines, consequently limiting activation of virulence gene expression (Rasko *et al.*, 2008; Curtis *et al.*, 2014). Importantly, LED209 showed no overt toxicity to mammalian or bacterial cells, and did not inhibit bacterial growth. In addition, secretion of the LEE-encoded proteins EspA and EspB was inhibited by LED209 *in vitro*, reducing formation of A/E lesions and activation of the bacterial SOS response, thus preventing Stx production. However, treatment of EHEC-infected rabbits with LED209 did not produce a statistically significant decrease in colonisation, which may be a reflection of the rapid absorption of the drug from the gastrointestinal tract that may be overcome by the development of a non-absorbable formulation of the drug (Rasko *et al.*, 2008). Furthermore, in several other plant and animal pathogens such as *S. Typhimurium* and *Francisella tularensis*, QseC expression is inhibited by LED209 (Curtis *et al.*, 2014), raising the possibility of its development as a broad-spectrum antimicrobial treatment.

Other attempts to develop therapies based largely on preventing Stx binding to Gb3 receptors have met with limited success. In clinical trials in which children with EHEC-associated HUS were treated with the drug SYNSORB Pk, designed to bind to Gb3 and thus limit Stx binding, no reduction of disease severity was observed (Trachtman *et al.*, 2003). Compounds that mimic Gb3 in order to bind Stx and prevent it from reaching its

1. INTRODUCTION

target have also been developed, showing efficacy both *in vitro* and *in vivo*, although successful clinical trials have remained elusive (Nishikawa *et al.*, 2005; Kitov *et al.*, 2000).

Given the importance of the T3SS in establishment of infection by a broad spectrum of Gram-negative pathogenic bacteria, many studies have investigated its inhibition as a therapeutic anti-virulence strategy, and a number of inhibitors effective against the T3SS of *Yersinia*, *Chlamydia*, *Salmonella* and *E. coli* species have been identified. One particularly well-characterised group of T3SS inhibitors are the salicylidene acylhydrazides (SAs), identified by high-throughput screening in *Yersinia pseudotuberculosis* (Kauppi *et al.*, 2003). These compounds are effective against a number of pathogenic species including *Shigella flexneri*, *S. Typhimurium* and EHEC, without showing any antibacterial activity (Veenendaal *et al.*, 2009; Hudson *et al.*, 2007; Tree *et al.*, 2009). Although the mode of action of the SAs is yet to be elucidated, their targets in O157:H7 have been identified as WrbA, Tpx and FolX, proteins conserved across many Gram-negative species and involved in regulation of T3SS gene expression. This has led to the working hypothesis that the SAs affect expression of the T3SS via a synergistic effect caused by perturbation of several regulatory proteins (Wang *et al.*, 2011).

1.7.2 Modified bacteriocins

Another potential bacterial treatment is the use of bacteriocins, toxic proteins produced by bacteria that target other bacterial strains, including those of the same species as the bacteriocin-producing strain. Colicins are bacteriocins synthesised exclusively by *E. coli* for use against other closely related *E. coli* strains, and display varying modes of action depending on the colicin type. These include inhibition of macromolecular synthesis, DNA breakdown, and inhibition of protein synthesis (Nomura, 1963). Unfortunately, the reported enhancement of Stx production by O157:H7 upon treatment with DNase colicins, caused by induction of the SOS response in response to colicin-produced DNA damage, limits their potential as treatments against Stx-producing pathogens (Toshima *et al.*, 2007).

However, pyocins produced by *Pseudomonas aeruginosa* strains that have been adapted to target *E. coli* instead of *P. aeruginosa* have shown promise. Of particular interest are

1. INTRODUCTION

the R-type pyocins, which form structures that resemble tails of bacteriophages and insert themselves into the bacterial cell membrane upon contact with specific cell receptors. Once in the membrane these pyocins form a pore, resulting in membrane depolarisation and death of the bacterium (reviewed by Michel-Briand & Baysse, 2002). Recent studies using modified pyocins have shown potential as a treatment of EHEC infections. A novel pyocin that targets O157:H7 by recognising and degrading the O157 lipopolysaccharide, AVR2-V10, was constructed by fusion of the tail spike protein from O157-specific phage ϕ V0 to an R-type pyocin tail fiber. Killing of O157:H7 by AVR2-V10 was highly efficient and specific, and did not induce Stx production (Scholl *et al.*, 2009). *In vivo* testing of the variant AVR2-V10.3 in an infant O157:H7 rabbit model showed that the pyocin reduced diarrhoea, intestinal inflammation, bacterial carriage and faecal shedding, and was equally effective if the pyocin was administered prophylactically or therapeutically (Ritchie *et al.*, 2011). This work clearly demonstrates the potential of pyocins in treatment of O157:H7, although further optimisation of delivery and clinical trials are required. The potent bactericidal activity of pyocins, combined with their ability to specifically target certain bacterial species, make them an attractive new development.

1.7 Project aims

The intent of this project is to further the understanding and development of new prophylactic and therapeutic treatments for O157:H7 and other *E. coli*. We aimed to test the hypotheses that a) the T3SS contributes towards colonisation of mice by EHEC, b) the potential vaccine candidate proteins EaeH and YghJ are expressed by EHEC O157:H7 and EAEC LF82, and c) Shiga toxin expression by O157:H7 is inhibited by a recently-identified small molecule.

The main objectives of this project are:

- 1. Establishment of a mouse model suitable for *in vivo* assessment of novel EHEC anti-virulence compounds.**

Animal models are an essential step in the development of new anti-virulence drugs, revealing whether compounds that have proven activity *in vitro* are able to work *in vivo*, identifying possible side-effects, and determining whether they can proceed to human clinical trials. They also allow the issue of drug delivery to the site of infection to be addressed; for example, a drug taken orally that targets an intestinal infection has to avoid being degraded by the stomach and intestine in order to reach the site of bacterial colonisation. We are interested in testing a number of different compounds that aim to prevent colonisation or toxin production in mice, and therefore require a model that can consistently replicate these features.

- 2. Investigation of two novel *E. coli* proteins identified by reverse vaccinology as protective antigens for ExPEC infection. This focuses on the suitability of these antigens as candidates for a general, broad-spectrum *E. coli* vaccine.**

Reverse vaccinology has identified a number of novel antigens that provide protection against ExPEC infection using a mouse transurethral challenge model (Moriel *et al.*, 2010). Many of these antigens are conserved across a large number of pathogenic *E. coli*, raising the possibility of their use in a broad-spectrum *E. coli* vaccine. We intend to investigate the expression and role in pathogenesis of two of these antigens, EaeH and YghJ, in

1. INTRODUCTION

O157:H7 (EHEC) and LF82 (EAEC) backgrounds, to evaluate their potential as candidates for a vaccine against these strains.

3. Characterisation of a novel compound identified by high-throughput screening as a potential inhibitor of Stx expression, with the aim of uncovering its mode of action.

A small compound has recently been identified by high-throughput screening by the group of Prof. David Gally at the University of Edinburgh as a potential inhibitor of Shiga toxin production. We intend to assess the Stx-inhibiting effect of this compound and several other modified versions, and to identify the mechanism by which this inhibition occurs. This may eventually determine whether these compounds have potential for use as therapeutic agents in humans.

Chapter 2: Materials & Methods

2.1 Chemicals, growth media and buffers

2.1.1 Chemicals

Chemicals used were purchased from Sigma-Aldrich, Invitrogen and Fisher Scientific, unless otherwise stated.

2.1.2 Bacterial growth media

Growth media was prepared in deionised water (dH₂O) and sterilised by autoclaving or filtration with 0.2 µm filters. Luria-Bertani broth (LB), tryptic soy broth (TSB) and M9 minimal media was prepared as described in Table 2-1. Dulbecco's Modified Eagle's Medium (DMEM) and Minimal Essential Media (MEM) with 4-(2-hydroxyethyl)-1-piperazineethanesulfonic acid (HEPES) modification (MEM-HEPES) was purchased from Sigma-Aldrich (#M7278). All media was prepared by addition of dH₂O to dry ingredients followed by autoclaving. For M9 minimal media, glucose was omitted from the dry ingredients prior to autoclaving, and added to media (in sterile H₂O, after filter sterilisation) after autoclaving. Solid media was prepared by addition of 15 g/L agar to liquid growth medium prior to autoclaving.

Table 2-1: Bacterial growth media recipes.

Media	Components per litre
Luria-Bertani (LB)	10 g tryptone
	5 g yeast extract
	10 g NaCl
Tryptic Soy Broth (TSB)	30 g TSB (Sigma Aldrich, #22092)
M9 Minimal Media	6.8 g Na ₂ HPO ₄
	3 g KH ₂ PO ₄
	0.5 g NaCl
	1 ml 1 M MgSO ₄
	100 µl 1 M CaCl ₂
	4 g glucose

2. MATERIALS & METHODS

2.1.3 Growth media supplements

Antibiotics were prepared as concentrated stock solutions in either dH₂O or 100% ethanol, and were filter sterilised. Stocks were stored at -20°C and used at final concentrations in Table 2-2.

Table 2-2: Antibiotic concentrations for bacterial growth media used in this study. Asterisks denote those antibiotics prepared in ethanol.

Antibiotic	Final concentration (µg/ml)
Ampicillin	100
Kanamycin	50
Chloramphenicol *	25
Erythromycin *	500
Ciprofloxacin	0.05
Tetracycline	6

Isopropyl β-D-1-thiogalactopyranoside (IPTG) was prepared as a 1 M stock in dH₂O, filter sterilised, and used at a final concentration of 1 mM to induce protein overexpression.

2.1.4 Buffers

All buffers were made using dH₂O and sterilised by autoclaving or filtering where necessary. Phosphate buffered saline was made according to Table 2-3. Tris-acetate-EDTA (TAE), 3-(N-morpholino)propanesulfonic acid (MOPS), Tris-borate-EDTA (TBE) and NOVEX Transfer buffer were purchased as concentrated stocks from Invitrogen.

Table 2-3: Components of phosphate buffered saline (PBS).

Component	Concentrations
NaCl	137 mM
KCl	2.7 mM
NaHPO ₄	10 mM
KH ₂ PO ₄	1.8 mM

2.2 Bacterial strains and plasmids

2.2.1 Bacterial strains

All bacterial strains used in this thesis are listed and described in Table 2-4.

Table 2-4: Bacterial strains used in this study.

Strain	Description and genotype	Source
<i>Escherichia coli</i>		
TUV93-0	Stx-negative derivative of O157:H7 EDL933	(Campellone <i>et al.</i> , 2002)
TUV93-0 <i>lux</i>	<i>lux</i> -positive derivative of TUV93-0	This study
TUV93-0 <i>lux</i> Str ^R	<i>lux</i> -positive Str-resistant K42T <i>rpsL</i> mutant	This study
TUV93-0 RFP	<i>rfp</i> -positive derivative of TUV93-0	Prof. D. Walker *
OI-148A <i>lux</i>	T3SS-negative, deletion of first half of LEE	(Campellone <i>et al.</i> , 2004)
ZAP0273	Stx-negative derivative of O157:H7 Sakai	Prof. D. Gally **
LF82	Crohn's Disease-associated ExPEC	(Miquel <i>et al.</i> , 2010)
LF82 <i>lux</i>	<i>lux</i> -positive derivative of LF82	This study
LF82 <i>lux</i> Str ^R	<i>lux</i> -positive Str-resistant K42T <i>rpsL</i> mutant	This study
LF82 Δ <i>eaeH</i>	Deletion of <i>eaeH</i> gene	This study
LF82 Δ <i>yghJ</i>	Deletion of <i>yghJ</i> gene	This study
H10407	Prototypical ETEC strain	(Crossman <i>et al.</i> , 2010)
E2348/69	Enteropathogenic O127:H6 serogroup	(Iguchi <i>et al.</i> , 2009)
JP10819	MG1655 strain lysogenic for ϕ P27, <i>stx2:tet</i>	(Quiles-Puchalt <i>et al.</i> , 2014)
MG1655	Non-lysogenic laboratory strain	(Blattner <i>et al.</i> , 1997)
BL21 Star (DE3)	Protein expression strain	New England Biolabs
XL1-Blue	Cloning strain	Agilent Technologies
<i>Staphylococcus aureus</i>		
JP5011	RN4220 strain lysogenic for ϕ SLT, <i>pvl::tet</i>	(Ferrer <i>et al.</i> , 2011)
RN10359	RN450 strain lysogenic for 80 α	(Ubeda <i>et al.</i> , 2007)
RN4220	Non-lysogenic laboratory strain	(Nair <i>et al.</i> , 2011)
<i>Citrobacter rodentium</i>		
<i>C. rodentium lux</i>	<i>lux</i> -positive <i>C. rodentium</i>	(Mallick <i>et al.</i> , 2012)
λ <i>stx</i> _{2dact} <i>lux</i>	<i>lux</i> -positive integrated Stx2 prophage	(Mallick <i>et al.</i> , 2012)
λ <i>stx</i> _{2dact} Δ <i>tir lux</i>	<i>lux</i> -positive integrated Stx2 prophage, <i>tir</i> mutant	(Mallick <i>et al.</i> , 2012)

* University of Glasgow

** University of Edinburgh

2. MATERIALS & METHODS

2.2.2 Storage of bacterial strains

Bacterial stocks for storage were prepared by addition 0.5 ml of an overnight bacterial culture to a cryovial containing 1 ml sterile glycerol (40%) and peptone (2%). Bacteria were stored at -80°C.

2.2.3 Bacterial growth conditions

Unless specified otherwise, bacterial cultures were propagated from a single colony obtained from agar plates streaked from frozen samples, and grown at 37°C and 200 rpm in an orbital incubator for aeration. Antibiotics were included when required using the concentrations described in Table 2-2.

2.2.4 Bacterial growth curves and calculation of colony-forming units

Growth curves were obtained by inoculating media with overnight cultures to give an initial starting OD₆₀₀ of 0.08 and grown at 37°C and 200 rpm. The OD₆₀₀ of cultures was measured hourly and plotted against time.

The number of colony-forming units (CFU) in bacterial cultures was measured by serial dilution of cultures in PBS. In brief, 10 µl of each dilution was inoculated in triplicate onto LB agar containing appropriate antibiotics. The average number of colony-forming units per ml of original culture (CFU/ml) was calculated by multiplication of the number of colonies that could be accurately counted (~5-50 colonies) and the dilution factor.

2.2.5 Plasmids

All plasmids used in this thesis are listed and described in Table 2-5.

2. MATERIALS & METHODS

Table 2-5: Plasmids used in this study.

Plasmid	Vector type	Antibiotic resistance	Source
p16 <i>Slux</i>	Integration	Erythromycin	(Riedel <i>et al.</i> , 2007)
pET-21b-EaeH	Expression	Ampicillin	Novartis Vaccines
pET-21b-YghJ	Expression	Ampicillin	Novartis Vaccines
pAJR70	Reporter	Chloramphenicol	(Roe <i>et al.</i> , 2003)
<i>prpsM::GFP</i>	Reporter	Chloramphenicol	(Roe <i>et al.</i> , 2003)
pzm_TE1	Reporter	Chloramphenicol	This study
pzm_LE1	Reporter	Chloramphenicol	This study
pzm_LY1	Reporter	Chloramphenicol	This study
<i>pstx2::GFP</i>	Reporter	Chloramphenicol	Prof D. Gally
pGB2	Resistance	Streptomycin	(Churchward <i>et al.</i> , 1984)
pKD4	Template	Kanamycin	(Datsenko & Wanner, 2000)
pKD46	Helper	Ampicillin	(Datsenko & Wanner, 2000)
StrataClone pSC-A-amp/kan vector	Storage	Ampicillin	Agilent Technologies

2.3 Eukaryotic cell lines and growth conditions

2.3.1 Eukaryotic growth media

Growth media for eukaryotic cells was prepared by addition of foetal calf serum (FCS; Invitrogen) to MEM-HEPES at a final concentration of 10%, along with penicillin and streptomycin at final concentrations of 100 units/ml and 100 µg/ml respectively. Prepared media was stored at 4°C and pre-warmed to 37°C before use.

2.3.2 Eukaryotic cell lines

All cell lines used in this thesis are listed and described in Table 2-6.

Table 2-6: Eukaryotic cell lines used in this study.

Strain	Biological source	Phenotype
Caco-2	Human colon	Epithelial
HeLa	Human cervix	Epithelial

2. MATERIALS & METHODS

2.3.3 Eukaryotic growth conditions and passage

Cells were grown at 37°C in a 5% CO₂ incubator. When confluency was reached, media was removed and cells washed twice with sterile HEPES solution. Trypsin-EDTA (Sigma-Aldrich) was added to flasks, which were left at room temperature until cells detached (5-10 minutes). An equal volume of MEM-HEPES to the trypsin was added to flasks, and cells transferred to new flasks containing growth media to achieve a dilution of 1/50 of the original concentration. Monolayers were considered near-confluent when approximately 90% confluent.

2.4 Molecular techniques

2.4.1 Preparation of genomic DNA

Genomic DNA (gDNA) was extracted using the ChargeSwitch gDNA Mini Bacteria kit (#CS11301, Invitrogen) from 1 ml of overnight LB cultures. The extracted DNA was resuspended in 200 µl nuclease-free water (Ambion) and stored at 4°C.

2.4.2 Oligonucleotide primers

Oligonucleotide primers used to amplify DNA were designed using MacVector and synthesised by Life Technologies. For molecular cloning and confirmation primers annealing regions complementary to template DNA were typically 20 bp in length, approximately 50% in GC content, and had a melting temperature of 55-60°C. All primers used in this thesis are listed in Table 2-7.

2. MATERIALS & METHODS

Table 2-7: Primers used in this study.

Name	Sequence 5' to 3'	Amplicon size (bp)
p16 <i>Slux</i> +ve 5'	ACACTGGAAGTGGACACGGTCCAGACTCC	1,150
p16 <i>Slux</i> +ve 3'	TTGTAAAACGACGGCCAGTGAGCGCGCG	
<i>rpsL</i> sequencing 5'	AATTCGGCGTCCTCATATTG	555
<i>rpsL</i> sequencing 3'	GTGGCATGGAAATACTCCGT	
<i>eaeH</i> promoter 5'	GGGGATCCTGTTATCCTTCCGTTATCGTTCATGAG	619
<i>eaeH</i> promoter 3'	GGCCATGGGTTTATGACCTGTTTTATAACG	
<i>yghJ</i> promoter 5'	GCGGATCCGAGCGTGAGAACATCTAT	424
<i>yghJ</i> promoter 3'	GCGGTACCGGCTAACAGGGTTGCGCTTAA	
Lambda red <i>eaeH</i> 5'	TTCAGGTTCTTTTTCCACTCGCTGTCACCTTTACGCC	1,579
Lambda red <i>eaeH</i> 3'	AGTAATGGCAGCAGTGTAGGCTGGAGCTGCTTC	
Lambda red <i>yghJ</i> 5'	GCAGTACGACCATTGCAACATTCAACACCCAGTCA	1,531
Lambda red <i>yghJ</i> 3'	GAAGCTGCGCGTAGCGTGTAGGCTGGAGCTGCTTC	
Δ <i>eaeH</i> +ve 5'	CCACCTGATGAGTGGCTACA	448
Δ <i>eaeH</i> +ve 3'	TCTACGTGTTCCGCTTCCTT	
Δ <i>eaeH</i> -ve 5'	GAAAAGGAAACCGGGAAATC	416
Δ <i>eaeH</i> -ve 3'	CTGGTTAGCTTTAGCGGTGG	
Δ <i>yghJ</i> +ve 5'	CGATGGCTTTACCTTTACGC	347
Δ <i>yghJ</i> +ve 3'	TGTAAGCCCACTGCAAGCTA	
Δ <i>yghJ</i> -ve 5'	CGACCATTGCAACATTCAAC	301
Δ <i>yghJ</i> -ve 3'	TCAGTCGCAGCATTGTTTTC	

2.4.3 Polymerase chain reaction (PCR)

PCR reactions were performed using a final volume of 25 μ l, and volumes of the PCR mixture components are shown in Table 2-8. Initial PCR temperature conditions are shown in Table 2-9 and, in general, amplification required 25 cycles. If no amplification occurred, a 15°C gradient of the annealing temperature was used to identify the optimal conditions. PCR of individual bacterial colonies was performed by inoculation of a single bacterial colony into 100 μ l PBS, and the sample boiled at 95°C for 10 minutes before brief centrifugation to remove cell debris. One microlitre of the supernatant was then used in a single PCR reaction.

2. MATERIALS & METHODS

Table 2-8: Components of a 25 µl PCR mixture.

Component	Volume used (µl)
2x PfuUltra Master Mix /2x GoTaq Green Master Mix	12.5
10 µM 5' primer	0.5
10 µM 3' primer	0.5
Template DNA	1
Nuclease-free H ₂ O	10.5

Table 2-9: Standard PCR protocol.

Step	Temperature (°C)	Duration (seconds)
Initial denaturing	95	300
Denaturing	95	45
Annealing	55	45
Extension	72	60 (per kb)
Final extension	72	600
Hold	4	∞

2.4.4 Agarose gel electrophoresis

To produce 1% agarose gels, agarose was added to 1x TAE buffer and heated until the agarose was dissolved. SYBR Safe gel stain (Life Technologies) was added at a dilution of 1:10,000 and the gel allowed to set in a gel tray. For all gels, 1x TAE was used as running buffer, 1 Kb Plus DNA ladder (Invitrogen) loaded to provide a standard marker of size, and 1x BlueJuice loading buffer (Invitrogen) added to samples to aid visualisation during loading. Gels were run at 100 V for 40 minutes, and visualised using an Alphamager transilluminator (Alpha Innotech).

2.5 Molecular cloning

2.5.1 Restriction enzyme digests

All restriction enzyme digests were performed according to the manufacturer's instructions (New England Biolabs). Reaction digests were performed in volumes of 10-20

2. MATERIALS & METHODS

μl , and volumes of the digest components are shown in Table 2-10. Reactions were incubated at 37°C for 2 hours, and digested products resolved by agarose gel electrophoresis to visualise and isolate fragments.

Table 2-10: Components of restriction enzyme digests for a 10 μl reaction.

Component	Volume (μl)
1 $\mu\text{g}/\mu\text{l}$ DNA	1
10 units / μl restriction enzyme	1
10x digestion buffer	1
Nuclease-free H_2O	7

2.5.2 DNA gel purification

Linear DNA products from PCR or restriction digests resolved by gel electrophoresis were excised from the gel and purified using the Gel Extraction Kit (Qiagen) as per manufacturer's instructions. Purified DNA was eluted into 30 μl dH_2O and the concentration determined by 280 nm absorbance using a NanoDrop 2000 (Thermo Fisher Scientific).

2.5.3 DNA ligation

All ligation reactions were performed according to the manufacturer's instructions (New England Biolabs). Ligation reactions used T4 DNA ligase (New England Biolabs) and were carried out in 10 μl volumes. Components of the ligation mixture are shown in Table 2-11. The ligation reaction was incubated overnight at 4°C.

Table 2-11: Components of DNA ligation mixture for a 10 μl reaction.

Component	Volume (μl)
100 $\text{ng}/\mu\text{l}$ vector DNA	1
100 $\text{ng}/\mu\text{l}$ insert DNA	3
400 units/ μl T4 DNA ligase	0.5
10x T4 DNA ligase buffer	1
Nuclease-free H_2O	4.5

2. MATERIALS & METHODS

2.5.4 Production of electrocompetent *E. coli*

An overnight culture of bacteria grown from a single colony was used to inoculate a 10 ml flask of pre-warmed LB at an OD₆₀₀ of 0.08. Bacteria were grown at 37°C until an OD₆₀₀ of 0.6 was reached. Cultures were chilled on ice for 10 minutes, centrifuged at 3,000 x *g* for 10 minutes at 4°C, and pellets resuspended in 20 ml ice-cold 10% (v/v) glycerol before a further centrifugation for 10 minutes. Pellets were then resuspended in 1 ml 10% glycerol and centrifuged for 2 minutes, and this step was repeated a further 4 times. After the final centrifugation, the pellet was resuspended in 100 µl of ice-cold 10% glycerol and 40 µl of cells were used per reaction.

2.5.5 Electroporation transformation

Electrocompetent cells were transformed by mixing 40 µl of cells with either 2 µl purified plasmid or 5 µl ligation reaction and immediately transformed using an Eporator electroporator (Eppendorf) at 2.5 kV and a capacitance of 25 µF. One ml of pre-warmed LB was added to the transformation mixture, which was incubated at 37°C or 30°C for 2 hours with shaking at 200 rpm. The mixture was plated onto LB agar containing appropriate antibiotics, and incubated at 37°C or 30°C overnight.

2.5.6 Heat-shock transformation

Chemically competent BL21 Star (DE3) and XL-1 Blue cells (Table 2-4) were transformed by adding either 2 µl purified plasmid or 5 µl ligation reaction to 50 µl chemically competent cells, which was incubated on ice for 30 minutes. Cells were then heat shocked by submersion in a 42°C water bath for 45 seconds. Cells were immediately returned to ice for 2 minutes before 1 ml of pre-warmed LB was added. The transformed bacteria were incubated at 37°C or 30°C for 2 hours with shaking, and the mixture plated onto LB agar containing appropriate antibiotics and incubated at 37°C or 30°C overnight.

2. MATERIALS & METHODS

2.5.7 p16S*lux* integration

All bacterial strains used in animal models were bioluminescently labelled by integration of the bacterially encoded luminescence genes (*lux*) into each genome. This allowed live imaging of infection within the whole animal using an *in vivo* imaging system (IVIS) Spectrum (PerkinElmer). The p16S*lux* plasmid encodes the *lux* operon from *Photobacterium luminescens*, a 16S RNA gene insertion site, and an erythromycin resistance cassette to allow for selection of successful integration. Bacterial strains were transformed with p16S*lux* by electroporation, plated onto agar containing 500 µg/ml erythromycin, and incubated at 30 °C for 48 hours. Colonies were examined for luminescence emission using the IVIS, and positive colonies inoculated into LB containing erythromycin and grown overnight at 30°C. The overnight culture was diluted 1:1000 into fresh erythromycin-containing LB, and grown for 18 hours at 42°C. Serial dilutions of the culture were plated onto agar containing erythromycin and incubated at 42°C overnight. Plasmid integration was confirmed by amplification of a 1,150 bp product from chromosomal DNA, using primers for chromosomal sequences flanking the integration site (Table 2-7).

2.5.8 Creation of *eaeH* and *yghJ* deletion mutants by lambda red phage mutagenesis

Lambda red mutagenesis is a technique used to create single step gene knockouts in bacteria. This involves PCR amplification of an antibiotic resistance cassette that contains 5' and 3' overhangs that directly flank the target gene, which is then transformed into bacterial cells. When integration occurs, the target gene is replaced with the resistance marker, which is used as a selection marker for identification of such mutants. This event is reliant on the bacteriophage Lambda Red genes *exo* (encoding a 5'3' dsDNA exonuclease), *bet* (encoding an ssDNA annealing protein) and *gam* (encoding an anti-exonuclease protein). These genes are encoded on the arabinose-inducible Red recombinase expression plasmid pKD46. When the resistance cassette is introduced to bacteria transformed with pKD46, the Gam protein prevents host degradation of foreign DNA by RecBCD and SbcCD nucleases, Exo converts the 5' ends of the PCR product into 3' ssDNA overhangs, and Bet uses these overhangs to pair them with their complementary target (Datsenko & Wanner, 2000).

2. MATERIALS & METHODS

To construct the kanamycin cassette with either the *eaeH* or *yghJ* flanking regions, the kanamycin resistance gene was amplified from the pKD4 plasmid using primers containing 50 bp of *eaeH* (5': +85 to +134, 3': +4009 to +4058) or 50 bp of *yghJ* (5': +669 to +718, 3': +4593 to +4642). The PCR products from 10 reactions were run on a 0.5% agarose gel, and DNA excised from the gel, purified and pooled.

Electrocompetent LF82 were transformed with the Amp^R pKD46 plasmid prior to transformation with the kanamycin cassette. Transformants were recovered in LB containing 0.1 M arabinose, which acts as the inducer for lambda red induction, plated onto LB agar containing arabinose and ampicillin, and grown overnight at 30°C.

Transformed LF82 were made electrocompetent again, transformed with approximately 3 µg of the kanamycin cassette DNA, and plated onto kanamycin agar plates which were then incubated overnight at 42°C. Colonies were re-streaked on LB agar containing kanamycin, and incubated at 42°C for 2-3 days to allow curing of the mutant strain of temperature-sensitive pKD46. Colonies with integration of the cassette and removal of the plasmid were able to grow on LB agar containing kanamycin, but not on agar containing ampicillin. Successful gene knockouts were identified by colony PCR with two sets of primers (Table 2-7). One set of primers amplified 300-400 bp DNA present only in the genome of LF82 in which either *eaeH* or *yghJ* had been replaced with the kanamycin cassette. The other set of primers amplified 300-400 bp DNA in the genome present only when *eaeH* or *yghJ* remained intact.

2.5.9 Creation of spontaneous streptomycin-resistant mutants

Spontaneous streptomycin-resistant *E. coli* mutants were created by growing the *lux*-marked strains in 25 ml LB until an OD₆₀₀ of 0.6 was reached. Bacteria were pelleted by centrifugation, resuspended in 500 µl fresh LB, and the entire inoculum plated onto agar containing 100 µg/ml streptomycin. Plates were incubated overnight at 37°C, and 8 colonies on each plate selected for further characterisation.

To determine the specific mutation in the *rpsL* gene of each Str^R mutant, the entire gene was amplified by PCR using primers described in Table 2-7. The resultant product was

2. MATERIALS & METHODS

cloned into StrataClone Cloning Vector pSC-A-amp/kan (Agilent Technologies). Clones containing the insert were verified by X-gal blue/white screening and sequenced by Eurofins MWG Operon using a T7 primer.

2.6 Protein overexpression and purification

2.6.1 Protein overexpression

For expression of recombinant proteins, plasmids encoding the genes were transformed into BL21(DE3) cells and cultured in LB until an OD₆₀₀ of 0.6 was reached, at which point expression of the proteins was induced by addition of 1 mM IPTG. Bacteria were incubated for a further 4 hours, harvested by centrifugation, and cell pellets stored at -20°C.

2.6.2 Protein purification

Cell pellets were resuspended in buffer A (Table 2-12) with DNAase (Sigma-Aldrich) and protease inhibitors (Enzo Life Sciences) added. Cells were lysed by sonication using a Soniprep 150 (MSE) sonicator at an amplitude of 40% for 5 minutes with pulses of 5 seconds on and 10 seconds off. The resultant cell lysate was centrifuged at 4000 x *g* for 15 minutes, and the supernatant containing the soluble recombinant protein removed. The His-tagged proteins were purified using immobilised metal affinity chromatography. Lysates were loaded onto a 5 ml Ni²⁺ HisTrap Column (GE Healthcare) pre-equilibrated with buffer A. Bound protein was eluted using buffer B in 1 ml fractions and protein identified by sodium dodecyl sulphate polyacrylamide gel electrophoresis (SDS-PAGE) analysis of fractions. To remove imidazole from the protein fractions, samples were dialysed against 2 litres of 20 mM Tris pH 7.5 and 500 mM NaCl for 4 hours.

2. MATERIALS & METHODS

Table 2-12: Components of protein purification buffers.

Buffer	Components
Buffer A	20 mM Tris pH 7.5
	500 mM NaCl
	20 mM imidazole
Buffer B	20 mM Tris pH 7.5
	500 mM NaCl
	300 mM imidazole

2.7 Phenotypic characterisation of strains

2.7.1 Secretion assays

To induce Type 3 expression and protein secretion, *E. coli* strains were grown in MEM-HEPES at 37°C with shaking until an OD₆₀₀ of 0.8 was reached. Cells were pelleted by centrifugation at 4000 x *g* for 15 minutes, and the supernatant removed and centrifuged again to remove any remaining bacteria. The supernatant was carefully removed to avoid disturbing the cell pellet, and trichloroacetic acid (TCA) added to the supernatant at a final concentration of 10%. Secreted proteins were precipitated overnight at 4°C, and pelleted by centrifugation at 4,000 x *g* for 45 minutes. The supernatant was removed, and the pellet dried and resuspended in 1.5 M Tris pH 8.8. Secreted proteins were then analysed by SDS-PAGE and/or Western blotting.

2.7.2 SDS-PAGE

Samples for analysis by SDS-PAGE were prepared in NuPAGE sample buffer (Invitrogen) at a final concentration of 1x. These were boiled for 10 minutes at 95°C before 10-20 µl of the sample was loaded onto NuPAGE 4-12% Bis-Tris pre-cast gels (Invitrogen). SeeBlue+2 molecular weight marker (Invitrogen) was included to allow differentiation of protein sizes and MES buffer (Invitrogen) was used as a running buffer. Gels were run at 150 V for 50 minutes and then stained using Coomassie Blue stain (Table 2-13) for one hour. Non-specific staining was removed using destain solution or water until the background staining of the gels was clear.

2. MATERIALS & METHODS

Table 2-13: Components of SDS-PAGE stains.

Stain	Volume used (μl)
Coomassie Blue	0.5 g Coomassie blue R250 400 ml methanol 100 ml acetic acid 500 ml dH ₂ O
Destain solution	400 ml methanol 100 ml acetic acid dH ₂ O

2.7.3 Western blotting

Proteins from SDS-PAGE gels were transferred onto Amersham Hybond enhanced chemiluminescence (ECL) nitrocellulose membrane (GE Healthcare) using the Sure-Lock Cell Blotting Module (Invitrogen) at 30 volts for 90 minutes. Membranes were blocked overnight in 3% skimmed milk (Marvel) in PBS containing 0.1% Tween (PBST) at 4°C. Primary antibody in 1% skimmed milk made with PBST was added to membranes at concentrations shown in Table 2-14. These were incubated for 1 hour at room temperature with gentle rocking, and unbound antibody removed with 3 x 15 minutes washes with PBST. The membrane was then incubated with secondary antibody conjugated to horseradish peroxidase (Invitrogen) for 1 hour at room temperature with rocking. Three 15 minute washes with PBST ensured removal of unbound antibody. Blots were developed by ECL, using SuperSignal West Pico Chemiluminescent Substrate (Thermo Fisher Scientific).

Table 2-14: Antibodies used in this study.

Primary antibody	Dilution	Secondary antibody	Origin of primary antibody
Rabbit anti-EaeH	1:5,000	Goat anti-Rabbit	Novartis Vaccines
Rabbit anti-YghJ	1:10,000	Goat anti-Rabbit	Novartis Vaccines
Rabbit anti-GroEL	1:10,000	Goat anti-Rabbit	Enzo

2. MATERIALS & METHODS

2.7.4 Motility assay

Bacterial motility was determined using LB agar plates containing 0.25% (w/v) agar. The center of the agar was inoculated with 5 μ l of a bacterial culture at an OD₆₀₀ of 0.8 and the plates were incubated at 30°C overnight. The diameter of the swimming zone was measured 18 hours after inoculation.

2.7.5 Bacterial adhesion assay

To determine bacterial adhesion to epithelial cells, Caco-2 cells resuspended in MEM-HEPES containing FCS and penicillin/streptomycin were used to seed 6-well plates with 9.5 cm² wells at 4x10⁴ cells/well. The plates were incubated at 37°C in a 5% CO₂ incubator until cells reached confluency. Overnight cultures of the bacterial strains were diluted 1/1,000 in MEM-HEPES containing the appropriate antibiotics and grown at 37°C with shaking until cultures reached an OD₆₀₀ of 0.6. Caco-2 cells were then washed 2x with 1 ml MEM-HEPES, and 5 ml fresh MEM-HEPES (without penicillin/streptomycin) added to the wells. One hundred microlitres of bacterial culture were added to each well, and plates centrifuged at 37 x *g* for 3 minutes before incubation at 37°C and 5% CO₂ for 4 hours. Non-adherent bacteria were harvested by removal and centrifugation of media, and resuspended in PBS. To remove adherent bacteria, wells were gently washed 3x with ice-cold sterile PBS, followed by addition of 1 ml ice-cold 1% saponin in PBS, or 0.1% Triton X-100 in adhesion assay buffer (Table 2-15). Plates were left on ice for 5 minutes, followed by removal of the wells contents from which the bacteria were harvested by centrifugation. Bacterial pellets were resuspended in PBS and serially diluted onto agar plates containing appropriate antibiotics to determine the total number of non- adherent and adherent bacteria per well.

Table 2-15: Components of adhesion assay buffer.

Component	Concentration (mM)
Na ₂ HPO ₄	60
NaH ₂ PO ₄	40
KCl	10
MgSO ₄	1

2. MATERIALS & METHODS

2.7.6 Immunofluorescence microscopy

To allow visualisation of bacterial/epithelial cell interactions, cover slips (pre-washed with 70% ethanol and HEPES buffer) were added to 24-well plates, and were seeded with 4×10^4 HeLa cells suspended in MEM-HEPES containing FCS and penicillin/streptomycin. Plates were incubated overnight at 37°C in a 5% CO₂ incubator. Overnight cultures of the bacterial strains were diluted 1/1,000 in MEM-HEPES containing the appropriate antibiotics and allowed to grow at 37°C with shaking until the cultures reached an OD₆₀₀ of 0.6. At that point, unattached HeLa cells were removed by washing the wells 2x with 1 ml MEM-HEPES, and 400 µl MEM-HEPES (without FCS and penicillin/streptomycin) added to each well. Bacterial cultures were diluted with warm MEM-HEPES to an OD₆₀₀ of 0.1, to achieve a multiplicity of infection (MOI) of approximately 100, and 100 µl of diluted bacteria added to each well. The appropriate antibiotics were also added to wells. Plates were centrifuged at 37 x g for 3 minutes and incubated for 1 hour at 37°C and 5% CO₂. Wells were then washed once to remove unattached bacteria, and 500 µl fresh MEM-HEPES (containing appropriate antibiotics) added to each well. Plates were incubated at 37°C and 5% CO₂ for a further 3 hours, after which media was removed.

To fix cells, the wells were initially washed 4x with PBS, and finally fixed by addition of 250 µl 2% paraformaldehyde (PFA) in PBS. Plates were incubated statically at room temperature for 15 minutes, followed by a further 15 minutes at room temperature with rocking. Wells were washed a further 3x with PBS, and cells permeabilised by addition of 250 µl 0.1% Triton X-100 (Sigma-Aldrich) in PBS for 5 minutes at room temperature with rocking. They were then washed 4x with PBS to remove the detergent.

To stain for actin, 250 µl (1 unit) Phalloidin 647 (Thermo Fisher Scientific) in PBS was added to wells, and plates incubated for 60 minutes at room temperature with rocking. From this point onwards, plates were kept in the dark using foil to prevent photobleaching. After incubation, wells were washed 3x with PBS. Cover slips were mounted using fluorescent mounting medium (Dako). Slides were left in the dark overnight to set and imaged on a Zeiss M1 Axioskop microscope. Cells were imaged at x100 and were captured using Velocity (PerkinElmer) software.

2. MATERIALS & METHODS

2.7.7 GFP reporter fusion assays

Measurement of gene expression as determined by GFP fluorescence was carried out using the promoter:GFP reporter fusion constructs listed in Table 2-5. Plasmids were transformed by electroporation into bacterial strains and transformants cultured overnight into LB containing chloramphenicol. Overnight cultures were diluted into fresh LB to an OD₆₀₀ of 0.08 and grown at 37°C for 6 hours, with OD₆₀₀ and fluorescence measured hourly. Fluorescence of GFP was recorded by analysis of 200 µl aliquots of culture supernatant placed in a 96-well black microtiter plate and fluorescence measured using a FLUOstar Optima plate reader (BMG Labtech). Three gain values were taken, and the measurement taken as the highest gain that did not reach maximum fluorescence. Fluorescence was plotted against either optical density or time.

2.7.8 Mitomycin C (MMC)-induced Stx-GFP reporter fusion assay

The Stx-GFP reporter fusion assay was performed as described in 2.7.7, however the AHU compounds and MMC were added to the culture only when it reached an OD₆₀₀ of 0.7-0.8. The AHU compounds were used at final concentrations of 10-200 µM, and MMC at a final concentration of 1 µg/ml. Cultures contained a dimethyl sulfoxide (DMSO) concentration of 1%, including the control containing 0 µM compound.

2.7.9 Phage transduction assays

The production and transduction of phages was performed using two strains: the strain carrying the specific prophage genes and lacking other lysogenic prophages, and a non-lysogenic acceptor strain. In *E. coli* the acceptor strain was MG1655, and in *S. aureus* was RN4220. The prophage strains were grown at 37 °C until an OD₆₀₀ of 0.25 was reached, using either LB (*E. coli* strains) or TSB (*S. aureus* strains). At this point, test compounds were added at a final concentration of 50 µM, MMC added at a final concentration of 2 µg/ml, or ciprofloxacin at a final concentration of 50 ng/ml. The final concentration of DMSO in cultures was 0.25%. Cultures were grown at 32°C with 80 rpm shaking for 4 hours then grown overnight at room temperature without shaking, and culture

2. MATERIALS & METHODS

containing the phage lysate filtered through a 0.2 μm filter. Phage lysate was diluted to 1:10⁵ in phage buffer (Table 2-16), and 100 μl of the diluted phage added to 1 ml of the acceptor strain, which was at an OD₆₀₀ of 1.4 and contained 10 mM CaCl₂. These were incubated without shaking at 37°C for 30 minutes. Three milliliters of LB containing 0.75% agar was added to bacteria, and this mixture poured onto LB agar plates containing 6 $\mu\text{g}/\text{ml}$ tetracycline and 1.7 mM sodium citrate. Plates were incubated at 37°C overnight, with each colony generated reflecting a successful single phage transduction event.

Table 2-16: Components of phage buffer.

Component	Concentration (mM)
NaCl	100
Tris pH 7.8	500
MgSO ₄	1
CaCl ₂	4

2.8 Biophysical techniques

2.8.1 Microscale thermophoresis

RecA was covalently labelled with NT.Red dye (NanoTemper Technologies), and unattached dye removed using a gravity flow column. AHU3 was prepared in 4% DMSO and PBS at concentrations between 12 pM and 200 μM , while RecA in PBS was kept at a constant concentration of 100 μM . After incubation at room temperature of 5 minutes, samples were loaded into MST NT.115 standard glass capillaries and the MST analysis was performed using a Monolith NT (NanoTemper Technologies).

2.8.2 Analytical ultracentrifugation

The effect of AHU3 on oligomerisation of RecA was assessed via sedimentation equilibrium (SE) analytical ultracentrifugation (AUC), following the methodology of Brenner *et al.* (1990). AUC was carried out in an Optima XL-I analytical ultracentrifuge (Beckman Coulter). Samples were dialysed for 2 hours against 2 litres of 50 mM Na-

2. MATERIALS & METHODS

citrate, 5% (w/v) glycerol pH 6.0, buffer conditions optimal for maximising the oligomeric state of RecA (Brenner *et al.*, 1990), and 80 μ l of each sample loaded into double sector centerpieces. Three samples were studied: 10 μ M RecA, 10 μ M RecA + 0.5% (v/v) DMSO, and 10 μ M RecA + 0.5% (v/v) DMSO + 100 μ M AHU3. Rotor speeds of 6, 10 and 14 k rpm at a temperature of 4°C and 20°C were used (Table 2-17). Scans were taken every 3 hours until analysis with WinMATCH indicated that equilibrium had been reached. Sedimentation equilibrium data was analysed with SEDPHAT (Vistica *et al.*, 2004) by Dr. Olwyn Byron, University of Glasgow, using the single species analysis model in order to gain a model-independent measure of the whole-cell average molecular weight.

Table 2-17: Partial specific volumes of proteins, and densities and intrinsic viscosities of buffers used in analytical ultracentrifugation. Values were calculated using SEDNTERP.

Temperature (°C)	Partial specific volume (g/ml)	Buffer density	Buffer viscosity
4	0.733	1.020	0.018
20	0.740	1.018	0.012

2.8.3 ATPase assays

Colourmetric ATPase assays were performed using a commercial ATPase assay kit (#601-0120, Innova Biosciences), which is based on the formation of coloured complexes between an inorganic phosphate and a dye molecule under acidic conditions. ATPase reactions were carried out in Costar clear flat-bottomed 96-well assay plates (Corning) following the manufacturer's protocol. RecA, poly dT single-stranded DNA (ssDNA; Midland Certified Reagent Company) and AHU were added to the substrate/buffer mix (assay buffer, MgCl₂, ATP) at volumes shown in Table 2-18. RecA was used at a final concentration of 250 nM, ssDNA at 5 μ M, and DMSO (required for AHU solubility) at 2% (v/v). AHU3 and AHU4 were used at concentrations between 0.1 μ M and 200 μ M. The reaction was incubated at 37°C for 30 minutes, then stopped by addition of 12.5 μ l Gold mix (P_iColorLock™ Gold with 1/100 vol. of Accelerator added), followed by addition of 5 μ l Stabiliser 2 minutes later. After 30 minutes at room temperature the plate was read at a wavelength of 650 nm. A negative control lacking RecA was included, as was a further

2. MATERIALS & METHODS

sample which lacked ssDNA, to confirm that the reaction was dependent on activation of RecA by ssDNA.

Table 2-18: Volumes of components in a single ATPase assay well.

Component	Volume used (μ l)
50 μ M RecA	0.25
500 μ M poly dT ssDNA	0.5
1-2000 μ M AHU3/AHU4 (in 20% DMSO)	5
Assay buffer	5
0.1 M $MgCl_2$	1.25
10 mM ATP	2.5
Nuclease-free water	35.5

2.8.4 AHU cytotoxicity testing

Cytotoxicity screening of the compounds AHU1-3 was undertaken by the European Screening Port (Hamburg, Germany). Briefly, Human Embryonic Kidney 293 (HEK 293) cells were grown until 80-90% confluency, before being harvested and resuspended in DMEM in 384-well plates containing the AHU compounds and 0.1 % (v/v) DMSO. After 24 hours of incubation at 37°C in the presence of 5% CO_2 , 20 μ l of CellTiter-Glo reagent (#G7571; Promega) was added to each well and incubated at room temperature for 10 minutes. Luminescence was recorded as a measure of cell survival; the CellTiter-Glo assay is a homogeneous method of determining the number of viable cells based on quantitation of ATP present, an indicator of metabolically active cells. All compounds were tested on three different days in duplicate. Raw data was processed using ActivityBase XE (IBDS), and the percentage cytotoxicity relative to the positive and negative controls calculated. Compounds were classed as actives when the calculated cytotoxicity was >50% of that relative to the positive and negative controls.

2.9 Animal experiments

2.9.1 Home Office animal licence

All procedures were carried out in strict accordance with the Animals Act (Scientific Procedures, 1986) and were approved by the Home Office, United Kingdom (project license number PPL60/4218, held by Dr. Gillian Douce).

2.9.2 Mouse maintenance

All mice, aged 6-8 weeks and female, were purchased from Harlan Laboratories, UK. Mouse strains used were inbred BALB/c, C57BL/6 and C3H/HeJ, and outbred ICR (also known as CD-1) mice. Mice were housed in groups of 5 at a controlled temperature (22°C) with a 12 hour light/dark cycle, and were fed BK001E Beekay rat and mouse diet (Special Diet Services) *at libitum* with free access to water at all times. Mice were culled by cervical dislocation or by terminal anaesthesia.

2.9.3 Bacterial infection of mice

Bacterial strains for mouse infections were grown in DMEM until an OD₆₀₀ of 0.8 was reached. Bacteria were pelleted by centrifugation and resuspended in PBS to concentrate the culture 100x. Bacterial viability to assess infection dose was determined by serial dilution of the inoculum and plating onto LB agar. This revealed the concentration of bacteria to be approximately 10¹¹ CFU/ml. Mice were infected by oral gavage with 100 µl each strain, or 10¹⁰ CFU/dose. Mice infected with *E. coli* were orally gavaged 30 minutes prior to infection with 100 µl of 0.1 M sodium bicarbonate to reduce the acid pH of the stomach.

2. MATERIALS & METHODS

2.9.4 Live imaging of infected mice

Progression of infection in individual mice was determined using the IVIS Spectrum. For imaging, mice were anaesthetised by inhalation of 2% isoflurane which was maintained during the imaging process. Luminescence as photons per second (p/s) was recorded using an exposure time of one minute, with large or medium binning.

2.9.5 Faecal shedding counts of infected mice

To determine bacterial colonisation by faecal shedding, faecal pellets were collected from individual mice and PBS added to give a faecal concentration of 100 mg/ml. Stools were softened by storage at 4°C for 30 minutes, then vortexed to ensure breakdown of the pellet and release of bacteria. After a brief centrifugation, the supernatant was serially diluted in PBS, and 10 µl of each dilution spotted in triplicate onto LB agar containing 500 µg/ml erythromycin, and other antibiotics if required. The average number of colony-forming units was calculated from the dilution at which colonies could most accurately be counted (~5-50 colonies).

2.9.6 Tissue collection and histology

In order to determine the extent of epithelial colonisation of the tissue, after necropsy the caecum, small intestine and large intestine were removed, opened longitudinally and washed in 5 ml sterile PBS. The washed material was removed and these samples diluted and plated to provide estimates of luminal-associated bacteria. The remaining tissue was washed in a further 10 ml PBS before being placed in 5 ml fresh PBS and homogenised for 5 minutes using a Stomacher Lab-Blender 80 (Seward). Mucosally-associated bacteria were measured by serial dilution of the PBS and agar plating as described previously.

For kidney histology, mouse kidneys were longitudinally divided and fixed in 10% buffered formalin, dehydrated, and embedded in paraffin blocks. Five-micrometer tissue sections were cut and stained with hematoxylin and eosin (H&E) and periodic acid-Schiff (PAS) stain by Lynn Stevenson, Veterinary Diagnostics, University of Glasgow. Slides were

2. MATERIALS & METHODS

visualised using an Axiovert 25 inverted microscope (Zeiss) at 400x magnifications and images collated using AxioVision (Zeiss) imaging software. Expert advice on the extent of kidney pathology was provided by Dr. Shana Coley, University of Glasgow.

2.10 Analysis of data

Data were analysed using Excel (Microsoft) and Prism 5 (GraphPad), and statistical analysis performed using Prism 5/Instat (Student's unpaired t-test, ANOVA, D'Agostino and Pearson omnibus test) or R software (General Linear Model). Statistical significance was indicated as a p-value of 0.05 or below. Significant differences between the means of two groups was determined by Student's unpaired t-test, and between the means of more than two groups by ANOVA. Unless stated otherwise, all data was determined to be parametric, after visualisation of data as a histogram, and for data sets with a large enough sample size, normality analysis using D'Agostino and Pearson omnibus test.

Chapter 3: Development and characterisation of mouse models of *E. coli* infection

3.1 Introduction

To effectively test novel anti-virulence compounds *in vivo*, appropriate animal models that allow bacteria to replicate those aspects of pathogenesis targeted by the drug are required. These features, such as colonisation by adhesion or invasion, or development of illness or tissue damage, should ideally be easily observable and sensitive to changes in the virulence factor of interest.

One of the main aims of this chapter is to assess colonisation of mice by *E. coli*, which is typically followed by shedding of bacteria in faeces. Quantification of the number of bacteria secreted in faecal matter is achieved by serial dilution of faecal supernatant and plating onto agar containing an antibiotic that the infecting *E. coli* strain is resistant to, with this resistance preferably carried on the chromosome rather than on a plasmid, as selective pressure to retain the plasmid may be lost *in vivo*. Another method for studying colonisation *in vivo* is by live-imaging of animals infected with bioluminescent bacteria, which enables assessment of infection in real time and without requiring sacrifice and analysis of infected animals.

The prerequisite for live imaging is the production of luminescence or fluorescence by the infecting bacteria, and this light release can then be quantified and localised using an *in vivo* imaging system (IVIS). Luminescence is commonly achieved using the *lux* operon from *Photobacterium luminescens*, a Gammaproteobacteria that lives in the gut of entomopathogenic nematodes. The *lux* operon can be introduced into bacteria either by plasmid or by integration into the chromosome via transposon mutagenesis. These methods, however, carry the risk of plasmid loss or integration that modifies gene expression, altering bacterial phenotype. One approach that avoids these risks is chromosomal integration of the *lux* operon into a specific site using the p16S*lux* vector, a plasmid containing the *P. luminescens lux* operon and a 16S rRNA gene insertion site. This has been designed to allow site-directed chromosomal integration by homologous recombination, and constitutive expression of high levels of luminescence in a wide range of Gram-negative bacteria (Riedel *et al.*, 2007). This location is a desirable site for chromosomal integration due to high conservation and 16S redundancy (Acinas *et al.*,

3. RESULTS: Mouse models of *E. coli* infection

2004), and integration of p16*Slux* has shown no significant influence on bacterial growth (Riedel *et al.*, 2007).

3.1.1 Aims of this chapter

- To identify a mouse model in which high, stable levels of *E. coli* O157:H7 colonisation can be observed over a significant period of 10-14 days, rather than clearance of bacteria within 2-3 days. While there are several animal species that are used as models for *E. coli*, we are limited to using mice by the available animal facilities. Additionally, as the O157:H7 strain requires a Category 3 containment laboratory, we chose to instead use TUV93-0, an Stx-negative derivative of the O157:H7 EDL933 strain, which does not produce any signs of illness in mice.
- To determine whether colonisation in this model is dependent, or is observably influenced by expression of the T3SS. As we aim to use this model to assess the influence of compounds that target the T3SS, we require the T3SS to play an essential role in colonisation of this model, so that the effects of treatments that successfully inhibit the T3SS *in vivo* are easily observed by significant decreases in faecal shedding and luminescence.
- To identify a mouse model that shows high and sustained levels of *E. coli* LF82 colonisation. LF82, considered a prototype AIEC strain associated with Crohn's disease, was chosen as unlike TUV93-0 and other EHEC, it carries the gene encoding YghJ, a potential vaccine candidate whose role in colonisation is unclear and warranted further evaluation (explored further in Chapter 4).
- To evaluate a recently developed *C. rodentium* mouse model that expresses Stx as a model for possible *in vivo* testing of compounds that inhibit Stx production. *C. rodentium* is often used as a surrogate model for *E. coli* as it is a closely related bacterial species that naturally colonises mice. As *C. rodentium* does not colonise humans, the Stx-expressing strain is classed as a Category 2 pathogen, and

3. RESULTS: Mouse models of *E. coli* infection

therefore does not require the safety precautions and facilities that a Category 3 pathogen like O157:H7 does.

3.2 Bioluminescent labelling of bacterial strains

To track bacterial infection in real time, all strains to be analysed *in vivo* were luminescently marked using the integrating p16S*lux* plasmid (Riedel *et al.*, 2007). All strains were checked for positive integration using PCR, and luminescence production using the IVIS (Figure 3-1). Integration of the *lux* operon produced a strong luminescent signal, detectable after an exposure of one second for bacteria on agar plates and one minute in mice infected with the strains. Luminescence was detected by the IVIS and displayed in colour as photons per second per cm² per steradian (p/s/cm²/sr), and luminescence in individual mice was quantified by selecting a region of interest, i.e. the whole mouse, and determining the total light emission in photons/second for that region.

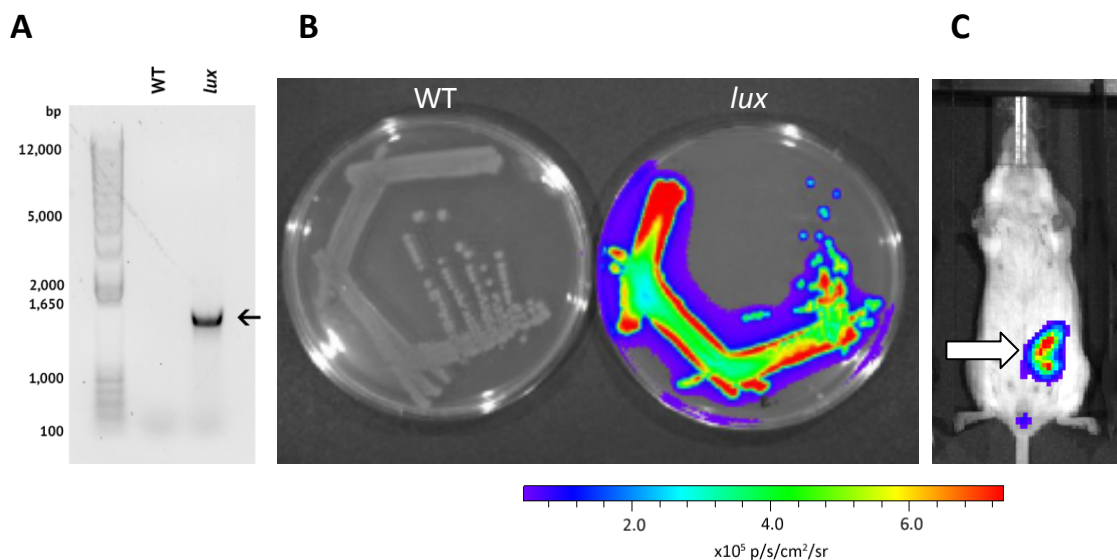


Figure 3-1: Integration of the *lux* operon into *E. coli* O157:H7 strain TUV93-0 and its luminescence on agar and in mice. To create strains capable of producing luminescence for live-image detection *in vivo*, *E. coli* strains were transformed with the p16S*lux* plasmid and the *lux* operon integrated using the method described by Riedel *et al.* (2007). Successful *lux*-positive integration was confirmed by colony PCR to amplify 1,250 bp of a chromosomal DNA sequence (indicated by arrow) present only when the *lux* operon was correctly inserted into the 16S locus (**A**). Luminescence production was confirmed by a 1 second IVIS exposure of WT and *lux*-marked strains grown on LB agar (**B**). *In vivo* production of luminescence by *lux*-marked bacteria were shown by an IVIS exposure of 1 minute of mice infected by oral gavage; a representative image of *in vivo* bacterial luminescence production in a BALB/c mouse three days after infection by oral gavage of 10⁹ CFU *lux*-integrated TUV93-0 is shown (**C**). The site of infection in the mouse is indicated by arrow and is likely to be the caecum, based on the location and shape of the signal. The colour scale bar below indicates luminescence intensity in p/s/cm²/sr for both the bacteria on agar and *in vivo*.

3.3 Colonisation of BALB/c, C57 and C3H/HeJ mouse strains by TUV93-0

As the genetic diversity of inbred mice is much lower than outbred strains, potentially decreasing the variety of host response to bacterial infection, we selected inbred mouse strains to investigate *E. coli* colonisation. Different inbred mouse populations show differing response to the severity of disease caused by the pathogen *Citrobacter rodentium* (Vallance *et al.*, 2003), a T3SS-producing natural mouse pathogen that is often used as a surrogate for *E. coli* in mice. To assess whether the susceptibility of different inbred mouse strains could also influence outcome of infection with O157:H7, three groups of the inbred mouse strains BALB/c, C57BL/6, and C3H/HeJ, consisting of five animals in each group, were infected with TUV93-0 and colonisation followed by live imaging and faecal shedding. BALB/c and C57BL/6 are both widely-used mouse strains which have been utilised in previous *E. coli* colonisation studies, while C3H/HeJ was chosen as it is a mouse strain highly vulnerable to *C. rodentium* (Vallance *et al.*, 2003). A spontaneous mutation in the Toll-like receptor 4 (TLR4) gene in C3H/HeJ mice confers a hyposensitivity to LPS (Hoshino *et al.*, 1999), but also makes them more susceptible to infection by Gram-negative organisms due to delayed TLR4-induced host immune responses (Khan *et al.*, 2006).

After infection by oral gavage of animals, similar levels of TUV93-0 faecal shedding was observed in C57BL/6 and C3H/HeJ mice with levels of shedding highest (10^5 - 10^6 CFU/mg faeces) 1 day after infection. This was followed by a decline until faecal shedding of TUV93-0 was no longer detectable ($<10^2$ CFU/mg faeces) 11 days post infection. While BALB/c mice shed TUV93-0 at significantly lower levels (10^2 CFU/mg faeces) than both C57BL/6 and C3H/HeJ 1 day after infection, faecal shedding rose to similar levels (10^4 CFU/mg faeces) 4 days post infection, followed by a decrease over the remaining post infection period, reaching undetectable levels after 8 days (Figure 3-2 A).

Analysis of bacterial luminescence revealed a high signal two days post infection in BALB/c mice (10^6 p/s), which then gradually declined. In contrast, luminescence in C57BL/6 mice remained at background levels (10^5 p/s) throughout the infection, and C3H/HeJ mice showed similar luminescence levels to BALB/c mice 1 day after infection, but these rapidly dropped to background levels (Figure 3-2 B). As similar levels of faecal

3. RESULTS: Mouse models of *E. coli* infection

shedding were observed in all three mouse strains, we concluded that the difference in observed luminescence probably reflected mouse coat colour, as darker coat colours (such as those associated with C57BL/6 mice) absorb bioluminescence more readily. We therefore chose to use BALB/c mice for future experiments as they produced the highest luminescence signal and were colonised as effectively (determined by faecal shedding) as the C57BL/6 and C3H/HeJ strains.

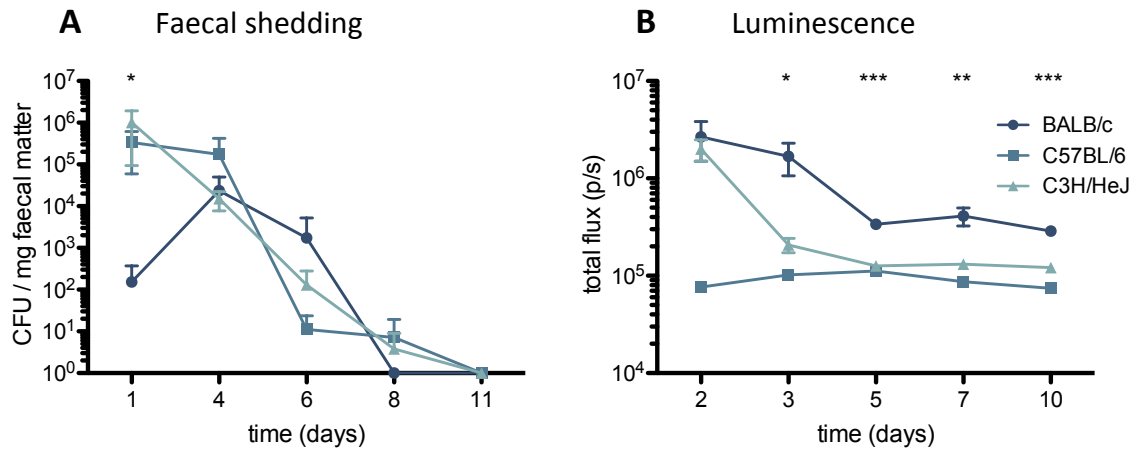


Figure 3-2: Colonisation of inbred mice by *E. coli* TUV93-0. Faecal shedding (A) and luminescence (B) of *lux*-marked TUV93-0 in BALB/c, C57BL/6, and C3H/HeJ mouse strains. Each group of mice consisted of five animals, and faecal shedding and luminescence were followed for 10 days after infection with 10⁹ CFU *lux*-marked TUV93-0. Data points shown are the mean of each group, and standard deviation from the mean displayed as error bars. Time points at which a significant difference between the means of groups, determined by one-way ANOVA, are denoted by an asterisk (* = p<0.05; ** = p<0.01; *** = p<0.001).

3.4 Colonisation of dextran sodium sulfate-treated BALB/c mice by TUV93-0 and LF82

While this first experiment revealed that high numbers of TUV93-0 were detected by faecal shedding and confirmed by live imaging 24 hours post infection, colonisation decreased steadily from this point reaching undetectable levels 8-11 days later, suggesting that bacteria were unable to successfully colonise the mouse intestine. This observation is consistent with previous studies (Mohawk & O'Brien, 2011) and has been associated with the competitive influence of the microbiome.

3. RESULTS: Mouse models of *E. coli* infection

Interestingly, recent studies in both human intestinal bowel disease patients and animal models of gut inflammation have shown that intestinal *E. coli* increase significantly and become a dominant species when the microbiota is disturbed by inflammation (Lupp *et al.*, 2007). Classically, mouse models of colitis have used dextran sodium sulphate (DSS), a water soluble polysaccharide, to induce intestinal inflammation by damaging the epithelial monolayer lining the large intestine. This leads to dissemination of proinflammatory intestinal bacteria and their products into underlying tissue. Histological changes caused by DSS at concentrations of 2-5% in drinking water include intestinal mucin depletion in the large intestine (Chassaing *et al.*, 2014a). To determine whether decreasing the intestinal mucosal layer and allowing TUV93-0 and LF82 greater access to the epithelial barrier may promote adhesion, we treated mice with a low concentration of DSS (0.25% in drinking water). We hypothesized that this concentration would be high enough to reduce mucus thickness, but not sufficient to induce colitis or significant intestinal inflammation.

To determine the effect of DSS on *E. coli* colonisation, mice were provided with drinking water three days prior to infection, with or without 0.25% DSS (~40 kDa). After infection with either TUV93-0 or LF82 all animals were provided with normal drinking water. Using both faecal shedding and bioluminescence as readouts, no difference in colonisation was observed for either strain in animals treated with DSS compared to untreated mice. TUV93-0 and LF82 faecal shedding levels of both pre-treated and untreated mice were highest 1 day after infection (10^5 - 10^6 CFU/mg faeces), and declined over the next 7 days, with no significant difference ($p > 0.05$) between pre-treated and untreated mice at any post infection time-point for either bacterial strain (Figure 3-3 A). Luminescence of bacteria also followed a similar trend over the post infection period (Figure 3-3 B). Therefore, we concluded that pretreatment of mice with 0.25% DSS had no discernible influence on persistence of either TUV93-0 or LF82 in the BALB/c host.

3. RESULTS: Mouse models of *E. coli* infection

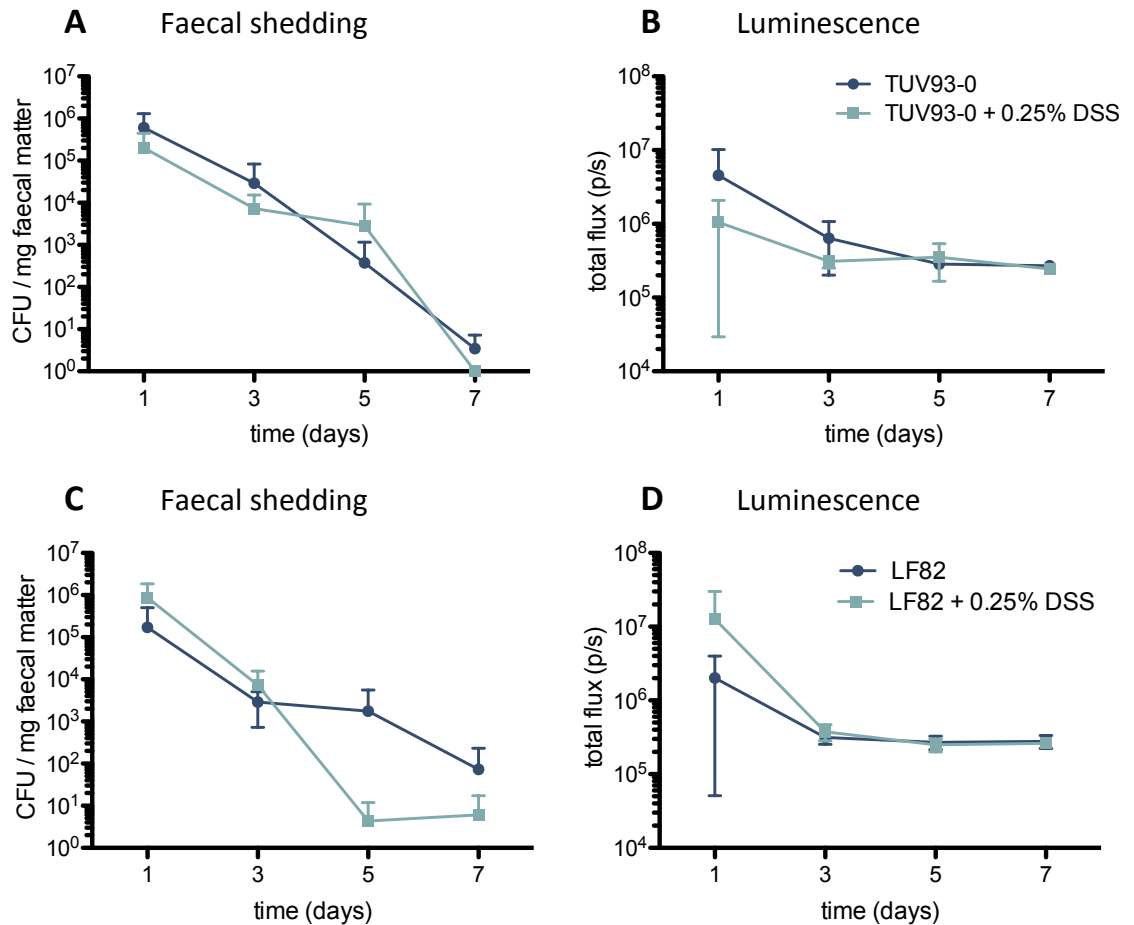


Figure 3-3: Effect of DSS pretreatment on *E. coli* colonisation. TUV93-0 (A, B) and LF82 (C, D) faecal shedding (A, C) and luminescence (B, D) in BALB/c mice. Each group of mice consisted of five animals, and faecal shedding and luminescence were followed for 7 days after infection with 10^9 CFU *lux*-marked TUV93-0 or LF82. Dark blue symbols represent colonisation in untreated animals, and light blue symbols DSS-treated animals. Data points shown are the mean of each group, and standard deviation from the mean displayed as error bars. No significant differences ($p < 0.05$) between the means of the treated and untreated groups, as determined by Student's unpaired t-test, were found for either strain at any time point. Both TUV93-0 and LF82 infections were performed concurrently.

Weight loss was monitored through the experiment as this has previously provided a reliable marker of acute colitis (Chassaing *et al.*, 2014a). However, no weight loss or other changes in behaviour were observed. While it is possible that increasing the concentration of DSS may have a greater influence on *E. coli* colonisation, it carries the risk of causing epithelial degeneration and induction of intestinal inflammation and colitis. We therefore chose not to raise the concentration of DSS above 0.25%.

3.5 Colonisation of streptomycin-treated ICR mice by *E. coli*

3.5.1 Colonisation of streptomycin-treated ICR mice by TUV93-0 carrying plasmid-borne Str^R

Further evaluation of the literature highlighted the potential influence of antibiotics on colonisation of mice with *E. coli* (Mohawk & O'Brien, 2011). In particular, the use of streptomycin, an aminoglycoside which inhibits protein synthesis, is capable of reducing the diversity of the microbiome, allowing more effective colonisation by Gram-negative enteric pathogens such as *E. coli* and *Salmonella* species (Wadolowski *et al.*, 1990; Barthel *et al.*, 2003). We chose to explore the use of this antibiotic in HaM/ICR mice, an outbred strain that is commonly used in streptomycin-treated O157:H7 models (Nagano *et al.*, 2003). These studies implied that O157:H7 colonises the untreated ICR mouse gut for longer periods than BALB/c mice, and also claimed to show *in vivo* evidence of T3SS-mediated bacterial adherence in the outbred strain.

In this model, mice were supplied with 5 g/L streptomycin in their drinking water three days prior to infection. To determine the long term impact of treatment, one group of animals was provided with regular drinking water, while the second continued with streptomycin water for a further 10 days, after which they were returned to regular water. This return to normal drinking water at 10 days was a restraint imposed by animal licence restrictions.

To ensure that *E. coli* was resistant to streptomycin, TUV93-0 was transformed with the pGB2 plasmid, which encodes the streptomycin resistance gene *aadA*. Faecal shedding and bioluminescence showed that 24 hours after infection, both groups were shedding TUV93-0 at 10^5 - 10^6 CFU/mg faeces (Figure 3-4). In mice that were subsequently returned to normal drinking water, colonisation decreased steadily, and 9 days post infection faecal shedding was undetectable. In animals with continuing streptomycin treatment, high and consistent levels of shedding were observed throughout the post infection period, with an average of 10^4 CFU/mg faeces observed at 14 days after infection.

3. RESULTS: Mouse models of *E. coli* infection

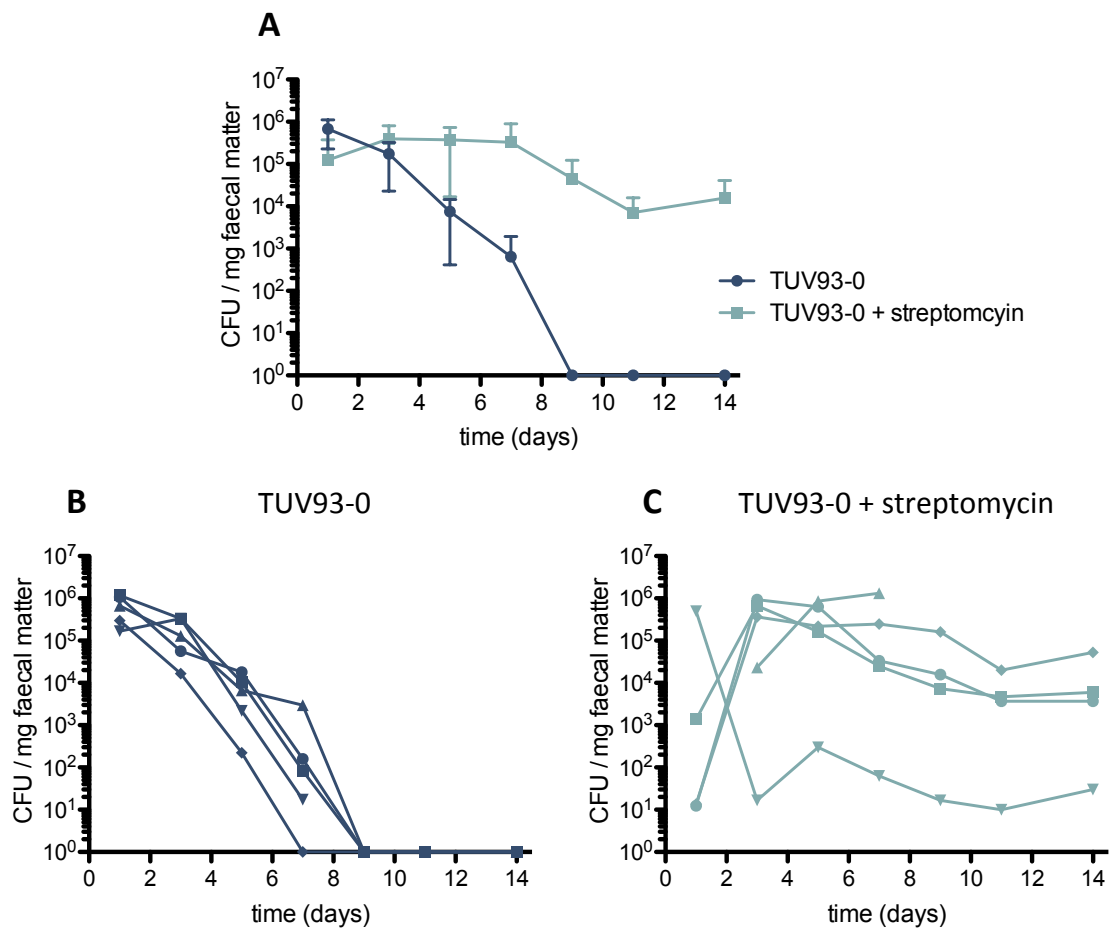


Figure 3-4: Effect of streptomycin-treated drinking water on faecal shedding of TUV93-0 in ICR mice. Average faecal shedding of two groups of ICR mice, five mice in each group, treated with 5 g/L streptomycin in drinking water for 3 days before infection with 10^9 CFU *lux*-marked TUV93-0 transformed with pGB2, and supplied with either normal drinking water (dark blue) or 5 g/L streptomycin-containing water (light blue) after infection (**A**). Individual faecal shedding of post infection untreated mice (**B**) and streptomycin-treated mice (**C**). Faecal shedding was followed for 14 days after infection. In (**A**), data points shown are the mean of each group, and standard deviation from the mean displayed as error bars.

Colonisation was confirmed using live imaging of mice, with luminescence reaching background levels ($<10^5$ p/s) in the untreated group 9 days post infection, while luminescence was not reduced to background levels until day 14 in the streptomycin treated group (Figure 3-5). While the average luminescence of the streptomycin-treated group 9-14 days after infection was relatively low compared to the level of faecal shedding at these time points, the main site of infection at that point of infection may be in a location that causes greater absorption of the luminescent signal, reducing the amount that is detectable. Alternatively, bacteria may be more dispersed throughout the intestine later in infection, which could result in a lower signal than when bacteria are more highly concentrated in a specific location.

3. RESULTS: Mouse models of *E. coli* infection

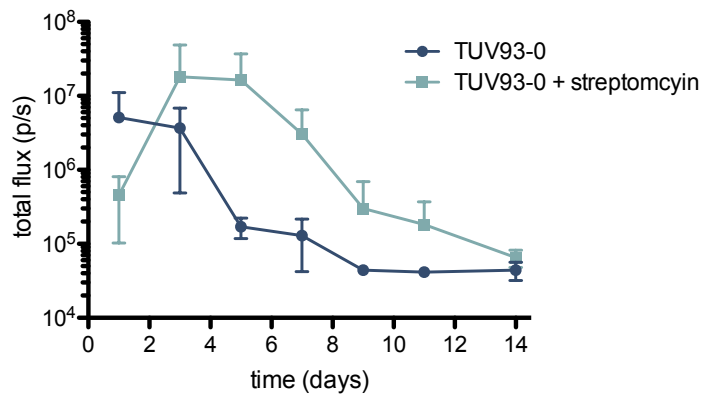


Figure 3-5: Effect of streptomycin-treated drinking water on TUV93-0 colonisation of ICR mice. Two groups of mice, five animals in each group, were treated with 5 g/L streptomycin in drinking water for 3 days before infection with 10^9 CFU *lux*-marked TUV93-0 transformed with pGB2, and supplied with either normal drinking water (dark blue) or 5 g/L streptomycin-containing water (light blue) after infection. Luminescence were monitored for 14 days after infection. Data points shown are the mean of each group with standard deviation from the mean displayed as error bars.

To monitor possible plasmid loss, faeces were plated on agar containing erythromycin alone, and on agar containing erythromycin and streptomycin. If plasmid loss were to occur, there should be a reduction in the number of colonies found on plates containing streptomycin compared to erythromycin plates. However, no significant difference in the faecal counts was observed, even when the bacteria were recovered from mice not supplied with streptomycin drinking water (Figure 3-6). Therefore, even in the absence of selection *in vivo*, the pGB2 plasmid is stably maintained in the *E. coli* strains colonising the mouse intestine.

3. RESULTS: Mouse models of *E. coli* infection

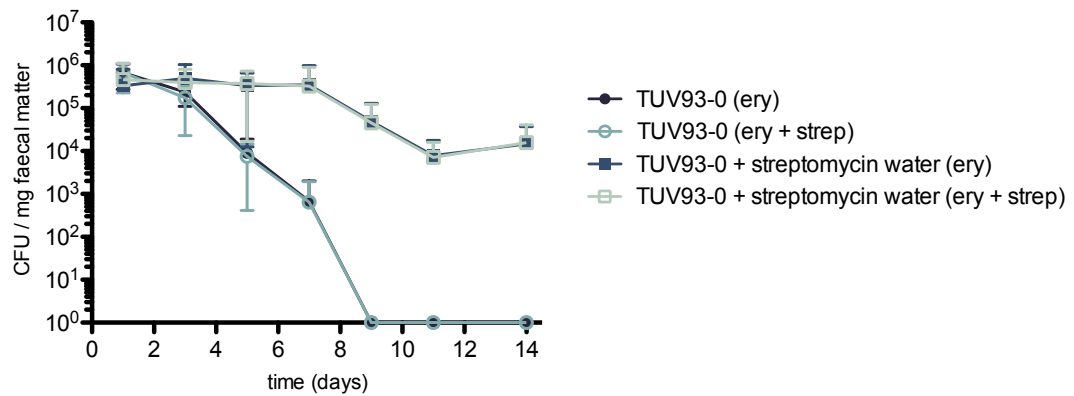


Figure 3-6: pGB2 plasmid stability. Faecal shedding of two groups of ICR mice, five mice in each group, treated with 5 g/L streptomycin in drinking water for 3 days before infection with 10^9 CFU *lux*-marked TUV93-0 transformed with pGB2 (conferring streptomycin resistance), and supplied with either normal drinking water (circular symbols) or 5 g/L streptomycin-containing water (square symbols) after infection. Faecal shedding was monitored for 14 days after infection, using agar plates containing erythromycin only, or erythromycin and streptomycin, with faecal counts from both plates displayed. Data points shown are the mean of each group, and standard deviation from the mean displayed as error bars.

3.5.2 Generation of Str^R bacterial strains

Although the pGB2 plasmid appeared to be stably maintained, for long term development of the model a strain in which antibiotic resistance is chromosomally encoded was considered desirable. Initially we attempted to confer streptomycin resistance to *E. coli* by replacing the erythromycin resistance gene in the p16S*lux* plasmid with the streptomycin resistance-encoding gene *aadA*. This strategy however proved unsuccessful and, as an alternative, spontaneous streptomycin-resistant mutants of *E. coli* were created and characterised.

Streptomycin is an antibiotic which functions by binding the small 16S rRNA of the bacterial 30S ribosome subunit, interfering with tRNA binding to the ribosome and resulting in codon misreading and inhibition of protein synthesis. Spontaneous streptomycin resistance in *E. coli* frequently arises as a consequence of mutation in the *rpsL* gene encoding the ribosomal protein S12. Mutations in S12 leads to slower but less translational error-prone ribosomes that are able to overcome the effects of streptomycin (Ruusala *et al.*, 1984).

3. RESULTS: Mouse models of *E. coli* infection

To generate spontaneous streptomycin-resistant mutants, *lux*-marked TUV93-0, LF82 and OI-148A (a TUV93-0 strain with a partial LEE deletion, rendering it unable to produce the T3SS) were grown on agar containing 100 µg/ml streptomycin. Eight colonies from each strain were selected and characterised to determine if acquisition of Str^R had altered the phenotypic characteristics of the organism. Mutants were tested for their ability to grow in LB, MEM and M9 media, to show motility on 0.25% agar, and to adhere to human epithelial cells (Appendices 9.1).

Additionally, the *rpsL* gene of each mutant was sequenced and each found to contain either one or two point mutations. In all three strains of *E. coli*, at least one mutant contained a single point mutation of an adenine to a cytosine at nucleotide 128, which resulted in a lysine to threonine change at amino acid 42 (K42T). This mutation has been reported to provide streptomycin resistance with a minimum inhibitory concentration (MIC) of 2 mg/ml, without making the bacteria dependent on the presence of streptomycin for growth (Carr *et al.*, 2005). Strains with this mutation also showed good growth, motility, secretion and adhesion profiles, and therefore those containing this mutation were selected for assessment in animal models.

3.5.3 Colonisation of streptomycin-treated ICR mice by Str^R TUV93-0 and OI-148A

The ability to produce T3SS-mediated attaching/effacing lesions on the surface of host cells is a defining characteristic of EHEC infection, and allows bacteria to colonise and persist within its host. To evaluate the importance of the T3SS in O157:H7 mouse colonisation, ICR mice given 5 g/L streptomycin in their drinking water for three days were infected with either Str^R *lux*-marked TUV-93 or T3SS-negative OI-148A. All animals were supplied with streptomycin in their drinking water after infection. Faecal shedding was followed for 9 days after infection, and there was no significant difference found between the two strains at any time point. Live imaging of the two groups also showed no difference in persistence (Figure 3-7).

3. RESULTS: Mouse models of *E. coli* infection

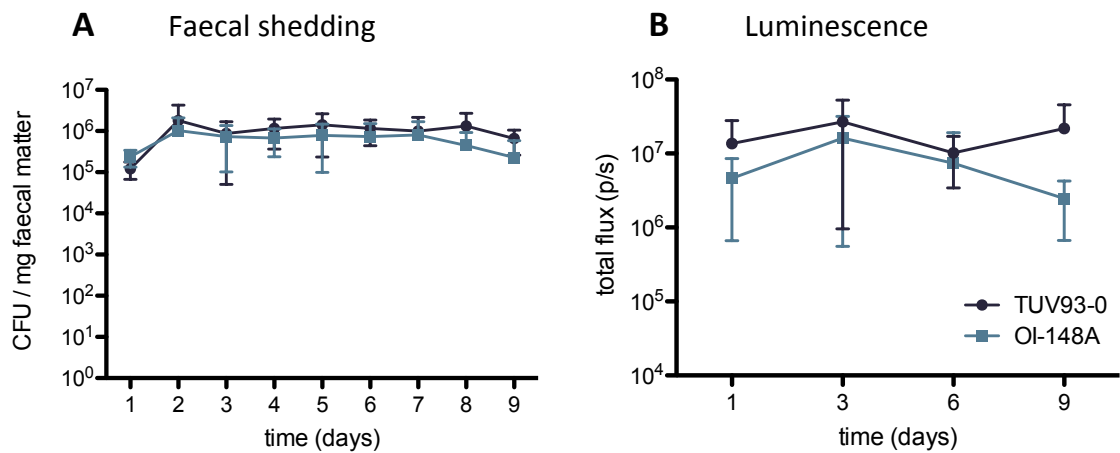


Figure 3-7: Colonisation of TUV93-0 and OI-148A. Two groups of streptomycin-treated ICR mice, 15 mice in each group, were infected with *lux*-marked Str^R TUV93-0 (dark blue) or the T3SS-negative OI-148A (light blue), and colonisation monitored by faecal shedding (A) and luminescence (B) for 9 days after infection. Drinking water containing 5 g/L streptomycin was provided to both groups throughout the post infection period. Five mice from each group were culled at days 3, 6 and 9. Data points shown are the mean of each group, and standard deviation from the mean displayed as error bars. No significant differences ($p < 0.05$) between the means of the two groups, as determined by Student's unpaired t-test, were found for at any time point

At 3, 5 and 9 days following challenge, 5 mice from each group were culled by cervical dislocation and subjected to post-mortem examination to determine the number of bacteria located in the lumen of the intestine and those more intimately attached to intestinal epithelial cells. The entire caecum, small intestine (from the duodenum to the ileum) and large intestine (from the ascending colon to the rectum) of each mouse was removed and separated from each other, contents removed to measure lumen bacteria, and tissue homogenised to release those bacteria adhered to epithelial cells. Bacteria were found to be associated with all areas of the gut, with the caecum and large intestine more heavily colonised than the small bowel. However, no significant difference in numbers of bacteria in either the lumen or tissue between the two strains was observed at any time point (Figure 3-8). This would suggest that while TUV93-0 is capable of adhesion mediated through expression of the T3SS, it does not appear relevant in this model as OI-148A, a strain unable to make this structure, was recovered at levels equivalent to that of TUV93-0.

3. RESULTS: Mouse models of *E. coli* infection

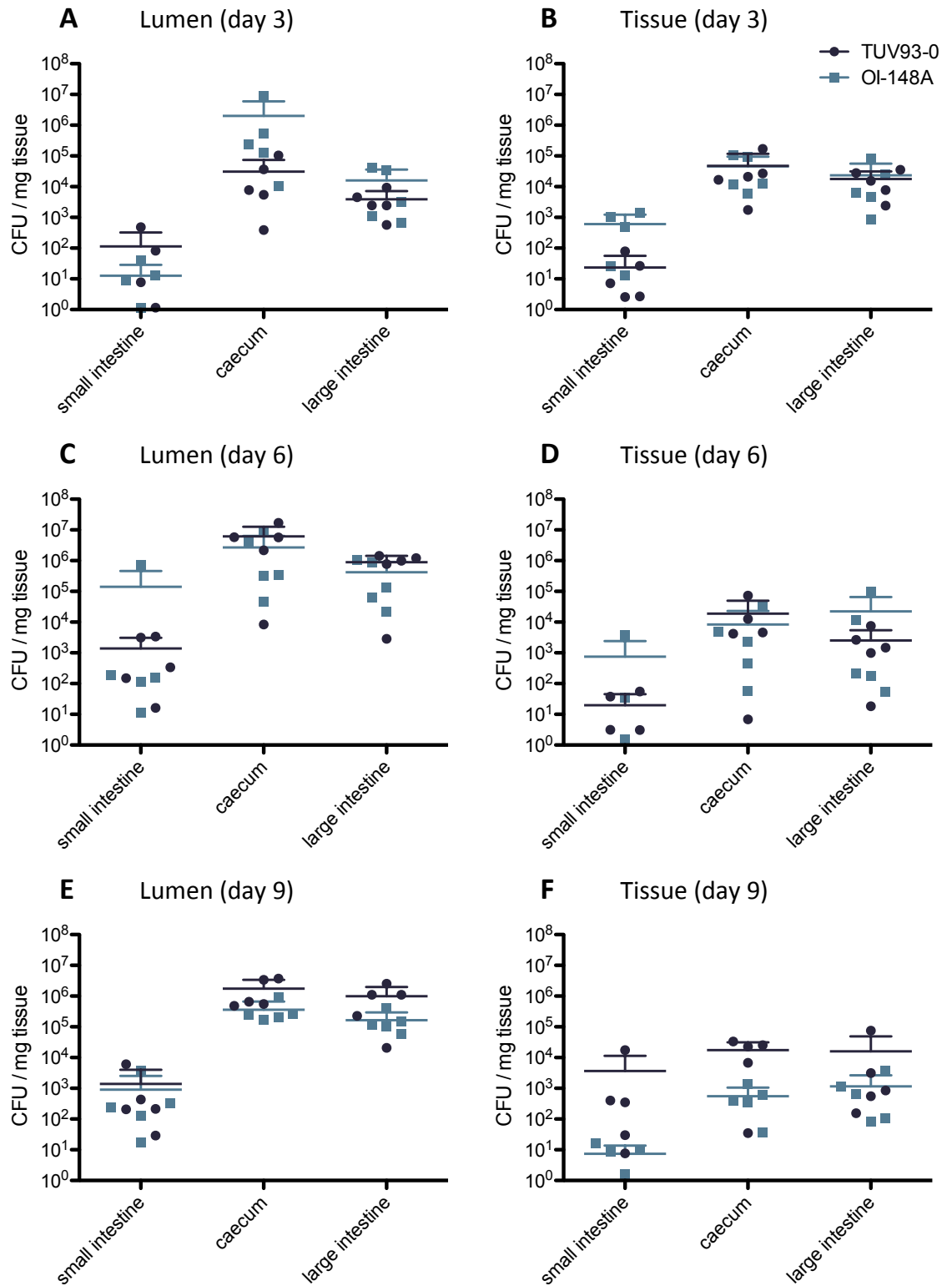


Figure 3-8: Intestinal bacterial recovery of TUV93-0 and OI-148A. Lumen (A, C, E) and tissue (B, D, F) colonisation of the small intestine, caecum and large intestine of streptomycin-treated ICR infected with 10⁹ CFU *lux*-marked Str^R TUV93-0 (dark blue) or OI-148A (light blue). Five mice from each group (which initially contained 15 mice in each group) were culled at time points of 3 (A, B), 6 (C, D) and 9 (E, F) days after infection and the concentration of TUV93-0 or OI-148A per mg organ tissue in the lumen or attached to tissue determined for the three organs. Symbols represent bacterial counts from a single animal. The mean bacterial count of each group (long line) and standard deviation from the mean (short line) are also

3. RESULTS: Mouse models of *E. coli* infection

indicated. No significant differences ($p < 0.05$) between the means of the two groups, as determined by Student's unpaired t-test, were found between strains in or attached to any organ at any time point.

As no significant difference between the two strains was observed either for faecal shedding, luminescence, or bacterial attachment to intestinal tissue, we concluded that persistence of the organism within the model is not dependent on the T3SS. This implies that colonisation is due to the bacteria's ability to survive and replicate in the intestinal lumen in the absence of competing natural gut microflora. Therefore this model is a poor replicator of T3SS-mediated colonisation, and would not be suitable for use in *in vivo* testing of anti-virulence drugs that target this structure.

3.5.4 Colonisation of streptomycin-treated ICR mice by Str^R LF82

LF82 is an adherent and invasive *E. coli* strain that does not encode the T3SS. However, this organism encodes the putative lipoprotein YghJ, whose involvement in LF82 colonisation of mice we were interested in exploring. To determine how effectively this strain colonised the streptomycin-treated model, ICR mice were infected with Str^R *lux*-marked LF82 and streptomycin treatment continued, as per the TUV93-0 infection model. In these experiments, LF82 was shed at high levels (10^5 - 10^7 CFU/mg faeces) for the first 6 days post infection, with the highest faecal shedding observed on day 4, followed by a gradual decrease in shedding (Figure 3-9 A). Luminescence of LF82 was also strong, with all animals showing strong colonisation throughout the post infection period (Figure 3-9 B). Both these levels were comparable to those of TUV93-0.

3. RESULTS: Mouse models of *E. coli* infection

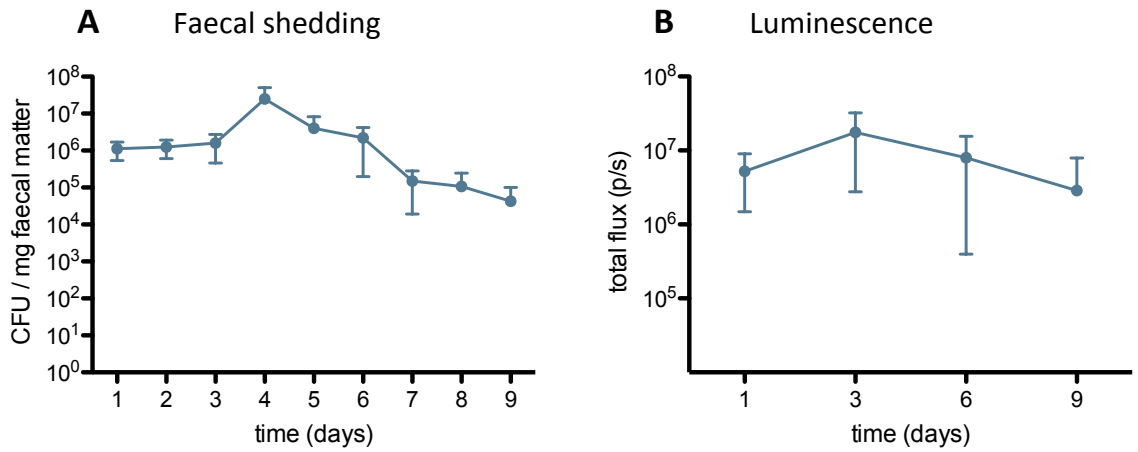


Figure 3-9: Colonisation of LF82. Fifteen streptomycin-treated ICR mice were infected with 10⁹ CFU *lux*-marked Str^R LF82 and drinking water containing 5 g/L streptomycin provided throughout the post infection period. Colonisation was monitored by faecal shedding (A) and luminescence (B) for 9 days after infection. Five mice were culled at 3, 6 and 9 days after infection. Data points shown are the mean of each group, and standard deviation from the mean displayed as error bars.

Recovery of intestinal LF82 from mice culled at 3, 6 and 9 days after infection found that colonisation was similar to that of TUV93-0; counts were highest in both the tissue and lumen of the caecum and large intestine, although the small intestine also showed colonisation throughout the post infection period (Figure 3-10). Although LF82 does not attach to host epithelial tissue via the T3SS, the high levels of bacteria in the lumen of the intestine coupled with how relative colonisation levels in the three organs remains consistent over time suggests that, like TUV93-0, LF82 displays persistence rather than true adherence and colonisation.

3. RESULTS: Mouse models of *E. coli* infection

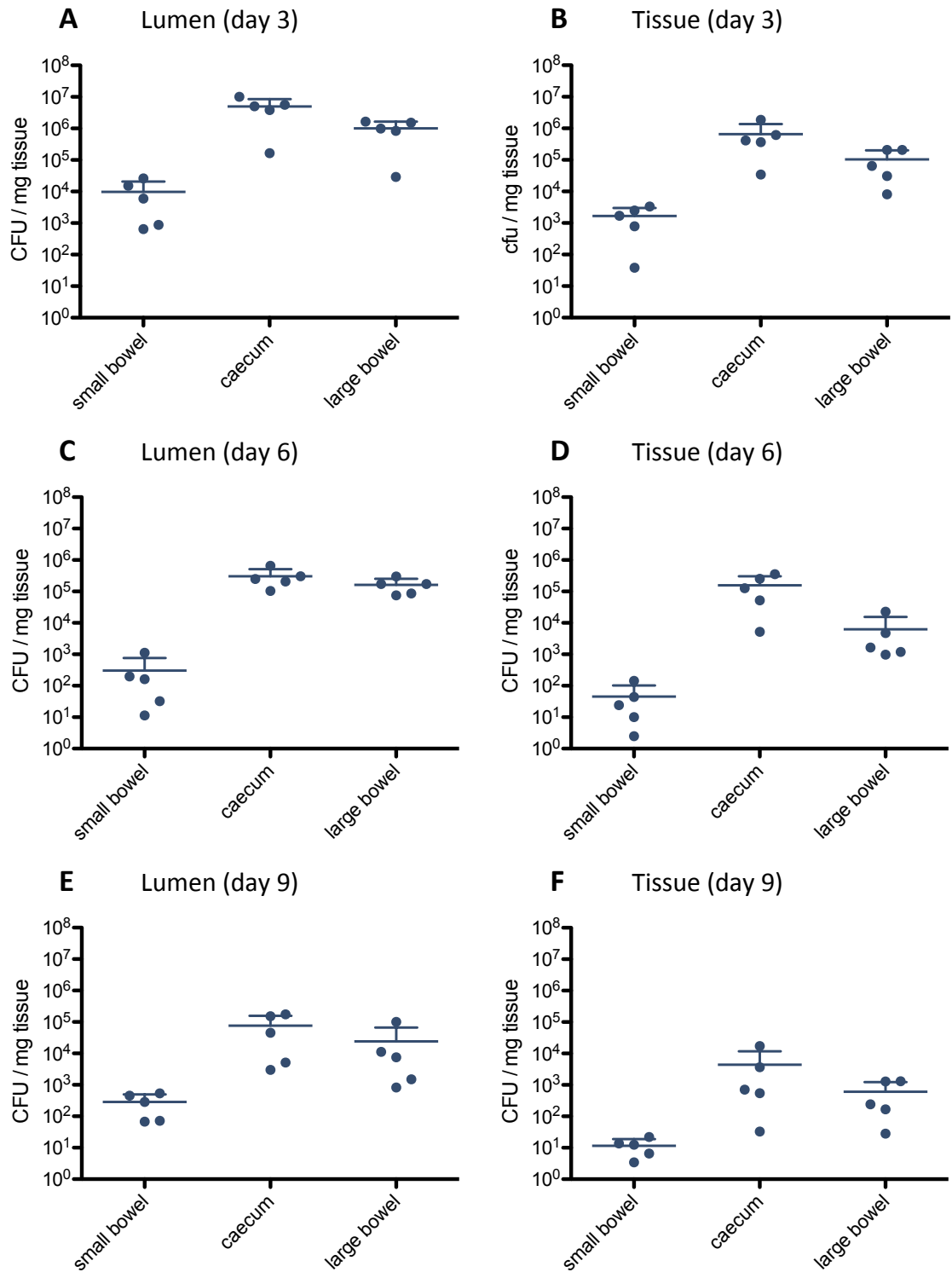


Figure 3-10: Intestinal bacterial recovery of LF82. Lumen (A, C, E) and tissue (B, D, F) colonisation of the small intestine, caecum and large intestine of streptomycin-treated ICR mice infected with 10^9 CFU *lux*-marked *Str^R* LF82. Five mice from each group (which initially contained 15 mice) were culled at time points of 3 (A, B), 6 (C, D) and 9 (E, F) days after infection and the number of LF82 per mg of organ tissue in the lumen or attached to tissue determined for the three organs. Symbols represent bacterial counts from a single animal. The mean bacterial count of each group (long line) and standard deviation from the mean (short line) are also indicated.

3.6 Stx-producing *Citrobacter rodentium*

3.6.1 Colonisation and pathogenesis of Stx-producing *C. rodentium*

As the streptomycin-treated ICR model showed no significant difference in colonisation levels between the wild type and T3SS-negative TUV93-0 strain, it would appear that this model cannot be used to screen drugs that target this structure. However, the capacity to generate the T3SS is not the only important virulence trait expressed by *E. coli* O157:H7 strains. The expression of Stx2 toxin results in significant kidney damage in infected individuals, and so drugs that modify Stx2 also warrant evaluation. Recently, a novel *Citrobacter rodentium* strain that produces Stx2 at comparable levels to O157:H7 was described in which the Stx2dact phage was inserted into the chromosome of *C. rodentium* (Mallick *et al.*, 2012). This strain, *C. rodentium* (λ stx_{2dact}), has been reported to result in lethal infection in C57BL/6 mice, as a consequence of Stx-mediated damage to kidney and intestinal tissues. The use of *C. rodentium* in this system is also attractive as adhesion of the bacteria to the host intestinal epithelial surface has been attributed to the expression of the T3SS (Mallick *et al.*, 2012). As we had additional interest in testing of compounds that target the Shiga toxin, characterisation of this model was undertaken.

The wild type *C. rodentium* and the λ stx_{2dact} strain, a kind gift from Prof. John Leong (Tufts University), were made luminescent by p16*Slux* integration. In order to replicate the original study findings (Mallick *et al.*, 2012), C57BL/6 and BALB/c mice were infected with either wild type or Stx2-expressing *C. rodentium*. As weight loss was used as a reliable indicator of illness in this model, animals were weighed daily and were culled once they lost more than of 15% of their weight at the start of the experiment.

While C57BL/6 and BALB/c mice infected with wild type *C. rodentium* maintained body weight throughout infection, BALB/c mice infected with *C. rodentium* (λ stx_{2dact}) rapidly lost weight. Shortly after infection, three animals reached experimental endpoint (loss of >15% of their starting body weight) 5 days after infection and the remaining two animals were culled by day 6 (Figure 3-11 A, B). Although these remaining two animals had not yet lost >15% of weight, strong visual and behavioural signs suggested significant illness.

3. RESULTS: Mouse models of *E. coli* infection

In contrast, C57BL/6 mice infected with the same *C. rodentium* (λ stx_{2dact}) strain showed no significant weight loss in the first week after infection, contrary to the Mallick *et al.* (2012) study. Two C57BL/6 mice from both the wild type and λ stx_{2dact} group were culled at day 6 for histological comparison to the BALB/c mice. Interestingly, during the second week after infection, body weight of all three C57BL/6 members of the λ stx_{2dact} group declined, with one mouse reaching a weight loss of >15% by day 10, although no visual or behavioural signs of illness were observed for any of the animals. The remaining two mice showed an increase in weight between days 12 and 14, presumably due to clearance of bacteria (Figure 3-11 C, D).

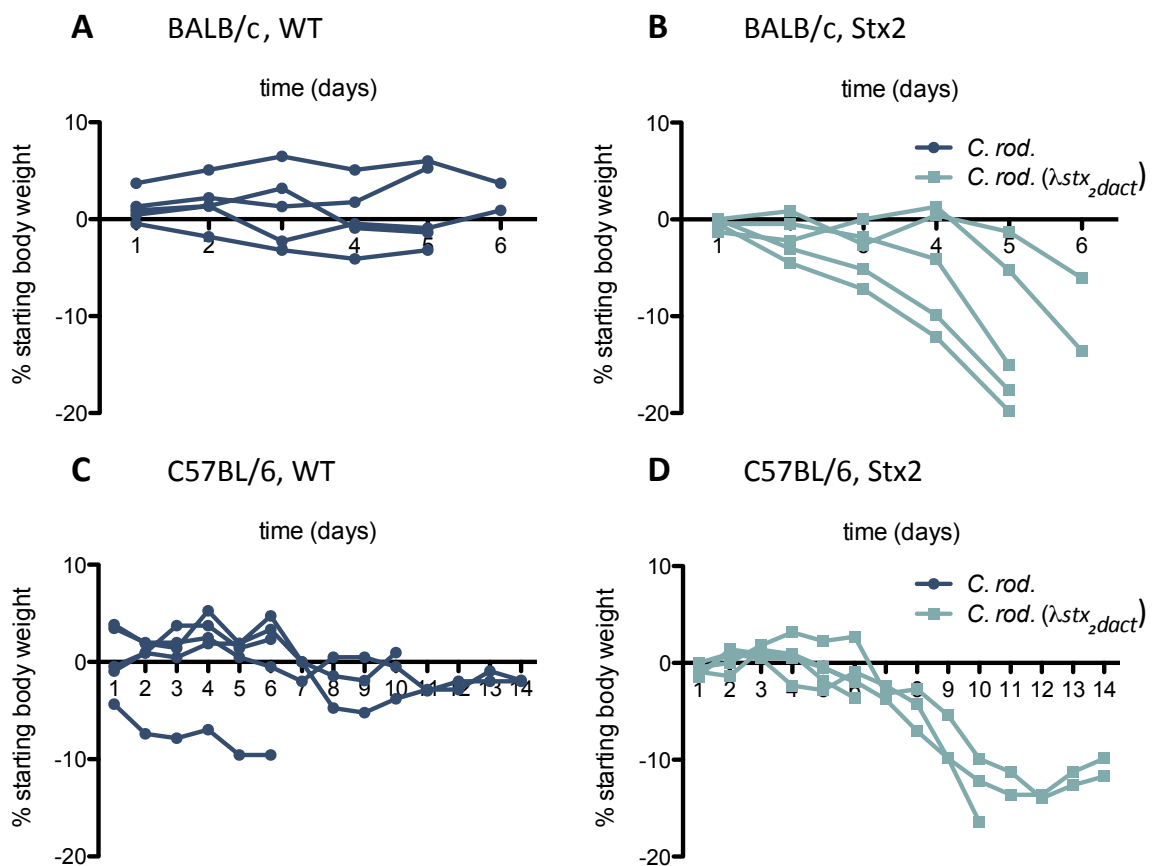


Figure 3-11: Weight changes of *C. rodentium* and *C. rodentium* (λ stx_{2dact})-infected mice. Five BALB/c (A, B) and five C57BL/6 (C, D) mice were infected with 10^9 CFU *lux*-marked *C. rodentium* (dark blue) or *C. rodentium* (λ stx_{2dact}) (light blue) by oral gavage. Animals were monitored for weight loss once daily after infection, and animals were culled once a >15% decrease in starting weight was reached. Data points represent the weights of individual mice.

Colonisation levels, as measured by faecal shedding and live imaging, indicated that both bacterial strains were present in the mice and were shed at equivalent levels in both BALB/c and C57BL/6 mice (Figure 3-12 A, C). High faecal shedding and luminescence in

3. RESULTS: Mouse models of *E. coli* infection

C57BL/6 mice during the first week of infection suggests that the lack of symptoms does not reflect poor bacterial colonisation. Colonisation levels in C57BL/6 mice decreased during the second week of infection, which is probably due to the natural clearance of the bacteria. Interestingly, the decrease in weight of C57BL/6 mice infected with λstx_{2dact} seen during the second week of infection occurs at the point at which bacterial colonisation starts to decrease due to natural clearance.

While both faecal shedding and luminescence levels of the λstx_{2dact} strain in C57BL/6 mice appeared lower than that of the wild type between days 10 and 14 of the post infection period, the small number (2-3) of mice in each group at these time points likely contributes to this variation in average colonisation levels.

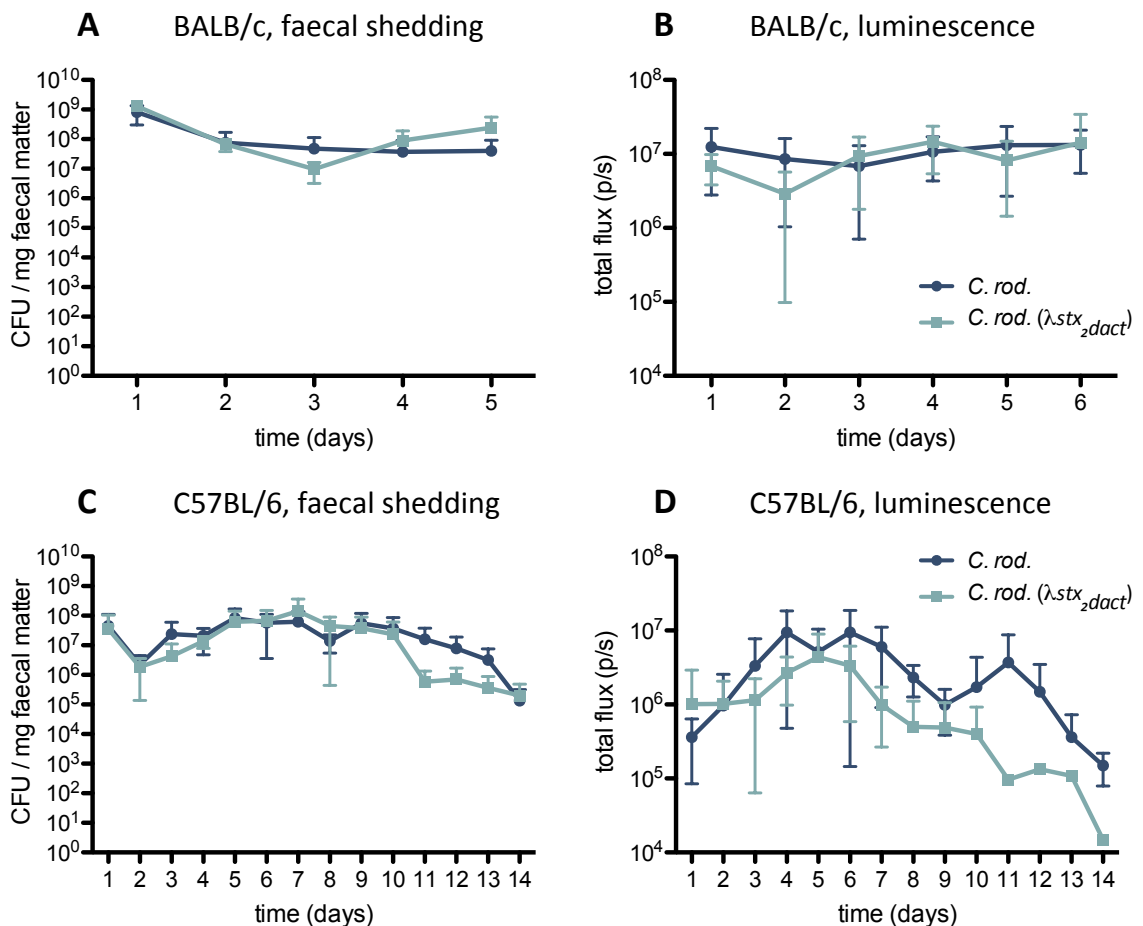


Figure 3-12: Colonisation of wild type *C. rodentium* and *C. rodentium* (λstx_{2dact}) in BALB/c and C57BL/6. Five BALB/c (A, B) and five C57BL/6 (C, D) mice were infected with *lux*-marked *C. rodentium* (dark blue) or *C. rodentium* (λstx_{2dact}) (light blue). Colonisation was monitored by faecal shedding (A, C) and luminescence (B, D). Data points represent the mean of each group with standard deviation from the mean displayed by error bars. As mice were culled once a >15% decrease in starting body weight was reached, the number of mice in each group does not stay consistent throughout the post infection period.

3. RESULTS: Mouse models of *E. coli* infection

After all animals were euthanised, kidneys were removed and prepared for histology using PAS and H&E staining, and examined by light microscopy. Stx-mediated pathology was observed in both BALB/c and C57BL/6 mice infected with the λ stx_{2dact} strain, while mice infected with the wild type strain showed no signs of tissue damage. Two main histological changes were seen in kidneys from λ stx_{2dact} mice: tubular injury and interstitial haemorrhage. Proximal tubules showed patchy degenerative changes that included a loss of apical brush borders, cytoplasmic simplification and vacuolisation, enlarged nuclei with prominent nucleoli, and luminal ectasia with focal sloughing of epithelial cells into tubular lumina (Figure 3-13). Microscopy images were blind scored for tissue damage, where 0 = no injury, 1 = mild damage, 2 = moderate damage, and 3 = severe damage, with scoring determined by comparison to representative renal biopsies published by D'Agati *et al.* (2005). Two images from each mouse were scored, with all BALB/c and C57BL/6 mice infected with *C. rodentium* scoring 0 for both PAS and H&E images. BALB/c mice infected with λ stx_{2dact} scored an average of 1.1 for PAS and 1.5 for H&E images, and C57BL/C mice infected with λ stx_{2dact} scored an average of 0.7 for PAS and 1.0 for H&E. These findings demonstrate that while λ stx_{2dact} only produces weak signs of illness in C57BL/6 mice, Stx-mediated kidney damage still occurs during infection.

3. RESULTS: Mouse models of *E. coli* infection

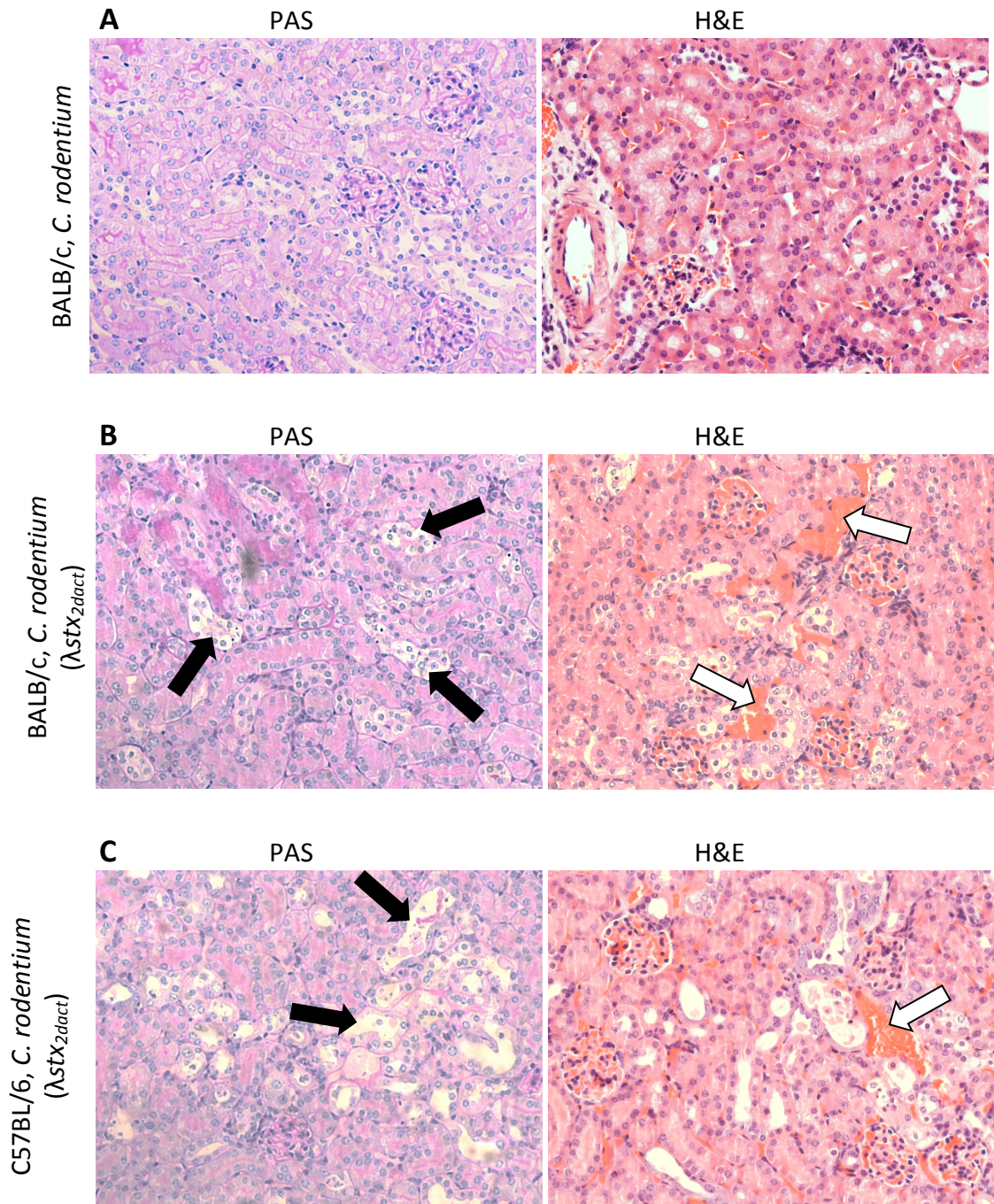


Figure 3-13: *C. rodentium* (λ stx_{2dact}) causes tubular injury and interstitial haemorrhage in kidneys of BALB/c and C57BL/6 mice. Representative images (400x magnification) of PAS and H&E-stained kidney sections from BALB/c mice infected with *lux*-marked *C. rodentium* (A) or *C. rodentium* (λ stx_{2dact}) (B), and C57BL/6 mice infected with *C. rodentium* (λ stx_{2dact}) (C). Black arrows indicate proximal tubules with degenerative changes including focal sloughed epithelial cells. White arrows indicate focal interstitial haemorrhages. BALB/c kidneys sections were from animals culled at 4 and 5 days after infection, and kidney sections from the C57BL/6 example were obtained from the single animal culled due to weight loss at 10 days after infection.

3. RESULTS: Mouse models of *E. coli* infection

3.6.2 Colonisation and production of disease by *C. rodentium* (λ stx_{2dact}) is dependent on the T3SS

To confirm that *C. rodentium* (λ stx_{2dact}) relies on the T3SS for colonisation and disease, BALB/c mice were infected with either *C. rodentium* or the Stx-2 expressing *tir* mutant *C. rodentium* (λ stx_{2dact}) Δ *tir*. Mice in the group with *C. rodentium* showed colonisation levels that gradually increased over time, while those infected with the Δ *tir* strain exhibited a rapid decline in the number of bacteria recovered by faecal shedding or detected by luminescence (Figure 3-14 A, B). Animals from both groups did not lose any body weight (Figure 3-14 C), or display any signs or behaviour indicating illness. These findings imply that when prevented from forming A/E lesions by the lack of Tir expression, *C. rodentium* is unable to colonise the mouse intestine effectively, resulting in faster clearance of the bacteria and no mortality or observable illness. This data confirms that the T3SS is an essential virulence factor during lethal infection of *C. rodentium*.

3. RESULTS: Mouse models of *E. coli* infection

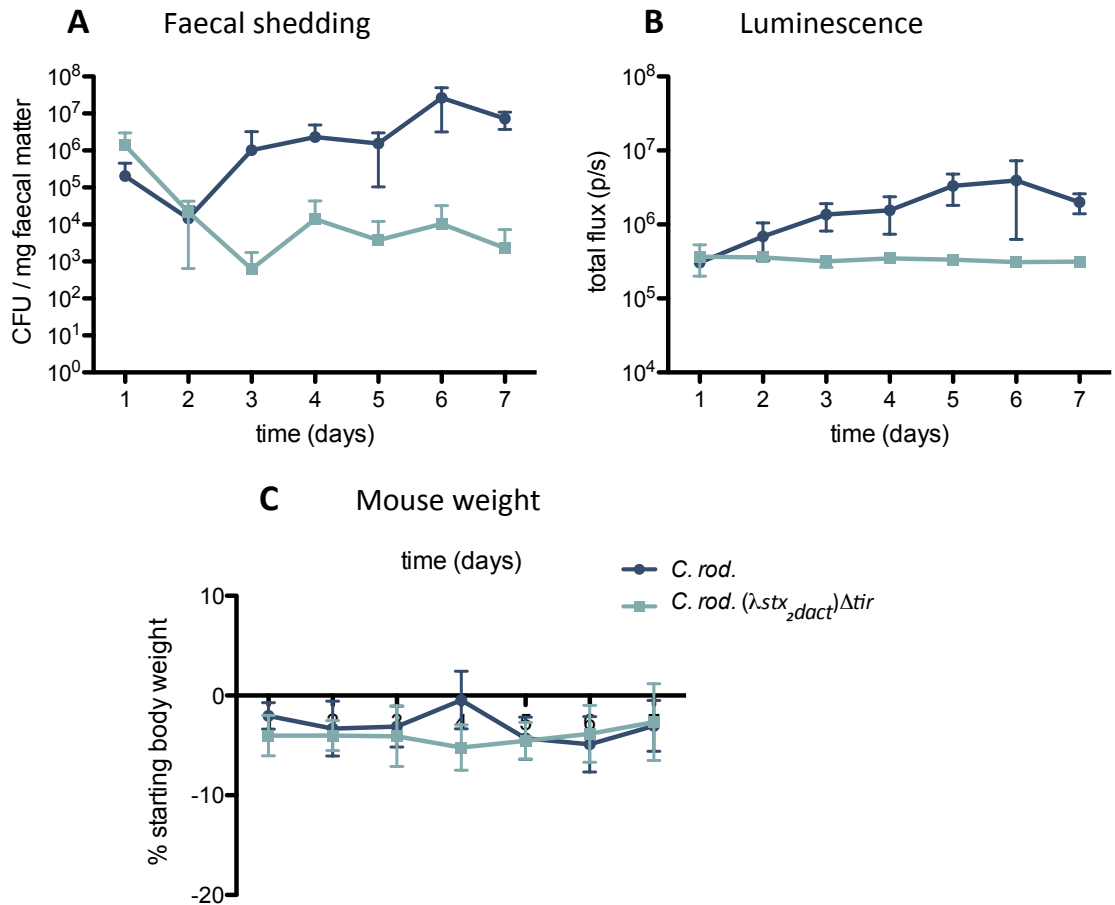


Figure 3-14: Production of Tir is required for colonisation and production of disease by *C. rodentium* (λ stx_{2dact}). Two groups of BALB/c mice, five mice in each group, were infected with 10⁰ CFU *lux*-marked *C. rodentium* (dark blue) or *C. rodentium* (λ stx_{2dact}) Δ tir (light blue). Colonisation was monitored by faecal shedding (A) and luminescence (B), and animals were weighed daily to monitor body weight changes (C). Data points represent the mean of each group with standard deviation from the mean shown by error bars.

3.7 Discussion

3.7.1 Streptomycin treatment of mice lowers colonisation resistance to *E. coli*

The original aim of this work was to establish a mouse model of *E. coli* colonisation using inbred mice, in which colonisation would be robust and dependent on T3SS production. Of the three inbred mouse strains tested, no differences in colonisation were observed, although BALB/c mice proved most suited to live-image monitoring. Pretreatment of BALB/c mice with DSS, in order to decrease the intestinal mucosal layer and allow *E. coli* to interact more directly with epithelial cells, produced no significant increase in either levels or length of colonisation by TUV93-0 or LF82.

In contrast, streptomycin pretreatment of the outbred ICR mouse strain followed by continuation of streptomycin after infection produced high, stable levels of bacterial colonisation by both TUV93-0 and LF82. The chromosomal integration of the *lux* operon provided an additional useful tool for monitoring colonisation. Despite the greater genetic variation that accompanies outbred mouse strains, all animals infected were successfully colonised and showed robust levels of colonisation.

Streptomycin treatment has a history of use in animal models of bacterial infections, including *E. coli* in cattle (Snider *et al.*, 2006), and mouse models of *Salmonella*, *Vibrio*, and *Klebsiella* (Barthel *et al.*, 2003; Olivier *et al.*, 2009; Favre-Bonté *et al.*, 1999). The exact mechanism by which streptomycin treatment lowers mouse resistance to *E. coli* colonisation is not yet fully understood. It is assumed that streptomycin treatment modifies the diversity of bacteria within the gut that under normal conditions prevent *E. coli* colonisation, either by competition for nutrients or by metabolic exclusion (Lawley & Walker, 2013). Mouse models using gnotobiotic animals, which require no antibiotic treatment for *E. coli* colonisation to occur, support this view. However, an alternate hypothesis has been presented by Spees *et al.* (2013) that suggests streptomycin produces conditions favourable to *E. coli* colonisation by initiating low-level intestinal inflammation. For example, streptomycin makes mice more susceptible to the development of DSS-induced colitis, implying that streptomycin lowers colonisation

3. RESULTS: Mouse models of *E. coli* infection

resistance by changing mucosal immune responses. In this published work, the caecal mucosa of streptomycin-treated mice showed a mild inflammatory infiltrate accompanied by raised expression of *nos2*, which encodes inducible nitric oxide synthase. Luminal growth of *E. coli* was increased by nitrate respiration in a NOS2-dependent manner, due to anaerobic respiration allowing *E. coli* to utilise non-fermentable carbon sources. These findings raise the possibility that streptomycin treatment allows *E. coli* to colonise by not only clearing competitive intestinal bacteria, but by creating a new niche in which the organism can flourish (Spees *et al.*, 2013).

It has also been suggested that streptomycin treatment promotes *E. coli* colonisation by altering the pH and volatile fatty acid (VFA) concentration in the caecum (Hentges *et al.*, 1990). When caecal contents of Str-treated mice were adjusted to match the pH and VFA conditions of untreated mice, the growth of *E. coli* was reduced and resembled that shown by *E. coli* in caecal contents of untreated mice. Additionally, when untreated caecal contents were adjusted to resemble the streptomycin-treated caecum, bacterial growth was increased (Hentges *et al.*, 1990).

3.7.2 The Str-treated TUV93-0 mouse model is not T3SS-dependent

As we required a T3SS-dependent TUV93-0 model for *in vivo* testing of novel compounds that target this virulence factor, the streptomycin-treated model needed to demonstrate an observable and significant change in colonisation when the T3SS was inhibited. To ensure persistence in the streptomycin-treated gut, spontaneous Str^R mutants of TUV93-0 and the T3SS-negative OI-148A were generated. Sequencing of the *rpsL* gene of these mutants allowed selection of strains with a common mutation. Str^R mutations can be classed as restrictive, decreasing the rate of translation and increasing cell doubling time, or non-restrictive, which behave in a similar manner to wild type strains. The K42T *rpsL* mutation that was present in all spontaneous Str^R *E. coli* strains is a restrictive mutation; however, growth, motility and adhesion profiles showed that none of these traits differed greatly from the behavior of the wild type strain, and these mutants were subsequently tested *in vivo*.

3. RESULTS: Mouse models of *E. coli* infection

Infection of streptomycin-treated ICR mice with Str^R TUV93-0 or the T3SS-negative O1-148A strain resulted in no significant difference in levels of colonisation. Bacterial counts recovered from all three regions of the gut were equivalent throughout the infection, with no difference between attached and lumen-associated bacteria observed. This implies that O157:H7 is able to persist in the intestinal lumen in the absence of natural gut microbiota, and that this is not dependent on T3SS expression. While our study did not find any measurable difference between wild type and T3SS-lacking O157:H7, this does not mean that bacteria do not form any A/E lesions using the T3SS, as A/E lesions have been previously reported in mice infected by O157:H7. Using the mouse loop model, Girard *et al.* (2008) directly infected mouse ileal loops with 10⁹ CFU of either O157:H7 or a *tir* mutant. After an incubation of three hours, tissue was removed and examined by electron microscopy, revealing A/E lesions present only in loops infected with the wild type. However, A/E lesions were observed infrequently, and the authors of the study conceded that these lesions may occur because of the high number of bacteria trapped in the mouse loops during the incubation (Girard *et al.*, 2008). Considering these experiments, it is unsurprising that we were unable to determine any T3SS effect on colonisation in the Str^R mouse model.

The influence of the T3SS on EHEC colonisation of mice has also been previously explored by Nagano *et al.* (2003). This study suggested that the T3SS may confer a persistence advantage at a time point later than considered in our study. When non-antibiotic-treated ICR mice were orally infected with O157:H7 GPU96MM, this strain was shed in faeces up to 4 weeks after infection. In contrast, a strain containing an *espA* deletion mutation was undetectable in faeces 1-2 weeks post infection (Nagano *et al.*, 2003). This implies that the T3SS may be important for prolonged colonisation. There are, however, notable differences between this experiment and the ones presented in this chapter. Aside from the different O157:H7 strains used, Nagano *et al.* (2003) used untreated mice in which colonisation of the O157:H7 strain was high and sustained for several weeks in the absence of antibiotic treatment. This contrasts our findings with TUV93-0 and non-streptomycin-treated mice. This is unsurprising, as colonisation of O157:H7 in mice with an intact commensal flora has been reported to be variable, possibly due to differences in both the O157:H7 strain and the microbiota composition of mice from different suppliers (Mohawk *et al.*, 2010). Additionally, confocal microscopy by Nagano *et al.* (2003) of

3. RESULTS: Mouse models of *E. coli* infection

intestinal tissue taken from 1 hour to 3 days after infection by GPU96MM found no evidence of A/E lesions on either the large or small intestine, despite bacteria being detected in the intestinal mucosa very soon after infection. However, in caecal tissue samples taken 18 hours to 3 days after infection, microcolonies and diffuse adherence of GPU96MM with accumulation of filamentous actin beneath the attached bacteria were observed (Nagano *et al.*, 2003). This has led to the hypothesis that the site of EHEC colonisation in mice is the caecum, and bacteria are shed into the caecal contents before passing into the large intestine, where they are then expelled in faecal matter (Nagano *et al.*, 2003; Mohawk *et al.*, 2010). It would therefore be interesting to explore whether a significant difference in colonisation levels would occur between TUV93-0 and OI-148A during an extended post infection period.

Shortly after completing our TUV93-0/OI-148A experimentation, a study by Chen *et al.* (2013) was published which indicated that Str^R mutants show significantly reduced Type 3 secretion. Spontaneous restrictive Str^R mutants, including the K42T mutant, displayed severely reduced secretion of EspA, the component of the T3SS syringe tip required for interaction with host cells, and EspB, a protein translocated into the host and necessary for formation of pores in the host membrane and translocation of Tir. The decreased secretion was due to a reduced rate of EspA and EspB protein synthesis, and mutants showed compromised adherence and A/E formation *in vitro*. Secretion assays and immunoblotting for EspD using the TUV93-0 K42T Str^R strain have also indicated a decrease in secretion of this T3SS protein (Tom Parker, personal communication). This study by Chen *et al.* (2013) suggests a currently unknown link between Str^R mutations and the T3SS-related virulence potential of this strain, although no *in vivo* experiments were performed (Chen *et al.*, 2013).

These findings suggested that the lack of a difference in colonisation levels between TUV93-0 and OI-148A may reflect the inability of the TUV93-0 Str^R strains to form A/E lesions. To address this issue, the experiments were repeated using TUV93-0 and OI-148A strains that were transformed with the streptomycin resistance-encoding pGB2 plasmid. Colonisation levels of these strains as measured by faecal shedding and live imaging were very similar to those of the *rpsL* mutants, and showed no significant difference between the wild type and the T3SS-negative strain. Luminal and tissue-attached bacteria in the

3. RESULTS: Mouse models of *E. coli* infection

caecum, small intestine and large intestine also appeared similar to the K42T mutants, and no significant difference between TUV93-0 and OI-148A was observed (Appendices 9.2). This suggests that our initial observation that persistence not associated with generation of a T3SS structure is reliable. Therefore, the ability of EHEC to persist in high numbers throughout infected mice without the model displaying dependence on the T3SS raises the issue of how useful EHEC mouse models are for *in vivo* testing of potential anti-virulence compounds.

3.7.3 The Stx-expressing *Citrobacter rodentium* mouse model is a strong replicator of T3SS-mediated adhesion and Stx-mediated kidney damage

As the Str^R-treated TUV93-0 model was deemed unsuitable for studying the T3SS' effect on colonisation, the Stx_{2dact}-expressing *C. rodentium* model, developed by Mallick *et al.* (2012), was investigated as an O157:H7 surrogate. BALB/c mice infected with this strain showed visual signs of illness a few days after infection along with decreasing body weight, while colonisation levels were high and stable throughout the infection. All λ Stx_{2dact}-infected animals became ill 5-6 days post infection and kidney histology revealed proximal tubule injury consistent with the Mallick *et al.* (2012) findings. A *C. rodentium* (λ Stx_{2dact}) Δ tir strain unable to produce A/E lesions resulted in poor colonisation and no signs of disease or mortality, making this an excellent surrogate *E. coli* model for studying both T3SS-mediated adhesion and Stx-mediated illness.

Surprisingly, C57BL/6 mice infected with *C. rodentium* (λ Stx_{2dact}) showed no weight loss until approximately 8 days after infection, despite strong colonisation levels. This weight loss in the second week of infection was not accompanied by any observable signs of illness, and only one out of the three λ Stx_{2dact} mice reached the >15% weight loss cull point. The remaining two mice showed a recovery in weight over the final two days of infection, likely due to the clearance of *C. rodentium*, as shown by faecal shedding levels. Interestingly, kidney histology found λ Stx_{2dact} C57BL/6 mice had signs of Stx-mediated damage, suggesting that Stx is being produced by *C. rodentium*, despite the poor indications of illness. The weight loss observed occurred at the point at which *C. rodentium* colonisation in mice typically begins to decrease, suggesting the explanation

3. RESULTS: Mouse models of *E. coli* infection

that bacterial clearance is associated with destruction of bacteria and subsequent release of Stx.

Immune differences between the two mouse strains may account for increased sensitivity of BALB/c mice to the λ Stx_{2dact} strain. The genetic background of mice is known to influence the Th1/Th2 balance, with C57BL/6 mice favouring Th1 and BALB/c mice biased towards Th2 (Mills *et al.*, 2000). This difference has been linked to impaired bactericidal activity of BALB/c macrophages and poor bacterial clearance relative to C57BL/6 mice (Watanabe *et al.*, 2004). Another possibility is that the intestinal environment of C57BL/6 mice produces lower Stx phage induction than the BALB/c host does.

Our C57BL/6 observations are however contradictory to those in the original Mallick *et al.* (2012) publication, which reported C57BL/6 weight loss and death within the first week of infection, similar to our results for BALB/c mice. As C57BL/6 mice are an inbred strain, it is unlikely that the varying results between our mice and those used by Mallick *et al.* (2012) are due to genetic differences. Instead, we suspect that differences in the microbiota of the mouse gut are responsible, as animals acquired from different suppliers will be subject to differences in the environment, diet, and exposure to maternal flora. Studies comparing the gut microbiota of lab mice have found that C57BL/6 mice obtained from two different suppliers displayed significant differences in their microbial composition, while mice raised in separate rooms of the same breeding facility showed no significant difference (Hufeldt *et al.*, 2010). We could therefore speculate that commensal bacterial strains present in our C57BL/6 mice confer a protective advantage to their host, for example by limiting the effect of Stx expression or Stx-mediated damage (although not *C. rodentium* colonisation). However, 16S ribosomal RNA sequencing of the gut microbiota of animals from both C57BL/6 suppliers would be required in order to investigate this further. Nonetheless, the results presented here demonstrate that despite these differences, with respect to final outcomes and damage to kidney tissue there is consistency between the two models. This is an important consideration in the use of animal models as a surrogate for infection in humans. The results presented in this chapter support the use of the *Citrobacter rodentium* Stx strains as a model for O157:H7 infection.

Chapter 4: Evaluation of EaeH and YghJ as potential vaccine candidates

4.1 Introduction

Surface-exposed bacterial proteins are considered good candidates for inclusion in vaccine formulations. These proteins are often associated with initial host-pathogen interactions, and thus generation of antibodies against them can both limit colonisation and enhance uptake and destruction of bacteria. Reverse vaccinology, which utilises bioinformatics to analyse sequenced genomes and recognise genes that encode proteins with extracellular regions, is a relatively recent approach to vaccine design which has been used to create a successful vaccine against Meningococcus B (Pizza *et al.*, 2000). In 2010, a reverse vaccinology screen identified nine proteins from ExPEC strains capable of inducing a significant level of protection in a mouse model of sepsis. The ExPEC group of strains, which colonise and induce disease outside of the intestinal tract, are a major health concern and responsible for diseases such as urinary tract infections, neonatal meningitis and pneumonia. However, comparative analysis of the genes encoding these antigens with genomic sequences from other pathogenic *E. coli* strains revealed many were conserved across other pathotypes, and were present in intestinal *E. coli* pathogens (Moriel *et al.*, 2010). The aim of our work was to investigate the role of two of these proteins, EaeH and YghJ, in EHEC and AIEC pathogenesis, and determine their potential as vaccine candidates against O157:H7 and LF82.

4.1.1 EaeH as a vaccine candidate

The *eaeH* gene (Figure 4-1 A) is predicted to encode an outer membrane adhesin with a putative amino-terminal signal sequence, and shares approximately 30% similarity with *eae*, which encodes intimin. Intimin functions as the bacterial receptor for the T3SS-translocated Tir in EHEC, and its inclusion in cattle vaccines reduces shedding of O157:H7 (McNeilly *et al.*, 2010). Although the protective efficacy of EaeH was relatively low (15%) in the initial screen study, it is highly conserved across many pathogens, including strains belonging to the serotypes O157:H7, O103:H2, and O26:H11, the latter of which is considered the most clinically important non-O157 EHEC (Bielaszewska *et al.*, 2007). Thus, inclusion of EaeH within a vaccine could broaden its potential as an efficacious vaccine against multiple *E. coli* strains.

4.1.2 YghJ as a vaccine candidate

The most effective antigen in the mouse sepsis model, YghJ, is a putative lipoprotein secreted by the Type 2 Secretion System (T2SS). YghJ shows significant similarity to accessory colonisation factor D (AcfD) of *Vibrio cholerae*, and provided extremely high protection from bacteraemia and mortality in mice (82% efficacy), both as a consequence of active or passive immunisation (Moriel *et al.*, 2010). Phylogenetic analysis has indicated that YghJ clusters into two main variants, although antibodies raised against one variant were protective against strains that encoded even the most distant variant of YghJ (Moriel *et al.*, 2010). The distribution of *yghJ* in 573 isolates representing the entire variation shown by *E. coli* phylogeny was analysed by Moriel *et al.* (2010), revealing that the gene is present across a wide range of pathogenic and non-pathogenic strains, although found more frequently in intestinal and extraintestinal pathogens (70-83%) than in commensal strains (59%). Interestingly, although YghJ was detected in total cell lysates from non-pathogenic strains, it was not secreted or surface associated. In non-pathogenic strains, the T2SS-encoding region adjacent to *yghJ* is truncated, and a fully-functional T2SS was demonstrated to be necessary for secretion of YghJ (Moriel *et al.*, 2010).

The *yghJ* gene is not present in O157:H7 EDL933. However, it is present in the genome of LF82 (Figure 4-1 B), which is why this gene was studied in this strain. LF82 colonises the intestinal mucosa of patients with Crohn's disease (Darfeuille-Michaud *et al.*, 1998), a chronic inflammatory bowel disease that is believed to have genetic, bacterial and environmental factors involved in its development (Cosnes *et al.*, 2011). The strong evidence for the involvement of LF82 and other AIEC strains in pathogenesis of Crohn's disease makes development of a vaccine that confers protection against these strains important.

4. RESULTS: EaeH and YghJ as vaccine candidates

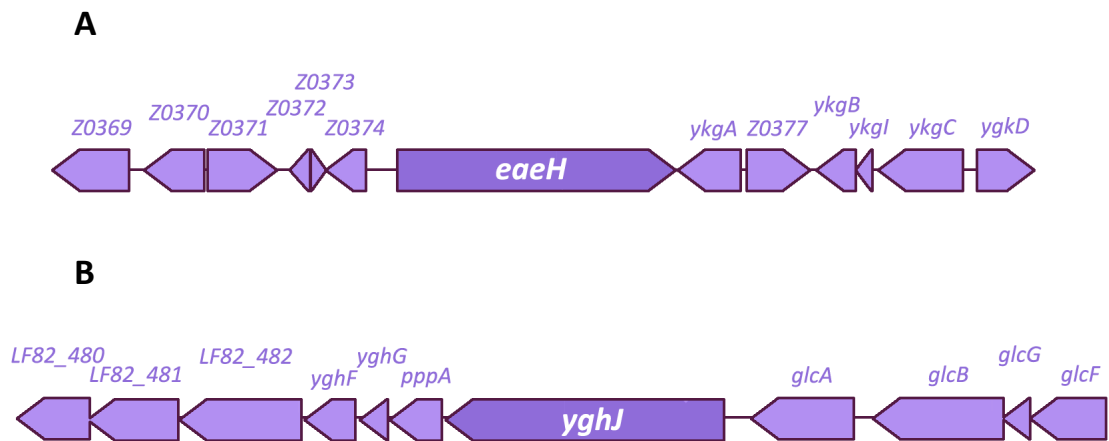


Figure 4-1: Genomic organisation of *eaeH* and *yghJ*. The *eaeH* organisation in O157:H7 EDL933 **(A)**, and *yghJ* organisation in LF82 **(B)**. Alignment of these genes in EDL933 and LF82 with those carried by the IHE3034 strain revealed both *eaeH* and *yghJ* were located in similar genomic positions.

4.1.3 Aims of this chapter

- To overexpress and purify His-tagged IHE3034 EaeH and YghJ from plasmids provided by Novartis Vaccines, and assess their suitability for use as positive controls in studies that explore expression of EaeH and YghJ by TUV93-0 and LF82 strains.
- To construct *eaeH* deletion mutant strains in both TUV93-0 and LF82, and a *yghJ* deletion mutant strain in LF82. These strains will be used as negative controls for expression studies, and potentially in animal experiments to determine the role of these genes in infection.
- To explore expression of EaeH and YghJ by TUV93-0 and LF82 under different growth conditions, including the use of different growth media and the presence of mammalian epithelial cells. Expression of these genes will be determined using fluorescence reporters, which will require the construction of gene promoter-GFP fusion plasmids, and by immunoblotting using anti-EaeH/YghJ antibodies provided by Novartis Vaccines.

4.2 Bacterial carriage of *eaeH* and *yghJ*

Bioinformatic analysis of *eaeH* and *yghJ* carriage in 1,591 *E. coli* isolates, carried out by Robert Goldstone (University of Glasgow) using the method described in Connolly *et al.* (2015), showed that *eaeH* is highly conserved across the *E. coli* lineage and found in all sub-groups. Carriage of *yghJ* was also very high, but noticeably absent from nearly all members of sub-group E (which includes the O157:H7 strain), which suggests that this gene was lost by an early ancestor of this phylogroup (Figure 4-2).

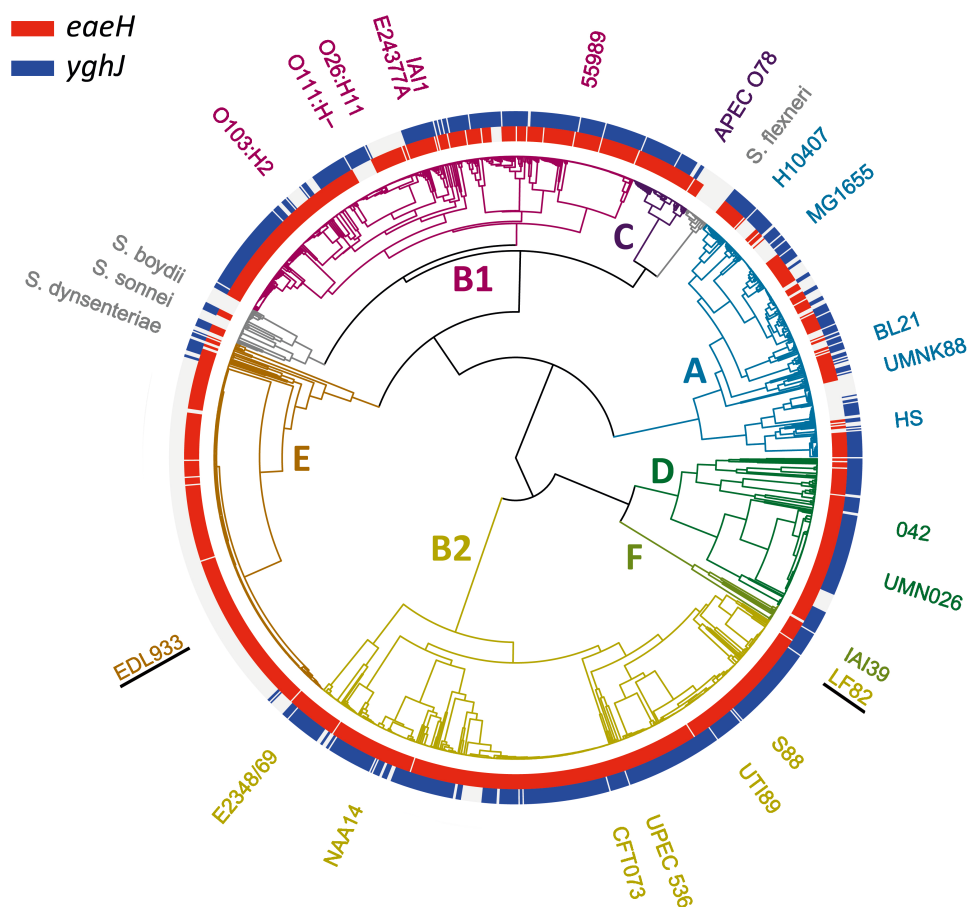


Figure 4-2: *E. coli* carriage of the *eaeH* and *yghJ* genes. Circularised phylogenetic tree of 1,591 *E. coli* and *Shigella* isolates overlaid with gene carriage (>80% identity over >80% of the coding sequence) for the *eaeH* (red) and *yghJ* (blue) genes. 1,406 isolates contained the *eaeH* gene, while 1,062 isolates carried the *yghJ* gene. Phylogenetic sub-grouping is indicated by branch colour coding as follows: Phylogroup A = blue; Phylogroup B1 = pink; Phylogroup B2: yellow; Phylogroup C = purple; Phylogroup D = green; Phylogroup E = orange; Phylogroup F = olive; *Shigella* = grey. Key strains are labelled according to their location on the tree, and the O157:H7 EDL933 and LF82 strains used in this study are indicated by underline. Bioinformatic analysis was performed by Robert Goldstone (University of Glasgow).

4.3 Overexpression of His-tagged EaeH and YghJ

The plasmids pET-21b-*eaeH* and pET-21b-*yghJ*, which encode polyhistidine-tagged EaeH and YghJ respectively, were constructed by Novartis Vaccines. The clones were generated using genomic DNA from the *E. coli* IHE3034 strain as a template. Protein expression was controlled using IPTG to induce the T7 promoter. These plasmids had originally been used to produce the purified EaeH and YghJ that were tested in the mouse sepsis model, and to raise antibodies in rabbits against both proteins (Moriel *et al.*, 2010). The amino acid sequence of the two proteins encoded by IHE3034 are highly homologous to those encoded by TUV93-0 and LF82 (92.2% identity between TUV93-0 and IHE3034 EaeH; 92.3% identity between LF82 and IHE3034 EaeH; 97.3% identity between LF82 and IHE3034 YghJ).

To overexpress EaeH and YghJ, plasmids were transformed into *E. coli* BL21(DE3) cells and expression induced by addition of 1 mM IPTG. Proteins were purified using nickel affinity columns and confirmed by Western blotting, using rabbit anti-EaeH and anti-YghJ supplied by Novartis Vaccines (Figure 4-3). Western blot analysis indicated that EaeH had a molecular weight of ~32 kDa, and YghJ a molecular weight of ~100 kDa, both significantly lower than the full peptide sequence of wild type EaeH (149 kDa) and YghJ (167 kDa). Sequencing of the *eaeH* and *yghJ* genes present in the pET-21b plasmids revealed that both genes were significantly truncated, with only ~1,650 bp of *eaeH* (full length = 4,254 bp) and 2,700 bp of *yghJ* (full length = 4,563 bp) present in the plasmids (Appendices 9.3). Therefore, these pET-21b-encoded proteins are poorly suited for comparison with EaeH and YghJ expressed by TUV93-0 and LF82.

4. RESULTS: EaeH and YghJ as vaccine candidates

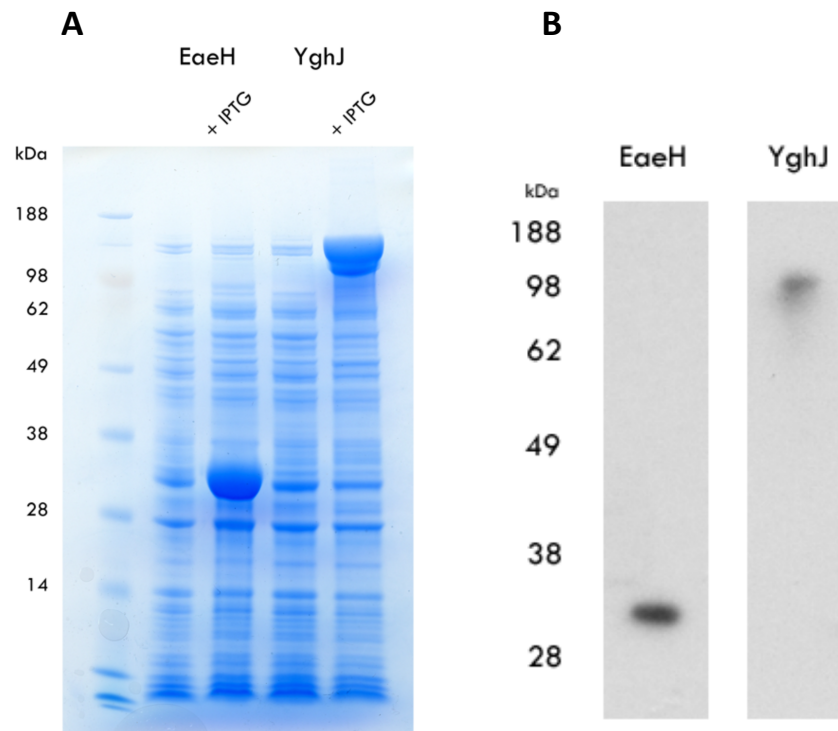


Figure 4-3: Expression of His-tagged EaeH and YghJ. Whole-cell lysate of BL21 transformed with the plasmids pET-21b-*eaeH* or pET-21b-*yghJ*, with and without addition of 1 mM IPTG when growth cultures reached an OD₆₀₀ of 0.6. Cultures were grown for a further 4 hours after the IPTG addition time point (A). Western blots of EaeH and YghJ from IPTG-induced cultures of BL21 transformed with pET-21b-*eaeH* or pET-21b-*yghJ*. Proteins were purified by affinity chromatography before Western blot analysis (B).

4.4 Construction of *eaeH* and *yghJ* deletion mutants

To explore the potential contribution played by EaeH and YghJ in *E. coli* colonisation *in vivo*, we planned to infect mice with TUV93-0 and LF82 strains containing *eaeH* or *yghJ* deletions and determine whether there was an effect on colonisation compared to wild type strains. Such deletion mutants could also be used as negative controls for exploring expression of these proteins by Western blot. Initial attempts to use allelic exchange to create a TUV93-0 $\Delta eaeH$ strain (Emmerson *et al.*, 2006) were unsuccessful. However, both $\Delta eaeH$ and $\Delta yghJ$ LF82 strains were created using lambda red mutagenesis, and confirmation that these genes had been successfully knocked out was demonstrated by PCR (Figure 4-4).

4. RESULTS: EaeH and YghJ as vaccine candidates

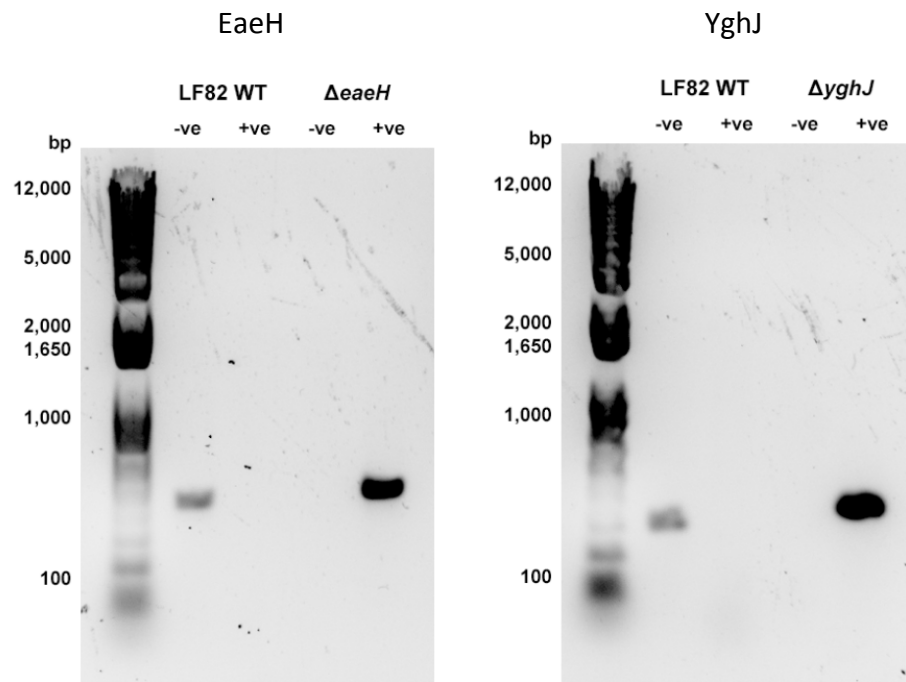


Figure 4-4: Confirmation of LF82 $\Delta eaeH$ and $\Delta yghJ$. The LF82 strains $\Delta eaeH$ and $\Delta yghJ$ were created by lambda red recombineering. These strains were checked for successful gene deletion by PCR; two sets of primers to amplify an ~800 bp region of DNA were used to test the knockout strains. The primers for negative integration (-ve) amplify a region of DNA only present when *eaeH* or *yghJ* is present in the chromosome, while the primers for positive integration (+ve) amplify a region of DNA only present when *eaeH* or *yghJ* replaced by the kanamycin resistance cassette. The gel shows DNA amplified from wild type LF82, $\Delta eaeH$, and $\Delta yghJ$ by the two sets of primers.

4.5 Reporter fusion analysis of *eaeH* and *yghJ* expression

4.5.1 Construction of GFP reporter fusions

To explore *eaeH* and *yghJ* gene expression by TUV93-0 and LF82, we used a fluorescence-based reporter system that allows monitoring of gene expression throughout the growth cycle. GFP reporter fusions were constructed using pAJR70, a promoterless plasmid containing the *gfp* gene, which encodes for green fluorescent protein (Cormack *et al.*, 1996). Briefly, the putative promoter regions of *eaeH* (-568 to +27, from both TUV93-0 and LF82) and *yghJ* (-346 to +66, from LF82 only) were amplified using PCR and cloned into pAJR70 directly upstream of *gfp*, ensuring that *gfp* remained in frame (Figure 4-5). Correct insertion of the promoters was confirmed by DNA sequencing. The reporter

4. RESULTS: EaeH and YghJ as vaccine candidates

fusions created were named pzm_TE1 (TUV93-0 *eaeH*), pzm_LE1 (LF82 *eaeH*), and pzm_LY1 (LF82 *yghJ*). For all experiments, the reporter fusions were transformed only into the strains from which the promoter region was obtained, i.e. pzm_TE1 transformed into the TUV93-0 background, and pzm_LE1 and pzm_LY1 transformed into the LF82 background.

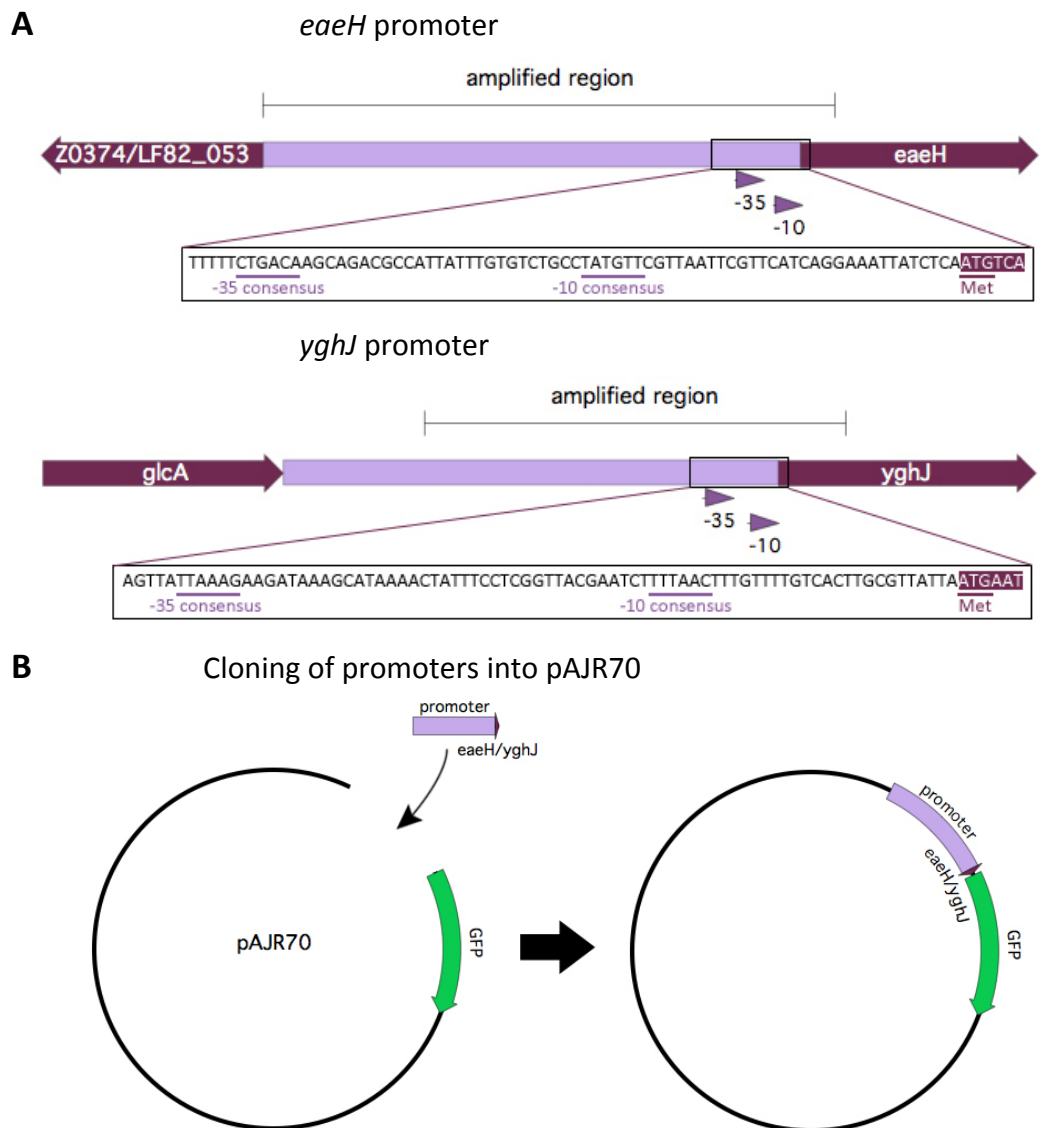


Figure 4-5: Construction of *eaeH* and *yghJ* reporter fusions. The potential promoter regions upstream of *eaeH* and *yghJ* were amplified by PCR. These amplified regions also contained the first few codons of *eaeH* and *yghJ*. The sequence immediately before and after the start codon of *eaeH* (from TUV93-0) and *yghJ* is shown. The putative promoter consensus sequences -10 (TATAAT) and -35 (TTGACA) are indicated by underline, and the ATG start codon encoding methionine labelled **(A)**. These amplified sequences were inserted directly upstream of *gfp* (green) in pAJR70, producing pzm_TE1, pzm_LE1, and pzm_LY1 **(B)**.

4. RESULTS: EaeH and YghJ as vaccine candidates

4.5.2 GFP reporter fusion assays

Expression of GFP by the *eaeH* and *yghJ* promoters was assessed during exponential growth of both TUV93-0 and LF82 transformed with the *pzm_TE1*, *pzm_LE1* and *pzm_LY1* plasmids respectively. Expression was monitored in LB, MEM and M9 medium for 6 hours. Positive expression of GFP was shown by *E. coli* transformed with the reporter plasmid *prpsM*:GFP, containing the promoter for *rpsM*, which encodes the 30S ribosomal subunit protein S13 and is strongly expressed in the growth medium used. Baseline fluorescence was determined by *E. coli* transformed with the promoterless *pAJR70* plasmid. Neither *eaeH* (in TUV93-0 and LF82) or *yghJ* (in LF82) reporter fusions produced fluorescence levels above that of the baseline during this time period (Figure 4-6), indicating that neither of these promoters are active at detectable levels under these conditions.

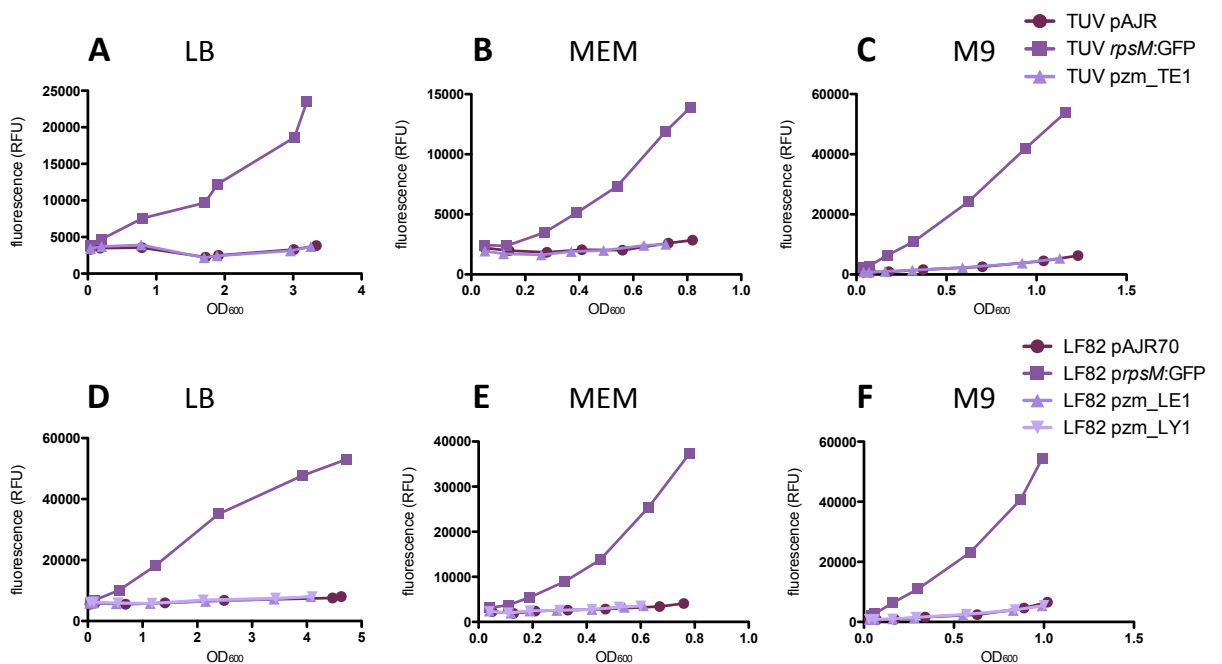


Figure 4-6: Expression of gene:GFP reporter fusions. TUV93-0 (A-C) and LF82 (D-F) transformed with the reporter fusions *pzm_TE1*, *pzm_LE1*, *pzm_LY1*, *pAJR70* (to obtain background fluorescence levels) or *prpsM*:GFP (for positive expression of GFP) were grown in LB (A, D), MEM (B, E), or M9 (C, F) growth medium for 6 hours. Fluorescence and OD₆₀₀ readings were taken hourly and fluorescence plotted against the corresponding OD₆₀₀. The data shown is from one growth experiment, but graphs are representative of triplicate experiments.

4.5.3 Expression of ETEC *eaeH* is upregulated by interaction with host cells

Many bacterial virulence genes have been demonstrably upregulated following contact with host epithelial cells (Zhang & Normark, 1996; Pettersson *et al.*, 1996). In 2013, a transcriptome analysis study that investigated how ETEC virulence genes were modulated upon contact with host epithelial cells indicated that *eaeH* expression was modified by this interaction (Kansal *et al.*, 2013). Using a β -galactosidase *eaeH* reporter fusion, gene expression was shown to be significantly increased in ETEC H10407 bacteria attached to human intestinal epithelial Caco-2 cells relative to planktonic bacteria. Additionally, immunofluorescence microscopy identified EaeH on the surface of ETEC attached to Caco-2 cells both at the point of cell contact and diffusely distributed on the H10407 surface. These findings suggested that similar upregulation of *eaeH* could potentially occur in O157:H7 and LF82.

4.5.4 Expression of GFP reporters upon contact with Caco-2 cells

To determine if epithelial contact resulted in expression of GFP by the *eaeH* and *yghJ* promoters, strains containing the reporter plasmids were used to infect near-confluent Caco-2 monolayers for 5 hours. To determine gene expression, fluorescence readings were taken hourly. While we were initially interested in *eaeH* expression, *yghJ* was included in this assay to investigate whether host cell contact modulates expression of this gene. Increased fluorescence over time was observed for TUV93-0 and LF82 containing the *rpsM* reporter, however, no fluorescence above baseline levels was detected for either the *eaeH* or *yghJ* reporter (Figure 4-7).

4. RESULTS: EaeH and YghJ as vaccine candidates

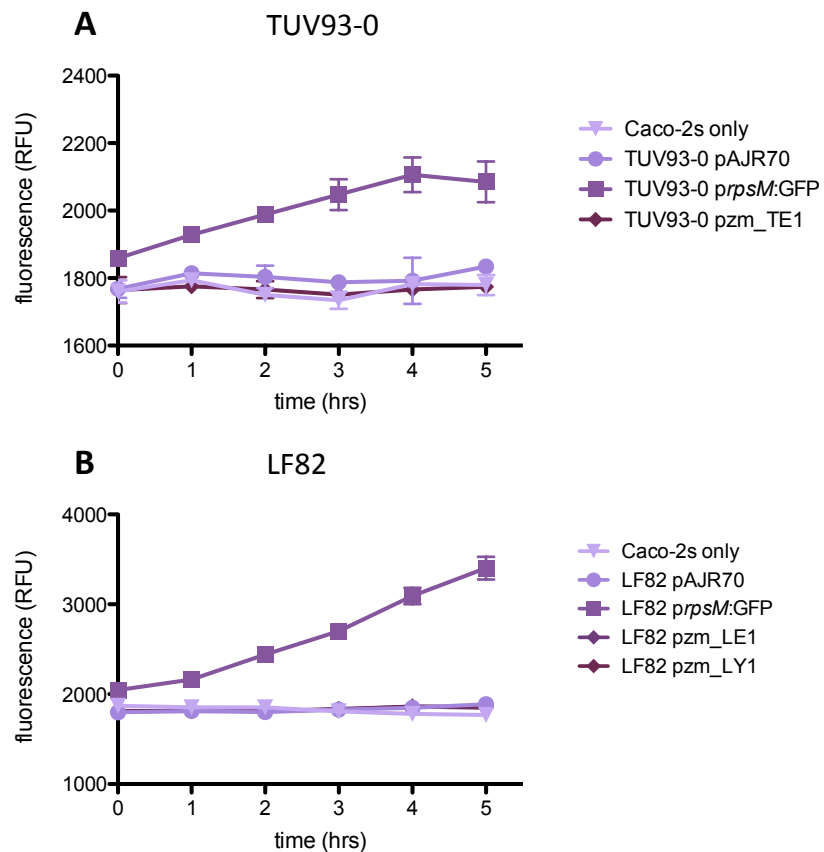


Figure 4-7: Expression of GFP by *eaeH* and *yghJ* reporter fusions in contact with Caco-2 cells. TUV93-0 and LF82 transformed with the plasmids *pzm*_TE1, *pzm*_LE1, *pzm*_LY1, pAJR70 (to obtain background fluorescence levels) or *prpsM*:GFP (for positive expression of GFP) were added to monolayers of Caco-2 cells at a final OD₆₀₀ of 0.1. Bacteria and Caco-2 cells were incubated together at 37°C and 5% CO₂ for 5 hours, and fluorescence measured directly from plates every hour. Experiments were performed in triplicate and data presented as the mean fluorescence, with error bars displaying standard deviation from the mean.

These reporter fusion assays demonstrated that no *eaeH* or *yghJ* promoter activity was detectable by this method. To more clearly visualise direct *eaeH* expression, immunofluorescence microscopy was used to examine expression of GFP by the *pzm*_TE1 plasmid upon contact with host cells. HeLa cells were used instead of Caco-2 cells for this experiment, as an established bacterial adhesion protocol was available for this cell line in which clear T3SS-mediated A/E lesions could be observed. Additionally, we selected a human cell line rather than a mouse intestinal cell line for these experiments, as we were interested in determining whether *eaeH* expression is upregulated on contact with human cells before assessing whether murine cells produce a similar response. For these studies, only TUV93-0 was tested. To further help bacterial visualisation, red fluorescence protein (RFP)-marked TUV93-0 was transformed with the *pzm*_TE1 reporter plasmid. This

4. RESULTS: EaeH and YghJ as vaccine candidates

strain was then incubated with near-confluent HeLa cells for 4 hours before fixing and staining with FITC Phalloidin 647 (far red) to allow visualization of host cell actin. Bacteria were identified using RFP, and *eaeH* promoter activity by GFP. TUV93-0 transformed with the *prpsM*:GFP reporter fusion or pAJR70 plasmid were used as a positive and negative control for GFP expression, respectively.

No GFP fluorescence from cells transformed with the *pzm_TE1* plasmid was detected, implying that the *eaeH* promoter region in the plasmid is inactive even when TUV93-0 is intimately attached to host cells (Figure 4-8). We also attempted to directly label cell surface-expressed EaeH using antisera; however, no EaeH could be detected in these experiments (data not shown).

4. RESULTS: EaeH and YghJ as vaccine candidates

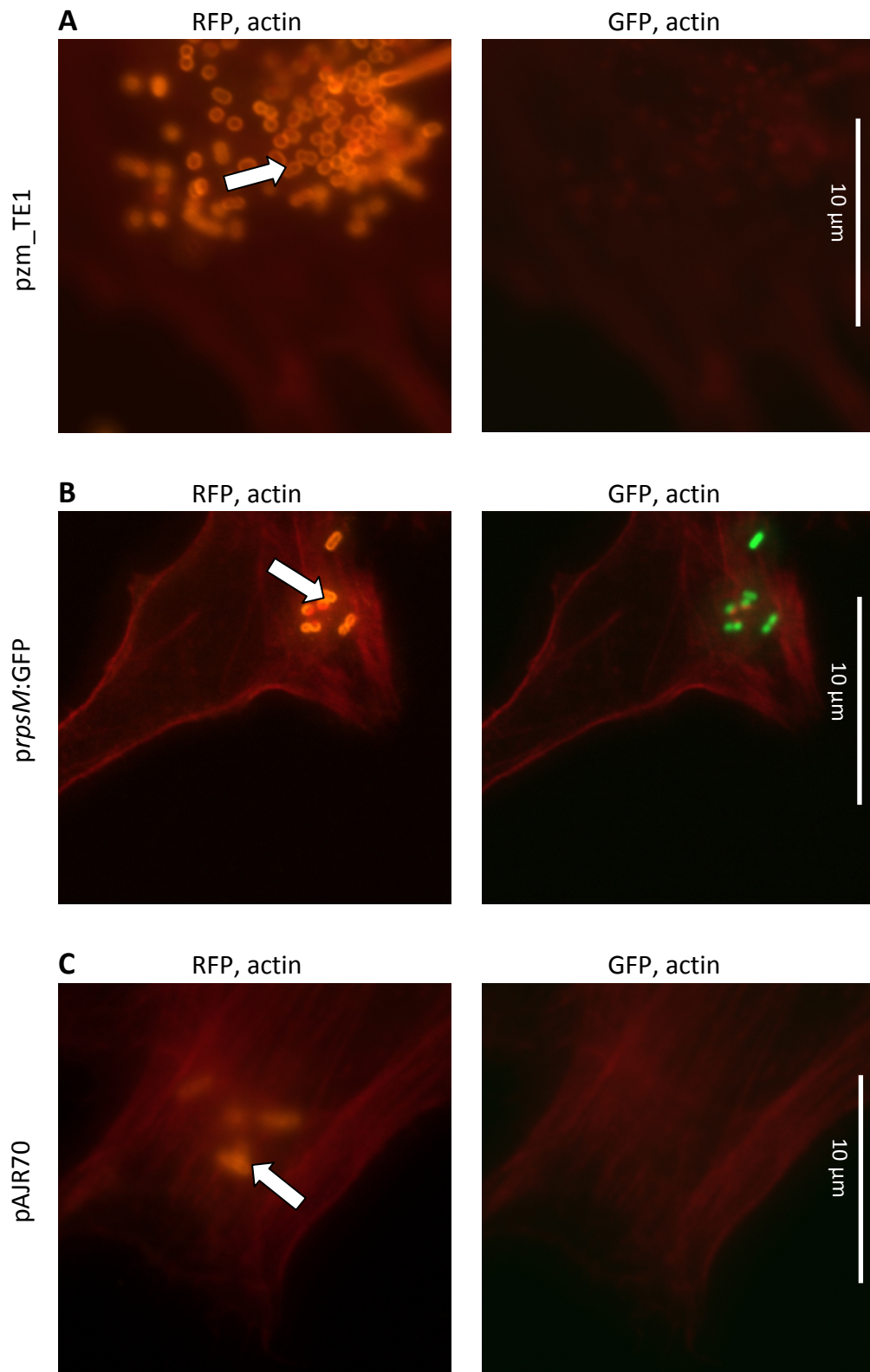


Figure 4-8: Expression of *eaeH*:GFP by TUV93-0 adhered to HeLa cells. Representative fluorescence microscopy images of HeLa cells with adhered TUV93-0 (indicated by arrows). RFP-expressing TUV93-0 transformed with *pzm_TE1* (A), *prpsM*:GFP (B) or pAJR70 (C). Bacteria were incubated with HeLa cells for 4 hours. After fixing and staining, cells were visualised for actin (far red), TUV93-0 (red) and *pzm_TE1/prpsM*:GFP expression (green). Images show a merge of the far red and red channels (images on left) or of the far red and green channels (images on right).

4.6 Western blot analysis of EaeH and YghJ expression

4.6.1 Expression and detection of EaeH and YghJ

Western analysis of whole-cell lysates of TUV93-0 and LF82 indicated that EaeH and YghJ were both expressed in these strains. In contrast, these bands were absent in the LF82 $\Delta eaeH$ and $\Delta yghJ$ strains (Figure 4-9). Although EaeH was expressed by both TUV and LF82 wild type strains, it was produced at very low levels, requiring large volumes of concentrated lysate (200 μ g total lysate protein) and a long exposure (10 minutes) to be detected. Both EaeH and YghJ ran at molecular weights approximately twice the size of the His-tagged proteins provided by Novartis as controls (Figure 4-3 B), although given that the pET-21b plasmids provided by Novartis encoded truncated His-tagged proteins, these differences were not unexpected.

Using the antibody against EaeH, we observed two distinct bands in the lysate of TUV93-0 at approximately 80-100 kDa, while LF82 lysate showed 3 bands at slightly higher and lower molecular sizes than TUV93-0. Presence of the lowest band in the $\Delta eaeH$ lysate suggests that the upper bands observed for LF82 are EaeH, while the lower band (at approximately 62 kDa) may be another surface protein to which the antibody is able to bind. EaeH contains tandem bacterial immunoglobulin-like domains that are similar to those present in eukaryotic cell surface adhesion proteins, and therefore if the EaeH antibody binds to these domains in EaeH, it is possible that it also targets proteins with similar domains (Dr. Alaullah Sheikh, personal communication). Identification of the EaeH band in TUV93-0 was not possible using this approach as the generation of a TUV93-0 $\Delta eaeH$ strain proved elusive.

4. RESULTS: EaeH and YghJ as vaccine candidates

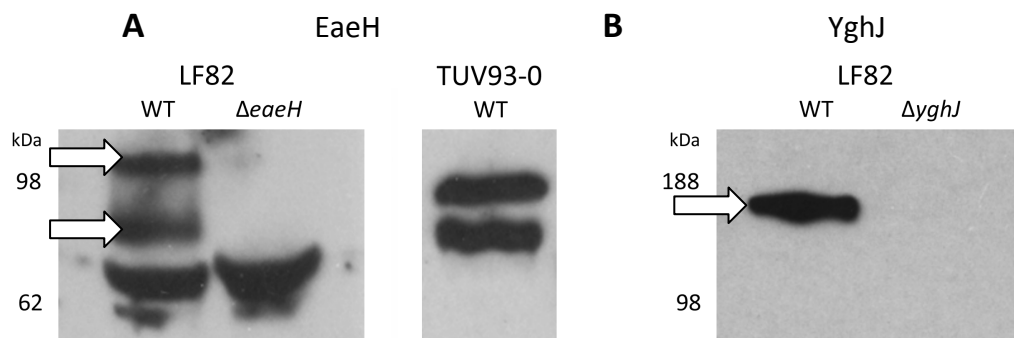


Figure 4-9: EaeH and YghJ expression by TUV93-0 and LF82. TUV93-0 and LF82 lysate after growth in MEM media showing EaeH (A) and YghJ (B). Lysate from LF82 $\Delta eaeH$ and $\Delta yghJ$ strains was run alongside the wild type to identify the EaeH and YghJ bands (indicated by arrows). Bacterial lysate was loaded into wells and contained a total of 200 μg (for EaeH blots) or 50 μg (for YghJ blots) protein. EaeH blots were exposed for 10 minutes and YghJ blots for 5 minutes.

4.6.2 Expression of EaeH upon contact with Caco-2 cells

As EaeH production by TUV93-0 and LF82 was detectable by Western blot, this technique was used to further explore whether expression of EaeH increased when the bacteria were in contact with host cells. Briefly, TUV93-0 and LF82 cultures grown in LB were used to infect monolayers of Caco-2 cells at an MOI of ~ 100 for four hours. Control TUV93-0 and LF82 were added to plates that did not contain Caco-2 cells, and grown under the same conditions. Unattached bacteria were harvested by removal and centrifugation of the media, and resuspended in PBS. After the Caco-2 cells were washed with PBS, adherent bacteria were removed using assay buffer containing 0.1% Triton X-100. To quantify the number of unattached and adherent bacteria, serial dilutions of the samples were performed and plated onto LB agar. This confirmed that approximately 100x less bacteria were attached to the cells than were unattached and in the medium. The number of bacteria were standardised to allow equal volumes of cell lysate from control, unattached and attached samples to be run on SDS-PAGE gels for analysis of EaeH expression by Western blot.

This analysis suggested that expression of EaeH in unattached bacteria in the presence of Caco-2 cells was slightly higher for the control bacteria. This finding was not unexpected, as expression of ETEC EaeH has been reported to be activated using media conditioned by Caco-2 cells (Sheikh *et al.*, 2014). Surprisingly, adherent TUV93-0 and LF82 appeared to

4. RESULTS: EaeH and YghJ as vaccine candidates

express EaeH at levels that were no different than the control bacteria (Figure 4-10). These results suggest that some upregulation of *eaeH* might occur in unattached bacteria, which we speculate could be caused by release of an unknown factor into the media that enhances expression of *eaeH*. This could be released by either the eukaryotic cells or by adherent bacteria to increase attachment of the local population.

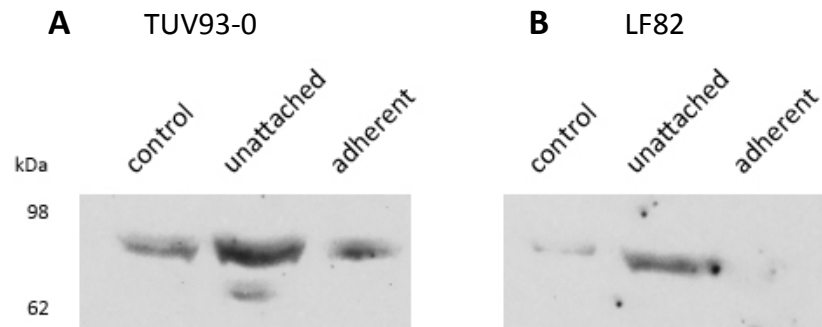


Figure 4-10: Expression of EaeH after host cell contact. TUV93-0 (A) and LF82 (B) lysate after cell adhesion assays were blotted for EaeH. Expression was examined in bacteria free in MEM media in the presence of Caco-2 cells and from bacteria intimately attached to Caco-2 cells. Bacteria were incubated with Caco-2 cells for 4 hours, and control TUV93-0 and LF82 grown in the same media but without the presence of Caco-2 cells. Gels were loaded with identical concentrations of protein (100 μ g total protein), and blots exposed for 10 minutes.

4.6.3 Expression of EaeH in Caco-2-conditioned MEM media

In ETEC strains, increased expression of EaeH has been shown to occur not only upon contact with epithelial mammalian cells, but also when H10407 is grown in media conditioned by growth of Caco-2 cells (Sheikh *et al.*, 2014), suggesting that molecules released by epithelial cells may be sufficient to initiate upregulation. To explore whether conditioned media also causes increased EaeH production in our strains, further analysis of bacterial lysates were performed. In brief, MEM medium supplemented with 10% foetal calf serum was conditioned by exposure to near-confluent Caco-2 cells for 24 hours. Both strains of bacteria were then grown in this media until an OD_{600} of 0.8 was reached. The ETEC H10407 strain was also included as a positive control for increased expression in conditioned media.

4. RESULTS: EaeH and YghJ as vaccine candidates

Growth in conditioned media showed no obvious influence on expression of EaeH by any of the three strains of *E. coli* (Figure 4-11 A). The lower band of each sample was presumed to be non-specific binding, based on Western blot analysis of our LF82 *eaeH* deletion mutant, and the reported ~150 kDa migration of EaeH observed in H10407 (Dr. Alaullah Sheikh, personal communication). Lysate was also stained for GroEL, a cytoplasmic chaperonin protein, to confirm standardisation of the amount of sample material used in this comparative analysis (Figure 4-11 B).

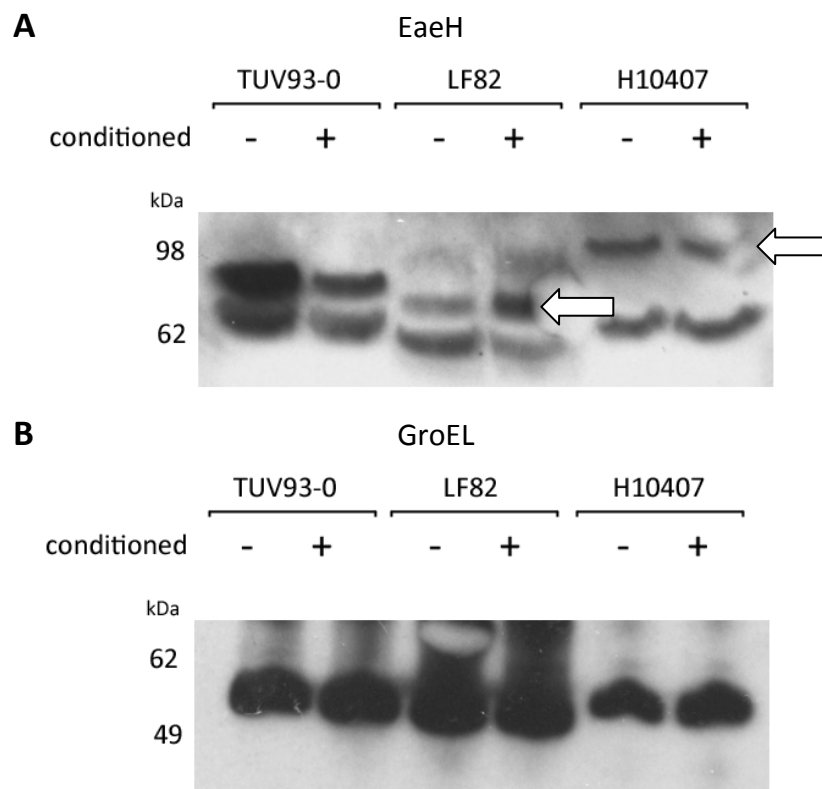


Figure 4-11: Expression of EaeH after growth in conditioned or unconditioned media. EaeH immunoblotting of TUV93-0, LF82 and H10407 lysate after growth in conditioned or unconditioned MEM (+ 10% FCS). A total of 200 μ g protein was loaded into each well, and blots were exposed for 10 minutes. Arrows indicates the presumed band for LF82 and H10407 EaeH (**A**). Samples were also blotted for GroEL to quantify the relative concentration of protein in the lysates (**B**).

4.7 Secretion of YghJ by LF82

YghJ has been reported to be secreted by the T2SS in *E. coli* strains, with those strains containing a truncated T2SS operon unable to secrete the protein. This was first demonstrated by Moriel *et al.* (2010) using Western blot analysis of *E. coli* cell lysate and culture supernatant. In these experiments, YghJ was detected in the cell lysates of all strains carrying the *yghJ* gene, but only detected in the culture supernatants of those strains with an intact T2SS operon (Moriel *et al.*, 2010).

Analysis of the sequenced LF82 genome reveals an intact T2SS operon (Miquel *et al.*, 2010), suggesting that this strain is capable of secreting YghJ. To examine this, analysis performed and described by Moriel *et al.* (2010) was replicated. Three strains were assessed: LF82, MG1655 (which carries the *yghJ* gene but has a truncated T2SS region), and the EPEC strain E2348/69. This strain was included as a positive control as T2SS-mediated secretion of YghJ has been reported in E2348/69 (Baldi *et al.*, 2012). Bacteria were grown in MEM media until an OD₆₀₀ of 0.8 was reached. Cells were harvested by centrifugation, and proteins in the culture media precipitated with 10% TCA. The presence of YghJ in both the lysate and culture supernatant was tested by Western blot. To ensure that culture supernatants did not contain protein released by lysed cells or inclusion of cell pellets, staining for the cytoplasmic protein GroEL was performed in parallel.

YghJ was detected in the cell lysate of all three strains, at similar concentrations. As expected, the MG1655 strain showed no presence of YghJ in the culture supernatant, while the EPEC strain demonstrated secretion of YghJ. However, no YghJ was detected in the culture supernatant of LF82 suggesting that although the LF82 genome appears to contain an intact T2SS operon, the T2SS is either not expressed or functional under these conditions (Figure 4-12).

4. RESULTS: EaeH and YghJ as vaccine candidates

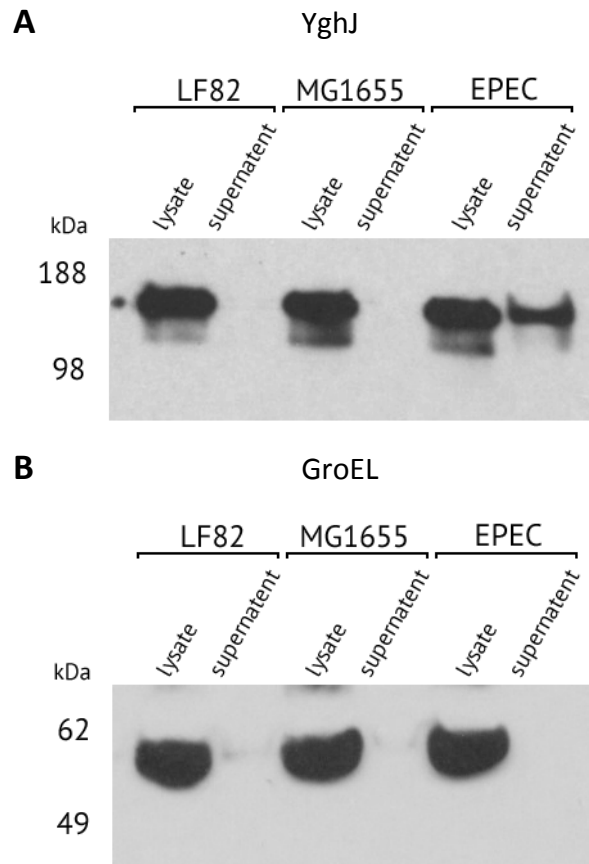


Figure 4-12: Expression and secretion of YghJ. Lysate and culture supernatant from *E. coli* LF82, MG1655 and E2348/69 (EPEC) strains grown to an OD₆₀₀ of 0.8 were blotted for YghJ (**A**). Samples were also blotted for GroEL to quantify the relative concentration of protein in the lysate, and to show that the culture supernatant did not contain cytoplasmic protein (**B**).

4.8 Discussion

4.8.1 Expression of EaeH by TUV93-0 and LF82

The bacterial protein EaeH, which had previously been identified as an antigen capable of conferring protection against ExPEC infections and thus a potential vaccine candidate, is highly conserved across a number of pathogenic *E. coli* strains (Moriel *et al.*, 2010). Our initial aim was to investigate EaeH expression in the strains TUV93-0 and LF82, in order to assess its suitability as a component of such a vaccine.

GFP reporter fusion assays revealed that when grown in LB, MEM or M9 media, expression of EaeH by TUV93-0 and LF82 was too low to be observed. These findings were consistent with our own RNAseq analysis of TUV93-0 gene expression in MEM (Dr. James Connolly, personal communication), which indicated that transcription of *eaeH* is extremely low in artificial growth media; with an average of 33 reads mapped for *eaeH* (4254 bp), compared to 7683 for intimin-encoding *eae* (2805 bp) and 920 for *rpsM* (357 bp).

Western blotting of EaeH in TUV93-0 and LF82 lysate revealed differences in band migration between the two strains, which was surprising given the high similarity between TUV93-0 and LF82 EaeH sequences (92.3% identity). As the protein sequence of TUV93-0 and LF82 EaeH differs in length by only one amino acid, it is possible that different post-translational modification results in the migration observed. The larger of the two EaeH bands remained unaffected by the length of time that samples were boiled prior to loading, or by addition of highly denaturing Laemmli loading buffer (data not shown). Alternatively, EaeH may be binding to unknown bacterial proteins, and this interaction does not dissociate under SDS denaturing conditions.

In recent years, studies investigating the expression of EaeH by ETEC strains have been published, and have emphasised the importance of bacterial-host cell interaction for upregulation of this gene. Transcriptome analysis of ETEC H10407 genes after interaction with human epithelial intestinal cells first identified *eaeH* as one such upregulated gene

4. RESULTS: EaeH and YghJ as vaccine candidates

(Kansal *et al.*, 2013). Further investigation of *eaeH* expression discovered that upregulation does not require direct contact with host cells, but can be initiated in media conditioned by intestinal Caco-2 cells (Sheikh *et al.*, 2014). In our TUV93-0 and LF82 strains, increased expression of EaeH was not observed in bacteria grown in conditioned media. However, expression of EaeH by the positive control strain H10407 strain also did not differ, contradicting the findings published by Sheikh *et al.* (2014). Discussions with the corresponding authors of this paper confirmed that an identical protocol for conditioning of media by Caco-2 cells was followed. However, it should be noted that increased EaeH expression reported by Sheikh *et al.* (2014) was observed by flow cytometry, whereas we studied expression by Western blotting.

While it is possible that the promoter region in the pzm_TE1 and pzm_LE1 plasmids did not contain the complete *eaeH* promoter sequence, the region we selected for cloning contained the entire region upstream of *eaeH*, and was highly similar to the promoter region used in the H10407 β -galactosidase reporter plasmid pQL002 (Figure 4-13). This region has been used successfully to show *eaeH* expression under similar cell contact conditions (Kansal *et al.*, 2013), making this explanation unlikely.

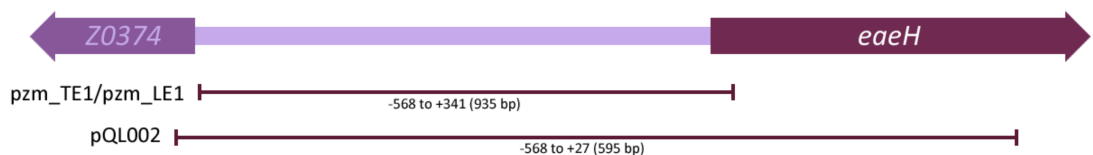


Figure 4-13: Comparison of the promoter regions used for *eaeH* expression reporters. The promoter region from our GFP reporters pzm_TE1/pzm_LE1 and the promoter region from the H10407 β -galactosidase reporter pQL002 (Sheikh *et al.*, 2014) are aligned against the full upstream region and start of the *eaeH* gene.

4.8.2 The function of EaeH in *E. coli*

The role of EaeH has also been explored in a recent study by Sheikh *et al.* (2014). EaeH was assumed to be an outer membrane adhesin as it shares a region of homology with intimin that is predicted to fold into a transmembrane β -barrel. EaeH also contains a series of tandem bacterial immunoglobulin-like domains similar to those found in other bacterial virulence proteins involved in adherence to eukaryotic host cells (Sheikh *et al.*,

4. RESULTS: EaeH and YghJ as vaccine candidates

2014). To examine the ability of EaeH to facilitate adhesion, Sheikh *et al.* (2014) added purified latex beads coated with recombinant EaeH to monolayers of Caco-2 cells. After a 3 hour incubation, scanning electron microscopy revealed that EaeH-coated beads bound to the cell surface, with some appearing partially engulfed by the Caco-2 cells. This implied that EaeH on its own was capable of promoting intimate attachment of bacteria to host cells. An ETEC H10407 *eaeH* deletion mutant showed decreased adhesion to Caco-2 cells when compared to the wild type strain, and was also impaired in delivery of LT toxin. Purified anti-EaeH antisera added to wild type H10407 and Caco-2 cells resulted in inhibition of bacterial adhesion to host cells, along with inhibition of bacterial activation of Caco-2 cyclic adenosine monophosphate (cAMP) (Sheikh *et al.*, 2014).

These findings imply that EaeH plays a role in ETEC interactions with its host. To explore this protein's contribution to colonisation *in vivo*, Sheikh *et al.* (2004) orally challenged streptomycin-treated mice with H10407 and an *eaeH* deletion mutant in competition experiments. No significant difference in total intestinal colonisation between the wild type and the mutant was observed; however, when the intestinal mucosa of mice was examined by immunofluorescence microscopy, significantly higher numbers of wild type bacteria were reported attached to the epithelial surface of the intestine compared to the mutant strain (Sheikh *et al.*, 2014).

4.8.3 Expression and secretion of YghJ by LF82

The location of *yghJ* immediately upstream of genes encoding a T2SS, and the significant similarity YghJ shares with the Type 2-secreted *Vibrio cholerae* AcfD protein implies that YghJ is an effector of this secretion system. Transcription of *yghJ* and the Type 2 *gsp* genes are also co-regulated in the *E. coli* H10407 strain (Yang *et al.*, 2006). Secretion assays initially performed by Moriel *et al.* (2010) involving a number of *E. coli* strains carrying the *yghJ* gene revealed that the T2SS is necessary for the secretion of YghJ into culture supernatant.

Comparison of the promoter region used in the construction of pzm_LY1 to the promoter region of *PssIE-luxCDABE*, an ExPEC IHE3034 *eaeH* expression reporter plasmid able to detect *in vivo* activity of the *eaeH* promoter (Nesta *et al.*, 2014), indicated that a similar

4. RESULTS: EaeH and YghJ as vaccine candidates

region was cloned (Figure 4-14). Despite this, fluorescence-based reporter fusion assays in various growth media did not demonstrate activation of the *yghJ* promoter in the LF82 strain.

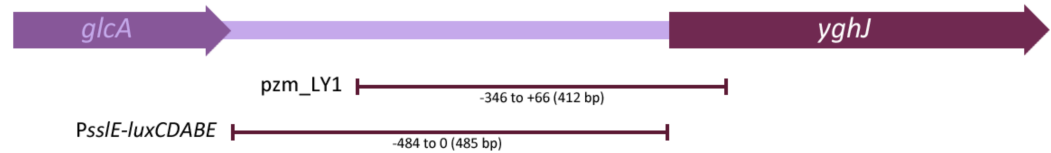


Figure 4-14: Comparison of the promoter regions used for *yghJ* expression reporters. The promoter region from our GFP reporter pzm_LY1 and the promoter region from the IHE3034 luciferase reporter *PssIE-luxCDABE* (Nesta *et al.*, 2014) are aligned against the full upstream region and start of the *yghJ* gene.

Expression of YghJ by LF82 was however detected in whole-cell lysate by Western blotting. As LF82 was not one of the strains previously investigated for YghJ secretion, we replicated the secretion assay, using the EPEC E2348/69 strain as a positive control for YghJ secretion (Baldi *et al.*, 2012). Surprisingly, as genome sequencing has indicated that LF82 contains an intact T2SS (Miquel *et al.*, 2010), YghJ was not detected in culture supernatants, and therefore was not being secreted under the conditions tested.

Two distinct and highly conserved T2SSs have been identified in *E. coli*, termed T2SS_α and T2SS_β (Strozen *et al.*, 2012). The LF82 strain carries a truncated T2SS_α operon and a complete T2SS_β operon, the latter of which contains the *yghJ* gene. The H10407 T2SS_β assembles and functions under standard laboratory conditions (Strozen *et al.*, 2012), although assembly of the LF82 T2SS was not investigated in this study. Further exploration of the T2SS in LF82 would be required to reveal whether this lack of secretion by LF82 is YghJ dependent, or a failure of T2SS functionality.

Our observation that LF82 does not secrete YghJ is supported by a recent comparative analysis of secretomes produced by the H10407 and LF82 strains. Using a mass spectrometry-based Stable Isotope Labeling with Amino acids in Cell culture (SILAC) quantitative proteomics method, Boysen *et al.* (2015) compared the protein levels in outer membrane vesicles (OMVs) and culture supernatant from LF82 and H10407 to those of the non-pathogenic MG1655 strain, identifying shared and unique proteins secreted or released in OMVs by the pathogenic strains. Notably, while YghJ was detected

4. RESULTS: EaeH and YghJ as vaccine candidates

in OMVs and culture supernatant of the H10407 strain, it was not detected in these fractions taken from the LF82 strain (Boysen *et al.*, 2015).

4.8.4 The function of YghJ

Several studies investigating the role of YghJ in *E. coli* have been recently published. In EPEC E2348/69, YghJ has been implicated in formation of biofilm, an aggregation of bacteria that protects against mechanical removal and phagocytosis (Baldi *et al.*, 2012). In this study, YghJ was determined to be located on the outer cell surface of this strain and secreted into culture supernatant. Deletion mutants of both *yghJ* and essential T2SS genes constructed by Baldi *et al.* (2012) did not show impaired growth or elicit the global stress response σ^E , but were attenuated for biofilm formation. When a *yghJ* deletion mutant in the rabbit-specific EPEC strain E22 was tested in a rabbit model of infection, lower bacterial counts were observed in rectal swabs post infection compared to the wild type strain. In addition, these animals had fewer days of diarrhoea and displayed normal weight gain (Baldi *et al.*, 2012). However, in atypical EPEC (aEPEC), diarrhoeal pathogens that carry the LEE but are negative for bundle-forming pilus production, the role of YghJ in pathogenicity is less defined; *yghJ* deletion mutants constructed in the aEPEC 1551-2 strain did not show changes in adherence to HeLa cells nor biofilm formation compared to the wild type strain (Hernandes *et al.*, 2013).

Although several non-pathogenic *E. coli* strains are deficient for secretion of YghJ, there is also evidence that secretion is not restricted to pathogenic strains, suggesting that YghJ may also play a role in colonisation by non-pathogenic strains. For example, the non-pathogenic W strain encodes a functional T2SS that secretes YghJ, and phenotypic microarray analysis revealed that deletion of *yghJ* or essential T2SS genes provided the mutants with a slight increase in urea tolerance. This implies that YghJ secretion or display of this protein on the bacterial cell surface influences the cell physiology, resulting in an increased sensitivity to urea. (Decanio *et al.*, 2013).

Further publications using ETEC strains have provided evidence that, in this pathotype, YghJ plays an important role in colonisation of the host intestine. YghJ is required for efficient delivery of the T2SS effector and major virulence factor LT enterotoxin, although

4. RESULTS: EaeH and YghJ as vaccine candidates

not for secretion of the toxin (Luo *et al.*, 2014). In this publication, both a *yghJ* deletion mutant and treatment of the wild type H10407 strain with antibodies raised against YghJ resulted in significantly impaired delivery of LT, determined by reduced activation of cAMP in host epithelial cells. This led the authors to hypothesise that YghJ acts to facilitate bacterial access to the enterocyte surface, allowing toxin access to host cell receptors.

A layer of heavily glycosylated proteins called mucins protects the surface of the small intestine. Bacteria must pass through this layer to gain access and attach to the epithelial cells. *In vitro* experiments by Luo *et al.* (2014) identified MUC2, the major luminal mucin in the small intestine, as a possible target of YghJ. When incubated in MUC2-containing media, the *yghJ* deletion mutant was more frequently coated with MUC2 relative to the wild type strain. Analysis of the YghJ protein sequence has identified a conserved putative metalloprotease motif suggesting that YghJ is a metalloprotease that degrades mucins, allowing bacterial access to the enterocyte layer. This hypothesis was supported by the finding that YghJ bound and degraded purified MUC2 in a dose-dependent manner, an activity that was abolished by chelation of metal from recombinant YghJ. This MUC2-degradation activity was subsequently restored by supplementation of divalent cations to the chelated protein. YghJ also degraded MUC3, the most abundant cell-bound mucin in the small intestine, but was inactive against mucin-like CD43, bovine submaxillary mucin, gelatin, or IgG (Luo *et al.*, 2014).

In vivo ETEC studies by Luo *et al.* (2014) using a streptomycin-treated ICR mouse model, however, provided limited evidence that YghJ plays a major role in bacterial pathogenesis. In the small intestine, MUC2 forms a barrier to the epithelial surface and contributes to removal of pathogens that are loosely associated with epithelial tissue by peristaltic flow. If YghJ degrades mucins and enables stronger persistence of EPEC within the host, it would be expected that the *yghJ* deletion mutant would show decreased faecal shedding. However, no significant difference in faecal shedding between the mutant and wild type was observed, which the authors postulated could be due to other proteins produced by EPEC that share YghJ's mucinase activity. Only when intestinal tissue was examined by immunofluorescence microscopy were differences seen between the strains; bacteria were identified in the lumen and on the enterocyte surface of mice

4. RESULTS: EaeH and YghJ as vaccine candidates

infected with both strains, but fewer organisms on the enterocyte surface were detected in mice infected with the *yghJ* mutant. Substantial decreases in cAMP activation by mouse intestinal epithelial cells compared to the wild type strain were also observed, supporting the hypothesis that YghJ is involved in efficient delivery of LT to host cells (Luo *et al.*, 2014).

The influence of YghJ on pathogenesis of the ExPEC strain IHE3034 also implies the mucin-degrading activity of this protein is utilised by different pathotypes of *E. coli*. Upregulation of YghJ production occurred when IHE3034 intimately attached to human mucus-producing intestinal cells. When gut cells were infected with a *yghJ* deletion mutant, fewer bacteria were able to reach the cell surface underneath the mucus layer compared to the wild type. Expression of YghJ may also provide a metabolic benefit as when bacteria were incubated with mucus-secreting cells, an enhanced growth rate was observed (Valeri *et al.*, 2015).

4.8.5 YghJ function in LF82

The hypothesis that YghJ plays a role in colonisation of the host intestine by facilitating bacterial traversal of the mucus barrier has been supported by recent research investigating its role in ETEC and ExPEC isolates. However, the function of YghJ in AIEC strains has not yet been explored. Comparison of the LF82 YghJ protein sequence with the H10407 sequence revealed LF82 contains the metalloprotease core motif HEXXHX (Nakjang *et al.*, 2012), along with conservation of the 22-amino acid region extending from the motif reported to contain the active site of YghJ (Luo *et al.*, 2014). This implies that LF82 YghJ is also capable of degrading mucin, and with techniques established to assess YghJ function in ETEC and ExPEC strains, given more time it would be interesting to determine whether LF82 YghJ also degrades MUC2 and MUC3 to enhance penetration of the mucus layer. As LF82 cells colonise the intestinal mucosa and are able to adhere to and invade intestinal epithelial cells, it is possible that YghJ aids colonisation of this strain.

4.8.6 YghJ and EaeH as vaccine candidates

Since YghJ was identified as a potential vaccine candidate in 2010, over 400 sequences of this gene from *E. coli* strains have been analysed. The sequences have revealed that variability is distributed along the entire protein, with identity ranging from 86-100%. Importantly, the metalloprotease motif was fully conserved in all sequences analysed (Nesta *et al.*, 2014). Despite this variation, polyclonal antibodies raised by Nesta *et al.* (2014) against a variant I YghJ inhibited the ability of all *E. coli* pathotypes tested to transverse the mucin-based matrix. Additionally, the structural similarity of YghJ was further demonstrated *in vivo* when mice immunised intranasally with recombinant variant I YghJ from an ExPEC strain were challenged with a ETEC strain expressing a YghJ variant II. A significant reduction in caecum-associated bacterial counts was observed in mice immunised with YghJ compared to those mock-immunised with saline, and anti-YghJ responses in immunised mice consisted of both IgG and IgA antibody isotypes (Nesta *et al.*, 2014). The authors of this study suggested that antibody cross-reactivity occurs due to immunogenicity of the conserved metalloprotease domain.

Although our work provides limited evidence for secretion of YghJ in LF82 and consequently implies it is unattractive as a vaccine candidate against AIEC strains, this protein still has strong potential for use in vaccines designed against ETEC, EPEC and ExPEC. The carriage of this protein by a large variety of pathogenic bacteria, along with the discovery of its role in colonisation and evidence of expression *in vivo* (Nesta *et al.*, 2014), make YghJ a viable candidate for the development of a broad-spectrum vaccine against pathogenic *E. coli*.

Expression of EaeH has, to date, been shown to be upregulated only in ETEC strains. As predicted by its protein sequence, EaeH has been identified on the outer surface of bacteria, making it an attractive target for vaccines. However, further study of how this protein is expressed and utilised in colonisation, particularly in clinically relevant strains, is required before its potential as an *E. coli* vaccine candidate can be determined.

4.8.7 LF82 *yghJ* and *eaeH* deletion mutants *in vivo*

Originally, one of the main aims of this work was to assess the contribution of EaeH and YghJ to bacterial colonisation in a mouse model of LF82 infection using deletion mutant strains. However, we ultimately decided not to test these strains in the streptomycin-treated ICR model of LF82 infection, as analysis of this model showed it to be ineffective for studying bacterial attachment to epithelial host cells. When LF82 colonisation of mice was explored (Chapter 3.5.4), high levels of bacterial prevalence in the intestinal lumen was observed throughout the infection, indicating that in the streptomycin-treated mouse gut, LF82 is able to persist without attachment and resist mechanical removal. As we could not directly confirm that bacterial attachment had a significant influence on colonisation of the mouse model, it was not deemed worthwhile to test the deletion mutants in mice. Complementation of the mutant strains was initially considered for controls in animal experiments, however, as we ultimately decided not to pursue these, complementation plasmids expressing EaeH and YghJ under control of their own promoters were not created.

Furthermore, in 2014 Fleckenstein and colleagues published studies in which *eaeH* and *yghJ* deletion mutants were tested in an ETEC murine model (Sheikh *et al.*, 2014; Luo *et al.*, 2014). Colonisation of mice by both mutants, monitored by faecal shedding, did not show a difference from that of the wild type strain. Only when sections of the infected mouse intestine were examined by immunofluorescence microscopy were significant differences in attachment to the intestinal epithelial surface reported. Therefore, the ability of *E. coli* to persist in the lumen without the need for attachment masks the true contribution of EaeH and YghJ to pathogenesis. An alternate animal model in which intimate attachment can be directly measured would thus be more appropriate for *in vivo* assessment of these two proteins.

Chapter 5: Development of novel inhibitors of the *E. coli* Shiga toxin

5.1 Introduction

Production of EHEC Shiga toxin, essential for manifestation of HUS, also limits treatment options as antibiotic use results in increased Stx release and thus greater risk of HUS development. Novel therapeutic treatments that aim to reduce or prevent the production of Stx may therefore lead to a reduction in clinical symptoms. EHEC can produce two types of Shiga toxin: Stx1 and Stx2, which are both encoded by temperate lysogenic bacteriophages but are controlled by different repressors. While inhibition of both Stx1 and Stx2 expression would be ideal, Stx2 is a more desirable target for inhibition than Stx1, as epidemiological and *in vitro* studies demonstrate that Stx2 is more likely to be associated with more serious human disease (Fuller *et al.*, 2011; Bergan *et al.*, 2012), and studies in primates have shown that Stx2 alone can produce symptoms of HUS while Stx1 administration at the same concentration does not (Mayer *et al.*, 2012).

Recently, high-throughput screening at the University of Edinburgh identified several small compounds as potential inhibitors of Stx2 expression (Prof. David Gally, personal communication). This was achieved through the use of fluorescence reporter constructs designed to monitor Stx2 expression, SOS induction and growth. These reporters were used to screen 17,500 chemically diverse compounds from the ChemBridge library (ChemBridge). This screen identified 77 inhibitors, 6 of which were selected for further studies after dose-response validation. The inhibitory potential of these lead compounds was further investigated using *E. coli* transformed with a plasmid containing an *stx2* promoter fused to a GFP gene, in which GFP expression could be induced by mitomycin C (MMC). The compound that was most effective at limiting MMC-induced *stx2*:GFP fluorescence was 5324835, which revealed concentration-dependent inhibition of GFP expression between 25 and 200 μM . The dose-response effect of 5324836 on MMC-induced Stx production was subsequently confirmed by enzyme-linked immunosorbent assay. This implies 5324836 inhibits Stx production, although does not reveal whether the compound directly interferes with *stx2* transcription or with events that modify transcription activation.

5.1.1 Aims of this chapter

- To validate the inhibition of Stx expression by compound 5324836, using the Stx-GFP reporter system in the Stx-negative O157:H7 ZAP0273 strain.
- To expand our knowledge regarding the active site of the 5324836 compound by evaluating modifications of the compound in the GFP reporter system, and to evaluate the efficacy of these modified compounds relative to that of 5324836.
- To uncover the mode of action of this compound and to identify the bacterial target or targets, and employ biophysical techniques to characterise these interaction.
- If the compounds show with potential as Stx-inhibiting drugs, to test them *in vivo* using the Stx-producing *C. rodentium* mouse model.

5.2 Modification of the hit compound 5324836 (AHU1)

The 258.1 Da compound 5324836, renamed AHU1, is a planar molecule composed of a maleimide and a morpholine moiety connected by a benzene ring (Figure 5-1). This compound is insoluble in water, and therefore was routinely solubilised in 100% DMSO at 20 mM stock concentration. However, the compound showed stability in much lower concentrations of DMSO (Alejandro Huerta Uribe, personal communication).

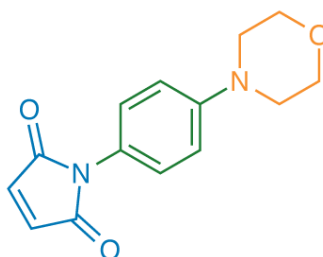


Figure 5-1: Structure of AHU1. The compound contains a maleimide (blue), benzene (green), and morpholine (orange) moiety, and has a molecular weight of 258.10 g/mol.

In order to understand the structure-activity of this compound, modifications were performed on AHU1 by Alejandro Huerta Uribe, a PhD student at the University of Glasgow. The morpholine moiety was initially selected for modification, as the presence of a heteroatom (a non-carbon atom in a ring structure) on the six-membered ring facilitates chemical manipulation. Briefly, the morpholine ring was replaced with an isostere piperazine in order to perform modifications on the nitrogen atom, and the addition of a methyl group and a butyl chain on this position gave the compounds AHU2 and AHU3, respectively (Figure 5-2 A, B). As we believed the maleimide of the compound was likely to be the active part of the molecule due to the reactivity of this moiety, the compound AHU4 was produced by the addition of a phenyl group to the maleimide moiety (Figure 5-2 C).

5. RESULTS: Shiga toxin inhibitors

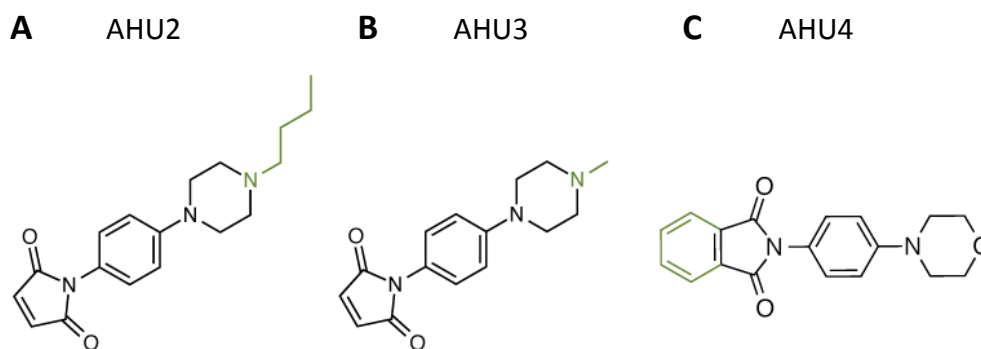


Figure 5-2: Structures of the modified AHU compounds. Compounds shown are AHU2 (**A**), AHU3 (**B**) and AHU4 (**C**). Butyl, methyl and phthalimide modifications are indicated in green. The molecular weights of the compounds are 271.13, 313.18, and 308.33 g/mol, respectively.

5.3 Stx2 reporter-fusion assays

5.3.1 Inhibition of bacterial lysis and *pstx2*:GFP expression by AHU1

Under normal growth conditions, Stx2 is expressed at very low levels. Expression can be upregulated by DNA-damaging agents that activate the SOS response, and is often induced experimentally by addition of MMC, a potent DNA crosslinker. To evaluate the effect of AHU1-4 on *stx2* expression, the *pstx2*:GFP promoter-fusion plasmid containing the *stx2c* promoter fused to a GFP gene was transformed into Stx-negative Sakai ZAP0273, a lysogenic strain. Bacteria in mid-logarithmic growth were exposed to AHU1 at concentrations between 10-200 μ M, and the SOS response activated by addition of 1 μ g/ml MMC, a concentration that initially allows growth to continue after MMC addition, but eventually results in bacterial lysis after 3-4 hours. Growth (OD_{600}) and GFP expression (fluorescence) was measured at intervals of 1 hour, for a maximum of 6 hours, following addition of compounds and MMC.

5. RESULTS: Shiga toxin inhibitors

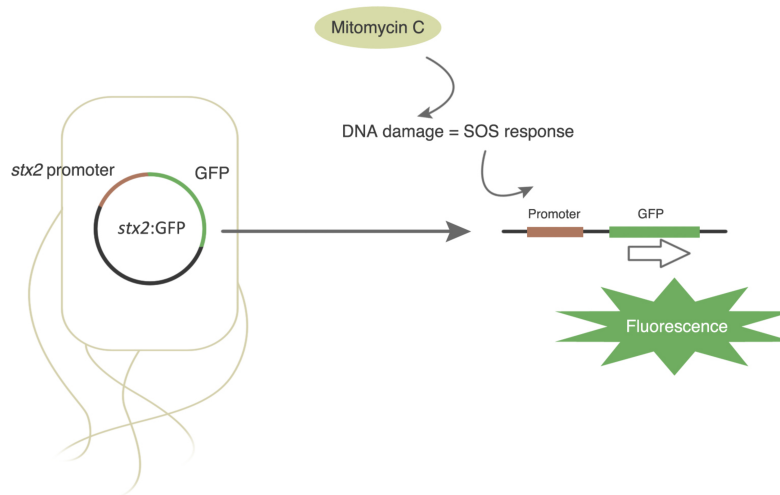


Figure 5-3: *Stx2:GFP* reporter assay. When *E. coli* transformed with the *pstx2:GFP* reporter fusion are treated with MMC to produce DNA damage and induction of the SOS response, the activated *stx2* promoter results in expression of GFP and production of fluorescence.

To determine any inhibitory effects of AHU1 on bacterial survival or replication, uninduced cultures containing 10-200 μM AHU1 were grown alongside MMC-induced cultures. Overall, AHU1 alone inhibited bacterial growth at high concentrations (200 μM) (Figure 5-4 A). In MMC-induced cultures, bacterial growth decreased 3 hours after addition of MMC when no AHU1 was present, an effect that reflects phage-mediated bacterial cell lysis initiated by activation of the SOS response by MMC. In contrast, at concentrations of 50-100 μM AHU1, some inhibition of this lysis was observed (Figure 5-4 B).

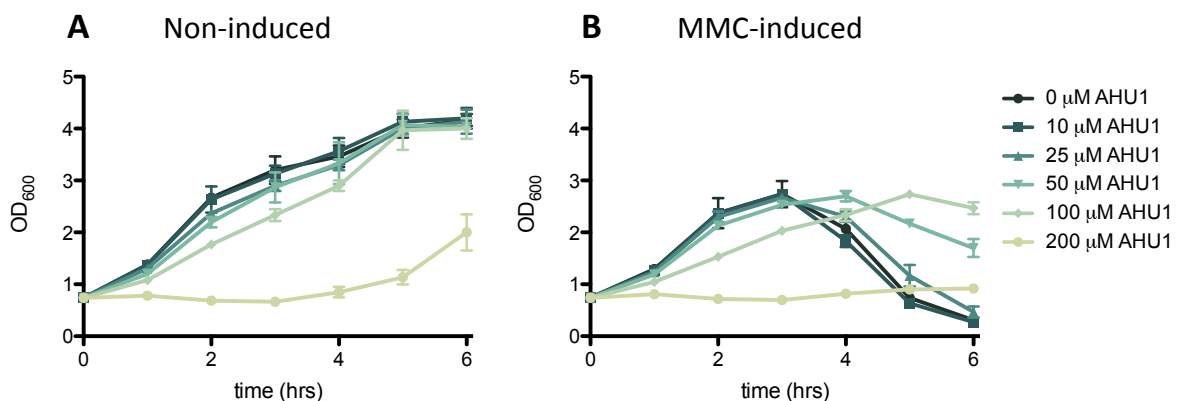


Figure 5-4: Inhibition of MMC-induced bacterial lysis by AHU1. ZAP0273 transformed with *pstx2:GFP* were grown in the presence or absence of 10-200 μM AHU1 (A) and induced with 1 $\mu\text{g/ml}$ MMC (B), and the OD₆₀₀ of cultures measured hourly. Asterisks denote those time points at which a significant difference was observed. Experiments were performed in triplicate with each replicate subcultured separately, and data plotted as the mean with standard deviation from the mean displayed by error bars.

5. RESULTS: Shiga toxin inhibitors

GFP expression was not observed in the absence of MMC, and was not influenced by the addition of AHU1 (Figure 5-5 A). As expected, *stx2*:GFP was detected 3-6 hours after induction with MMC, coinciding with the lysis stage, and was inhibited in a dose-dependent manner by AHU1 (Figure 5-5 B). Our results have therefore confirmed the original observation that this compound influences expression through the *stx2* promoter.

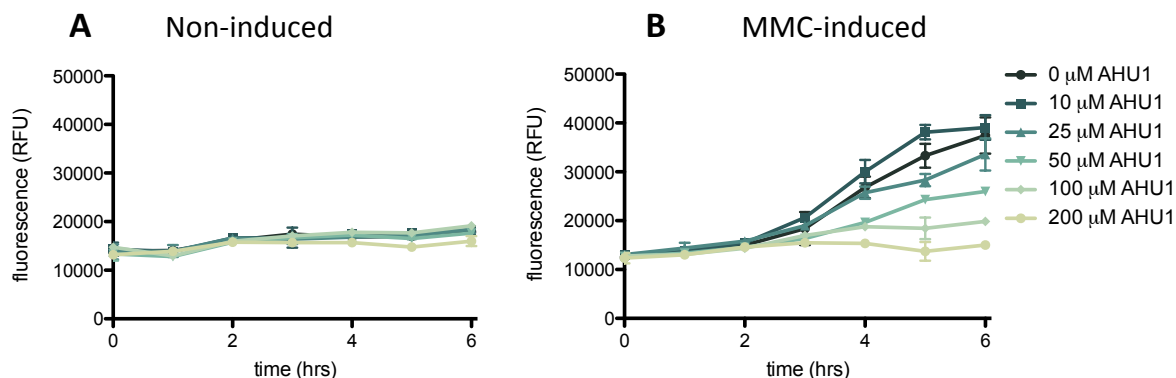


Figure 5-5: Dose-dependent inhibition of MMC-induced *stx2*:GFP expression by AHU1. ZAP0273 transformed with *pstx2*:GFP were grown in the presence or absence of 10-200 μM AHU1 (A) and induced with 1 μg/ml MMC (B), and fluorescence measured hourly. Experiments were performed in triplicate with each replicate subcultured separately, and data plotted as the mean with standard deviation from the mean displayed by error bars.

5.3.2 Inhibition of bacterial lysis and *stx2*:GFP expression by AHU2 and AHU3.

The *stx2*:GFP reporter system was used to evaluate the inhibitory effects of the modified compounds AHU2 and AHU3 on growth, lysis, and GFP expression. Both AHU2 and AHU3 showed increased efficacy, with concentrations of 50 μM inhibiting bacterial lysis and *stx2*:GFP expression (Figure 5-6), approximately halving the dose required for optimal inhibition by AHU1.

5. RESULTS: Shiga toxin inhibitors

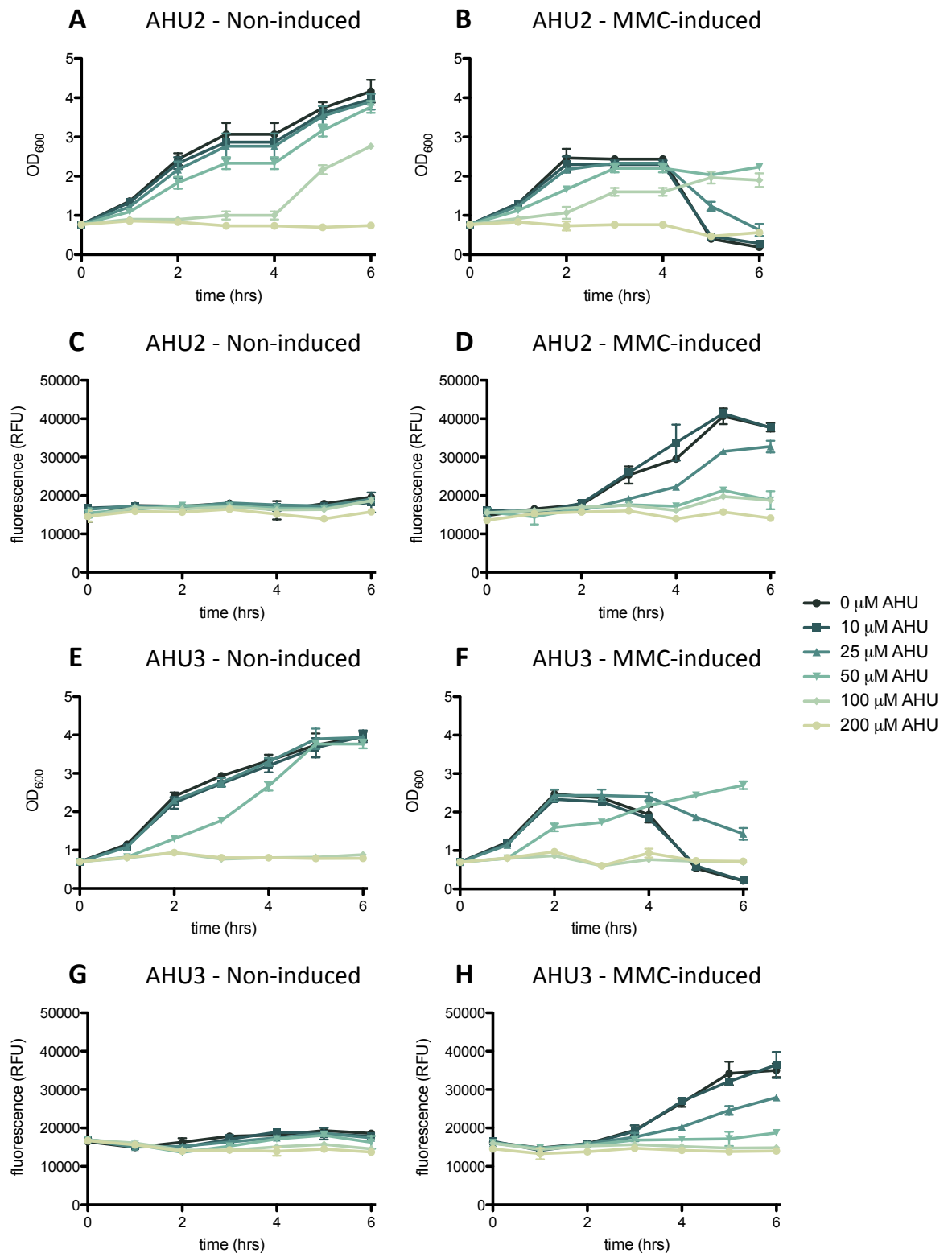


Figure 5-6: Effect of AHU2 and AHU3 on bacterial growth, MMC-induced lysis, and MMC-induced *stx2*:GFP expression. ZAP0273 transformed with *pstx2*:GFP were grown in the presence of 10-200 μM AHU2 (A-D) or AHU3 (E-H) and uninduced (left) or induced with 1 μg/ml MMC (right). Growth (OD₆₀₀) and *stx2* expression (GFP) were measured hourly. Both AHU2 and AHU3 cause inhibition of growth at higher concentrations (A, E), inhibition of bacterial lysis at 25-100 μM (B, F) and inhibition of MMC-induced lysis (D, H). Experiments were performed in triplicate with each replicate subcultured separately, and data plotted as the mean with standard deviation from the mean displayed by error bars.

5. RESULTS: Shiga toxin inhibitors

To compare the *stx2*:GFP inhibitory properties of AHU1, AHU2 and AHU3, the percentage inhibition of *stx2*:GFP expression at 6 hours post-MMC induction was calculated using the following formula:

$$100\left(1 - \left(\frac{F_{AHU} - F_{min}}{F_{max} - F_{min}}\right)\right)$$

where F_{AHU} = fluorescence at 6 hours with MMC induction and AHU present, F_{min} = fluorescence at 6 hours with no MMC induction, and F_{max} = fluorescence at 6 hours with MMC induction. Two concentrations of AHU1-3 were selected: 25 μ M and 50 μ M, as inhibition of lysis and GFP expression was effective at these concentrations for all three compounds. All showed inhibition at 25 μ M, although AHU3 had significantly more inhibitory activity than AHU1. At 50 μ M, both AHU2 and AHU3 produced near-complete inhibition of *stx2*:GFP expression, which was significantly higher than that of AHU1 (Figure 5-7). As AHU3 was the most effective of the three compounds, this was selected for use in all further experiments.

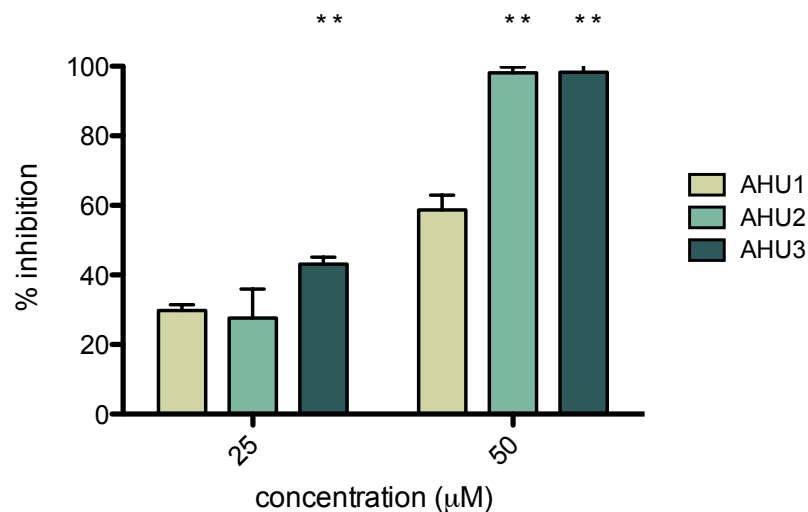


Figure 5-7: Inhibition of *stx2*:GFP expression by 25 and 50 μ M AHU1, AHU2 and AHU3 at 6 hours after addition of AHU1-3 and MMC. Data was calculated from triplicate experiments and displayed as the mean inhibition with error bars showing the standard deviation from the mean. Asterisks indicate a significant difference (** = $p < 0.001$) from inhibition by AHU1 at the same concentration inhibition. Inhibition by AHU2 at 50 μ M was significantly higher than that of AHU1 ($p < 0.001$, 4 degrees of freedom, $t = 14.942$), and inhibition by AHU3 was significantly higher than that of AHU1 at both 25 μ M ($p < 0.001$, 4 degrees of freedom, $t = 9.056$) and 50 μ M ($p < 0.001$, 4 degrees of freedom, $t = 14.597$). Statistical significance was determined by Student's unpaired t-test.

5.3.3 Inhibition of bacterial lysis and *stx2*:GFP expression by AHU4.

The final compound to be tested was AHU4, in which a phthalimide group was added to the maleimide ring of the compound. This change resulted in a loss of activity of the drug, with bacterial lysis and GFP expression equivalent to untreated cells. Bacterial growth was also unaffected (Figure 5-8). From this, it would appear that the maleimide ring is essential for the inhibitory property of the compounds, and is the active site of this molecule.

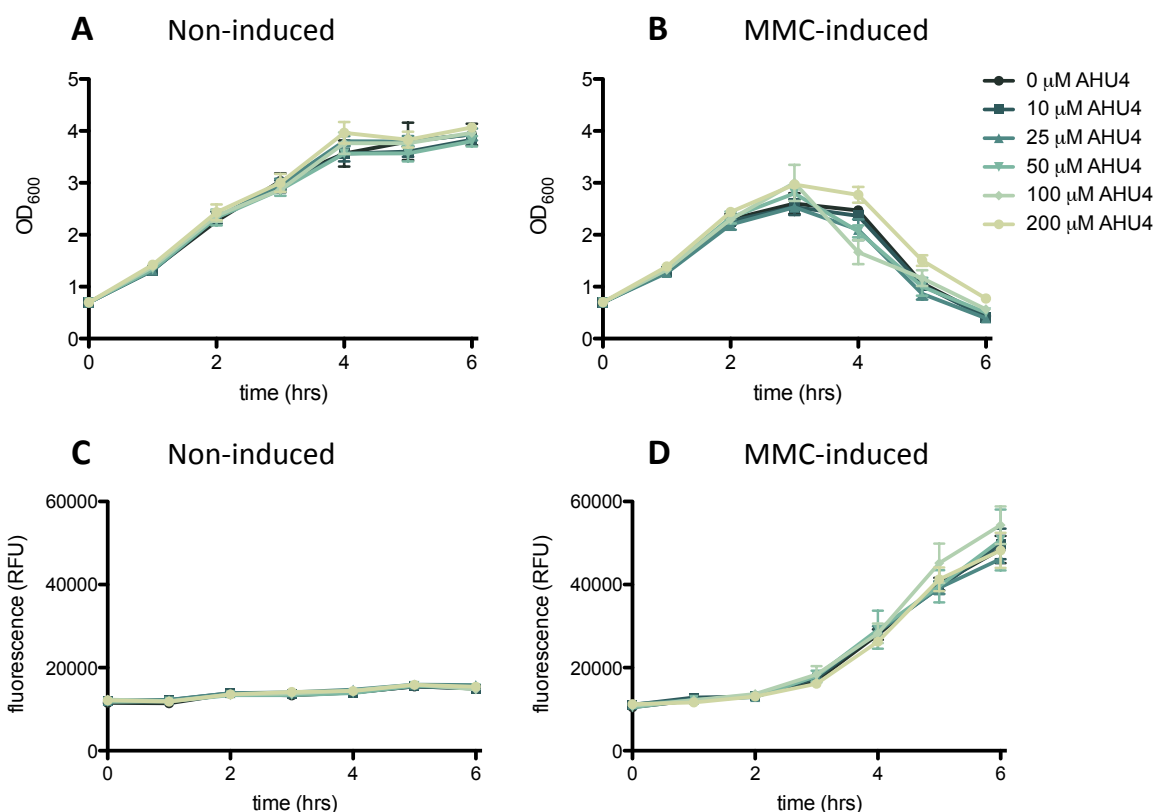


Figure 5-8: Effect of AHU4 on bacterial growth, MMC-induced lysis, and MMC-induced *stx2*:GFP expression. ZAP0273 transformed with *pstx2*:GFP were grown in the presence or absence of 10-200 μM AHU4, (A, C) and induced with 1 μg/ml MMC (B, D). Growth (OD₆₀₀) and *stx2* expression (GFP) were measured hourly. Growth (A), MMC-induced lysis (B), and both *stx2*:GFP expression in the absence (C) and presence (D) of MMC remained unaffected by AHU4. Experiments were performed in triplicate with each replicate subcultured separately, and data plotted as the mean with standard deviation from the mean displayed as error bars.

5.3.4 The maleimide group on its own can inhibit lysis and *Stx* expression

As the maleimide moiety appeared responsible for the inhibition of MMC-induced lysis and *stx2*:GFP expression by the AHU compounds, the impact of purified maleimide (#129585, Sigma-Aldrich) on these activities was tested. In comparative experiments with AHU3, maleimide elicited a stronger inhibitory effect on growth than AHU3 (Figure 5-9 A), with the OD₆₀₀ of culture containing 50 μ M maleimide decreasing over the last two hours of the experiment (Figure 5-9 B), which contrasted with cultures treated with 50 μ M AHU3. Inhibition of *stx2*:GFP expression by maleimide occurred at similar efficacy to AHU3 (Figure 5-9 C, D). These results indicated that cell lysis was occurring in the maleimide-containing culture and thus inhibition of phage-mediated lysis by maleimide was less efficient than AHU3.

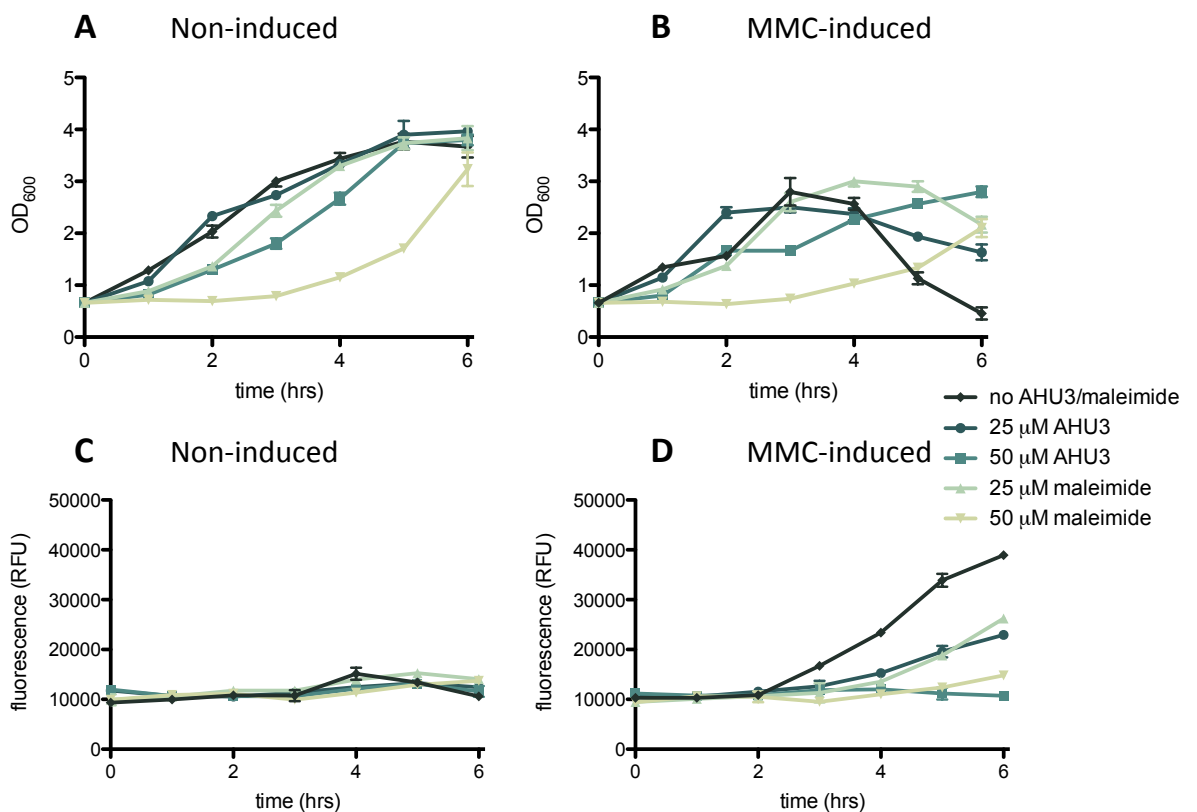


Figure 5-9: Comparison of inhibitory effects of AHU3 and maleimide. ZAP0273 transformed with *pstx2*:GFP were grown in the presence or absence of 25 or 50 μ M AHU3 or maleimide (A, C), and induced with 1 μ g/ml MMC (B, D). Growth (OD₆₀₀) and *stx2* expression (GFP) were measured hourly. While AHU3 and maleimide demonstrated similar *stx2*:GFP inhibition efficacy, maleimide had a stronger inhibitory effect on bacterial growth at 25 μ M than AHU3 at the same concentration (A). Experiments were performed in triplicate with each replicate subcultured separately, and data plotted as the mean with standard deviation from the mean displayed as error bars.

5. RESULTS: Shiga toxin inhibitors

These findings suggest that the non-maleimide groups of AHU3 have an unknown role in increasing the specificity of the molecule. Therefore, we chose to further evaluate AHU3, which appeared to be an effective inhibitor of Stx expression without strong limitation of bacterial growth.

5.3.5 AHU3 does not inhibit expression of *rpsM* and *tir*

The specificity of AHU3 was explored using expression reporters for *rpsM*, which encodes the 30S ribosomal protein S13 and is a commonly used growth control in biological assays, and *tir*, encoding the Type 3-secreted receptor protein Tir. To determine if the presence of AHU3 has any influence on the expression of these genes, reporter constructs were transformed into ZAP0273 cells. These were grown in the presence or absence of 50 μ M AHU3, and fluorescence measured against OD₆₀₀. As expression of T3SS genes is dependent on environmental signals, bacteria were grown in MEM-HEPES media to induce expression of *tir*. AHU3 did not affect expression of GFP controlled by either the *rpsM* and *tir* promoters (Figure 5-10), implying that AHU3 does not influence expression of either of these genes.

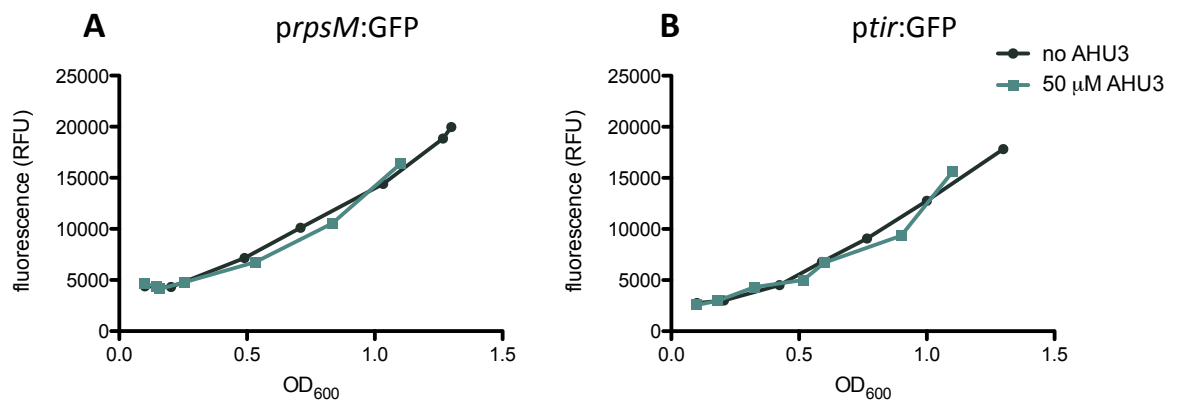


Figure 5-10: Effect of AHU3 on *rpsM:GFP* and *tir:GFP* expression. ZAP0273 transformed with *prpsM:GFP* (A) or *ptir:GFP* (B) were grown in the presence or absence of 50 μ M AHU3 for 6 hours. OD₆₀₀ and fluorescence were measured hourly, and fluorescence plotted against the OD₆₀₀ of that time point.

5.4 AHU3 inhibits phage production

5.4.1 Inhibition of Stx phage production by AHU3

The *stx2*:GFP reporter assays demonstrate that the AHU compounds inhibit general phage-mediated lysis of ZAP0273. Although this strain has had the Stx2 phage deleted, it undergoes lysis in the presence of MMC, suggesting that other integrated lysogenic phages are responsible and that the AHU compounds interfere with their expression. To confirm that AHU3 directly inhibits production of the Stx2 phage, phage transduction assays were performed using *E. coli* JP10819, which only carries the lysogenic Stx prophage ϕ P27. This prophage contains a tetracycline resistance cassette inserted into the *stx2* toxin gene providing tetracycline resistance and preventing production of Stx. Phage production was induced by 2 μ g/ml MMC in the presence and absence of 50 μ M AHU3, the concentration at which *stx2*:GFP expression and bacterial lysis were effectively inhibited in the GFP reporter assay, and the phages produced isolated by filtration. The non-lysogenic *E. coli* strain MG1655 was incubated with serial dilutions of the recovered phage and grown on agar containing tetracycline, as MG1655 infected with the Stx phage acquire resistance against this antibiotic. Each colony was counted as a single phage transductant, and differences in phage production by the four samples were analysed using the general linear model (GLM) test.

Bacteria that were not induced with MMC produced low levels of Stx phage ($\sim 10^4$ transductants/ml JP10819), which significantly increased to $\sim 10^8$ transductants/ml when induced with MMC. Inclusion of 50 μ M AHU3 resulted in a highly significant decrease in the amount of phage produced by MMC-induced bacteria (Figure 5-11). However, the difference in phage production between non-induced bacteria with and without AHU3 treatment was also significant, which probably reflects the inhibition of growth by AHU3. GLM analysis of the interaction between MMC induction and AHU3 treatment was determined to be highly significant. This demonstrated that the statistically significant reduction in phage production by MMC-induced cells observed is not merely the result of the inhibitory effect AHU3 has on bacterial growth. This implies that MMC-induced expression of Stx phage genes is inhibited by AHU3.

5. RESULTS: Shiga toxin inhibitors

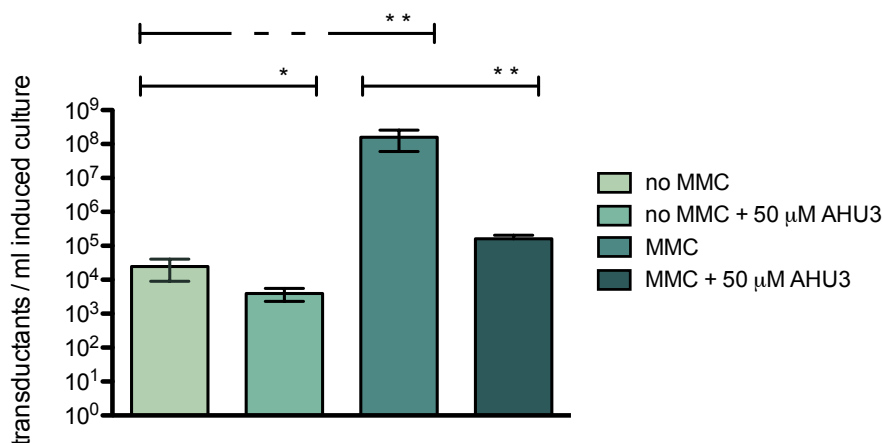


Figure 5-11: Reduction of MMC-induced Stx phage production by 50 µM AHU3. Induction of JP10819 with 2 µg/ml MMC resulted in significantly increased phage production ($p < 0.001$, 4 degrees of freedom, $t = 17.780$). Addition of 50 µM AHU3 produced a significant decrease in phage production by both non-induced ($p = 0.0158$, 4 degrees of freedom, $t = 4.022$) JP10819 and MMC-induced JP10819 ($p < 0.001$, 4 degrees of freedom, $t = 18.840$), and the interaction between MMC and AHU3 determined significant ($p < 0.001$, 8 degrees of freedom, $t = 8.884$). Asterisks indicate a significant difference (* = $p < 0.05$, ** = $p < 0.001$) in phage production. The data shown is the average of triplicate individual experiments with each replicate subcultured separately, with standard deviation from the mean displayed as error bars. Statistical significance was determined by GLM analysis.

5.4.2 Inhibition of Gram-positive phage production by AHU3

As the AHU compounds appeared to inhibit phage-mediated bacterial lysis, we next explored whether these drugs could inhibit other non-Stx phages, including those carried by Gram-positive bacteria. To evaluate their activity, two strains of *S. aureus* harbouring different phages were tested with AHU3: JP5011, which carries the ϕ SLT phage that produces the pore-forming Panton-Valentine leukocidin toxin (Ferrer *et al.*, 2011), and RN10359, which carries the prophage 80 α , involved in mobilisation of *S. aureus* pathogenicity islands.

Similar to the Stx2 phage in JP10819, the SLT phage in the JP5011 strain contains a tetracycline resistance gene integrated into the phage *p_{lv}* gene that encodes the toxin. When induced by MMC, approximately 10⁶ transductants/ml of JP5011 culture were produced. In contrast, only 10² transductants/ml were generated from uninduced JP5011. Treatment of the MMC-induced culture with 50 µM AHU3 showed at least a log-fold

5. RESULTS: Shiga toxin inhibitors

reduction in the number of transductants generated, but did not reduce this to levels observed in non-induced controls, while treatment of the uninduced culture did not result in a significant change in phage transduction (Figure 5-12).

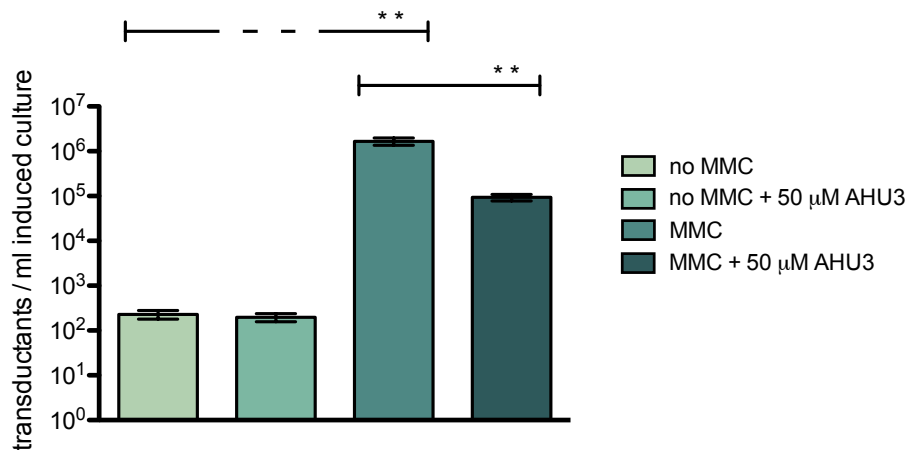


Figure 5-12: Reduction of MMC-induced SLT phage production by AHU3. Induction of JP5011 with 2 μg/ml MMC resulted in significantly increased phage production ($p < 0.001$, 4 degrees of freedom, $t = 53.94$). Addition of 50 μM AHU3 produced a significant decrease in phage production by MMC-induced JP5011 ($p < 0.001$, 4 degrees of freedom, $t = 19.97$). Asterisks indicate a significant difference (** = $p < 0.001$) in phage production. The data shown is the average of triplicate individual experiments with each replicate subcultured separately, with standard deviation from the mean displayed as error bars. Statistical significance was determined by GLM analysis.

Inhibition of 80α phage production, a highly lysogenic phage, was measured by following growth of RN10359 in LB. Cultures were induced with 500 ng/ml MMC and AHU3 added at concentrations between 10-200 μM, and OD₆₀₀ measured for 6 hours. While growth and lysis of *S. aureus* in the presence of AHU3 was not as noticeably different to the control, 50 μM AHU3 resulted in a significant reduction of OD₆₀₀ compared to the control at the 3-6 hour time points (Figure 5-13). Concentrations of 100 and 200 μM AHU3 showed lower OD₆₀₀ values than the control, indicating that AHU3 also slows bacterial growth in *S. aureus*.

5. RESULTS: Shiga toxin inhibitors

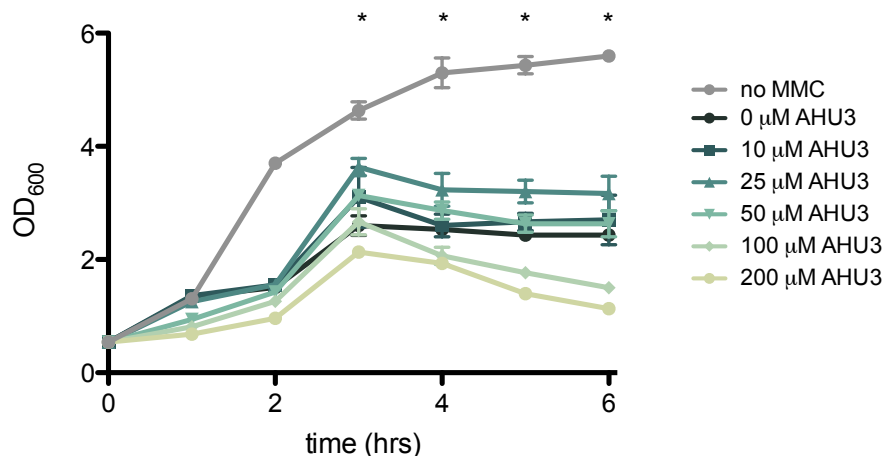


Figure 5-13: Effect of AHU3 on MMC-induced bacterial lysis by 80α. RN10359 were grown in the presence or absence of 10-200 μM AHU3 and induced with 500 ng/ml MMC. The OD₆₀₀ of cultures was measured hourly, and the time points at which the OD₆₀₀ of the 50 μM AHU3 culture were significantly higher than the untreated culture are indicated by asterisks (* = p<0.05). Experiments were performed in triplicate with each replicate subcultured separately, with data plotted as the mean, and standard deviation from the mean displayed by error bars. Statistical significance was determined by Student's unpaired t-test.

While inhibition of phage production in *S. aureus* by AHU3 is less effective than that seen in *E. coli*, it provides some evidence that AHU3 can affect Gram-positive phage production. It also demonstrates that AHU3 does not specifically target expression or production of only the Stx2 phage, but has a broader and more general impact on phage biology.

5.5 AHU3 does not target mitomycin C

One mechanism by which the AHU compounds could work is through direct interaction with MMC, preventing its capacity to damage bacterial DNA. To determine whether MMC was the target of AHU3, Stx phage transduction and GFP-Stx reporter fusion assays were repeated using ciprofloxacin instead of MMC. Ciprofloxacin is a member of the fluoroquinolone group of antibiotics which induce Stx bacteriophage *in vivo* (Zhang *et al.*, 2000). The bactericidal action of ciprofloxacin is achieved by inhibition of topoisomerases II and IV, which are essential for DNA replication, transcription, repair and recombination, thus resulting in DNA damage and activation of the SOS response. If AHU3 inhibits MMC

5. RESULTS: Shiga toxin inhibitors

directly, bacterial lysis and Stx expression would be unaffected if AHU3 is used in combination with ciprofloxacin.

The SOS response was effectively induced using a concentration of 50 ng/ml ciprofloxacin. Importantly, the presence of AHU3 resulted in dose-dependent inhibition of both lysis and *stx2*:GFP expression similar to that seen when MMC was used as the inducing agent (Figure 5-14 A, B). Additionally, AHU3 was able to significantly reduce Stx phage production by ciprofloxacin-induced JP10819 (Figure 5-14 C). From this, we concluded that the inhibition observed in previous assays was not the result of direct interaction of AHU3 with MMC.

5. RESULTS: Shiga toxin inhibitors

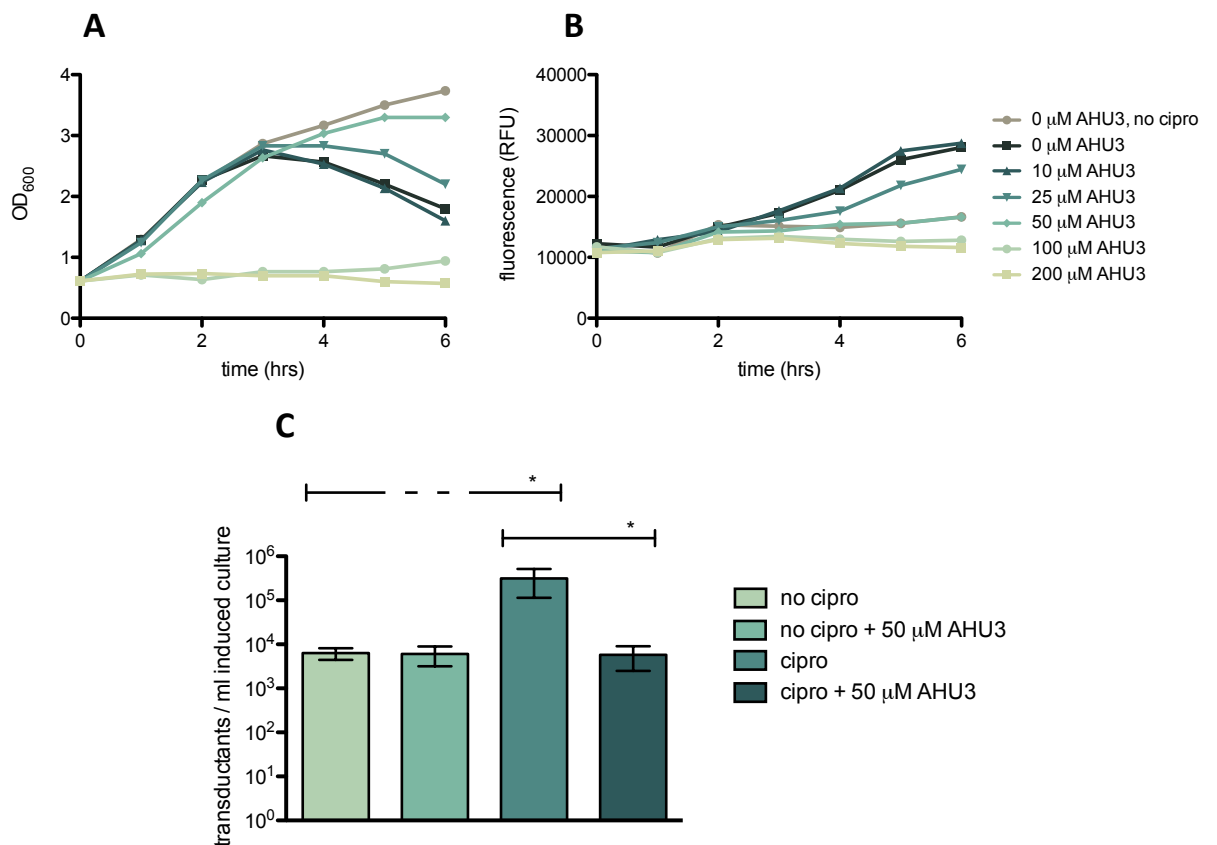


Figure 5-14: AHU3 prevents ciprofloxacin-mediated SOS response. ZAP0273 transformed with *pstx2*:GFP were grown the presence or absence of 10-200 μ M AHU3, and induced with 50 ng/ml ciprofloxacin. AHU3 inhibited ciprofloxacin-induced bacterial lysis (**A**) and *stx2*:GFP expression (**B**). AHU3 also inhibited ciprofloxacin-induced Stx phage production (**C**). Induction of JP10819 with 50 ng/ml ciprofloxacin resulted in significantly increased phage production ($p=0.002$, 4 degrees of freedom, $t=7.295$). Addition of 50 μ M AHU3 produced a significant decrease in phage production by ciprofloxacin-induced bacteria ($p=0.002$, 4 degrees of freedom, $t=6.868$). Asterisks indicate a significant difference ($* = p<0.05$) in phage production. The data shown is the average of triplicate individual experiments with each replicate subcultured separately, with standard deviation from the mean displayed as error bars. Statistical significance was determined by GLM analysis.

5.6 Identifying the possible target of AHU3

As AHU3 inhibits phage production in both Gram-negative and Gram-positive bacteria, including phages unrelated to Stx, it appeared likely that AHU3 acts on an essential component of the SOS response involved in the induction of phage expression. Prophage genes are under the control of phage repressors that, under non-stressed cell conditions, prevent the phage from entering the lytic cycle and causing bacterial host lysis. When the SOS response is initiated, RecA filaments mediate autocleavage of the key SOS response

5. RESULTS: Shiga toxin inhibitors

repressor LexA as well as autocleavage of phage repressors, thus allowing gene expression and production of assembled phage particles and toxins. Therefore, inhibition of the SOS response by AHU3 through prevention of RecA-mediated autocleavage of prophage repressors could help to explain the results observed: inhibition of both Gram-negative and Gram-positive phage production, inhibition of prophage-encoded toxin expression, and inhibition of phage-mediated bacterial lysis. To be effective in both Gram-negative and Gram-positive bacteria, AHU3 would need to target a protein highly conserved across the bacterial species.

We therefore hypothesised that the most likely target of the AHU compounds was RecA, which fits the above criteria. Inactivation of this protein by AHU3, either by preventing it binding damaged DNA, forming activated filaments, or interacting with prophage repressors, would block expression of phage genes (Figure 5-15). LexA was also considered but, as this would require the compounds to bind to a region of the protein that shared high similarity with many different phage repressors, RecA was thought more likely to be the target. Inhibition of either gene expression or protein function of other SOS components is unlikely, as while this would inhibit the SOS response, phage gene expression would be unaffected.

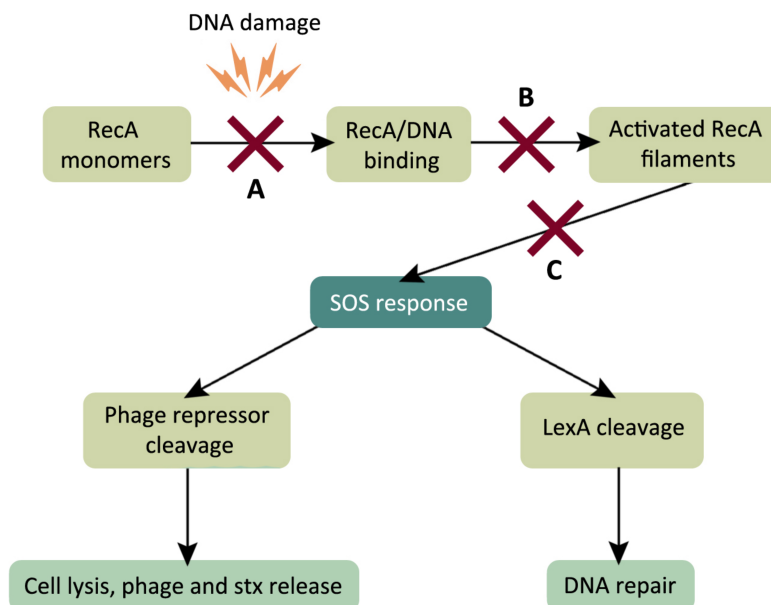


Figure 5-15: Possible stages of SOS response activation that AHU3 may inhibit. LexA and prophage repressor autocleavage, which results in expression of SOS response and prophage genes, is mediated by activated RecA filaments. These are assembled when RecA monomers recognise damaged DNA. AHU3 may therefore inhibit induction of the SOS response either by preventing RecA from recognising DNA (**A**), inhibiting oligomerisation of RecA into activated filaments (**B**), or by blocking the RecA filament's ability to mediate autocleavage of LexA/prophage repressors (**C**).

5.7 Microscale thermophoresis of AHU3 and RecA

Microscale thermophoresis (MST) was used to determine whether AHU3 interacts with RecA directly. MST analyses biomolecule interaction by measuring the directed movement of molecules in a microscopic temperature gradient. This molecular behaviour, termed thermophoresis, is detected through fluorescence of one of the binding partners, either by labelling the molecule with a fluorescent tag or using its intrinsic fluorescence. Thermophoresis is dependent on factors such as size, charge, and solvation shell of the molecule, and therefore when the labelled molecule binds a target these properties are altered, resulting in a detectable change in thermophoresis. MST has several advantages over other well-established techniques for molecule interaction investigation such as isothermal titration calorimetry and surface plasmon resonance. Notably, it does not require immobilisation of one of the molecules, a step that can cause binding difficulties due to steric hindrance at the interface. In addition, lysate or whole cell extract can be used in place of purified proteins.

5. RESULTS: Shiga toxin inhibitors

To assess RecA and AHU3 binding, we fluorescently labelled RecA through covalent attachment of NT.Red dye. In these experiments the inactive derivative AHU4 was used as a negative control. The concentration of RecA was kept constant at 100 μM , while AHU3 and AHU4 concentrations ranged from 12-200 μM . Incubation of RecA with AHU3 provided supportive evidence that binding occurred between RecA and AHU3, while AHU4 showed no affinity for RecA (Figure 5-16).

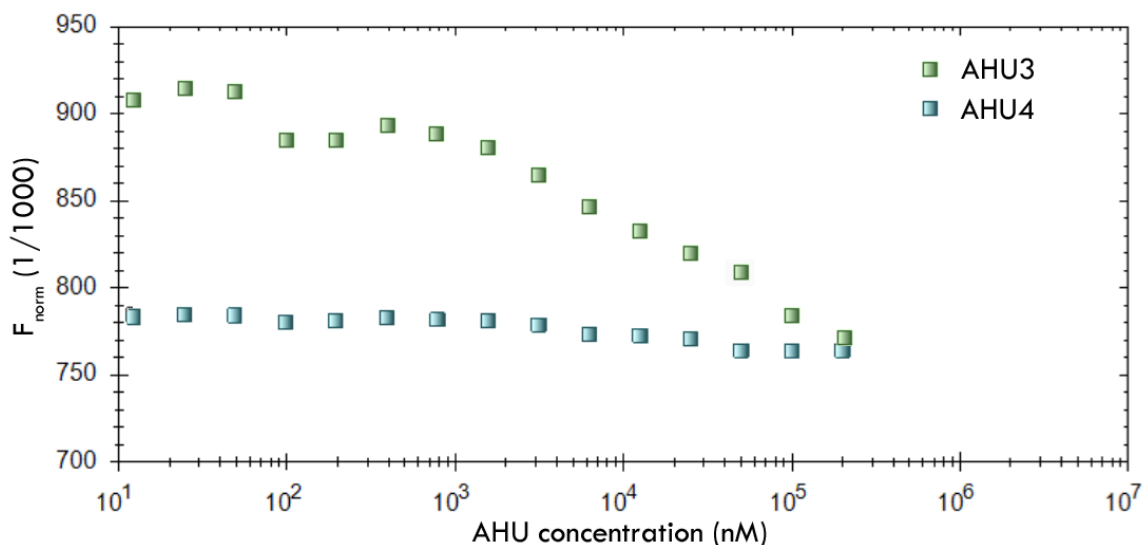


Figure 5-16: Interaction of RecA with AHU3 and AHU4. AHU3 (green) and AHU4 (blue) in 4% DMSO and PBS were added at concentrations between 12-200 μM to 100 μM fluorescently-labelled RecA in PBS. The signal corresponds to the fraction of fluorescence formed as a consequence of complex formation.

5.8 AHU3 inhibits the ATPase activity of RecA

Previous studies of RecA inhibitors have used ATP assays which quantify the amount of free phosphate as a measure of ATP hydrolysis, as an indirect measure of RecA nucleoprotein filament assembly (Wigle & Singleton, 2007; Wigle *et al.*, 2009; Sexton *et al.*, 2010). We attempted to replicate the phosphomolybdate-blue ATPase assay as used by Sexton *et al.* (2010), wherein compounds that inhibit RecA produce a decrease in A₈₂₅. However, we were unable to reproduce this assay. We therefore used the Innova Biosciences ATPase assay kit, which produces a Pⁱ-dye complex when free phosphate is produced by ATPase-mediated hydrolysis of ATP. Optimal final concentrations of RecA and ssDNA were 250 nM and 5 μM respectively, with higher concentrations of RecA

5. RESULTS: Shiga toxin inhibitors

causing precipitation due to the presence of detergent in the RecA buffer. DMSO was required for solubility of AHU3 and kept at a final concentration of 2%, as >5% DMSO inhibited the reaction. A reaction lacking RecA was used as a background absorbance control, and a reaction that included RecA but no ssDNA was used to confirm that ATP hydrolysis was dependent on the presence of ssDNA. AHU3 was included at concentrations between 0.1-100 μM , and a positive control with no AHU3 present included. The presence of AHU3 resulted in a concentration-dependent decrease in A_{650} , implying that AHU3 inhibits RecA in a manner that prevents it from catalysing ATP hydrolysis. While the ATPase assay is not a direct measure of nucleoprotein filament formation, it provides further evidence that the AHU compounds are inhibitors of RecA, and validates our MST findings.

The data, as a percentage of the average absorbance of the 0 μM control, generated a dose-response curve that was used to determine IC_{50} values (Figure 5-17). The relative IC_{50} calculated was 7.721 μM , similar to the single-digit micromolar values obtained for the most potent of other previously studied RecA inhibitors, and a shallow Hill slope of 0.109, which was lower than the >5.0 values of the other reported RecA inhibitors (Sexton *et al.*, 2010; Peterson *et al.*, 2012).

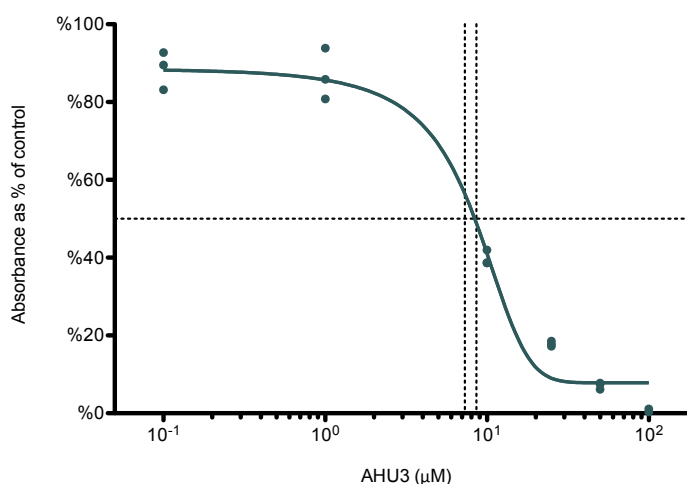


Figure 5-17: AHU3 inhibits RecA-mediated ATP hydrolysis. Dose-response curve of AHU3 showing the inhibition of ATPase activity by different concentrations of 0.1-100 μM AHU3. Data is plotted as a percentage of the average absorbance of the assay wells containing 0 μM AHU3. The curve exhibits an IC_{50} value of 7.721 μM and a Hill slope of 0.109.

5. RESULTS: Shiga toxin inhibitors

The inactive AHU4 compound was also tested for ATPase inhibition and showed no evidence of ATPase activity (Figure 5-18), confirming that the maleimide is responsible for ATPase inhibition.

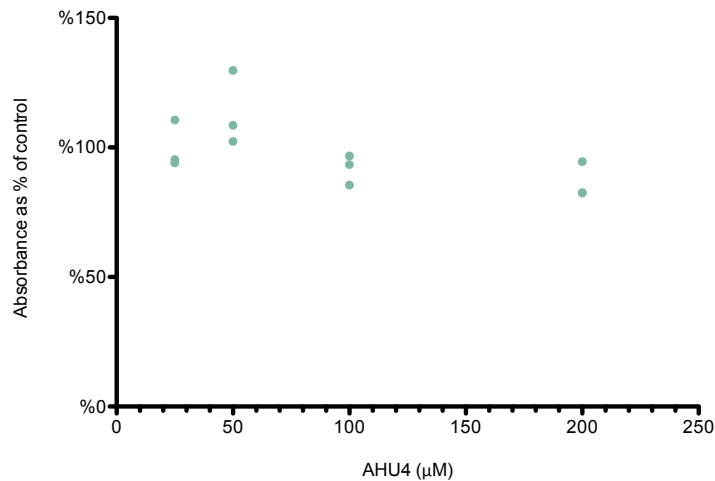


Figure 5-18: AHU4 does not inhibit RecA-mediated ATP hydrolysis. Concentrations of AHU4 between 25-200 μM showed no dose-dependent effect on RecA-mediated ATP hydrolysis and no dose-response curve could be fitted. Data is plotted as a percentage of the average absorbance of the assay wells containing 0 μM AHU4.

5.9 AHU3 inhibits RecA oligomerisation

Analytical ultracentrifugation (AUC), a versatile method for the quantitative analysis of macromolecules, employs a centrifugal field to study the sedimentation of proteins in solution. Centrifugation at high speed separates proteins according to their shapes and masses, and concentrations of these different protein species are measured using absorbance or interference optics, allowing for characterisation of the oligomeric state of the protein and its gross shape. There are two main types of AUC used: sedimentation velocity (SV), which interprets the movement of macromolecules using hydrodynamic theory to determine the size, shape, and interactions of the protein, and sedimentation equilibrium (SE), which uses equilibrium concentration gradients to define molecule mass, assembly stoichiometry, association constants, and solution non-ideality (Cole *et al.*, 2008).

5. RESULTS: Shiga toxin inhibitors

The oligomerisation of *E. coli* RecA has previously been thoroughly characterised by SE. Brenner *et al.* (1990) observed monomeric RecA in reversible equilibrium with trimers, hexamers and dodecamers under specific solution conditions. Equilibrium was strongly temperature dependent; as the temperature was raised from 1°C to 21°C polymerisation was favoured and shown to be reversible upon lowering of temperature. Distribution of RecA oligomers was dependent on solution conditions, and thermodynamic analysis indicated that these different species were in reversible equilibrium with each other (Brenner *et al.*, 1990). To assess whether AHU3 affects the oligomerisation dynamics of RecA, we studied RecA sedimentation under similar conditions to those described by Brenner *et al.* (1990) in the presence and absence of AHU3.

The overall oligomerisation state of RecA was studied under three conditions: RecA alone, RecA + 0.5% DMSO, and RecA + 0.5% DMSO + 100 µM AHU3. The concentration of RecA was 10 µM in all samples, while AHU3 was included in a 10-fold excess. RecA was dialysed into 50 mM Na-citrate, 5% glycerol pH 6.0, in order to maximise the oligomeric state of RecA (Brenner *et al.*, 1990), and rotor speeds of 6, 10 and 14k rpm at a temperature of 4°C and 20°C used to explore the landscapes of molecular weights in the system.

Raw sedimentation data showed AHU3 had an effect on RecA oligomerisation; RecA in the presence of AHU3 produced a markedly shallower equilibrium distribution (Figure 5-19 A). The SE data was analysed with SEDPHAT by Dr. Olwyn Byron (University of Glasgow) using the single species analysis model in order to gain a model-independent measure of the whole-cell weight average molecular weight. The average molecular mass of RecA oligomers in the absence of both AHU3 and DMSO was 661.8 kDa at 6k rpm, 556.0 kDa at 10k rpm, and 404.0 kDa at 14k rpm. When DMSO was present there was a decrease in the average molecular mass at rotor speeds of 10k rpm and 14k rpm, although at 6k rpm the average mass increased to 791.7 kDa. However, when AHU3 was present in the sample, the average molecular mass of RecA oligomers was greatly reduced at all rotor speeds, with kDas below both those for RecA alone and RecA + DMSO (Figure 5-19 B). This implies that AHU3 is inhibiting the formation of larger oligomeric RecA species, resulting in an increase in lower molecular weight oligomers observed. While SE only measures the average molecular weight of RecA and does not give an indication of the proportion of different oligomeric species present, it still provides

5. RESULTS: Shiga toxin inhibitors

evidence to support our hypothesis that AHU3 inhibits the SOS response by targeting and inhibiting RecA. It also further indicates that it is the initial oligomerisation stage of RecA activation inhibited, rather than a later step such as ATP hydrolysis.

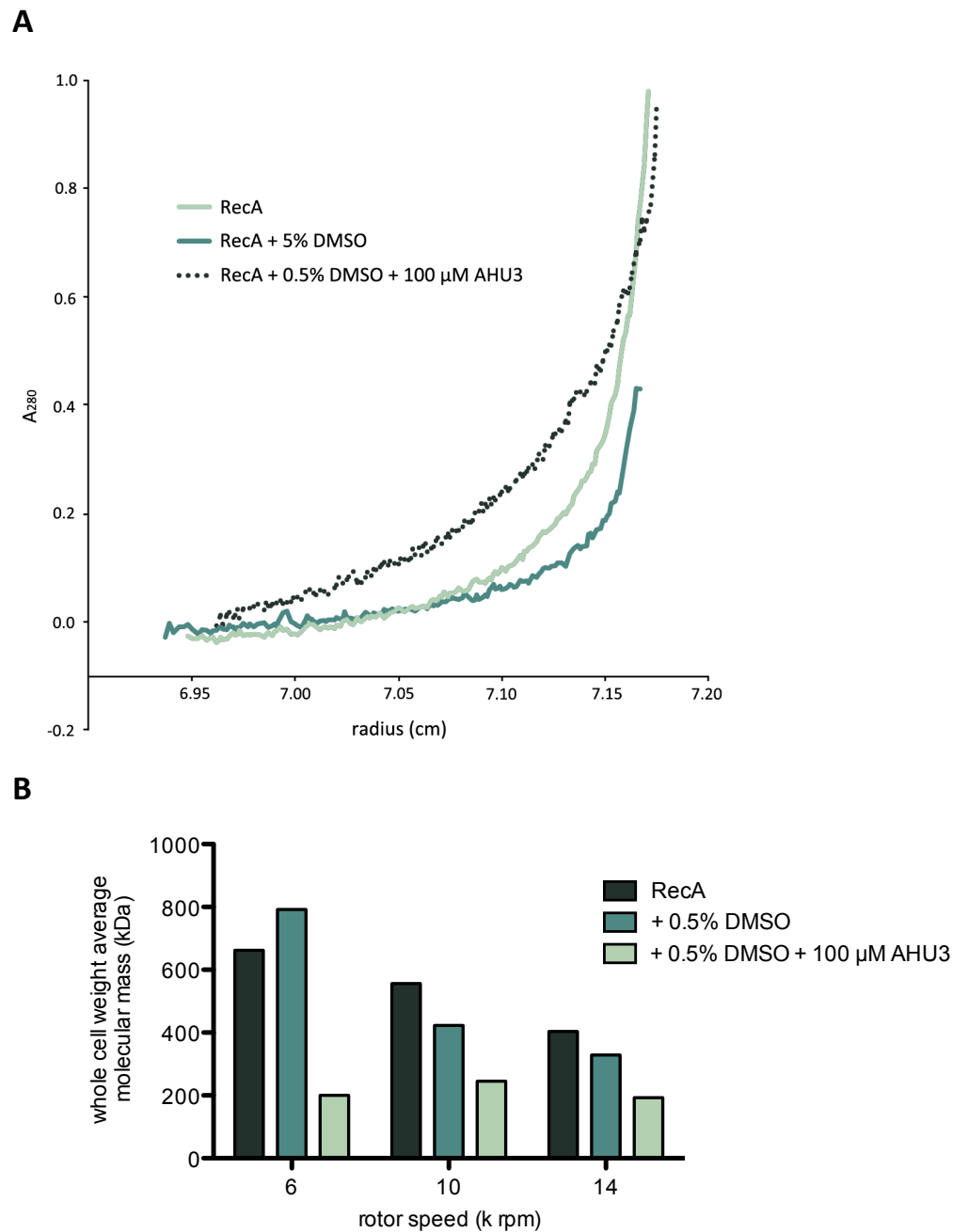


Figure 5-19: AHU3 decreases RecA oligomerisation. Raw sedimentation equilibrium data for RecA, RecA in the presence of 0.5% DMSO, and RecA in 0.5% DMSO and 100 μ M AHU3 (**A**). Oligomeric RecA species at 6, 10 and 14k rpm rotor speeds (**B**). SEDPHAT analysis was performed by Dr. Olwyn Byron (University of Glasgow).

5.10 Cytotoxicity of the AHU compounds

Before considering *in vivo* testing of the AHU compounds, we required confirmation that they were not toxic to eukaryotic cells. AHU1-3 were tested for cytotoxicity against HEK 293 cells by the European Screening Port (Hamburg, Germany). At a concentration of 100 μ M, all three compounds were highly toxic with no viable cells remaining after treatment. Full dose-response curves were generated and all three compounds revealed an IC₅₀ value of approximately 5 μ M (Table 5-1). While there is a selectivity window based on the dose required to inhibit bacterial virulence, at this stage of drug discovery a lead compound should ideally show no cytotoxicity at a dose of 10 μ M. Therefore, these compounds are not considered suitable for testing in the Stx-expressing *Citrobacter rodentium* model, and will require further modification to reduce cytotoxicity before they can be considered for inclusion in future animal trials.

Table 5-1: Cytotoxicity of AHU1-3. Toxicity of the compounds to HEK293 cells was calculated at concentrations of AHU1-3 between 0.01-1 mM. Dose-response curves for the three compounds were used to calculate the IC₅₀ and Hill slope values.

Compound	Toxicity at 100 μ M	Hill slope	pIC ₅₀ (μ M)
AHU1	100%	5.19 \pm 0.47	5.10 \pm 0.01
AHU2	100%	4.30 \pm 0.25	5.30 \pm 0.01
AHU3	100%	5.30 \pm 0.30	5.09 \pm 0.01

5.11 Discussion

Our studies confirmed that the compound AHU1 inhibits MMC-induced *stx2* expression, and the efficacy of this inhibition was increased by modification of the morpholine ring. The AHU compounds also caused inhibition of MMC-induced bacterial lysis, implying that their action was not limited to *stx2* expression, but had a broader effect on lysogenic prophages encoded by the *E. coli* Sakai genome. This was validated by the observation that AHU3 additionally inhibited transduction of Gram-positive phages. The ability of AHU3 to inhibit a wide range of very different phages suggests that instead of directly inhibiting expression of phage genes, AHU3 works by inhibiting an earlier process that controls expression of all phage genes: the SOS response. We hypothesised that the AHU compounds target RecA, an early and essential component of the SOS response, and have shown that AHU3 interacts with RecA, inhibiting its ability to oligomerise and hydrolyse ATP and thus preventing it from mediating cleavage of the SOS and prophage repressors.

5.11.1 The AHU compounds target the SOS response protein RecA

To determine whether AHU3 targets RecA, several techniques to explore interaction were performed. AHU3 was shown to inhibit ATP hydrolysis by RecA, an event that plays an essential role in repair of DNA by homologous recombination. Microscale thermophoresis, which analyses the interaction of two molecules by measuring their movement in temperature gradients, implied that AHU3 binds RecA. Finally, AHU3 was shown by AUC to reduce oligomerisation of RecA, the essential first step in activation of the SOS response. Together, this data provides compelling evidence that the AHU compounds interact with and inhibit RecA.

Under non-stressed growth conditions, RecA exists in an inactive state and is unable to initiate high expression of SOS or prophage genes. Activity first requires the formation of a helical homopolymeric filament of ATP-bound RecA on ssDNA, followed by hydrolysis of ATP. The active RecA-DNA filament is then able to mediate recombinant DNA repair and homologous exchange, as well as autocleavage of the LexA and prophage repressors. The ability of AHU3 to inhibit this essential initial step of the SOS response was studied using

5. RESULTS: Shiga toxin inhibitors

SE-AUC, which revealed that the presence of AHU3 results in lower numbers of larger oligomeric RecA species, suggesting that AHU3 is inhibiting RecA oligomerisation. Additionally, ATPase assays showed that AHU3 inhibits RecA-mediated ATP hydrolysis. As ATPase activity by RecA requires the binding of RecA to ssDNA and formation of RecA filaments, we propose that AHU3 binds inactive RecA monomers, preventing them from forming filaments that can hydrolyse ATP, and thereby inhibiting activation of the SOS response.

It is also likely that the AHU compounds target other bacterial proteins, as at higher concentrations (100-200 μM) bacterial growth was either slowed or completely inhibited. However, growth was minimally inhibited at the lower concentrations which modified RecA activity. Additionally, expression of *rpsM* and *tir* was unaffected when bacteria were grown in the presence of 50 μM AHU3, suggesting AHU3 displays specificity for RecA. We attempted to identify other non-RecA proteins with which AHU3 interacts by synthesising affinity-tagged AHU3, which could be attached to an immobile surface and incubated with bacterial cell lysate. After washing to remove unbound material, the proteins bound to AHU3 could then be eluted with an excess of free drug or denaturing conditions, and analysed by SDS-PAGE with protein bands identified by mass spectrometry. Unfortunately, attempts to synthesise a biotinylated derivative of AHU3 were unsuccessful, and thus further targets of AHU3 remain to be identified.

5.11.2 The maleimide moiety of the AHU compounds inhibits bacterial RecA

The role of the maleimide moiety with respect to the inhibitory activity of the AHU compounds was always considered to be significant, and was confirmed by the synthesis of AHU4. In this drug, addition of a phenyl group resulted in blocking of the maleimide double bond. When tested in the GFP reporter assay, this compound did not exhibit activity against bacterial growth, *stx2*:GFP expression, or MMC-induced bacterial lysis, confirming that the maleimide is essential for all inhibitory abilities. Interestingly, maleimide on its own was sufficient to cause inhibition of *stx2*:GFP expression. However, at 50 μM maleimide strongly affected bacterial growth, and therefore the additional moieties of AHU3 may increase its specificity for RecA while decreasing its influence on other cellular processes.

5. RESULTS: Shiga toxin inhibitors

Maleimide is a 5-membered ring whose reactivity is derived from its electrophilic nature, and readily forms covalent bonds with thiols. The carbons on either side of the double bond are susceptible to addition either by Michael or via Diels-Alder reactions, and could react with the nucleophilic thiol group (-SH) of a surface-exposed cysteine residue, forming a stable carbon-sulfur covalent bond between RecA and AHU3 (Figure 5-20). Although some other amino acids are also nucleophilic, maleimides specifically target cysteine residues at intracellular pH levels, due to the much higher susceptibility of the sulfhydryl group to oxidation (Bednar, 1990). The protein sequence of RecA reveals that it contains three cysteine residues that may interact with the electrophilic carbons in the AHU3 maleimide. Covalent binding between the inhibitor and protein is an irreversible event, and therefore while our MST experiment suggests binding is occurring, this analysis cannot be used to determine the kinetics of binding. Although further experiments are required to confirm that AHU3 is binding covalently, the known selectivity of the thiol-maleimide reaction in aqueous environments, rapid kinetics associated with this reaction, and stability of the thiol-maleimide product (Nair *et al.*, 2014) support our hypothesis that this reaction is occurring between AHU3 and RecA.

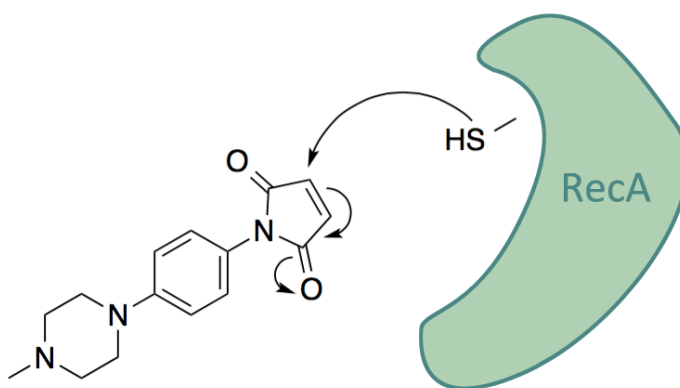


Figure 5-20: Proposed covalent attachment of AHU3 to RecA. The electrophilic maleimide moiety of AHU3 undergoes nucleophilic attack by the thiol group (-SH) of a surface-exposed cysteine residue of RecA, forming a stable covalent bond between compound and protein.

Cysteine residues in proteins are often involved in disulphide bonds, covalent bonds formed from two thiol groups. These occur between pairs of cysteines that are in close proximity to each other, and can enhance the stability of the protein structure. A free thiol group is however required for covalent binding with AHU3. Non-disulphide cysteine residues exposed on the surface of proteins are often found in the active sites of proteins

5. RESULTS: Shiga toxin inhibitors

due to their high reactivity, but are also found on protein surfaces in locations not directly involved with protein function. The three cysteines in RecA are located at positions 91, 117, and 130. PyMol analysis of the RecA monomer structure in the biological hexamer crystal of RecA (Xing & Bell, 2004) suggests that only one of these residues, Cys117, is predicted to be on the surface of the protein and therefore easily accessible to AHU3 (Figure 5-21 A). This residue is not located in the ATP hydrolysis site of RecA, but is found in one of the two RecA-RecA interfaces. When the RecA monomer is bound to another monomer, the cysteine residue in this interface is inaccessible to the surface (Figure 5-21 B). Labelling of surface accessible cysteines in the hexameric structure of RecA revealed that Cys117 is only surface-located on the RecA monomer at one end of the filament, and all other cysteines in the filament are inaccessible (Figure 5-21 C).

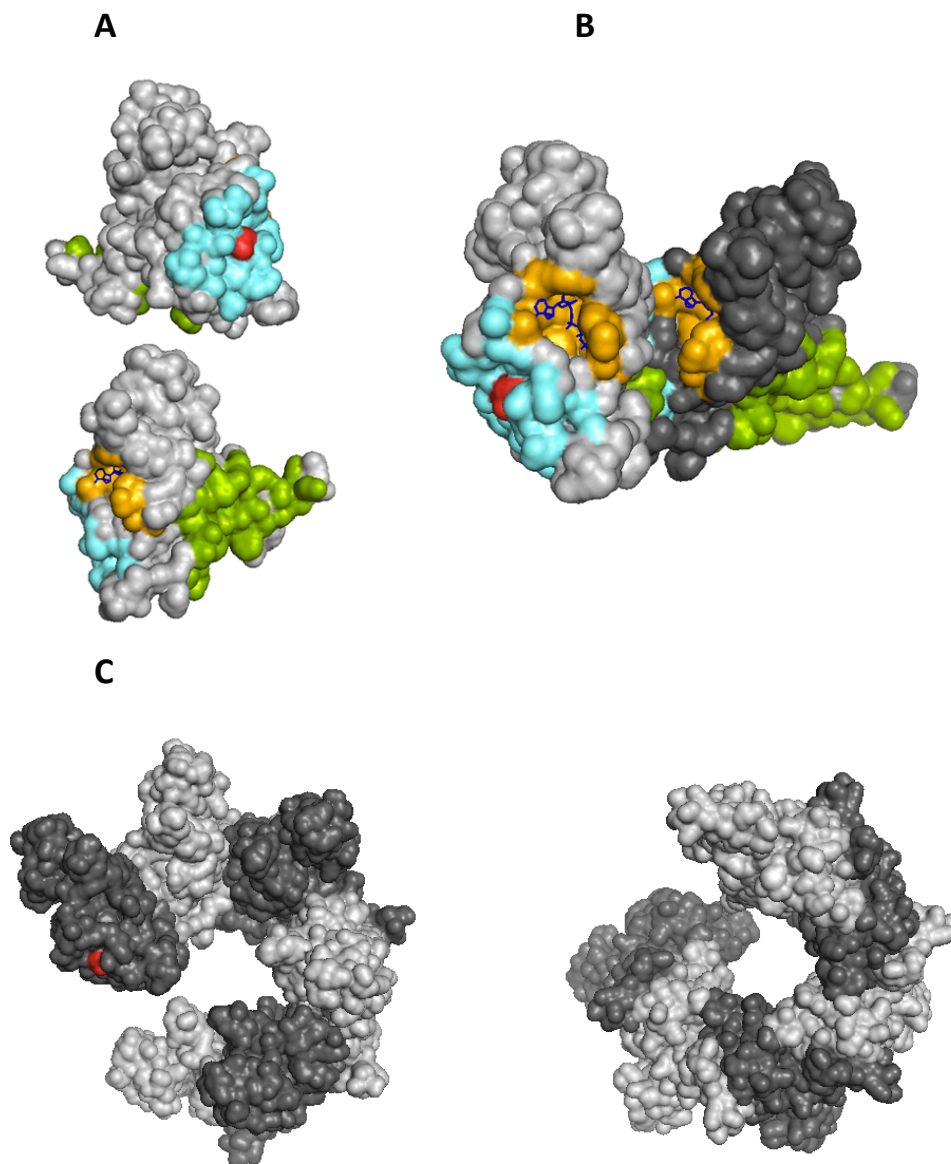


Figure 5-21: Cysteine residues are not solvent accessible in oligomeric RecA. The solvent accessible surface of *E. coli* RecA as a monomer displaying both sides of the molecule (**A**), and two monomers coloured light and dark grey (**B**) from the biological hexamer of RecA (Xing & Bell, 2004; PDB id 1XMS). Cysteine residues are coloured red, and the monomer-monomer interfaces (residues within 4 Å of each other) are coloured green and cyan. Residues within 4 Å of the non-hydrolysable analogue of ATP (MnAMP-PNP, blue sticks) are coloured orange. The solvent accessible surface of RecA as a hexamer with cysteine residues coloured red (**C**) shows that the solvent accessible cysteine residues in the filament are inaccessible when RecA undergoes oligomerisation, due to their position in the monomer-monomer interface.

The position of Cys117 in oligomeric RecA supports our hypothesis that AHU3 inhibits the SOS response by preventing RecA monomers from binding to each other and forming active filaments. By covalently attaching to cysteines present in the RecA-RecA interface on monomers or at the end of RecA oligomers, AHU3 would inhibit filamentation of RecA. However, further experiments are required to confirm that Cys117 is the target of AHU3.

5. RESULTS: Shiga toxin inhibitors

One approach to determine the impact of AHU3 binding to Cys117 would be to genetically modify this amino acid. However, as mutagenesis of Cys117 could also render RecA unable to oligomerise and therefore non-functional due to modification of the interface site, this is not a favoured method. *In silico* digest and mass spectrometry of AHU3-bound RecA would therefore be better suited for investigation of which cysteine residues interact with RecA.

5.11.3 Antimicrobial properties of maleimide compounds

Very few natural maleimides have been identified to date. Pencolide, a maleimide-containing metabolite produced by fungal *Penicillium* strains, is bacteriostatic against the non-pathogenic *E. coli* ATCC 25922 strain, as well as *Streptococcus pyogenes*, *S. aureus*, and *Salmonella* Typhimurium, and exhibits fungicidal activity against *Candida albicans* (Lucas *et al.*, 2007). Another fungal maleimide compound is farinomalein, produced by *Isaria farinosa*, and has shown potent activity against plant pathogen oomycetes (Putri *et al.*, 2014).

A maleimide compound produced by bacteria has also been identified; showdomycin, first isolated from *Streptomyces showdoensis* (Nishimura *et al.*, 1964), which has a high structural similarity to uridine and pseudouridine. This compound has shown activity against both Gram-positive and Gram-negative strains, and was particularly active against *Streptococcus hemolyticus* and *S. pyogenes* (Böttcher & Sieber, 2010). To investigate the target of showdomycin, Böttcher and Sieber (2010) synthesised a showdomycin probe which identified 13 different enzymes from *S. aureus*, multidrug resistant *S. aureus* (MRSA), *Pseudomonas aeruginosa*, and *Listeria monocytogenes*. These showdomycin-binding enzymes were subsequently placed into two major classes, oxidoreductases and transferases, for which several substrates that contain nucleosides such as uridine have been identified. Many targets contain a cysteine residue in their active site, which could interact with the double bond of the maleimide moiety. All targets are enzymes with important cellular functions or involved in virulence, growth and persistence, with roles such as primary metabolism, nucleotide biosynthesis, cell wall biosynthesis and oxidative stress resistance (Böttcher & Sieber, 2010).

5. RESULTS: Shiga toxin inhibitors

As the electrophilic maleimide has the potential to interact with any available cysteine residue, the authors hypothesised that the maleimide moiety in showdomycin is sterically restricted by its ribose moiety, preventing it from non-specific interactions. To test this, *S. aureus* proteome lysates were incubated with either labelled maleimide or labelled showdomycin and their targets identified; while maleimide bound to nearly all the proteins present in the lysate, showdomycin was far more selective, only binding to a very limited number of proteins. Showdomycin was particularly effective against the *S. aureus* proteins MurA1 and MurA2, important antibacterial targets due to their essential roles in catalysing the first step of cell wall biosynthesis. A substrate inhibition assay found that showdomycin inhibited MurA1 with an IC_{50} of 10 μ M, while full saturation of the majority of the other targets was achieved by 50 μ M showdomycin (Böttcher & Sieber, 2010).

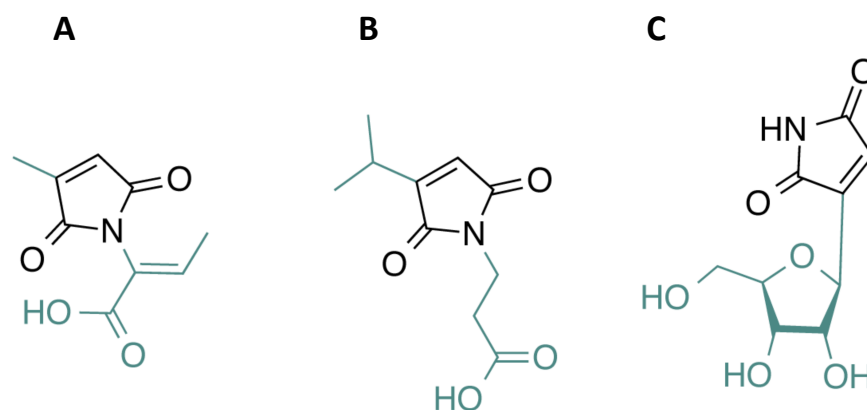


Figure 5-22: Structures of natural maleimides. The structures of pencolide from *Penicillium* species (A), farinomalein from *Isaria farinosa* (B), and showdomycin from *Streptomyces showdoensis* (C). The maleimide ring of each molecule is coloured black, with the rest of the compound in green.

Like AHU3, these three natural maleimides are small compounds, allowing them to be cell permeable and enter bacteria to inhibit cytosolic proteins. Unlike AHU3, however, all three natural maleimides contain a substituted maleimide, with an additional group adjacent to the double bond. This makes the maleimide moiety less reactive as it contains only one electrophilic carbon, which may limit the number of cysteine-containing proteins to which it covalently binds. Further work to explore this speculation would involve testing of a synthesised AHU3 derivative with this maleimide modification for cytotoxicity and RecA inhibition.

5.11.4 RecA as a target of anti-virulence therapies

RecA is a particularly appealing target for novel anti-virulence therapies. Not only does it allow bacteria to survive potentially lethal stress caused by DNA-damaging agents by mediating repair and homologous recombination, but late genes involved in the SOS response promote genome-wide mutations and therefore the potential development of genetic mutations. Additionally, the production and release of phages by the SOS response can lead to transmission of virulence factors across pathogenic bacterial strains. In the case of EHEC, antibiotic treatment can result in further release of toxins via activation of the SOS response, increasing the severity of disease. Therefore, therapeutic treatments that prevent initiation of the bacterial SOS response could be valuable when used in combination with conventional antibiotics. Such drugs could be used to limit the harmful impact of antibiotic treatment such as Shiga toxin release, and prevent horizontal transfer of resistance or virulence genes. RecA is also a highly conserved protein found in all bacteria, raising the possibility of drugs that inhibit this protein being used against a wide range of pathogenic bacteria. However, this also makes the effect of RecA inhibitors very broad spectrum, and they are probably best considered for use alongside strongly selective treatments, to minimise disruption of the microbiota. RecA inhibitors may therefore have greatest potential when used to limit the harmful side-effects of drug treatment (such as Stx release), *de novo* development of antibiotic resistance genes, or horizontal transfer of antibiotic resistance and phage-borne virulence genes.

Not all reported RecA inhibitors are suitable for therapeutic use, due to their molecular size. ATPase and *stx2*:GFP assays performed by Dr. James Connolly, University of Glasgow, have found that the reported RecA inhibitors Congo Red, Suramin and Bis-ANS show activity in the ATPase assay but are unable to inhibit *stx2*:GFP production (Dr. James Connolly, personal communication). This is likely to reflect the large molecular sizes and negative charges of these compounds (Wigle & Singleton, 2007) which renders them membrane-impermeable.

5.11.5 The future of AHU3 as an anti-virulence therapy

Although the AHU compounds have shown potential as anti-virulence compounds, the finding that they are cytotoxic to eukaryotic cells, even at very low concentrations, makes them unsuitable in their current form for further testing *in vivo*. This cytotoxicity is likely due to the maleimide moiety of the compound binding to available cysteine residues on other essential eukaryotic proteins, which may limit the options for modification as the maleimide is essential for RecA inhibition. There are, however, possible solutions to the issue of cytotoxicity, such as steric hindrance by addition of compounds to the maleimide to increase their selectivity, or modification of the maleimide group to reduce its toxicity while retaining its RecA-binding activity. While eukaryotic cells produce the RecA homologue Rad51, also involved in DNA repair, the low protein sequence similarity (27%) between Rad51 and RecA makes it unlikely that Rad51 is targeted in a similar fashion by AHU3, although this would need to be confirmed experimentally.

The work presented in this chapter has shown that the AHU compounds inhibit the SOS response rather than specifically targeting Stx expression. While RecA and the SOS response are appealing targets for novel therapeutic treatments in their own right, the assays we have developed for exploring the effect of AHU3 on Stx expression and phage production are well-suited for evaluating other compounds that have been reported to inhibit EHEC Shiga toxin expression and release. Additionally, the availability of the Stx-producing *C. rodentium* mouse model means that ultimately *in vivo* assessment of Stx-targeting compounds can be carried out in a well-characterised small animal model of the disease.

Chapter 6: Evaluation of alternative therapeutic treatments within mouse models of infection.

6.1 Introduction

Work undertaken for this thesis revealed that while the T3SS-specific colonisation of EHEC can be modeled by *C. rodentium* in mice, infection using the EHEC strain TUV93-0 results in persistence that is not dependent on the T3SS specifically. This information provides the opportunity to choose the most appropriate model when evaluating new potential interventional strategies. In this chapter, work is described in which two models were used, in collaboration with other researchers at the University of Glasgow, to test several different compounds that have shown anti-virulence activity *in vitro*. These include three which target the T3SS and one with potential bactericidal activity.

6.1.1 Aims of this chapter

- To investigate the effect of disulfiram, an acetaldehyde dehydrogenase inhibitor currently licenced for treatment of alcoholism, on *C. rodentium* colonisation of mice. We hypothesise that inhibition of the bacterial protein AdhE by disulfiram will result in downregulation of the T3SS, leading to reduced A/E lesions and a decrease in colonisation.
- To test the effect of the RCZ20 compound, a derivative of a salicylidene acylhydrazide (SA), on *C. rodentium* colonisation of mice. This compound has demonstrated downregulation of T3SS proteins *in vitro*, and we therefore aim to explore any potential effect on colonisation *in vivo* when mice are treated with this compound after infection.
- To investigate the effect of the amino acid D-serine, which causes repression of T3SS genes *in vitro*, on colonisation of mice by *C. rodentium* when D-serine is provided in drinking water. We will also explore any effect D-serine or *C. rodentium* colonisation has on the mouse gut flora by short-chain fatty acid (SCFA) analysis of faecal matter.

6. RESULTS: *In vivo* testing of novel therapies

- To assess the effect of colicin E1, which has *in vitro* antibacterial activity against LF82, on colonisation of mice by this strain. This colicin has also been encapsulated, allowing it to avoid degradation in the stomach and be released in the colon, to increase the likelihood of it reaching the site of LF82 colonisation.

6.2 The effect of disulfiram on *C. rodentium* colonisation

6.2.1 Salicylidene acylhydrazides, AdhE and the T3SS

The salicylidene acylhydrazides are a group of T3SS inhibitors effective against several species of Gram-negative pathogens, including EHEC, whose bacterial targets in O157:H7 have been identified by affinity pull-down assay and mass spectrometry (Wang *et al.*, 2011). One of the nineteen putative targets of the SAs was AdhE, a metabolic enzyme involved in the fermentation of glucose, leading to production of ethanol (Clark & Cronan, 1980). Evidence of a possible role in bacterial virulence for AdhE has also come from studies suggesting a link between this protein and expression of the T3SS (Bäumler *et al.*, 1994; Abernathy *et al.*, 2013), although the mechanism by which AdhE affects T3SS expression was not elucidated.

An O157:H7 TUV93-0 *adhE* deletion mutant constructed by Beckham *et al.* (2014) generated a strain with no growth defects in a range of minimal and rich media, but which displayed a decrease in Type 3 secretion and an increased level of flagellar expression, a phenotype similar to wild type *E. coli* treated with SA compounds. The expression of T3SS and flagellar genes is cross-regulated (Saini *et al.*, 2010), and the switch from expression of the flagella to expression of the T3SS is an important event in bacterial infection. The flagella are required for motility, and mediate initial attachment of bacteria to host cells (Mahajan *et al.*, 2009). However, flagella are also potent activators of the host immune system. The flagellar filament is composed of polymerised flagellin protein, which stimulate the Toll-like receptor 5 (TLR5) response, resulting in production of inflammatory cytokines and thus leading to inflammation and infiltration of immune cells (Hayashi *et al.*, 2001). To avoid host immune responses, the downregulation of flagellar genes occurs after initial host cell contact, and the T3SS is produced to mediate intimate attachment (Iyoda *et al.*, 2006). Previous analysis of the $\Delta adhE$ mutant confirmed that it secreted more flagellin than the wild type, and produced a correspondingly stronger TLR5 response (Beckham *et al.*, 2014). Furthermore, the flagella of the $\Delta adhE$ mutant appeared to be non-functional, reducing the motility of the mutant and rendering it unable to interact with host cells to initiate contact. As AdhE is involved

6. RESULTS: *In vivo* testing of novel therapies

in the generation of acetaldehyde and ethanol, deletion of AdhE increases the concentration of metabolites in this pathway. Two of these metabolites are acetate and cAMP, both of which stimulate expression of flagellar genes. Accumulation of these metabolites has been proposed by Beckham *et al.* (2014) to result in strong upregulation of flagella that correspondingly reduces expression and secretion of T3SS proteins. It has been suggested by Beckham *et al.* (2014) that the assembled flagella are unable to rotate properly due to either misassembly of a key component or inappropriate acetylation of a flagellar component (Figure 6-1).

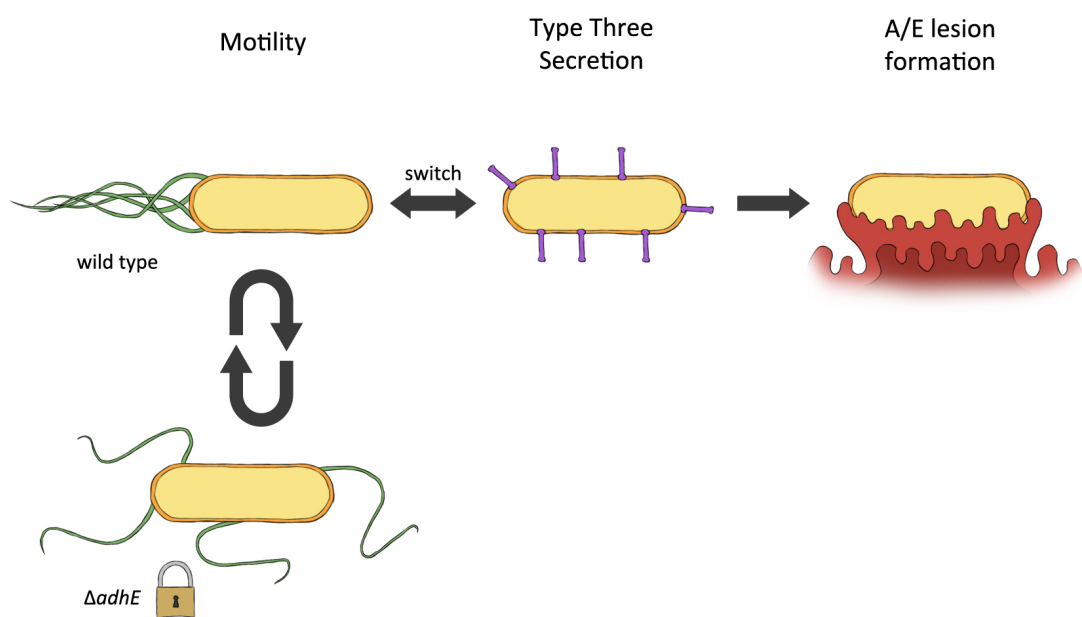


Figure 6-1: Proposed model of *adhE* deletion in *E. coli* O157:H7. By switching from flagellar expression to T3SS expression, *E. coli* are able to move from a motile state to a phenotype that allows intimate attachment to host cells and formation of A/E lesions. The $\Delta adhE$ mutant is prevented from changing to the T3SS-expressing phenotype, and has reduced motility due to non-functional flagella. Figure is adapted from Beckham (2014, p.228).

6.2.2 Disulfiram as a potential inhibitor of AdhE

AdhE is an attractive drug target as inhibition of its activity could result in a decrease in the proteins associated with T3SS production, thus limiting adhesion and subsequently colonisation of *E. coli*. An increase of flagellar production may also aid removal of bacteria by the immune system due to the immunogenic nature of flagellin, while inhibition of motility could further decrease bacterial pathogenicity (Beckham, 2014).

The drug disulfiram, which is licensed for use in the treatment of chronic alcoholism, has been explored as a possible inhibitor of AdhE (Beckham, 2014). Disulfiram functions by inhibiting human acetaldehyde dehydrogenase, which is one of the functional domains of AdhE (Membrillo-Hernandez *et al.*, 2000). Addition of disulfiram to TUV93-0 produced a similar bacterial phenotype to that of the $\Delta adhE$ mutant: strongly repressed secretion of the T3SS effectors EspA and Tir, an increase in FliC expression, reduced attachment to host cells, and reduced bacterial motility (Beckham, 2014). Disulfiram is a prodrug, requiring enzymatic metabolism *in vivo* to produce multiple metabolites, including intermediary metabolites, and thus evidence of direct binding to AdhE was not possible. However, as disulfiram treatment significantly affected major virulence factors *in vitro*, we were interested in determining its impact *in vivo*.

6.2.3 Effect of disulfiram on *C. rodentium* colonisation *in vivo*

The *lux*-marked *C. rodentium* mouse model was selected for *in vivo* testing of disulfiram, as this strain is dependent on T3SS-mediated attachment for successful colonisation and thus any decrease in T3SS expression should be detected by reduced faecal shedding. The use of this model was thought relevant as the AdhE of *C. rodentium* is highly homologous to AdhE from *E. coli* O157:H7, sharing 91% protein sequence identity.

Three groups of mice, consisting of five animals each, were orally infected with 10^9 CFU *lux*-marked *C. rodentium*. The first group was given *C. rodentium* (untreated) while the second group was given *C. rodentium* cultured in the presence of 10 μ M disulfiram (pre-DSF), and the third group given *C. rodentium* cultured in the presence of 10 μ M disulfiram and treated daily with 2 mg disulfiram in 100 μ l corn oil by oral gavage from one day after

6. RESULTS: *In vivo* testing of novel therapies

infection until the end of the experiment (pre-/post-DSF). Colonisation was followed for 9 days after infection by faecal shedding and live imaging. All groups of mice displayed strong levels of colonisation post infection (Figure 6-2 A), and analysis of the three groups by ANOVA identified a significant difference between the mean luminescence of each group at 6 and 8 days after infection (Figure 6-2 B). Post-test Tukey's Multiple Comparison showed that on day 6 there was a significant difference between the untreated and pre-DSF group, and on day 8 the untreated group was significantly different from both the pre-DSF and the pre/post-DSF group. However, no significant difference in faecal shedding between the three groups was identified at any time point.

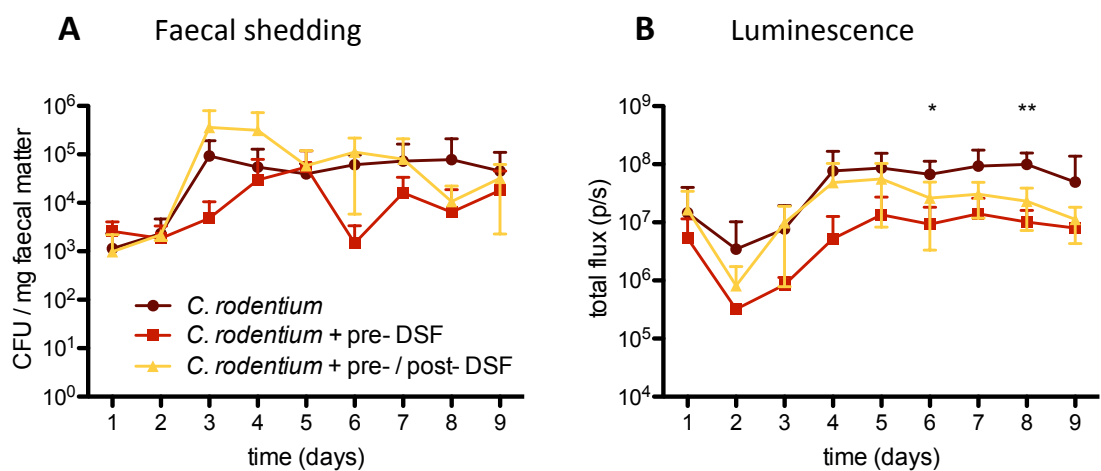


Figure 6-2: Effect of disulfiram on colonisation of BALB/c mice by lux-marked *C. rodentium*. BALB/c mice were infected with 10⁹ CFU lux-marked *C. rodentium* grown in DMEM (dark red), 10⁹ CFU lux-marked *C. rodentium* grown in DMEM and 10 μM disulfiram (red), or 10⁹ CFU lux-marked *C. rodentium* grown in DMEM and 10 μM disulfiram and 2 mg disulfiram in 100 μl corn oil administered to mice daily by oral gavage (yellow). Each group of mice consisted of five animals, and colonisation was monitored by faecal shedding (**A**) and luminescence (**B**). A significant difference between the mean luminescence of mouse groups was present on day 6 (p=0.028) and day 8 (p=0.002). Data points shown are the mean of each group, and standard deviation from the mean displayed as error bars. Significant differences between the means of groups are denoted by an asterisk (*=p<0.05; **=p<0.01) and were determined by one-way ANOVA with post-test Tukey's Multiple Comparison.

6.3 The effect of RCZ20 on *C. rodentium* colonisation

6.3.1 RCZ20 is a derivative of the salicylidene acylhydrazide ME0055

ME0055, one of the most effective members of the SAs, is a highly efficient inhibitor of O157:H7 T3SS expression *in vitro*, reducing expression of Tir and EspD to undetectable levels (Tree *et al.*, 2009). Transcriptome analysis and reporter fusion assays by Tree *et al.* (2009) of TUV93-0 grown in the presence of 20 μ M ME0055 revealed this compound produces significant downregulation of genes in all 5 LEE operons, including that of the gene encoding Ler, the master regulator of T3SS. ME0055 treatment of TUV93-0 cultured with HeLa cells also reduced the number of bacteria on the cell surface associated with A/E lesions.

Although ME0055 has shown potential as an anti-virulence compound *in vitro*, it has low solubility and is hydrolysed by both basic and acidic conditions, undesirable traits for a therapeutic drug. The compound was subsequently structurally modified by Riccardo Zambelloni (University of Glasgow) to optimise its stability and improve its activity. The most effective derivative of ME0055, RCZ20 (Figure 6-3), had no influence on bacterial growth and when incubated with growing cultures of TUV93-0 at a concentration of 50 μ M, significantly reduced expression and secretion of EspD (Riccardo Zambelloni, personal communication).

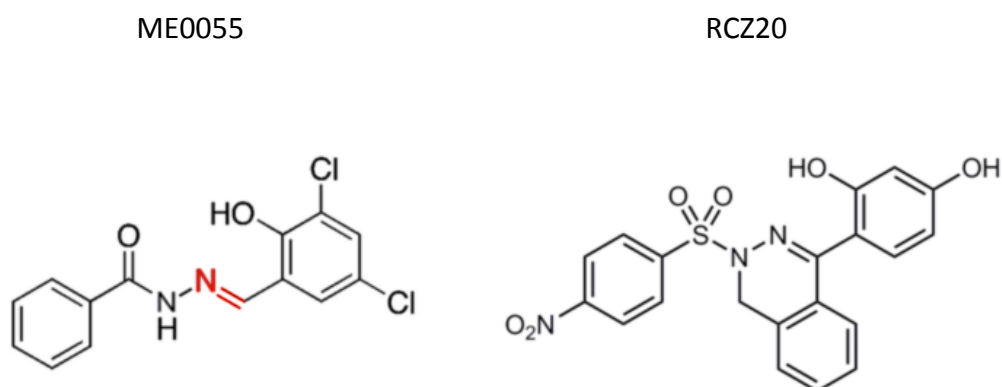


Figure 6-3: Structures of ME0055 and RCZ20. Alkylation of the imine bond (red) of ME0055 results in a more stable compound that is not easily hydrolysed.

6.3.2 Effect of RCZ20 on *C. rodentium* colonisation *in vivo*

To investigate the potential of RCZ20 to reduce colonisation of EHEC *in vivo*, mice infected with *lux*-marked *C. rodentium* were treated with RCZ20 both before and after infection, and colonisation monitored by faecal shedding and luminescence.

For delivery of the compound by oral gavage, RCZ20 was solubilised in 10% DMSO, 40% PEG400 at a concentration of 2.5 mg/ml (5.88 mM), and administered in a 200 µl dose. This dose is similar to that of the T3SS inhibitor aurodox which protects mice from a lethal dose of *C. rodentium* (Kimura *et al.*, 2011). RCZ20 was not tested at higher concentrations as this would require addition of further DMSO to aid solubility, which was not feasible given its toxicity in mice at high concentrations (Jacob & Rosenbaum, 1966).

Two groups of mice, consisting of 5 animals each, were orally dosed with either RCZ20 in DMSO/PEG400 or mock-treated with DMSO/PEG400 buffer one day prior to infection with 10^9 CFU *lux*-marked *C. rodentium*. Both groups were also given daily doses of RCZ20 or the control after infection, for 9 days. No significant difference in either faecal shedding or luminescence was observed between groups at any time point (Figure 6-4), implying that oral administration of RCZ20 has no significant effect on *C. rodentium* T3SS expression *in vivo*. Mouse weight was also monitored throughout the post infection period, with neither group displaying an obvious change in body weight (data not shown), suggesting that RCZ20 treatment and the solution it was administered in have no adverse effect on mice.

6. RESULTS: *In vivo* testing of novel therapies

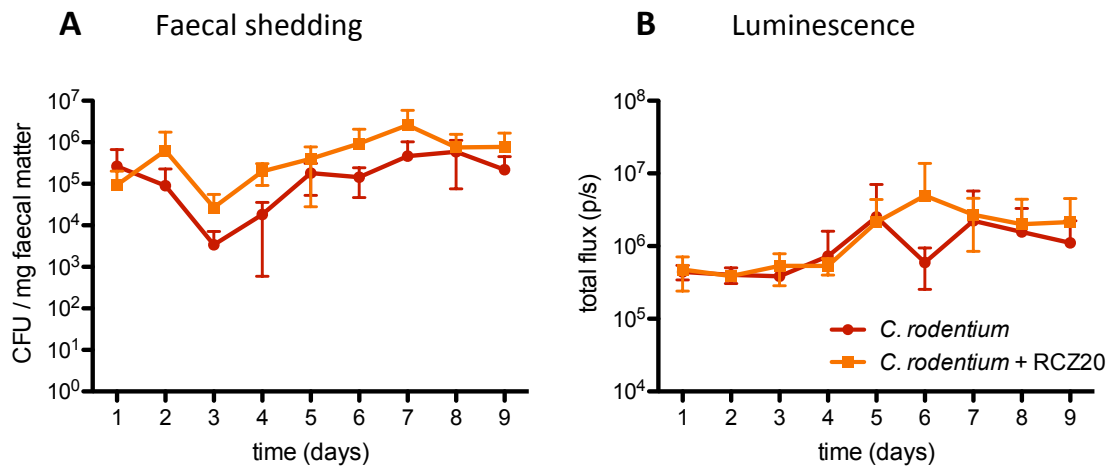


Figure 6-4: Effect of RCZ20 on colonisation of BALB/c mice by *lux*-marked *C. rodentium*. BALB/c mice were infected with 10⁹ CFU *lux*-marked *C. rodentium* and dosed once daily (including one pre-infection treatment) with either 200 μ l 10% DMSO, 40% PEG400 (red), or 0.5 mg RCZ20 in 200 μ l 10% DMSO, 40% PEG400 (orange). Each group of mice consisted of five animals, and colonisation was monitored by faecal shedding (**A**) and luminescence (**B**). Data points shown are the mean of each group, and standard deviation from the mean displayed as error bars. No significant differences ($p < 0.05$) between the means of the treated and untreated groups, as determined by Student's unpaired t-test, were found for either strain at any time point.

6.4 The effect of D-serine on *Citrobacter rodentium* colonisation and microflora short-chain fatty acid (SCFA) production

6.4.1 D-serine metabolism by *E. coli*

The ability to compete with the gut microbiome and occupy a distinct niche is an essential trait for colonisation by enteric bacterial pathogens. To achieve this, pathogenic *E. coli* have evolved to utilise various host metabolites as their energy source, allowing them to colonise specific sites within the gastrointestinal tract, with distinct pathotypes of *E. coli* able to metabolise different types of sugars (Meador *et al.*, 2014). As well as sugars, *E. coli* can also make use of different chiral forms of amino acids; UPEC strains are capable of using the D form of serine as a carbon source, a useful trait given that the urinary tract, the site of UPEC colonisation, contains the highest concentration of D-serine in the body (Huang *et al.*, 1998).

6. RESULTS: *In vivo* testing of novel therapies

Although both D- and L-amino acids are chemically identical and available to living organisms in the environment, their abundance and role in biological systems is very different. L-amino acids are the predominant form in cells, as D-amino acids cannot be incorporated into proteins by ribosomes. However, D-amino acids have functions in both eukaryotic and prokaryotic cells, for example in proteins not synthesised by ribosomes, or as signalling molecules in the brain (reviewed by Cava *et al.*, 2011). In bacteria, D-amino acids are also present in the peptidoglycan layer of the bacterial cell wall (Vollmer *et al.*, 2008).

The ability of UPEC to metabolise D-serine is due to the presence of the *dsdCXA* locus which encodes three proteins that transport and metabolise D-serine, enabling UPEC to utilise D-serine as a sole carbon source (Anfora & Welch, 2006). EHEC strains, including O157:H7, carry a truncated *dsdCXA* locus that renders them unable to convert D-serine, as well as making them susceptible to the bacteriostatic consequences of high D-serine concentrations (Cosloy & McFall, 1973). As it is likely that EHEC strains encounter D-serine both in the intestine and outside the host (such as in animal waste), this raises the question of why EHEC strains have lost the ability to utilise this amino acid.

6.4.2 D-serine represses the T3SS and induces the SOS response

A recent study by Connolly *et al.* (2015) explored the role of D-serine in modulation of O157:H7 virulence factors and showed that D-serine causes repression of T3SS genes and induces the SOS response. Transcriptome analysis of the TUV93-0 strain revealed that treatment with 1 mM D-serine led to downregulation of 26 out of the 42 LEE genes, including those encoding both structural and effector T3SS proteins. Attachment of TUV93-0 to epithelial cells *in vitro* was also significantly reduced by D-serine, with treatment resulting in lower numbers of infected host cells, as well as lower numbers of bacteria on infected cells and fewer actin pedestals formed by attached bacteria. This implied that two LEE-associated transcriptional activators, IhfA and YhiF, which are differentially expressed in response to D-serine, regulated T3SS expression. Additionally, intracellular accumulation of D-serine led to upregulation of 21 genes from the SOS regulon, including *recA* and *lexA*, and was independent of T3SS repression (Connolly *et al.*, 2015). The authors of this study also analysed the prevalence of *dsdCXA* and the LEE

6. RESULTS: *In vivo* testing of novel therapies

sequences in chromosomes of 1,591 *E. coli* strains, revealing that carriage of both is extremely rare due to incompatibility between these two loci caused by a strong selective pressure to lose *dsdCX* when bacteria obtain the LEE operon.

6.4.3 Effect of D-serine on *C. rodentium* colonisation of mice

Downregulation of the T3SS by D-serine could potentially limit colonisation of those strains of pathogenic *E. coli* that rely on this virulence factor for pathogenicity. To explore the effect of D-serine on bacterial colonisation *in vivo*, two groups of 5 BALB/c mice were given either normal drinking water or drinking water supplemented with 125 µg/ml D-serine 3 days prior to infection with 10^{10} CFU *C. rodentium*. The mouse group given D-serine water was continued on this treatment throughout the post infection period. Colonisation, as followed by faecal shedding and live imaging, was not significantly different at any time point in the D-serine-treated mice compared to the non-treated mice (Figure 6-5), implying that D-serine in drinking water has no discernible influence on T3SS expression *in vivo*.

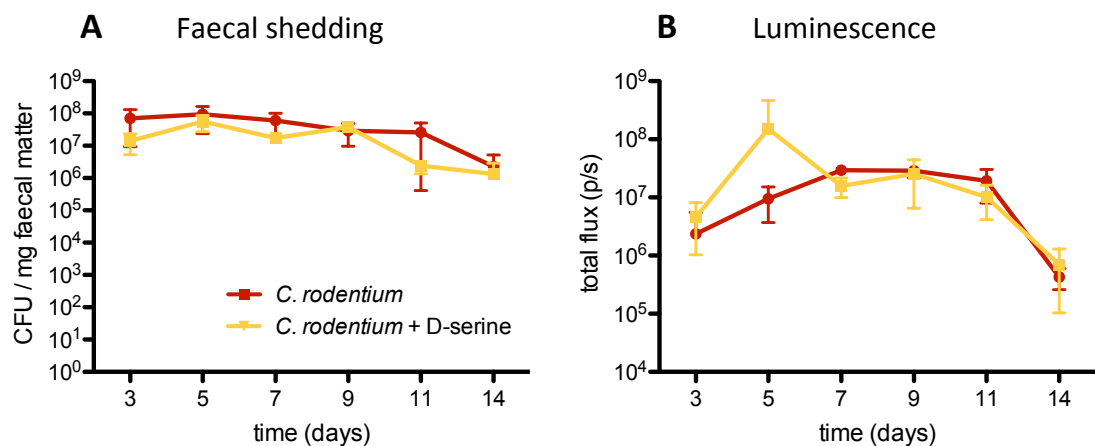


Figure 6-5: Effect of D-serine treatment on colonisation of *C. rodentium*. Two groups of mice, consisting of five mice in each group, were given normal drinking water (red) or drinking water containing 125 µg/ml D-serine (yellow) 3 days prior to infection. Mice were infected with 10^{10} CFU *lux*-marked *C. rodentium*, and colonisation monitored by faecal shedding (**A**) and luminescence (**B**). Data points shown are the mean of each group, and standard deviation from the mean displayed as error bars. No significant differences ($p < 0.05$) between the means of the treated and untreated groups, as determined by Student's unpaired t-test, were found for either strain at any time point.

6.4.4 Effect of D-serine on SCFA production

D-serine's potential influence on SCFA production by host microflora was also explored in both infected and uninfected mice, as an indication of population changes within the microflora. SCFAs are metabolites 1-6 carbons in length, and are derived from fermentation of non-digestible polysaccharides by bacteria in the colon. In humans, the most abundant SCFAs in the gut are acetate, propionate and butyrate. SCFAs are utilised by the host organism for a wide range of purposes, including energy sources for colonocytes, modulators of intracellular pH and cell volume, regulation of cell proliferation and differentiation, and regulation of gene expression (Wong *et al.*, 2006). They also have anti-inflammatory properties, inducing differentiation of regulatory T cells that prevents proinflammatory responses by the host immune system in response to intestinal commensal bacteria (Smith *et al.*, 2013).

To assess the effect of D-serine on SCFA production in uninfected or *C. rodentium*-infected mice, 4 groups of mice consisting of 5 animals in each were given either normal drinking water or drinking water supplemented with 125 µg/ml D-serine 3 days prior to infection. Two groups of mice, one on regular water and one on D-serine water, were infected with 10^{10} CFU *C. rodentium* (the same two groups of mice used in the experiment in Chapter 6.5.3), and the other two groups of mice given a mock infection of PBS. Individual mouse weights and food weight consumed by groups was measured daily, showing no difference between groups (data not shown). Faecal samples were obtained from animals at 0, 3, 7 and 14 days after infection (faecal samples from day 0 were collected prior to infection), and faecal water analysed for SCFA composition by gas chromatography by Michael Logan (University of Glasgow). Total levels of SCFA production showed an eventual decline over the post infection period in all four groups, and no significant difference between groups was observed at any time point (Figure 6-6).

6. RESULTS: *In vivo* testing of novel therapies

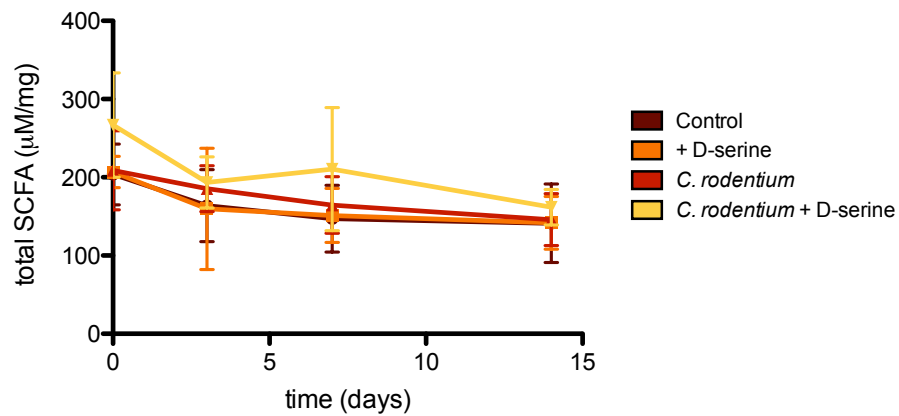


Figure 6-6: SCFA production in mice treated with D-serine and infected with *C. rodentium*. Total faecal SCFA was analysed from faecal water by gas chromatography, from mice either uninfected (dark red, orange), or infected with 10^{10} CFU *C. rodentium* (red, yellow), and provided with either regular drinking water (dark red, red) or 125 µg/ml D-serine-supplemented water (orange, yellow). Each group of mice consisted of five animals. Data represent the average SCFA concentration in µM/mg faecal matter of each group, with standard deviation displayed as error bars. No significant differences ($p < 0.05$) between the means of the groups, as determined by ANOVA, were found for either strain at any time point.

To determine any possible difference in the SCFA profile between groups of mice, the relative percentages of the three major SCFAs detected, acetate, propionate and butyrate, were analysed. Acetate was the predominant SCFA from all samples, ranging from 75.8-98.9% throughout the post infection period, while propionate and butyrate were 0-10% of total SCFA detected. However, a significant difference in relative percentages between groups was only found for acetate and butyrate faecal samples taken at day 0, and not at any other time point (Figure 6-7). Although some groups appeared to show large variation in relative percentage at certain time points, such as the *C. rodentium* + D-serine group on day 0, this was often due to an individual mouse in the group. Therefore, we concluded that neither D-serine nor *C. rodentium* are able to significantly alter the production of these SCFAs by intestinal bacteria to an extent that any changes can be detected from faecal matter.

6. RESULTS: *In vivo* testing of novel therapies

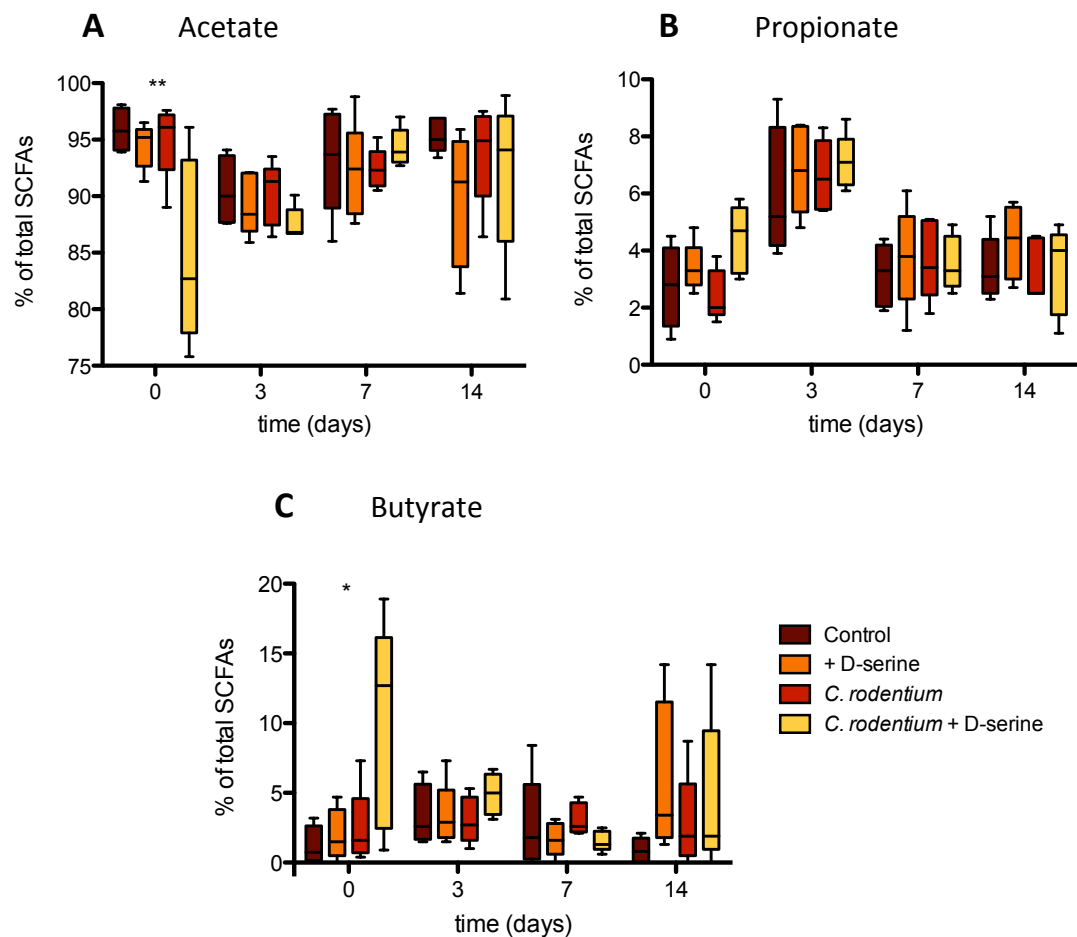


Figure 6-7: Effect of D-serine treatment and *C. rodentium* infection on faecal SCFA composition. The amount of acetate (A), propionate (B) and butyrate (C) as a percentage of total SCFA was analysed from faecal water by gas chromatography, from mice either uninfected (dark red, orange), or infected with 10^{10} CFU *C. rodentium* (red, yellow), and provided with either regular drinking water (dark red, red) or 125 $\mu\text{g/ml}$ D-serine-supplemented water (orange, yellow). Each group of mice consisted of five animals. Boxes represent the standard deviation of each group, and whiskers represent the range of data values in that group. SCFA analysis was performed by Michael Logan (University of Glasgow). Significant differences between the means of groups are denoted by an asterisk (*= $p < 0.05$; **= $p < 0.01$) and were determined by one-way ANOVA with post-test Tukey's Multiple Comparison.

6.4.5 D-serine concentration in urine is higher in mice treated with D-serine in drinking water

Although D-serine was supplied to mice in drinking water, this is not the only source of serine for them, as both forms of serine can be obtained from diet or synthesised by mice themselves (Foltyn *et al.*, 2010). To examine the impact providing additional dietary D-serine had on the amount of D-serine in the urine, the relative levels of L- and D-serine

6. RESULTS: *In vivo* testing of novel therapies

from mice treated with and without D-serine were measured (Glasgow Polyomics, University of Glasgow). Mice that had been given normal drinking water had very low levels of D-serine in their urine (3.93% average), with no D-serine detected in 7 out of the 11 samples analysed. Mice treated with D-serine showed significantly higher levels of D-serine (25.75% average) (Figure 6-8).

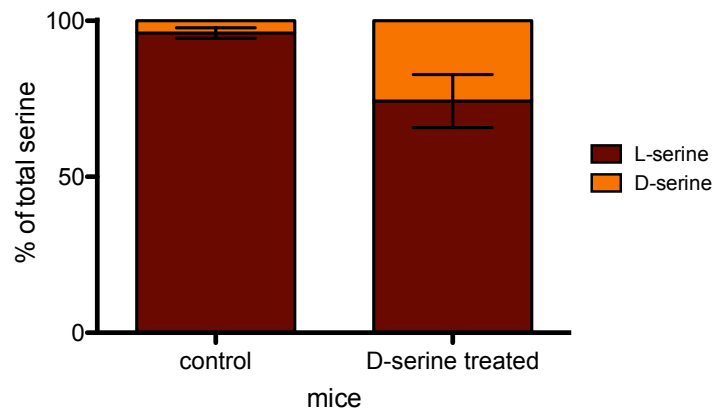


Figure 6-8: D-serine treatment increases the relative abundance of urinary D-serine. Urine was collected from mice given drinking water with or without 125 $\mu\text{g}/\text{ml}$ D-serine supplementation. Data represents the average percentages of L- (dark red) and D-serine (orange) present in 11 samples from each treated/untreated group taken 3, 6, 10 and 17 days after D-serine treatment was started, with standard deviation displayed as error bars. The increase in D-serine resulted in a significant increase from an average of 3.93% to an average of 25.75% ($p=0.0204$, 20 degrees of freedom, $t=2.518$), determined using Student's unpaired t-test.

6.5 The effect of colicin E1 on LF82 colonisation

6.5.1 Colicin E1 is an antimicrobial against AIEC LF82

One class of antimicrobial agents that have shown promise as potential interventional therapies are the bacteriocins. These are antimicrobial peptides produced by bacteria that enable the bacteriocin-producing strain to compete effectively within an established microbial niche through killing of closely related, competitive neighbouring strains. Colicins, bacteriocins produced by *E. coli* and encoded on colicinogenic plasmids, are high molecular weight proteins that specifically target other *E. coli* strains. Their activity is highly specific, which means that they can potentially be used to kill pathogenic strains

6. RESULTS: *In vivo* testing of novel therapies

without significant modification to the healthy microbiota (Rea *et al.*, 2011; Smith *et al.*, 2012). Recent work by Carla Brown (University of Glasgow) has explored the efficacy of colicins against AIEC infection associated with Crohn's disease.

Colicin E1, which kills bacteria by forming a pore and depolarising the inner membrane, has *in vitro* antibacterial activity against the AIEC LF82 strain. This colicin was also found to be effective against LF82 both when bound to intestinal epithelial cells or located within macrophages (Brown *et al.*, 2015). To determine the potential of this colicin *in vivo*, we considered its use in reduction of LF82 persistence in the streptomycin-treated mouse model. Before *in vivo* testing, colicin E1 was encapsulated to protect it from degradation in the stomach and duodenum. Pectin was used as a delivery system for the colicin as it is a natural gastroresistant polysaccharide selectively digested by microflora in the colon, and is considered an ideal carrier for colon-specific treatments (Wong *et al.*, 2011). Purified colicin E1 was encapsulated in pectin/zein hydrogel, forming small beads containing approximately 700 ng colicin per bead, and these beads retained the cytotoxic activity of the colicin (Brown, 2015).

6.5.2 Effect of encapsulated colicin E1 on LF82 colonisation *in vivo*

Two groups of ICR mice, consisting of 6 animals in each, were treated with 5 g/L streptomycin in their drinking water 3 days prior to infection with 10^9 CFU *lux*-marked Str^R LF82. One group was treated with daily with 10 colicin beads per mouse, a total of approximately 7 µg colicin E1/mouse, while the other was given 10 control beads per mouse. Administration of colicin E1 or control beads continued for seven days after infection, and colonisation was monitored by faecal shedding and live imaging until 9 days after infection. Although both faecal shedding and luminescence of LF82 by the colicin-treated mice appeared slightly lower than that of the non-treated group throughout the post infection period, this difference was not significant at any time point (Figure 6-9).

6. RESULTS: *In vivo* testing of novel therapies

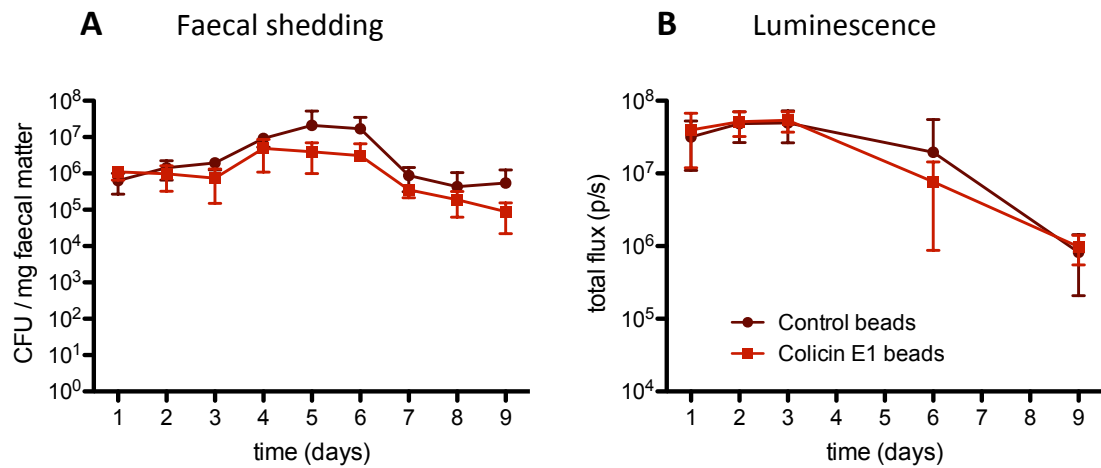


Figure 6-9: Effect of colicin E1 treatment on LF82 colonisation. BALB/c mice pre-treated with 5 g/L streptomycin in drinking water for three days were infected with 10⁹ CFU *lux*-marked Str^R LF82. Animals were dosed daily with either control beads (dark red) or colicin beads containing a total of ~7 µg colicin E1 (red) for the first 7 days after infection. Each group of mice consisted of six animals. Streptomycin treatment was continued throughout the post infection period. Colonisation was monitored by faecal shedding (**A**) and luminescence (**B**). Data points shown are the mean of each group, and standard deviation from the mean displayed as error bars. No significant differences ($p < 0.05$) between the means of the treated and untreated groups, as determined by Student's unpaired t-test, were found for either strain at any time point.

6.6 Discussion

6.6.1 Disulfiram does not reduce *Citrobacter rodentium* colonisation of mice

Prior treatment of *C. rodentium* with the acetaldehyde dehydrogenase inhibitor disulfiram before infection resulted in slightly lower levels of colonisation compared to those animals given disulfiram daily. However, colonisation of mice treated daily with disulfiram was similar to that of the untreated group, and only two time points reported a significant difference in bacterial luminescence between the untreated and treated groups. While it is possible that the significant decrease in bacterial colonisation seen at days 6 and 8 is a result of lower initial T3SS-mediated attachment of treated bacteria to host tissues, the lack of a significant difference in colonisation at other time points suggests that neither disulfiram treatment of bacteria before nor after infection have a major influence on bacterial colonisation.

This finding probably reflects the treatment of an intestinal bacterial infection with a drug that is rapidly absorbed and metabolised by the body. Post ingestion, disulfiram is rapidly absorbed from the gastrointestinal tract and reduced to diethyldithiocarbamate. This compound is then converted by hepatic thiol methyltransferases to multiple different metabolites that are distributed in different body tissues. These metabolites are excreted via the kidneys, lungs, and faeces, with 5-20% of an oral dose excreted in the faeces alone (reviewed by Johansson, 1992). It is therefore likely that disulfiram and its metabolites reach the site of *C. rodentium* colonisation in the caecum and lower colon at very low concentrations.

Although disulfiram is converted into its active metabolites by human methyltransferases, bacteria are also believed to be capable of metabolising disulfiram. The effect of disulfiram on T3SS and flagellar expression, and experimentally linked to inhibition of AdhE, strongly suggests that *E. coli* can convert the prodrug into the metabolites that have binding activity. Disulfiram also displays antitubercular activity against a large number of *Mycobacterium tuberculosis* clinical isolates, and is capable of killing *M. tuberculosis* both within macrophages and in a mouse model of chronic tuberculosis

6. RESULTS: *In vivo* testing of novel therapies

(Horita *et al.*, 2012). Additionally, while it has weak antibiotic activity against *S. aureus*, disulfiram produces a strongly synergistic inhibition of bacterial growth when administered alongside the antibiotic minocycline (Ejim *et al.*, 2011). Therefore, disulfiram does not require metabolism by human enzymes in order to inhibit AdhE, although delivery to the site of infection still remains an issue. Although repurposing of disulfiram is appealing as it is already licenced for human use, the difficulty of its rapid absorption and distribution throughout the body means that novel AdhE inhibitors may be better suited for an anti-virulence strategy that targets this protein.

Although *C. rodentium* is dependent on the T3SS for colonisation, making it a good surrogate for EHEC mouse infections, this model is limited by the inability of *C. rodentium* to express functional flagella, which renders the bacteria non-motile. A lack of flagella may also limit the TLR5 response, and thus the influence of the host immune system on bacterial clearance may be lower in the *C. rodentium* model than it would be for O157:H7. However, our discovery that the T3SS has no perceptible effect on *E. coli* colonisation in mice means that the *E. coli* mouse model cannot be used for assessment of disulfiram's effect *in vivo*. The infant rabbit O157:H7 model may therefore be better suited for exploration of the effect of potential AdhE inhibitors on both T3SS inhibition and flagella-mediated stimulation of the host immune response.

Another point of consideration is the large infectious dose of *C. rodentium* used, which may result in colonisation levels that are too high to be significantly affected by the amount of disulfiram that reach the site of infection. Mice were treated with 10^9 CFU *C. rodentium* in order to produce high and easily detected colonisation, however this is not representative of natural infection of mice. Transmission of *C. rodentium* occurs between infected and uninfected littermates via coprophagy, and faecally-shed bacteria are much more infectious than those grown in culture (Wiles *et al.*, 2005). As inhibition of AdhE is hypothesised to inhibit the switch from flagellar to T3SS expression and thus prevent initial attachment of bacteria to host tissues, AdhE inhibitors will potentially function more effectively as prophylactic treatments for at-risk individuals rather than therapeutic treatment of infected patients. Therefore, a mouse model that mixes *C. rodentium*-infected mice with uninfected mice that are treated with AdhE inhibitors may be a more suitable model of infection for assessing this type of anti-virulence compound.

6.6.2 The RCZ20 compound does not reduce colonisation *in vivo*

Treatment of mice with RCZ20 before and after infection with *C. rodentium* had no significant effect on bacterial colonisation. While it is possible that RCZ20 has limited or no influence on T3SS modulation *in vivo*, the therapeutic concentration of RCZ20 at the site of *C. rodentium* infection remains unknown. Mice were treated with 200 μ l of 5.88 mM RCZ20 daily, a concentration much higher than that required to see significant downregulation of T3SS genes and decrease in T3 effector secretion *in vitro* (20-50 μ M). RCZ20 may, however, be metabolised before it reaches the intestine. Use of a labeled compound in future *in vivo* experiments would allow the compound to be tracked within the mouse after administration, and the relative RCZ20 abundance in the colon estimated.

6.6.3 D-serine does not affect *C. rodentium* colonisation or SCFA metabolism by the gut microflora

Supplementation of drinking water with 125 μ g/ml D-serine resulted in significantly higher amounts of D-serine in the urine of mice compared to untreated control animals. This led us to conclude that using this approach, D-serine levels in mice can be increased through diet. Although D-serine modulates expression of the T3SS *in vitro*, resulting in decreased bacterial adhesion to host cells, mice infected with *C. rodentium* and supplied with D-serine in drinking water showed no discernible difference in colonisation when compared to infected mice given normal drinking water. This suggests that either D-serine is unable to modulate the T3SS *in vivo*, or that the concentration of D-serine in the intestine of *C. rodentium*-infected mice is simply not high enough to influence T3SS expression. Although the concentration of D-serine in the drinking water (1.19 mM) was similar to that used to reduce T3SS expression *in vitro* (1 mM) (Connolly *et al.*, 2015), it might not reflect the concentration of D-serine at the site of *C. rodentium* colonisation. While the average amount of D-serine in the urine of treated mice was found to be higher (approximately 25% of total D-serine), the proportion of D-serine in the intestine is likely to be lower than that observed in urine. Additionally, although *C. rodentium* expresses a highly similar T3SS to O157:H7, it differs from O157:H7 by carriage of both the LEE and the *dsdCXA* locus (Petty *et al.*, 2010), and thus this strain's ability to

6. RESULTS: *In vivo* testing of novel therapies

metabolise D-serine may prevent intracellular accumulation of D-serine at sufficient concentrations to influence T3SS expression.

The second aim of our D-serine and *C. rodentium* experiment was to assess the effect both had on the production of SCFAs produced by intestinal bacteria, as these are metabolites important to colonic health. Interestingly, treatment of mice with D-serine did not result in significant changes to either the total amount of SCFAs produced or the relative abundances of the three most prevalent SCFAs. The lack of changes in the SCFA profile may be because additional D-serine in the intestine has no noticeable impact on the microbiota in the context of SCFA metabolism, or is due to limited D-serine concentration in the gastrointestinal tract for reasons discussed previously. It should also be noted that the SCFA compositions obtained were measured from faecal material. This may not provide an accurate reflection of SCFAs in the intestine as SCFAs are absorbed from the intestine and transported to other sites of the body.

While the total amount and profile of SCFAs was also unaffected by *C. rodentium* infection, colonisation of the mouse intestine by this strain is known to be accompanied by changes in both intestinal mucosally adhered and luminal bacteria. In particular, alterations in relative abundance of *Protobacteria*, *Deferribacteres*, *Lactobacillaceae* and *Clostridia* have been observed (Hoffmann *et al.*, 2009). These changes have been attributed to either direct competition between *C. rodentium* and the microbiota, or to immune responses elicited by *C. rodentium* that affect the microbiota. However, we must conclude that these alterations do not result in any major changes to the overall production of SCFAs.

While the ability of D-serine to decrease T3SS expression *in vitro* suggests it may have a use in treatment of bacterial infections that rely on this virulence factor for colonisation, the independent upregulation of the SOS response may also produce a result that is highly undesirable for EHEC infections. The SOS response modulates the expression of Shiga toxin and therefore an increase in SOS gene expression may lead to increased Stx release, resulting in a higher risk of HUS development. As the *C. rodentium* mouse model does not carry Stx, we were unable to determine whether D-serine treatment affects the

6. RESULTS: *In vivo* testing of novel therapies

SOS response *in vivo*. However, this could potentially be explored using the Stx-producing *C. rodentium* (λ stx_{2dact}) model.

6.6.4 Colicin treatment does not affect LF82 colonisation *in vivo*

Colicin E1 treatment, delivered by oral gavage of purified colicin in pectin/zein hydrogel beads, failed to show any significant influence on LF82 infection in streptomycin-treated mice. Further mouse infection studies performed by Carla Brown and Dr. Gill Douce (University of Glasgow) in which mice were orally administered 1 mg purified unencapsulated colicin E1 daily also failed to show a significant decrease in LF82 faecal shedding. Testing for colicin activity in the intestinal organs of uninfected mice harvested shortly after treatment with purified colicin E1 revealed that while colicin activity was detectable in stomach samples, no colicin activity was found in small intestine, caecum and colon tissues, implying that colicin E1 is degraded in the small intestine (Brown, 2015).

These findings indicate that colicin E1 is not effective against LF82 in this mouse model. However, lack of an effective delivery system for the colicin to the site of LF82 infection is relevant. The poor efficiency of colicin encapsulation resulted in mice being treated with ~7 µg colicin/mouse/day, far lower than the 100 µg/ml concentration at which colicin E1 is toxic to LF82 *in vitro* (Brown *et al.*, 2015). Furthermore, as release of colicin from the hydrogel requires digestion of pectin by the gut microbiota, clearance of the natural gut flora by streptomycin treatment may potentially decrease the amount of pectinase activity in the intestine, limiting or slowing the delivery of colicin.

Colicin treatment was explored by Brown (2015) as a potential therapy targeting AIEC that are associated with Crohn's disease. The streptomycin-treated ICR mouse model is therefore perhaps not the most appropriate small animal model in this context as the model does not replicate any aspects of Crohn's disease. Alternative murine models that induce colitis and thus more accurately depict the role of LF82 in Crohn's disease, such as LF82 infection of TLR5-deficient germ-free mice (Chassaing *et al.*, 2014b) or LF82 infection of transgenic mice expressing human CEACAMs (Carvalho *et al.*, 2009), may be better

6. RESULTS: *In vivo* testing of novel therapies

suites for *in vivo* assessment of colicin E1. Use of these models would allow the effect of colicins on AIEC-induced symptoms to be assessed alongside bacterial persistence.

Chapter 7: Final Discussion

7.1 Mouse models of EHEC infection

Our initial aim was to establish a mouse model of a Shiga toxin-negative O157:H7 strain that showed high and consistent levels of colonisation over approximately 10-14 days, and then determine the influence of the T3SS on colonisation. Although this strain was a poor coloniser of inbred mice, streptomycin-treated outbred ICR mice were strongly colonised. However, this colonisation was revealed to be non-dependent on the T3SS, making it unsuitable for testing T3SS-inhibiting anti-virulence compounds.

7.1.1 *C. rodentium* and *C. rodentium* (λ stx_{2dact}) as *in vivo* EHEC surrogates

As O157:H7 was deemed unsuitable for T3SS-focused mouse studies, the *C. rodentium* model was explored as a surrogate for EHEC infection, as this strain is highly dependent on the T3SS for colonisation. Infection of BALB/c mice by an Stx2-expressing *C. rodentium* strain produced strong symptoms of disease, including weight loss, kidney damage, and death within the first week of infection. This model was particularly appealing as it allows the testing of compounds that potentially inhibit Stx production. Interestingly, disease was very poor in C57BL/6 mice despite high bacterial colonisation levels, in contrast to the original study by Mallick *et al.* (2012), probably reflecting the significant role that the host intestinal flora has on bacterial pathogenesis. The differences in microbiota composition of mice obtained from different suppliers is a major issue when it comes to the reproducibility of models, as commensal bacteria are known to not just affect the intestinal colonisation of introduced strains and their ability to cause illness, but also to influence host immune responses (Macpherson & Harris, 2004). Therefore, a better understanding of the intestinal strains that are involved in colonisation resistance to pathogenic *E. coli* may aid the development of a more reproducible mouse infection model.

Although the Stx-producing *C. rodentium* (λ stx_{2dact}) mouse model demonstrates both strong colonisation and manifestation of disease without the requirement for alteration of the normal gut flora, there are several notable limitations of this model. Unlike EHEC, *C. rodentium* does not produce flagella, which provide motility and act as primary

7. FINAL DISCUSSION

adhesins. Expression of the flagella is also coordinated with T3SS expression in EHEC, and therefore therapies that target regulation of the T3SS may show limited effect in the *C. rodentium* model. A number of other EHEC proteins are not found within the *C. rodentium* genome, making the study of treatments that influence the regulation or function of anti-virulence factors difficult to assess. In addition, while useful as a surrogate for O157:H7 infection, the λ stx_{2dact} model produces the Stx2dact variant of Shiga toxin, which has not been identified in O157:H7 strains.

Irrespective of these obstacles, *C. rodentium* is still a strong model for *in vivo* studies that focus on the T3SS compared to the current alternatives. Intestinal xenograft murine models are also a recent development with the potential for use in colonisation studies, as they have demonstrated T3SS-dependent lesion formation on human intestinal tissue (Golan *et al.*, 2011). However, the infant rabbit model of EHEC infection is perhaps the most appropriate small animal model currently available for colonisation studies, as it is strongly dependent on the T3SS and uses the original EHEC strain instead of a surrogate, allowing the influence of other non-T3SS EHEC virulence factors to be assessed. This model has previously been used to identify non-T3SS factors that contribute to intestinal colonisation and disease, with studies implying that surface-exposed structures such as the long polar fimbriae, curli, and the O-antigen capsule have a significant effect on colonisation and survival within the intestine (Ritchie & Waldor, 2005; Shifrin *et al.*, 2008; Lloyd *et al.*, 2012).

7.1.2 The importance of the T3SS in human pathogenesis

The question of whether the T3SS dependence and A/E lesions observed in these animal models is actually a true reflection of what occurs in humans needs to be considered. Due to the unavailability of human studies, our understanding of the processes involved in human intestinal colonisation by EHEC is relatively limited, and both the site of bacterial colonisation and the significance of the T3SS varies between the different animal models (reviewed by Ritchie, 2014). Human volunteer studies of EPEC infection, however, which do not carry the risk of kidney damage and death, have provided insights into the role of the T3SS in virulence, which may be similar to its function in EHEC. In two separate human studies exploring the virulence of *eae* and *espB* deletion mutants relative to the

7. FINAL DISCUSSION

wild type, the mutants produced a significantly lower incidence and severity of diarrhoea (Donnenberg *et al.*, 1993; Tacket *et al.*, 2000), although the similar level of mutant bacteria shed in stool samples to that of the wild type-infected control group implies that other adhesion factors are also important.

In conclusion, although different animal models of EHEC have shown varying results when assessing the role of the T3SS in pathogenesis, they provide strong evidence that it plays an important function in colonisation, and that inhibitors of the T3SS have potential as new therapeutic strategies. Furthermore, selection of the most appropriate animal model and consideration of its differences in bacterial pathogenesis, host responses, and host microbiota influence needs to be carefully contemplated during *in vivo* evaluation of novel T3SS-targeting drugs.

7.2 Candidates for a broadly protective vaccine against *E. coli*

The development of a vaccine that could effectively protect against O157:H7 and other EHEC strains would have a major impact on human health and economy. Broad-range vaccines that target not only EHEC but other *E. coli* pathotypes are highly desirable, given the wide range of clinically important diseases they cause. Reverse vaccinology is an approach designed to rapidly identify protein candidates that offer protection and has been used successfully to develop vaccines against other pathogenic bacteria such as Meningococcus B and Group A Streptococcus. Recently, Moriel *et al.* (2010) used this technique to identify conserved antigens that could be used in a broad-spectrum vaccine against *E. coli* pathogens. The intention of work outlined in this thesis was to explore the expression and function of two of these antigens, EaeH and YghJ, to determine their protective potential against EHEC and AIEC strains.

7.2.1 Expression of EaeH and YghJ in *E. coli* strains

Expression of EaeH in both TUV93-0 and LF82 was very low, and no upregulation of transcription was identified under any of the conditions we tested, including the presence of human intestinal epithelial cells. Expression of YghJ in LF82 occurred at a similar level

7. FINAL DISCUSSION

to that of EPEC YghJ but, despite encoding the genes required for a functional T2SS, YghJ was not secreted by LF82 under the same conditions as EPEC YghJ. While this difference is not surprising given that LF82 belongs to a very different pathotype, the similar level of LF82 YghJ expression to that of EPEC despite its lack of secretion is intriguing, and raises the possibility of another intracellular function for LF82 YghJ. Further work to characterise the T2SS of LF82 and determine its role in pathogenesis could therefore help reveal if YghJ is secreted by this *E. coli* strain.

Although our studies did not demonstrate strong expression or secretion of EaeH and YghJ in the two strains tested, in the last few years their functions in colonisation and disease have been elucidated in ETEC and ExPEC strains. Studies focusing on YghJ have implied that this protein has strong potential as a vaccine component and, despite the variation present in YghJ from different strains, conserved motifs within the protein have allowed the production of antibodies that show broad cross-reactivity between variants (Nesta *et al.*, 2014). Further exploration of the production of YghJ by a greater number of clinically important *E. coli* strains and the ability of YghJ to confer protection against them could advance the development of a vaccine against pathogenic *E. coli*.

7.2.2 Recent insights into the other identified ExPEC vaccine candidates

Further exploration of the other potential *E. coli* vaccine candidates identified by the Moriel *et al.* (2010) study has also been undertaken. Hemolysin A, one of the most protective candidates in the sepsis mouse model, has also been evaluated in an acute cystitis mouse model. Mice immunised with a hemolysin A toxoid showed significantly lowered severity of cystitis and 10-fold lower bacterial titers in their urine, implying that vaccination with hemolysin A reduces UPEC-produced bladder pathology (Smith *et al.*, 2015). Other studies have also investigated the expression and function of some of the vaccine candidates that were poorly understood at the time of identification. One of these, IrmA, was found to be coexpressed with factors associated with biofilm formation, and secreted into culture supernatant. The structure of IrmA displayed similarity to human cytokine receptor binding domains, and purified IrmA shown to bind to their cognate cytokines, suggesting this protein manipulates host immune responses (Moriel *et al.*, 2016). Another antigen, EsiB, also has implied immunomodulatory functions. EsiB

7. FINAL DISCUSSION

interacts with secretory immunoglobulin A (SigA), inhibiting SigA-mediated signalling events (Pastorello *et al.*, 2013). The authors of this study proposed that EsiB interference with immune signalling may help the bacteria avoid clearance by neutrophils, and reduce immune cell recruitment to the site of infection.

7.3 Inhibitors of Shiga toxin production and the bacterial SOS response

Therapeutic treatments that disrupt production and release of bacterial toxins are widely regarded as suitable strategies for effectively reducing the impact of bacterial infections without applying selective pressure on the organism. The Shiga toxin of EHEC is a particularly appealing target for new anti-virulence drugs, as use of conventional antibiotic treatment is associated with serious and life-threatening secondary sequelae.

7.3.1 The AHU compounds prevent Stx expression by inhibiting RecA

The aim of our work with the AHU compounds was to validate and explore the structure-activity relationship of these potential Stx inhibitors. Using expression reporter assays, we determined the maleimide ring of the compounds to be essential for both inhibition of Stx production and MMC-induced bacterial lysis, while phage transduction studies using both *E. coli* and *S. aureus* strains revealed that these compounds inhibit the production of phages other than Stx. RecA, the major regulator of the SOS response, was ultimately identified as the target of the AHU compounds, with biophysical studies indicating that AHU3 acts by preventing oligomerisation of RecA, an essential first step in activation of the SOS response and phage expression. Analysis of the structure of RecA and the known propensity of maleimide to readily form covalent bonds with thiols suggested that covalent binding of AHU3 to an exposed cysteine residue on RecA prevents monomers from binding to each other. Further work to confirm this activity is currently being undertaken.

7.3.2 Covalent binding as a mode of action for therapeutic drugs

Although covalently-binding drugs comprise a significant percentage of approved treatments on the market, including well-known drugs such as aspirin and penicillin, they have previously been considered toxic due to their irreversible mode of binding and potential for non-specific reactivity. In recent years, however, there has been a renewed interest in covalent drugs and the benefits to drug development they offer. The advantages they have include high potency and selectivity, a dissociation of pharmacokinetics from pharmacodynamics as the latter will be dependent on protein resynthesis, and the potential for proteins with a shallow binding site to be effectively targeted (Mah *et al.*, 2014). Thus, we did not consider AHU3's mode of action with RecA to be a considerable impediment.

7.3.3 The AHU compounds are toxic to mammalian cells

Cytotoxicity testing of the AHU compounds revealed that they were highly toxic, with this toxicity most probably due to non-specific interaction of the maleimide moiety with eukaryotic proteins. As the maleimide is essential for inhibition of RecA, the potential of this compound to be successfully modified is likely to be limited. However, our characterisation of the AHU3/RecA interaction has required the development and optimisation of assays that can be applied to rigorously test other compounds with potential Stx- or RecA-inhibiting activity. These may potentially be used to study a large number of small compounds reported to reduce Stx production that have been identified by high-throughput screening (reviewed by Upadhyay *et al.*, 2015). Characterisation of some of these compounds is currently ongoing by Alejandro Huerta Uribe, and the most promising inhibitors will eventually be tested in the *C. rodentium* (λ Stx_{2dact}) mouse model.

7.4 Future directions

The work presented in this thesis demonstrates that future *in vivo* studies testing potential anti-virulence therapies that target the T3SS should involve the *C. rodentium* infection mouse model, or, if possible, the EHEC infant rabbit model, which allows the

7. FINAL DISCUSSION

influence of other *E. coli* genes on pathogenesis to be assessed. One major consideration raised by *in vivo* testing of the anti-virulence drugs in Chapter 6 is the problem of delivering an active compound to the site of bacterial infection at a high enough concentration for it to be effective. With the exception of the E1 colicin tested in the LF82 mouse model, the compounds we evaluated *in vivo* were not encapsulated to protect them from being degraded or absorbed before reaching their target, and before further assessment of these compounds in animals is undertaken, encapsulation should perhaps be explored. Additionally, as the terminal rectum is the main site of *C. rodentium* colonisation, alternative delivery of compounds tested in this model, such as rectal administration, could be considered.

Although the function of EaeH as an adhesin has in recent years been elucidated, its mammalian protein target is currently unknown. Experiments to uncover the identity of this receptor, for example pull-down assays, co-immunoprecipitation, or the yeast two-hybrid screen, may help to further our knowledge of this vaccine candidate. While the function and targets of YghJ has also been revealed in the last few years, our work has shown LF82 to be the only reported strain which contains an apparently intact T2SS operon but does not secrete YghJ under conditions that other strains do. The T2SS of LF82, which is relatively unexplored, is therefore worth investigating to determine whether it is assembled and functional, possibly by methods such as the use of antibodies against T2SS structural proteins to identify the T2SS in LF82 membrane fractions.

Our studies with the AHU3 compound have demonstrated that suppression of the bacterial SOS response is a potential route to inhibition of prophage-encoded virulence factors such as the Shiga toxin. We have shown evidence that AHU3 binds RecA monomers and inhibits their polymerisation, and this binding is currently believed to be covalent. Further investigation into this interaction to examine this hypothesis is currently being undertaken as part of the PhD project of Alejandro Huerta Uribe, and will involve *in silico* digest and crystallisation of the AHU3-RecA complex. While cytotoxicity testing of the AHU compounds has indicated that they are ultimately unsuitable as therapeutic drugs for humans, the assays we have developed to assess Stx inhibition and RecA binding can be applied to many of the other SOS-inhibiting compounds that have been identified but not yet fully characterised. Finally, little is currently understood about the

7. FINAL DISCUSSION

three natural maleimide-containing metabolites, and given the scarcity of this moiety in nature, studies to characterise these compounds and determine their targets and mode of action, as well as any potential for leads as antibacterial therapies, would be of great interest.

7.5 Concluding remarks

In conclusion, the work presented in this thesis has provided new insights into several different and important areas of prevention and treatment of EHEC infections: assessment of mouse models for the study of T3SS-mediated bacterial colonisation, evaluation of the role and vaccine candidate potential of two antigens in two clinically important *E. coli* strains, and characterisation of the AHU group of compounds with elucidation of their target and mode of action. In the long-term, the work presented may contribute to the development of novel strategies to limit EHEC infection.

Chapter 8: References

8. REFERENCES

- Abernathy J, Corkill C, Hinojosa C, Li X & Zhou H (2013). Deletions in the pyruvate pathway of *Salmonella* Typhimurium alter SPI1-mediated gene expression and infectivity. *Journal of Animal Science and Biotechnology* 4(1) 5.
- Acinas SG, Marcelino LA, Klepac-Ceraj V & Polz MF (2004). Divergence and redundancy of 16S rRNA sequences in genomes with multiple *rrn* operons. *Journal of Bacteriology* 186(9) 2629–35.
- Akeda Y & Galán JE (2005). Chaperone release and unfolding of substrates in type III secretion. *Nature* 437 911–5.
- Allen RC, Papat R, Diggle SP & Brown SP (2014). Targeting virulence: can we make evolution-proof drugs? *Nature Reviews Microbiology* 12(4) 300–8.
- Anfora AT & Welch RA (2006). DsdX is the second D-serine transporter in uropathogenic *Escherichia coli* clinical isolate CFT073. *Journal of Bacteriology* 188(18) 6622–8.
- Arenson TA, Tsodikov OV & Cox MM (1999). Quantitative analysis of the kinetics of end-dependent disassembly of RecA filaments from ssDNA. *Journal of Molecular Biology* 288(3) 391–401.
- Baldi DL, Higginson EE, Hocking DM, Praszker J, Cavaliere R, James CE, Bennett-Wood V, Azzopardi KI, Turnbull L, Lithgow T *et al.* (2012). The type II secretion system and its ubiquitous lipoprotein substrate, SslE, are required for biofilm formation and virulence of enteropathogenic *Escherichia coli*. *Infection and Immunity* 80(6) 2042–52.
- Barthel M, Hapfelmeier S, Quintanilla-Martínez L, Kremer M, Rohde M, Hogardt M, Pfeffer K, Rüssmann H & Hardt WD (2003). Pretreatment of mice with streptomycin provides a *Salmonella enterica* serovar Typhimurium colitis model that allows analysis of both pathogen and host. *Infection and Immunity* 71(5) 2839–58.
- Bäumler AJ, Kusters JG, Stojiljkovic I & Heffron F (1994). *Salmonella typhimurium* loci involved in survival within macrophages. *Infection and Immunity* 62(5) 1623–30.
- Beckham KSH (2014). *Structural and functional characterisation of the protein targets of the anti-virulence compounds, the salicylidene acylhydrazides*. University of Glasgow.
- Beckham KSH, Connolly JPR, Ritchie JM, Wang D, Gawthorne JA, Tahoun A, Gally DL, Burgess K, Burchmore RJ, Smith BO *et al.*, (2014) The metabolic enzyme AdhE controls the virulence of *Escherichia coli* O157:H7. *Molecular Microbiology* 93(1) 199–211.
- Bednar RA (1990). Reactivity and pH dependence of thiol conjugation to N-ethylmaleimide: detection of a conformational change in chalcone isomerase. *Biochemistry* 29(15) 3684–90.
- Bellmeyer A, Cotton C, Kanteti R, Koutsouris A, Viswanathan VK & Hecht G (2009). Enterohemorrhagic *Escherichia coli* suppresses inflammatory response to cytokines and its own toxin. *American Journal of Physiology. Gastrointestinal and Liver Physiology* 297(3) G576–81.
- Bentancor LV, Bilen M, Brando RJF, Ramos MV, Ferreira LCS, Ghiringhelli PD & Palermo MS (2009). A DNA vaccine encoding the enterohemorrhagic *Escherichia coli* Shiga-like toxin 2 A2 and B subunits confers protective immunity to Shiga toxin challenge in the murine model. *Clinical and Vaccine Immunology: CVI* 16(5) 712–8.
- Bergan J, Dyve Lingelem AB, Simm R, Skotland T & Sandvig K (2012). Shiga toxins. *Toxicon* 60(6) 1085–107.
- Bielaszewska M, Friedrich AW, Aldick T, Schürk-Bulgrin R & Karch H (2006). Shiga toxin activatable by intestinal mucus in *Escherichia coli* isolated from humans: predictor for a severe clinical outcome. *Clinical Infectious Diseases: An Official Publication of the Infectious Diseases Society of America* 43(9) 1160–7.

8. REFERENCES

- Bielaszewska M, Zhang W, Mellmann A & Karch H (2007). Enterohaemorrhagic *Escherichia coli* O26:H11/H-: a human pathogen in emergence. *Berliner Und Münchener Tierärztliche Wochenschrift* 120(7-8) 279–87.
- Blattner FR, Plunkett G, Bloch CA, Perna NT, Burland V, Riley M, Collado-Vides J, Glasner JD, Rode CK, Mayhew GF *et al.* (1997). The complete genome sequence of *Escherichia coli* K-12. *Science (New York, N.Y.)* 277(5331) 1453–62.
- Böttcher T & Sieber S (2010). Showdomycin as a versatile chemical tool for the detection of pathogenesis-associated enzymes in bacteria. *Journal of the American Chemical Society* 132(20) 6964–72.
- Boysen A, Borch J, Krogh TJ, Hjernø K & Møller-Jensen J (2015). SILAC-based comparative analysis of pathogenic *Escherichia coli* secretomes. *Journal of Microbiological Methods* 116 66–79.
- Brenner SL, Zlotnick A & Stafford WF (1990). RecA protein self-assembly. II. Analytical equilibrium ultracentrifugation studies of the entropy-driven self-association of RecA. *Journal of Molecular Biology* 216(4) 949–64.
- Brown CL (2015) *The activity of colicins against Crohn's disease associated adherent-invasive Escherichia coli infection*. University of Glasgow.
- Brown CL, Smith K, Wall DM & Walker D (2015). Activity of species-specific antibiotics against Crohn's disease-associated adherent-invasive *Escherichia coli*. *Inflammatory Bowel Diseases* 21(10) 2372–82.
- Brumbaugh AR & Mobley HL (2012). Preventing urinary tract infection: progress toward an effective *Escherichia coli* vaccine. *Expert Review of Vaccines* 11(6) 663–76.
- Buchholz U, Bernard H, Werber D, Böhmer MM, Remschmidt C, Wilking H, Deleré Y, an der Heiden M, Adlhoch C, Dreesman J *et al.* (2011). German outbreak of *Escherichia coli* O104:H4 associated with sprouts. *The New England Journal of Medicine* 365(19) 1763–70.
- Bunger JC, Melton-Celsa AR & O'Brien AD (2013). Shiga toxin type 2dct displays increased binding to globotriaosulceramide *in vitro* and increased lethality in mice after activation by elastase. *Toxins* 5(11) 2074-92.
- Calderwood SB & Mekalanos JJ (1987). Iron regulation of Shiga-like toxin expression in *Escherichia coli* is mediated by the fur locus. *Journal of Bacteriology* 169(10) 4759–64.
- Campellone KG, Giese N, Tipper OJ & Leong JM (2002). A tyrosine-phosphorylated 12-amino-acid sequence of enteropathogenic *Escherichia coli* Tir binds the host adaptor protein Nck and is required for Nck localization to actin pedestals. *Molecular Microbiology* 43(5) 1227–41.
- Campellone KG, Robbins D & Leong JM (2004). EspFU is a translocated EHEC effector that interacts with Tir and N-WASP and promotes Nck-independent actin assembly. *Developmental Cell* 7(2) 217–28.
- Carr JF, Gregory ST & Dahlberg AE (2005). Severity of the streptomycin resistance and streptomycin dependence phenotypes of ribosomal protein S12 of *Thermus thermophilus* depends on the identity of highly conserved amino acid residues. *Journal of Bacteriology* 187(10) 3548–50.
- Carvalho FA, Barnich N, Sivignon A, Darcha C, Chan CHF, Stanners CP & Darfeuille-Michaud A (2009). Crohn's disease adherent-invasive *Escherichia coli* colonize and induce strong gut inflammation in transgenic mice expressing human CEACAM. *The Journal of Experimental Medicine* 206(10) 2179–89.
- Cava F, Lam H, de Pedro MA & Waldor MK (2011). Emerging knowledge of regulatory roles of D-amino acids in bacteria. *Cellular and Molecular Life Sciences: CMLS* 68(5) 817–31.
- Chapman PA, Siddons CA, Malo AT & Harkin MA (1996). Lamb products as a potential source of *E. coli* O157. *The Veterinary Record* 139(17) 427–8.

8. REFERENCES

- Chassaing B, Aitken JD, Malleshappa M & Vijay-Kumar M (2014). Dextran sulfate sodium (DSS)-induced colitis in mice. *Current Protocols in Immunology* 104 Unit 15.25.
- Chassaing B, Koren O, Carvalho FA, Ley RE & Gewirtz AT (2014). AIEC pathobiont instigates chronic colitis in susceptible hosts by altering microbiota composition. *Gut* 63(7) 1069–80.
- Chen C, Blumentritt CA, Curtis MM, Sperandio V, Torres AG & Dudley EG (2013). Restrictive streptomycin-resistant mutations decrease the formation of attaching and effacing lesions in *Escherichia coli* O157:H7 strains. *Antimicrobial Agents and Chemotherapy* 57(9) 4260-66.
- Churchward G, Belin D & Nagamine Y (1984). A pSC101-derived plasmid which shows no sequence homology to other commonly used cloning vectors. *Gene* 31(1-3) 165–71.
- Clark D & Cronan JE (1980). *Escherichia coli* mutants with altered control of alcohol dehydrogenase and nitrate reductase. *Journal of Bacteriology* 141(1) 177–83.
- Clarke MB, Hughes DT, Zhu C, Boedeker EC & Sperandio V (2006). The QseC sensor kinase: a bacterial adrenergic receptor. *Proceedings of the National Academy of Sciences of the United States of America* 103(27) 10420–5.
- Clermont O, Christenson JK, Denamur E & Gordon DM (2013). The Clermont *Escherichia coli* phylo-typing method revisited: improvement of specificity and detection of new phylo-groups. *Environmental Microbiology Reports* 5(1): 58-65.
- Cobbold RN, Hancock DD, Rice DH, Berg J, Stilborn R, Hovde CJ & Besser TE (2007). Rectoanal junction colonization of feedlot cattle by *Escherichia coli* O157:H7 and its association with supershedders and excretion dynamics. *Applied and Environmental Microbiology* 73(5) 1563–8.
- Cole JL, Lary JW, P Moody T & Laue TM, (2008) Analytical ultracentrifugation: sedimentation velocity and sedimentation equilibrium. *Methods in Cell Biology* 84 143–79.
- Connolly JPR, Goldstone RJ, Burgess K, Cogdell RJ, Beatson SA, Vollmer W, Smith DGE & Roe AJ (2015). The host metabolite D-serine contributes to bacterial niche specificity through gene selection. *The ISME Journal* 9(4) 1039–51.
- Cookson AL, Taylor SCS & Attwood GT (2006). The prevalence of Shiga toxin-producing *Escherichia coli* in cattle and sheep in the lower North Island, New Zealand. *New Zealand Veterinary Journal* 54(1) 28–33.
- Cormack BP, Valdivia RH & Falkow S (1996). FACS-optimized mutants of the green fluorescent protein (GFP). *Gene* 173(1) 33–8.
- Cornelis GR (2006). The type III secretion injectisome. *Nature Reviews. Microbiology* 4(11) 811–25.
- Cosloy SD & McFall E (1973). Metabolism of D-serine in *Escherichia coli* K-12: mechanism of growth inhibition. *Journal of Bacteriology* 114(2) 685–94.
- Cosnes J, Gower-Rousseau C, Seksik P & Cortot A (2011). Epidemiology and natural history of inflammatory bowel diseases. *Gastroenterology* 140(6) 1785–94.
- Courcelle J, Khodursky A, Peter B, Brown PO & Hanawalt PC (2001). Comparative gene expression profiles following UV exposure in wild-type and SOS-deficient *Escherichia coli*. *Genetics* 158(1) 41–64.
- Crossman LC, Chaudhuri RR, Beatson SA, Wells TJ, Desvaux M, Cunningham AF, Petty NK, Mahon V, Brinkley C, Hobman JL *et al.* (2010). A commensal gene bad: complete genome sequence of the prototypical enterotoxigenic *Escherichia coli* strain H10407. *Journal of Bacteriology* 192(21) 5822–31.
- Croxen MA, Law RJ, Scholz R, Keeney KM, Wlodarska M & Finlay BB (2013). Recent advances in understanding enteric pathogenic *Escherichia coli*. *Clinical Microbiology Reviews* 26(4) 822-80.

8. REFERENCES

- Curtis MM, Russell R, Moreira CG, Adebesein AM, Wang C, Williams NS, Taussig R, Stewart D, Zimmern P, Lu B *et al.* (2014). QseC inhibitors as an antivirulence approach for Gram-negative pathogens. *mBio* 5(6) e02165.
- D'Agati VD, Jenette JC & Silva FG (2005). *Non-neoplastic Kidney Diseases*. American Registry of Pathology.
- Daniell SJ, Kocsis E, Morris E, Knutton S, Booy FP & Frankel G (2003). 3D structure of EspA filaments from enteropathogenic *Escherichia coli*. *Molecular Microbiology* 49(2) 301–8.
- Darfeuille-Michaud A, Neut C, Barnich N, Lederman E, Di Martino P, Desreumaux P, Gambiez L, Joly B, Cortot A & Colombel JF (1998). Presence of adherent *Escherichia coli* strains in ileal mucosa of patients with Crohn's disease. *Gastroenterology* 115(6) 1405–13.
- Datsenko KA & Wanner BL (2000). One-step inactivation of chromosomal genes in *Escherichia coli* K-12 using PCR products. *Proceedings of the National Academy of Sciences of the United States of America* 97(12) 6640–5.
- Dean P, Scott JA, Knox AA, Quitard S, Watkins NJ & Kenny B (2010). The enteropathogenic *E. coli* effector EspF targets and disrupts the nucleolus by a process regulated by mitochondrial dysfunction. *PLoS Pathogens* 6(6) e1000961.
- Decanio MS, Landick R & Haft RJF (2013). The non-pathogenic *Escherichia coli* strain W secretes SsIE via the virulence-associated type II secretion system beta. *BMC Microbiology* 13 130.
- Deng W, Li Y, Vallance BA & Finlay BB (2001). Locus of enterocyte effacement from *Citrobacter rodentium*: sequence analysis and evidence for horizontal transfer among attaching and effacing pathogens. *Infection and Immunity* 69(10) 6323–35.
- Dho-Moulin M & Fairbrother JM (1999). Avian pathogenic *Escherichia coli* (APEC). *Veterinary Research* 30(2-3) 299-316.
- Donnenberg MS, Tacket CO, James SP, Losonsky G, Nataro JP, Wasserman SS, Kaper JB & Levine MM (1993). Role of the *eaeA* gene in experimental enteropathogenic *Escherichia coli* infection. *The Journal of Clinical Investigation* 92(3) 1412–7.
- Dziva F (2004). Identification of *Escherichia coli* O157:H7 genes influencing colonization of the bovine gastrointestinal tract using signature-tagged mutagenesis. *Microbiology* 150(11) 3631–45.
- Ejim L, Farha MA, Falconer SB, Wildenhain J, Coombes BK, Tyers M, Brown ED & Wright GD (2011). Combinations of antibiotics and nonantibiotic drugs enhance antimicrobial efficacy. *Nature Chemical Biology* 7(6) 348–50.
- Elliott SJ, Sperandio V, Girón JA, Shin S, Mellies JL, Wainwright L, Hutcheson SW, McDaniel TK & Kaper JB (2000). The locus of enterocyte effacement (LEE)-encoded regulator controls expression of both LEE- and non-LEE-encoded virulence factors in enteropathogenic and enterohemorrhagic *Escherichia coli*. *Infection and Immunity* 68(11) 6115–26.
- Emmerson JR, Gally DL & Roe AJ (2006). Generation of gene deletions and gene replacements in *Escherichia coli* O157:H7 using a temperature sensitive allelic exchange system. *Biological Procedures Online* 8(1) 153–62.
- Endo Y, Tsurugi K, Yutsude T, Takeda Y, Ogasawara T & Igarashi K (1988). Site of action of a Vero toxin (VT2) from *Escherichia coli* O157:H7 and of Shiga toxin on eukaryotic ribosomes. *European Journal of Biochemistry* 50 45–50.
- Eppinger M, Mammel MK, Leclerc JE, Ravel J & Cebula TA (2011). Genomic anatomy of *Escherichia coli* O157:H7 outbreaks. *Proceedings of the National Academy of Sciences* 108(50) 20142–7.

8. REFERENCES

- Favre-Bonté S, Licht TR, Forestier C & Krogfelt KA (1999). *Klebsiella pneumoniae* capsule expression is necessary for colonization of large intestines of streptomycin-treated mice. *Infection and Immunity* 67(11) 6152–6.
- Ferens WA, Cobbold R & Hovde CJ (2006). Intestinal Shiga toxin-producing *Escherichia coli* bacteria mitigate bovine leukemia virus infection in experimentally infected sheep. *Infection and Immunity* 74(5) 2906–16.
- Ferens WA, Grauke LJ & Hovde CJ (2004). Shiga toxin 1 targets bovine leukemia virus-expressing cells. *Infection and Immunity* 72(3) 1837–40.
- Ferens WA, Haruna J, Cobbold R & Hovde CJ (2008). Low numbers of intestinal Shiga toxin-producing *E. coli* correlate with a poor prognosis in sheep infected with bovine leukemia virus. *Journal of Veterinary Science* 9(4) 375–9.
- Ferrer MD, Quiles-Puchalt N, Harwich MD, Tormo-Más MÁ, Campoy S, Barbé J, Lasa I, Novick RP, Christie GE & Penadés JR (2011). RinA controls phage-mediated packaging and transfer of virulence genes in Gram-positive bacteria. *Nucleic Acids Research* 39(14) 5866–78.
- Foltyn VN, Zehl M, Dikopoltsev E, Jensen ON & Wolosker H (2010). Phosphorylation of mouse serine racemase regulates D-serine synthesis. *FEBS Letters* 584(13) 2937–41.
- Fox JT, Thomson DU, Drouillard JS, Thornton AB, Burkhardt DT, Emery DA & Nagaraja TG (2009). Efficacy of *Escherichia coli* O157:H7 siderophore receptor/porin proteins-based vaccine in feedlot cattle naturally shedding *E. coli* O157. *Foodborne Pathogens and Disease* 6(7) 893–9.
- Foxman B, Manning SD, Tallman P, Bauer R, Koopman JS, Gillespie B, Sobel JD & Marrs CF (2002). Uropathogenic *Escherichia coli* are more likely than commensal *E. coli* to be shared between heterosexual sex partners. *American Journal of Epidemiology* 156(12) 1133–40.
- Foxman B (2003). Epidemiology of urinary tract infections: incidence, morbidity, and economic costs. *Disease-A-Month* 49(2) 53–70.
- Fraser ME, Fujinaga M, Cherney MM, Melton-Celsa AR, Twiddy EM, O'Brien AD & James MNG (2004). Structure of shiga toxin type 2 (Stx2) from *Escherichia coli* O157:H7. *The Journal of Biological Chemistry* 279(26) 27511–7.
- Frenzen PD, Drake A, Angulo FJ & The Emerging Infections Program Foodnet Working Group (2005). Economic cost of illness due to *Escherichia coli* O157 Infections in the United States. *Journal of Food Protection* 12 2502–720.
- Friedman N, Vardi S, Ronen M, Alon U & Stavans J (2005). Precise temporal modulation in the response of the SOS DNA repair network in individual bacteria. *PLoS Biology* 3(7) e238.
- Fuller CA, Pellino CA, Flagler MJ, Strasser J & Weiss AA (2011). Shiga toxin subtypes display dramatic differences in potency. *Infection and Immunity* 79(3) 1329–37.
- Ginisty H, Sicard H, Roger B & Bouvet P (1999). Structure and functions of nucleolin. *J. Cell Sci.* 112(6) 761–72.
- Girard F, Frankel G, Phillips AD, Cooley W, Weyer U, Dugdale AH, Woodward MJ & La Ragione RM (2008). Interaction of enterohemorrhagic *Escherichia coli* O157:H7 with mouse intestinal mucosa. *FEMS Microbiology Letters* 283(2) 196–202.
- Girón JA, Torres AG, Freer E & Kaper JB (2002). The flagella of enteropathogenic *Escherichia coli* mediate adherence to epithelial cells. *Molecular Microbiology* 44(2) 361–79.

8. REFERENCES

- Golan L, Gonen E, Yagel S, Rosenshine I & Shpigel NY (2011). Enterohemorrhagic *Escherichia coli* induce attaching and effacing lesions and hemorrhagic colitis in human and bovine intestinal xenograft models. *Disease Models & Mechanisms* 4(1) 86–94.
- Gohar A, Abseltawab NF, Fahmy A & Amin MA (2016). Development of safe, effective and immunogenic vaccine candidate for diarrheagenic *Escherichia coli* main pathotypes in a mouse model. *BMC Research Notes* 9:80 doi: 10.1186/s13104-016-1891-z
- Grant J, Wendelboe AM, Wendel A, Jepson B, Torres P, Smelser C & Rolfs RT (2008). Spinach-associated *Escherichia coli* O157:H7 outbreak, Utah and New Mexico, 2006. *Emerging Infectious Diseases* 14(10) 1633–6.
- Hao W, Allen VG, Jamieson FB, Low DE & Alexander DC (2012). Phylogenetic incongruence in *E. coli* O104: understanding the evolutionary relationships of emerging pathogens in the face of homologous Recombination. *PLoS ONE* 7(4) e33971.
- Harari I & Arnon R (1990). Carboxy-terminal peptides from the B subunit of Shiga toxin induce a local and parenteral protective effect. *Molecular Immunology* 27(7) 613–21.
- Harel Y, Silva M, Giroir B, Weinberg A, Cleary TB & Beutler B (1993). A reporter transgene indicates renal-specific induction of tumor necrosis factor (TNF) by shiga-like toxin. Possible involvement of TNF in hemolytic uremic syndrome. *Journal of Clinical Investigation* 92(5) 2110–6.
- Hayashi F, Smith KD, Ozinsky A, Hawn TR, Yi EC, Goodlett DR, Eng JK, Akira S, Underhill DM & Aderem A (2001). The innate immune response to bacterial flagellin is mediated by Toll-like receptor 5. *Nature* 410 1099–103.
- Hentges DJ, Pongpech P & Que JU (1990). How streptomycin treatment compromises colonisation resistance against enteric pathogens in mice. *Microbial Ecology in Health and Disease* 3(3) 105–11.
- Hernandes RT, de la Cruz MA, Yamamoto D, Giron JA & Gomes TAT (2013). Dissection of the role of pili and type 2 and 3 secretion systems in adherence and biofilm formation of an atypical enteropathogenic *Escherichia coli* strain. *Infection and Immunity* 81(10) 3793–802.
- Heuvelink AE, van den Biggelaar FL, de Boer E, Herbes RG, Melchers WJ, Huis in 't Veld JH & Monnens LA (1998). Isolation and characterization of verocytotoxin-producing *Escherichia coli* O157 strains from Dutch cattle and sheep. *Journal of Clinical Microbiology* 36(4) 878–82.
- Hoffmann C, Hill DA, Minkah N, Kirn T, Troy A, Artis D & Bushman F (2009). Community-wide response of the gut microbiota to enteropathogenic *Citrobacter rodentium* infection revealed by deep sequencing. *Infection and Immunity* 77(10) 4668–78.
- Horita Y, Takii T, Yagi T, Ogawa K, Fujiwara N, Inagaki E, Kremer L, Sato Y, Kuroishi R, Lee Y *et al.* (2012). Antitubercular activity of disulfiram, an antialcoholism drug, against multidrug- and extensively drug-resistant *Mycobacterium tuberculosis* isolates. *Antimicrobial Agents and Chemotherapy* 56(8) 4140–5.
- Hoshino K, Takeuchi O, Kawai T, Sanjo H, Ogawa T, Takeda Y, Takeda K & Akira S (1999). Cutting edge: Toll-like receptor 4 (TLR4)-deficient mice are hyporesponsive to lipopolysaccharide: evidence for TLR4 as the LPS gene product. *Journal of Immunology* 162(7): 3749-52.
- Huang Y, Nishikawa T, Satoh K, Iwata T, Fukushima T, Santa T, Homma H & Imai K (1998). Urinary excretion of D-serine in human: comparison of different ages and species. *Biological & Pharmaceutical Bulletin* 21(2) 156–62.
- Hudson DL, Layton AN, Field TR, Bowen AJ, Wolf-Watz H, Elofsson M, Stevens MP & Galyov EE (2007). Inhibition of type III secretion in *Salmonella enterica* serovar Typhimurium by small-molecule inhibitors. *Antimicrobial Agents and Chemotherapy* 51(7) 2631–5.

8. REFERENCES

- Hufeldt MR, Nielsen DS, Vogensen FK, Midtvedt T & Hansen AK (2010). Variation in the gut microbiota of laboratory mice is related to both genetic and environmental factors. *Comparative Medicine* 60(5) 336–47.
- Hughes DT, Clarke MB, Yamamoto K, Rasko DA & Sperandio V (2009). The QseC adrenergic signaling cascade in enterohemorrhagic *E. coli* (EHEC). *PLoS Pathogens* 5(8) e1000553.
- Iguchi A, Thomson NR, Ogura Y, Saunders D, Ooka T, Henderson IR, Harris D, Asadulghani M, Kurokawa K, Dean P *et al.* (2009). Complete genome sequence and comparative genome analysis of enteropathogenic *Escherichia coli* O127:H6 strain E2348/69. *Journal of Bacteriology* 191(1) 347–54.
- Imlay JA & Linn S (1987). Mutagenesis and stress responses induced in *Escherichia coli* by hydrogen peroxide. *Journal of Bacteriology* 169(7) 2967–76.
- Ishikawa S, Kawahara K, Kagami Y, Isshiki Y, Kaneko A, Matsui H, Okada N & Danbara H (2003). Protection against Shiga toxin 1 challenge by immunization of mice with purified mutant Shiga toxin 1. *Infection and Immunity* 71(6) 3235–9.
- Isogai E, Isogai H, Kimura K, Hayashi S, Kubota T, Fujii N & Takeshi K, (1998) Role of tumor necrosis factor alpha in gnotobiotic mice Infected with an *Escherichia coli* O157:H7 strain. *Infection and Immunity* 66(1) 197–202.
- Iyoda S, Koizumi N, Satou H, Lu Y, Saitoh T, Ohnishi M & Watanabe H (2006). The GrlR-GrlA regulatory system coordinately controls the expression of flagellar and LEE-encoded type III protein secretion systems in enterohemorrhagic *Escherichia coli*. *Journal of Bacteriology* 188(16) 5682–92.
- Jacob SW & Rosenbaum EE (1966). The toxicology of dimethyl sulfoxide (DMSO). *Headache: The Journal of Head and Face Pain* 6(3) 127–36.
- Jandhyala DM, Rogers TJ, Kane A, Paton AW, Paton JC & Thorpe CM (2010). Shiga toxin 2 and flagellin from shiga-toxigenic *Escherichia coli* superinduce interleukin-8 through synergistic effects on host stress-activated protein kinase activation. *Infection and Immunity* 78(7) 2984–94.
- Johansson B (1992). A review of the pharmacokinetics and pharmacodynamics of disulfiram and its metabolites. *Acta Psychiatrica Scandinavica* 86(S369) 15–26.
- Khan MA, Ma C, Knodler LA, Valdez Y, Rosenberger CM, Deng W, Finlay BB & Vallance BA (2006). Toll-like receptor 4 contributes to colitis development but not to host defense during *Citrobacter rodentium* infection in mice. *Infection and Immunity* 74(5): 2522-36.
- Kanamaru K, Tatsuno I, Tobe T & Sasakawa C (2000). SdiA, an *Escherichia coli* homologue of quorum-sensing regulators, controls the expression of virulence factors in enterohaemorrhagic *Escherichia coli* O157:H7. *Molecular Microbiology* 38(4) 805–16.
- Kansal R, Rasko DA, Sahl JW, Munson GP, Roy K, Luo Q, Sheikh A, Kuhne KJ & Fleckenstein JM (2013). Transcriptional modulation of enterotoxigenic *Escherichia coli* virulence genes in response to epithelial cell interactions. *Infection and Immunity* 81(1) 259–70.
- van de Kar NC, Monnens LA, Karmali MA & van Hinsbergh VW (1992). Tumor necrosis factor and interleukin-1 induce expression of the verocytotoxin receptor globotriaosylceramide on human endothelial cells: implications for the pathogenesis of the hemolytic uremic syndrome. *Blood* 80(11) 2755–64.
- Karmali MA, Steele BT, Petric M & Lim C (1983). Sporadic cases of haemolytic-uraemic syndrome associated with faecal cytotoxin and cytotoxin-producing *Escherichia coli* in stools. *Lancet* 1 619–20.
- Kauppi AM, Nordfelth R, Uvell H, Wolf-Watz H & Elofsson M (2003). Targeting bacterial virulence. *Chemistry & Biology* 10(3) 241–9.

8. REFERENCES

- Keepers TR, Psocka MA, Gross LK & Obrig TG (2006). A murine model of HUS: Shiga toxin with lipopolysaccharide mimics the renal damage and physiologic response of human disease. *Journal of the American Society of Nephrology* 17(12) 3404–14.
- Kenny B, DeVinney R, Stein M, Reinscheid DJ, Frey EA & Finlay BB (1997). Enteropathogenic *E. coli* (EPEC) transfers its receptor for intimate adherence into mammalian cells. *Cell* 91(4) 511–20.
- Kim SH, Lee YH, Lee SH, Lee SR, Huh JW, Kim SU & Chang KT (2011). Mouse model for hemolytic uremic syndrome induced by outer membrane vesicles of *Escherichia coli* O157:H7. *FEMS Immunology and Medical Microbiology* 63(3) 427–34.
- Kimura K, Iwatsuki M, Nagai T, Matsumoto A, Takahashi Y, Shiomi K, Omura S & Abe A (2011). A small-molecule inhibitor of the bacterial type III secretion system protects against *in vivo* infection with *Citrobacter rodentium*. *The Journal of Antibiotics* 64(2) 197–203.
- Kitov PI, Sadowska JM, Mulvey G, Armstrong GD, Ling H, Pannu NS, Read RJ & Bundle DR (2000). Shiga-like toxins are neutralized by tailored multivalent carbohydrate ligands. *Nature* 403 669–72.
- Kodama T, Akeda Y, Kono G, Takahashi A, Imura K, Iida T & Honda T (2002). The EspB protein of enterohaemorrhagic *Escherichia coli* interacts directly with alpha-catenin. *Cellular Microbiology* 4(4) 213–22.
- Kokai-Kun JF (2000). Elastase in intestinal mucus enhances the cytotoxicity of Shiga toxin type 2d. *Journal of Biological Chemistry* 275(5) 3713–21.
- Kolodkin-Gal I, Romero D, Cao S, Clardy J, Kolter R & Losick R (2010). D-Amino acids trigger biofilm disassembly. *Science* 328 627–9.
- Konadu E, Donohue-Rolfe A, Calderwood SB, Pozsgay V, Shiloach J, Robbins JB & Szu SC (1999). Syntheses and immunologic properties of *Escherichia coli* O157 O-specific polysaccharide and Shiga toxin 1 B subunit conjugates in mice. *Infection and Immunity* 67(11) 6191–3.
- Kurioka T, Yunou Y & Kita E (1998). Enhancement of susceptibility to shiga toxin-producing *Escherichia coli* O157:H7 by protein calorie malnutrition in mice. *Infection and Immunity* 66(4) 1726–34.
- Lainhart W, Stofa G & Koudelka GB, (2009) Shiga toxin as a bacterial defense against a eukaryotic predator, *Tetrahymena thermophila*. *Journal of Bacteriology* 191(16) 5116–5122.
- Langermann S, Palaszynski S, Barnhart M, Auguste G, Pinkner JS, Burlein J, Barren P, Koenig S, Leath S, Jones CH *et al.* (1997). Prevention of mucosal *Escherichia coli* infection by FimH-adhesin-based systemic vaccination. *Science* 276 607–11.
- Lawley TD & Walker AW (2013). Intestinal colonization resistance. *Immunology* 138(1) 1–11.
- Lee MS, Kim MH & Tesh VL (2013). Shiga toxins expressed by human pathogenic bacteria induce immune responses in host cells. *Journal of Microbiology* 51(6) 724–30.
- Levine MM, Ferreccio C, Prado V, Cayazzo M, Abrego P, Martinez J, Maggi L, Baldini MM, Martin W, Maneval D, Kay B, Guers L, Lior H, Wasserman SS & Nataro JP (1993). Epidemiologic studies of *Escherichia coli* diarrheal infections in a low socioeconomic level peri-urban community in Santiago, Chile. *American Journal of Epidemiology* 138(10) 849-69.
- Lindgren SW, Samuel JE, Schmitt CK & O'Brien AD (1994). The specific activities of Shiga-like toxin II (SLT-II) and SLT-II-related toxins of enterohemorrhagic *Escherichia coli* differ when measured by Vero cell cytotoxicity but not by mouse lethality. *Infection and Immunity* 62(2) 623–31.
- Liu J, Sun Y, Feng S, Zhu L, Guo X & Qi C (2009). Towards an attenuated enterohemorrhagic *Escherichia coli* O157:H7 vaccine characterized by a deleted *ler* gene and containing apathogenic Shiga toxins. *Vaccine* 27(43) 5929–35.

8. REFERENCES

- Livny J & Friedman DI (2004). Characterizing spontaneous induction of Stx encoding phages using a selectable reporter system. *Molecular Microbiology* 51(6) 1691–704.
- Lloyd SJ, Ritchie JM, Rojas-Lopez M, Blumentritt CA, Popov VL, Greenwich JL, Waldor MK & Torres AG (2012). A double, long polar fimbria mutant of *Escherichia coli* O157:H7 expresses Curli and exhibits reduced in vivo colonization. *Infection and Immunity* 80(3): 914-20.
- Loftus EV Jr (2004). Clinical epidemiology of inflammatory bowel disease: incidence, prevalence, and environmental influences. *Gastroenterology* 126(6) 1504-17.
- Loś JM, Loś M, Węgrzyn A & Węgrzyn G (2012). Altruism of Shiga toxin-producing *Escherichia coli*: recent hypothesis versus experimental results. *Frontiers in Cellular and Infection Microbiology* 2 166.
- Lucas EMF, Castro MCM de & Takahashi JA (2007). Antimicrobial properties of sclerotiorin, isochromophilone VI and pencolide, metabolites from a Brazilian cerrado isolate of *Penicillium sclerotiorum* van Beyma. *Brazilian Journal of Microbiology* 38(4) 785–9.
- Luo Q, Kumar P, Vickers TJ, Sheikh A, Lewis WG, Rasko DA, Sistrunk J & Fleckenstein JM (2014). Enterotoxigenic *Escherichia coli* secretes a highly conserved mucin-degrading metalloprotease to effectively engage intestinal epithelial cells. *Infection and Immunity* 82(2) 509–21.
- Lupp C, Robertson ML, Wickham ME, Sekirov I, Champion OL, Gaynor EC & Finlay BB (2007). Host-mediated inflammation disrupts the intestinal microbiota and promotes the overgrowth of Enterobacteriaceae. *Cell Host & Microbe* 2(2) 119–29.
- Macpherson AJ & Harris NL (2004). Interactions between commensal intestinal bacteria and the immune system. *Nature Reviews Immunology* 4(6) 478–85.
- Mah R, Thomas JR & Shafer CM (2014). Drug discovery considerations in the development of covalent inhibitors. *Bioorganic & Medicinal Chemistry Letters* 24(1) 33–9.
- Mahajan A, Currie CG, Mackie S, Tree J, McAteer S, McKendrick I, McNeilly TN, Roe A, La Ragione RM, Woodward MJ *et al.* (2009). An investigation of the expression and adhesin function of H7 flagella in the interaction of *Escherichia coli* O157:H7 with bovine intestinal epithelium. *Cellular Microbiology* 11(1) 121–37.
- Makino K, Yokoyama K, Kubota Y, Yutsudo CH, Kimura S, Kurokawa K, Ishii K, Hattori M, Tatsuno I, Abe H *et al.* (1999). Complete nucleotide sequence of the prophage VT2-Sakai carrying the verotoxin 2 genes of the enterohemorrhagic *Escherichia coli* O157:H7 derived from the Sakai outbreak. *Genes & Genetic Systems* 74(5) 227–39.
- Mallick E, McBee M, Vanguri VK, Melton-Celsea AR, Schlieper K, Karalius BJ, O'Brien A, Butterson J, Leong JM & Schauer D (2012). A novel murine infection model for Shiga toxin-producing *Escherichia coli*. *The Journal of Clinical Investigation* 122(11) 4012–24.
- Marcato P, Griener TP, Mulvey GL & Armstrong GD (2005). Recombinant Shiga toxin B-subunit-keyhole limpet hemocyanin conjugate vaccine protects mice from Shigatoxemia. *Infection and Immunity* 73(10) 6523–9.
- Matthews L, Low JC, Gally DL, Pearce MC, Mellor DJ, Heesterbeek JAP, Chase-Topping M, Naylor SW, Shaw DJ, Reid SWJ *et al.* (2006). Heterogeneous shedding of *Escherichia coli* O157 in cattle and its implications for control. *Proceedings of the National Academy of Sciences of the United States of America* 103 547–52.
- Matthews L, Reeve R, Gally DL, Low JC, Woolhouse MEJ, McAteer SP, Locking ME, Chase-Topping ME, Haydon DT, Allison LJ *et al.* (2013). Predicting the public health benefit of vaccinating cattle against *Escherichia coli* O157. *Proceedings of the National Academy of Sciences of the United States of America* 110(40) 16265–70.

8. REFERENCES

- Mauro S a. & Koudelka GB (2011). Shiga toxin: expression, distribution, and its role in the environment. *Toxins* 3 608–25.
- Mayer CL, Leibowitz CS, Kurosawa S & Stearns-Kurosawa DJ (2012). Shiga toxins and the pathophysiology of hemolytic uremic syndrome in humans and animals. *Toxins* 4(11) 1261-87.
- McGann P, Snesrud E, Maybank R, Corey B, Ong AC, Clifford R, Hinkle M, Whitman T, Lesho E & Schaecher KE (2016). *Escherichia coli* harboring *mc-1* and *bla*_{CTX-M} on a novel IncF plasmid: First report of *mcr-1* in the USA. *Antimicrobial Agents and Chemotherapy* 60(7) 4420-1.
- McGannon CM, Fuller CA & Weiss AA (2010). Different classes of antibiotics differentially influence shiga toxin production. *Antimicrobial Agents and Chemotherapy* 54(9) 3790–8.
- McNeilly TN, Mitchell MC, Rosser T, McAteer S, Low JC, Smith DGE, Huntley JF, Mahajan A & Gally DL (2010). Immunization of cattle with a combination of purified intimin-531, EspA and Tir significantly reduces shedding of *Escherichia coli* O157:H7 following oral challenge. *Vaccine* 28(5) 1422–8.
- Meador JP, Caldwell ME, Cohen PS & Conway T (2014). *Escherichia coli* pathotypes occupy distinct niches in the mouse intestine. *Infection and Immunity* 82(5) 1931–8.
- Melton-Celsa AR, Darnell SC & O'Brien AD (1996). Activation of Shiga-like toxins by mouse and human intestinal mucus correlates with virulence of enterohemorrhagic *Escherichia coli* O91:H21 isolates in orally infected, streptomycin-treated mice. *Infection and Immunity* 64(5) 1569–76.
- Membrillo-Hernandez J, Echave P, Cabisco E, Tamarit J, Ros J & Lin EC (2000). Evolution of the *adhE* gene product of *Escherichia coli* from a functional reductase to a dehydrogenase. Genetic and biochemical studies of the mutant proteins. *The Journal of Biological Chemistry* 275(43) 33869–75.
- Michel-Briand Y & Baysse C (2002). The pyocins of *Pseudomonas aeruginosa*. *Biochimie* 84(5-6) 499–510.
- Michino H, Araki K, Minami S, Takaya S, Sakai N, Miyazaki M, Ono A & Yanagawa H (1999). Massive outbreak of *Escherichia coli* O157:H7 infection in schoolchildren in Sakai City, Japan, associated with consumption of white radish sprouts. *American Journal of Epidemiology* 150(8) 787–96.
- Mills CD, Kincaid K, Alt JM, Heilman MJ & Hill AM (2000). M-1/M-2 macrophages and the Th1/Th2 paradigm. *Journal of Immunology* 164(12) 6166–73.
- Miquel S, Peyretailade E, Claret L, de Vallée A, Dossat C, Vacherie B, Zineb EH, Segurens B, Barbe V, Sauvanet P *et al.* (2010). Complete genome sequence of Crohn's disease-associated adherent-invasive *E. coli* strain LF82. *PloS One* 5(9) e12714.
- Mohawk KL, Melton-Celsa AR, Zangari T, Carroll EE & O'Brien AD (2010). Pathogenesis of *Escherichia coli* O157:H7 strain 86-24 following oral infection of BALB/c mice with an intact commensal flora. *Microbial Pathogenesis* 48(3-4) 131–42.
- Mohawk KL & O'Brien AD (2011). Mouse models of *Escherichia coli* O157:H7 infection and shiga toxin injection. *Journal of Biomedicine & Biotechnology* 2011 id258185.
- Moriel DG, Bertoldi I, Spagnuolo A, Marchi S, Rosini R, Nesta B, Pastorello I, Corea V AM, Torricelli G, Cartocci E *et al.* (2010). Identification of protective and broadly conserved vaccine antigens from the genome of extraintestinal pathogenic *Escherichia coli*. *Proceedings of the National Academy of Sciences of the United States of America* 107(20) 9072–7.
- Moriel DG, Heras B, Paxman JJ, Lo AW, Tan L, Sullivan MJ, Dando SJ, Beatson SA, Ulett GC & Schembri MA (2016). Molecular and structural characterization of a novel *Escherichia coli* interleukin receptor mimic protein. *mBio* 7(2) e02046-15

8. REFERENCES

- Myhal ML, Laux DC & Cohen PS (1982). Relative colonizing abilities of human fecal and K 12 strains of *Escherichia coli* in the large intestines of streptomycin-treated mice. *European Journal of Clinical Microbiology* 1(3) 186–92.
- Nagano K, Taguchi K, Hara T, Yokoyama S, Kawada K & Mori H (2003). Adhesion and colonization of enterohemorrhagic *Escherichia coli* O157:H7 in cecum of mice. *Microbiology and Immunology* 47(2) 125–32.
- Nair D, Memmi G, Hernandez D, Bard J, Beaume M, Gill S, Francois P & Cheung AL (2011). Whole-genome sequencing of *Staphylococcus aureus* strain RN4220, a key laboratory strain used in virulence research, identifies mutations that affect not only virulence factors but also the fitness of the strain. *Journal of Bacteriology* 193(9) 2332–5.
- Nair DP, Podgórski M, Chatani S, Gong T, Xi W, Fenoli CR & Bowman CN (2014). The Thiol-Michael addition click reaction: a powerful and widely used tool in materials chemistry. *Chemistry of Materials* 26(1) 724–44.
- Nakjang S, Ndeh DA, Wipat A, Bolam DN & Hirt RP (2012). A novel extracellular metallopeptidase domain shared by animal host-associated mutualistic and pathogenic microbes. *PLoS One* 7(1) e30287.
- Nataro JP, Mai V, Johnson J, Blackwelder WC, Heimer R, Tirrell S, Edberg SC, Braden CR, Glenn Morris J Jr & Hirshon JM (2006). Diarrheagenic *Escherichia coli* infection in Baltimore, Maryland, and New Haven, Connecticut. *Clinical Infectious Diseases* 43(4) 402-7.
- Naylor SW (2005). *Escherichia coli* O157:H7 forms attaching and effacing lesions at the terminal rectum of cattle and colonization requires the LEE4 operon. *Microbiology* 151(8) 2773–81.
- Neil KP, Biggerstaff G, MacDonald JK, Trees E, Medus C, Musser KA, Stroika SG, Zink D & Sotir MJ (2012). A novel vehicle for transmission of *Escherichia coli* O157:H7 to humans: multistate outbreak of *E. coli* O157:H7 infections associated with consumption of ready-to-bake commercial prepackaged cookie dough - United States, 2009. *Clinical Infectious Diseases* 54(4) 511–8.
- Nesta B, Valeri M, Spagnuolo A, Rosini R, Mora M, Donato P, Alteri CJ, Del Vecchio M, Buccato S, Pezzicoli A *et al.* (2014). SsIE elicits functional antibodies that impair in vitro mucinase activity and In vivo colonization by both intestinal and extraintestinal *Escherichia coli* strains. *PLoS Pathogens* 10(5) e1004124.
- Newman J V, Zabel BA, Jha SS & Schauer DB (1999). *Citrobacter rodentium* espB is necessary for signal transduction and for infection of laboratory mice. *Infection and Immunity* 67(11) 6019–25.
- Nguyen Y & Sperandio V, (2012) Enterohemorrhagic *E. coli* (EHEC) pathogenesis. *Frontiers in Cellular and Infection Microbiology* 2 90.
- Nishikawa K, Matsuoka K, Watanabe M, Igai K, Hino K, Hatano K, Yamada A, Abe N, Terunuma D, Kuzuhara H *et al.* (2005). Identification of the optimal structure required for a Shiga toxin neutralizer with oriented carbohydrates to function in the circulation. *The Journal of Infectious Diseases* 191(12) 2097–105.
- Nishimura H, Mayama M, Komatsu Y, Kato H, Shimaoka N & Tanaka Y (1964). Showdomycin, a new antibiotic from a *Streptomyces* sp. *The Journal of Antibiotics* 17 148–55.
- Nomura M (1963). Mode of action of colicines. *Cold Spring Harbor Symposia on Quantitative Biology* 28 315–24.
- Noris M & Remuzzi G (2005). Hemolytic uremic syndrome. *Journal of the American Society of Nephrology* 16(4) 1035–50.
- O'Brien AD, Lively TA, Chang TW & Gorbach SL (1983). Purification of *Shigella dysenteriae* 1 (Shiga)-like toxin from *Escherichia coli* O157:H7 strain associated with haemorrhagic colitis. *Lancet* 2 573.

8. REFERENCES

- Olivier V, Queen J & Satchell KJF (2009). Successful small intestine colonization of adult mice by *Vibrio cholerae* requires ketamine anesthesia and accessory toxins. *PLoS One* 4(10) e7352.
- Olsnes S, Reisbig R & Eiklid K (1981). Subunit structure of *Shigella* cytotoxin. *The Journal of Biological Chemistry* 256(16) 8732–8.
- Pacheco AR & Sperandio V (2012). Shiga toxin and enterohemorrhagic *E. coli*: regulation and novel anti-virulence strategies. *Frontiers in Cellular and Infection Biology* 2(81) doi: 10.3389/fcimb.2012.00081.
- Pai CH, Kelly JK & Meyers GL (1986). Experimental infection of infant rabbits with verotoxin-producing *Escherichia coli*. *Infection and Immunity* 51(1) 16–23.
- Pastorello I, Paccani SR, Rosini R, Mattera R, Navarro MF, Urosev D, Nesta B, Surdo PL, Vecchio MD, Ripa V *et al.* (2013). EsiB, a novel pathogenic *Escherichia coli* secretory immunoglobulin A-binding protein impairing neutrophil activation.
- Pennington H (2010). *Escherichia coli* O157. *Lancet* 376 1428–35.
- Peterson EJR, Janzen WP, Kireev D & Singleton SF (2012). High-throughput screening for RecA inhibitors using a transcriber adenosine 5'-O-diphosphate assay. *ASSAY and Drug Development Technologies* 10(3) 260–8. *mBio* 4(4) e00206–13.
- Pettersson J, Nordfelth R, Dubinina E, Bergman T, Gustafsson M, Magnusson KE & Wolf-Watz H (1996). Modulation of virulence factor expression by pathogen target cell contact. *Science* 273 1231–3.
- Petty NK, Bulgin R, Crepin VF, Cerdeño-Tárraga AM, Schroeder GN, Quail MA, Lennard N, Corton C, Barron A, Clark L *et al.* (2010). The *Citrobacter rodentium* genome sequence reveals convergent evolution with human pathogenic *Escherichia coli*. *Journal of Bacteriology* 192(2) 525–38.
- Pizza M, Scarlato V, Masignani V, Giuliani MM, Aricò B, Comanducci M, Jennings GT, Baldi L, Bartolini E, Capecchi B *et al.* (2000). Identification of vaccine candidates against serogroup B meningococcus by whole-genome sequencing. *Science* 287 1816–20.
- Potter AA, Klashinsky S, Li Y, Frey E, Townsend H, Rogan D, Erickson G, Hinkley S, Klopfenstein T, Moxley RA *et al.* (2004). Decreased shedding of *Escherichia coli* O157:H7 by cattle following vaccination with type III secreted proteins. *Vaccine* 22(3-4) 362–9.
- Pruimboom-Brees IM, Morgan TW, Ackermann MR, Nystrom ED, Samuel JE, Cornick NA & Moon HW (2000). Cattle lack vascular receptors for *Escherichia coli* O157:H7 Shiga toxins. *Proceedings of the National Academy of Sciences of the United States of America* 97(19) 10325–9.
- Putri SP, Ishido K-I, Kinoshita H, Kitani S, Ihara F, Sakihama Y, Igarashi Y & Nihira T (2014). Production of antioomycete compounds active against the phytopathogens *Phytophthora sojae* and *Aphanomyces cochlioides* by clavicipitoid entomopathogenic fungi. *Journal of Bioscience and Bioengineering* 117(5) 557–62.
- Quiles-Puchalt N, Carpena N, Alonso JC, Novick RP, Marina A & Penadés JR (2014). Staphylococcal pathogenicity island DNA packaging system involving cos-site packaging and phage-encoded HNH endonucleases. *Proceedings of the National Academy of Sciences of the United States of America* 111(16) 6016–21.
- Rappuoli R (2000). Reverse vaccinology. *Current Opinion in Microbiology* 3(5) 445–50.
- Rasko DA, Moreira CG, Li DR, Reading NC, Ritchie JM, Waldor MK, Williams N, Taussig R, Wei S, Roth M *et al.* (2008). Targeting QseC signaling and virulence for antibiotic development. *Science* 321 1078–80.

8. REFERENCES

- Rea MC, Dobson A, O'Sullivan O, Crispie F, Fouhy F, Cotter PD, Shanahan F, Kiely B, Hill C & Ross RP (2011). Effect of broad- and narrow-spectrum antimicrobials on *Clostridium difficile* and microbial diversity in a model of the distal colon. *Proceedings of the National Academy of Sciences of the United States of America* 108 (Suppl 1) 4639–44.
- Riedel CU, Casey PG, Mulcahy H, Gara FO, Gahan CGM & Hill C (2007). Construction of p16Slux, a novel vector for improved bioluminescent labeling of Gram-negative bacteria. *Applied and Environmental Microbiology* 73(21) 7092–5.
- Riley LW, Remis RS, Helgerson SD, McGee HB, Wells JG, Davis BR, Hebert RJ, Olcott ES, Johnson LM, Hargrett NT *et al.* (1983). Hemorrhagic colitis associated with a rare *Escherichia coli* serotype. *The New England Journal of Medicine* 308(12) 681–5.
- Ritchie JM (2014). Animal models of enterohemorrhagic *Escherichia coli* infection. *Microbiology Spectrum* 2(4) e0022–2013.
- Ritchie JM, Greenwich JL, Davis BM, Bronson RT, Gebhart D, Williams SR, Martin D, Scholl D & Waldor MK (2011). An *Escherichia coli* O157-specific engineered pyocin prevents and ameliorates infection by *E. coli* O157:H7 in an animal model of diarrheal disease. *Antimicrobial Agents and Chemotherapy* 55(12) 5469–74.
- Ritchie JM & Waldor MK (2005). The locus of enterocyte effacement-encoded effector proteins all promote enterohemorrhagic *Escherichia coli* pathogenicity in infant rabbits. *Infection and Immunity* 73(3): 1466–74.
- Ritchie JM, Thorpe CM, Rogers AB & Waldor MK (2003). Critical roles for stx2, eae, and tir in enterohemorrhagic *Escherichia coli*-induced diarrhea and intestinal inflammation in infant rabbits. *Infection and Immunity* 71(12) 7129–39.
- Roberts JA, Kaack MB, Baskin G, Chapman MR, Hunstad DA, Pinkner JS & Hultgren SJ (2004). Antibody responses and protection from pyelonephritis following vaccination with purified *Escherichia coli* PapDG protein. *The Journal of Urology* 171(4) 1682–5.
- Roberts JA, Upton PA & Azene G (2000). *Escherichia coli* O157:H7: an economic assessment of an outbreak. *Journal of Public Health Medicine* 22(1) 99–107.
- Roberts JW, Yarnell W, Bartlett E, Guo J, Marr M, Ko DC, Sun H & Roberts CW (1998). Antitermination by bacteriophage lambda Q protein. *Cold Spring Harbor Symposia on Quantitative Biology* 63 319–25.
- Robinson CM, Sinclair JF, Smith MJ & O'Brien AD (2006). Shiga toxin of enterohemorrhagic *Escherichia coli* type O157:H7 promotes intestinal colonization. *Proceedings of the National Academy of Sciences of the United States of America* 103(25) 9667–72.
- Roe AJ, Yull H, Naylor SW, Woodward MJ, Smith DGE & Gally DL (2003). Heterogeneous surface expression of EspA translocon filaments by *Escherichia coli* O157:H7 is controlled at the posttranscriptional level. *Infection and Immunity* 71(10) 5900–9.
- Russo TA, Stapleton A, Wenderoth S, Hooton TM & Stamm EW (1995). Chromosomal restriction fragment length polymorphism analysis of *Escherichia coli* strains causing recurrent urinary tract infections in young women. *Journal of Infectious Diseases* 172(2) 440–5.
- Ruusala T, Andersson D, Ehrenberg M & Kurland CG (1984). Hyper-accurate ribosomes inhibit growth. *The EMBO Journal* 3(11) 2575–80.
- Saini S, Slauch JM, Aldridge PD & Rao CV (2010). Role of cross talk in regulating the dynamic expression of the flagellar Salmonella pathogenicity island 1 and type 1 fimbrial genes. *Journal of Bacteriology* 192(21) 5767–77.

8. REFERENCES

- Sassanfar M & Roberts JW (1990). Nature of the SOS-inducing signal in *Escherichia coli*. The involvement of DNA replication. *Journal of Molecular Biology* 212(1) 79–96.
- Sauer RT, Ross MJ & Ptashne M (1982). Cleavage of the lambda and P22 repressors by recA protein. *The Journal of Biological Chemistry* 257(8) 4458–62.
- Sauter KAD, Melton-Celsa AR, Larkin K, Troxell ML, O'Brien AD & Magun BE (2008). Mouse model of hemolytic-uremic syndrome caused by endotoxin-free Shiga toxin 2 (Stx2) and protection from lethal outcome by anti-Stx2 antibody. *Infection and Immunity* 76(10) 4469–78.
- Schauer DB & Falkow S (1993). The eae gene of *Citrobacter freundii* biotype 4280 is necessary for colonization in transmissible murine colonic hyperplasia. *Infection and Immunity* 61(11) 4654–61.
- Scheutz F, Nielsen EM, Frimodt-Møller J, Boisen N, Morabito S, Tozzoli R, Nataro JP & Caprioli A (2011). Characteristics of the enteroaggregative Shiga toxin/verotoxin-producing *Escherichia coli* O104:H4 strain causing the outbreak of haemolytic uraemic syndrome in Germany, May to June 2011. *Euro Surveillance: Bulletin Européen Sur Les Maladies Transmissibles = European Communicable Disease Bulletin* 16(24) pii19889.
- Scheutz F, Teel LD, Beutin L, Piérard D, Buvens G, Karch H, Mellmann A, Caprioli A, Tozzoli R, Morabito S, Strockbine NA, Melton-Celsa AR, Sanchez M, Persson S & O'Brien AD (2012). Multicenter evaluation of a sequence-based protocol for subtyping Shiga toxins and standardizing Stx nomenclature. *Journal of Clinical Microbiology* 50(9) 2951–63.
- Scholl D, Cooley M, Williams SR, Gebhart D, Martin D, Bates A & Mandrell R (2009). An engineered R-type pyocin is a highly specific and sensitive bactericidal agent for the food-borne pathogen *Escherichia coli* O157:H7. *Antimicrobial Agents and Chemotherapy* 53(7) 3074–80.
- Sexton JZ, Wigle TJ, He Q, Hughes MA, Smith GR, Singleton SF, Williams AL & Yeh LA (2010). Novel inhibitors of *E. coli* RecA ATPase activity. *Current Chemical Genomics* 4 34–42.
- Sheikh A, Luo Q, Roy K, Shabaan S, Kumar P, Qadri F & Fleckenstein JM (2014). Contribution of the highly conserved EaeH surface protein to enterotoxigenic *Escherichia coli* pathogenesis. *Infection and Immunity* 82(9) 3657–66.
- Shifrin Y, Peleg A, Ilan O, Nadler C, Kobi S, Baruch K, Yerushalmi G, Berdichevsky T, Altuvia S, Elgrably-Weiss M, Abe C, Knutton S, Sasakawa C, Ritchie JM, Waldor MK & Rosenshine I (2008). Transient shielding of intimin and the type III secretion system of enterohemorrhagic and enteropathogenic *Escherichia coli* by a group 4 capsule. *Journal of Bacteriology* 190(14): 5063–74.
- Shimizu T, Ohta Y & Noda M (2009). Shiga toxin 2 is specifically released from bacterial cells by two different mechanisms. *Infection and Immunity* 77(7) 2813–23.
- Sinclair JF & O'Brien AD (2002). Cell surface-localized nucleolin is a eukaryotic receptor for the adhesin intimin-gamma of enterohemorrhagic *Escherichia coli* O157:H7. *The Journal of Biological Chemistry* 277(4) 2876–85.
- Smith K, Martin L, Rinaldi A, Rajendran R, Ramage G & Walker D (2012). Activity of pyocin S2 against *Pseudomonas aeruginosa* biofilms. *Antimicrobial Agents and Chemotherapy* 56(3) 1599–601.
- Smith MA, Weingarten RA, Russo LM, Ventura CL & O'Brien AD (2015). Antibodies against hemolysin and cytotoxic necrotizing factor type 1 (CNF1) reduce bladder inflammation in a mouse model of urinary tract infection with toxigenic uropathogenic *Escherichia coli*. *Infection and Immunity* 83(4) 1661-73.
- Smith PM, Howitt MR, Panikov N, Michaud M, Gallini CA, Bohlooly YM, Glickman JN & Garrett WS (2013). The microbial metabolites, short-chain fatty acids, regulate colonic Treg cell homeostasis. *Science* 341 569–73.

8. REFERENCES

- Smith WE, Kane A V, Campbell ST, Acheson DWK, Cochran BH & Thorpe CM (2003). Shiga toxin 1 triggers a ribotoxic stress response leading to p38 and JNK activation and induction of apoptosis in intestinal epithelial cells. *Infection and Immunity* 71(3) 1497–504.
- Snedeker KG, Shaw DJ, Locking ME & Prescott RJ (2009). Primary and secondary cases in *Escherichia coli* O157 outbreaks: a statistical analysis. *BMC Infectious Diseases* 9 144.
- Snider TA, Fabich AJ, Washburn KE, Sims WP, Blair JL, Cohen PS, Conway T & Clinkenbeard KD (2006). Evaluation of a model for *Escherichia coli* O157:H7 colonization in streptomycin-treated adult cattle. *American Journal of Veterinary Research* 67(11) 1914–20.
- Spees AM, Wangdi T, Lopez CA, Kingsbury DD, Xavier MN, Winter SE, Tsois RM & Bäumlner AJ (2013). Streptomycin-induced inflammation enhances *Escherichia coli* gut colonization through nitrate respiration. *mBio* 4(4) e00430–13.
- Sperandio V, Torres AG, Giron JA & Kaper JB (2001). Quorum sensing is a global regulatory mechanism in enterohemorrhagic *Escherichia coli* O157:H7. *Journal of Bacteriology* 183(17) 5187–97.
- Sperandio V, Torres AG & Kaper JB (2002). Quorum sensing *Escherichia coli* regulators B and C (QseBC): a novel two-component regulatory system involved in the regulation of flagella and motility by quorum sensing in *E. coli*. *Molecular Microbiology* 43(3) 809–21.
- Steinberg KM & Levin BR (2007). Grazing protozoa and the evolution of the *Escherichia coli* O157:H7 Shiga toxin-encoding prophage. *Proceedings of the Royal Society of Biological Sciences* 274(1621) 1921–9.
- Strober W (2011). Adherent-invasive *E. coli* in Crohn disease: bacterial "agent provocateur". *The Journal of Clinical Investigation* 121(3) 841–4.
- Strozen TG, Li G & Howard SP (2012). YghG (GspS β) is a novel pilot protein required for localization of the GspS β type II secretion system secretin of enterotoxigenic *Escherichia coli*. *Infection and Immunity* 80(8) 2608–22.
- Tacket CO, Sztein MB, Losonsky G, Abe A, Finlay BB, McNamara BP, Fantry GT, James SP, Nataro JP, Levine MM *et al.* (2000). Role of EspB in experimental human enteropathogenic *Escherichia coli* infection. *Infection and Immunity* 68(6) 3689–95.
- Tarr PI, Gordon CA & Chandler WL (2005). Shiga-toxin-producing *Escherichia coli* and haemolytic uraemic syndrome. *Lancet* 365 1073–86.
- Thliveris AT, Little JW & Mount DW (1991). Repression of the *E coli* recA gene requires at least two LexA protein monomers. *Biochimie* 73(4) 449–56.
- Toshima H, Yoshimura A, Arikawa K, Hidaka A, Ogasawara J, Hase A, Masaki H & Nishikawa Y (2007). Enhancement of Shiga toxin production in enterohemorrhagic *Escherichia coli* serotype O157:H7 by DNase colicins. *Applied and Environmental Microbiology* 73(23) 7582–8.
- Totsika M, Moriel DG, Idris A, Rogers BA, Wurpel DJ, Phan MD, Paterson DL & Schembri MA (2012). Uropathogenic *Escherichia coli* mediated urinary tract infection. *Current Drug Targets* 13(11) 1386–99.
- Trachtman H, Cnaan A, Christen E, Gibbs K, Zhao S, Acheson DWK, Weiss R, Kaskel FJ, Spitzer A & Hirschman GH (2003). Effect of an oral Shiga toxin-binding agent on diarrhea-associated hemolytic uremic syndrome in children: a randomized controlled trial. *JAMA* 290(10) 1337–44.
- Tree JJ, Wang D, McNally C, Mahajan A, Layton A, Houghton I, Eloffson M, Stevens MP, Gally DL & Roe AJ (2009). Characterization of the effects of salicylidene acylhydrazide compounds on type III secretion in *Escherichia coli* O157:H7. *Infection and Immunity* 77(10) 4209–20.
- Ubeda C, Barry P, Penades JR & Novick RP (2007). A pathogenicity island replicon in *Staphylococcus aureus* replicates as an unstable plasmid. *Proceedings of the National Academy of Sciences* 104(36) 14182–8.

8. REFERENCES

- Upadhyay A, Mooyottu S, Yin H, Nair M, Bhattaram V & Venkitanarayanan K (2015). Inhibiting microbial toxins using plant-derived compounds and plant extracts. *Medicines* 2(3) 186–211.
- Valeri M, Rossi Paccani S, Kasendra M, Nesta B, Serino L, Pizza M & Soriani M (2015). Pathogenic *E. coli* exploits SsIE mucinase activity to translocate through the mucosal barrier and get access to host cells. *PLoS One* 10(3) e0117486.
- Vallance BA, Deng W, Jacobson K & Finlay BB (2003). Host susceptibility to the attaching and effacing bacterial pathogen *Citrobacter rodentium*. *Infection and Immunity* 71(6) 3443–53.
- Vareille M, de Sablet T, Hindré T, Martin C & Gobert AP (2007). Nitric oxide inhibits Shiga-toxin synthesis by enterohemorrhagic *Escherichia coli*. *Proceedings of the National Academy of Sciences of the United States of America* 104(24) 10199–204.
- Veenendaal AKJ, Sundin C & Blocker AJ (2009). Small-molecule type III secretion system inhibitors block assembly of the *Shigella* type III secretion. *Journal of Bacteriology* 191(2) 563–70.
- Vistica J, Dam J, Balbo A, Yikilmaz E, Mariuzza RA, Rouault TA & Schuck P (2004). Sedimentation equilibrium analysis of protein interactions with global implicit mass conservation constraints and systematic noise decomposition. *Analytical Biochemistry* 326(2) 234–56.
- Vollmer W, Blanot D & de Pedro MA (2008). Peptidoglycan structure and architecture. *FEMS Microbiology Reviews* 32(2) 149–67.
- Wadolkowski EA, Burris JA & Brienl ADO (1990). Mouse model for colonization and disease caused by enterohemorrhagic *Escherichia coli* O157:H7. *Infection and Immunity* 58(8) 2438–45.
- Wang D, Zetterström CE, Gabrielsen M, Beckham KSH, Tree JJ, Macdonald SE, Byron O, Mitchell TJ, Gally DL, Herzyk P *et al.* (2011). Identification of bacterial target proteins for the salicylidene acylhydrazide class of virulence-blocking compounds. *The Journal of Biological Chemistry* 286(34) 29922–31.
- Watanabe H, Numata K, Ito T, Takagi K & Matsukawa A (2004). Innate immune response in Th1- and Th2-dominant mouse strains. *Shock* 22(5) 460–6.
- Wennerås C & Erling V (2004). Prevalence of enterotoxigenic *Escherichia coli*-associated diarrhoea and carrier state in the developing world. *Journal of Health, Population, and Nutrition* 22(4) 270–82.
- Wigle TJ, Sexton JZ, Gromova A V, Hadimani MB, Hughes M a, Smith GR, Yeh L-A & Singleton SF (2009). Inhibitors of RecA activity discovered by high-throughput screening: cell-permeable small molecules attenuate the SOS response in *Escherichia coli*. *Journal of Biomolecular Screening: The Official Journal of the Society for Biomolecular Screening* 14(9) 1092–101.
- Wigle TJ & Singleton SF (2007). Directed molecular screening for RecA ATPase inhibitors. *Bioorganic and Medicinal Chemistry Letters* 17(12) 3249–53.
- Wiles S, Clare S, Harker J, Huett A, Young D, Dougan G & Frankel G (2004). Organ specificity, colonization and clearance dynamics in vivo following oral challenges with the murine pathogen *Citrobacter rodentium*. *Cellular Microbiology* 6(10) 963–72.
- Wiles S, Dougan G & Frankel G (2005). Emergence of a “hyperinfectious” bacterial state after passage of *Citrobacter rodentium* through the host gastrointestinal tract. *Cellular Microbiology* 7(8) 1163–72.
- Wong CS, Jelacic S, Habeeb RL, Watkins SL & Tarr PI (2000). The risk of the hemolytic-uremic syndrome after antibiotic treatment of *Escherichia coli* O157:H7 infections. *The New England Journal of Medicine* 342(26) 1930–6.
- Wong JMW, de Souza R, Kendall CWC, Emam A & Jenkins DJA (2006). Colonic health: fermentation and short chain fatty acids. *Journal of Clinical Gastroenterology* 40(3) 235–43.

8. REFERENCES

- Wong TW, Colombo G & Sonvico F (2011). Pectin matrix as oral drug delivery vehicle for colon cancer treatment. *AAPS PharmSciTech* 12(1) 201–14.
- Xing X & Bell CE (2004). Crystal structures of *Escherichia coli* RecA in complex with MgADP and MnAMP-PNP. *Biochemistry* 43(51) 16142–52.
- Xu X, McAteer SP, Tree JJ, Shaw DJ, Wolfson EBK, Beatson SA, Roe AJ, Allison LJ, Chase-Topping ME, Mahajan A *et al.* (2012). Lysogeny with Shiga toxin 2-encoding bacteriophages represses type III secretion in enterohemorrhagic *Escherichia coli*. *PLoS Pathogens* 8(5) e1002672.
- Yang J, Baldi DL, Tauschek M, Strugnell RA & Robins-Browne RM (2006). Transcriptional regulation of the yghJ-pppA-yghG-gspCDEFGHIJKLM cluster, encoding the type II secretion pathway in enterotoxigenic *Escherichia coli*. *Journal of Bacteriology* 189(1) 142–150.
- Yip CK, Finlay BB & Strynadka NCJ (2005). Structural characterization of a type III secretion system filament protein in complex with its chaperone. *Nature Structural & Molecular Biology* 12(1) 75–81.
- Yip CK & Strynadka NCJ (2006). New structural insights into the bacterial type III secretion system. *Trends in Biochemical Sciences* 31(4) 223–30.
- Yokoyama K, Makino K, Kubota Y, Watanabe M, Kimura S, Yutsudo CH, Kurokawa K, Ishii K, Hattori M, Tatsuno I *et al.* (2000). Complete nucleotide sequence of the prophage VT1-Sakai carrying the Shiga toxin 1 genes of the enterohemorrhagic *Escherichia coli* O157:H7 strain derived from the Sakai outbreak. *Gene* 258(1-2) 127–39.
- Zhang JP & Normark S (1996). Induction of gene expression in *Escherichia coli* after pilus-mediated adherence. *Science* 273(5279) 1234–6.
- Zhang X, McDaniel AD, Wolf LE, Keusch GT, Waldor MK & Acheson DW (2000). Quinolone antibiotics induce Shiga toxin-encoding bacteriophages, toxin production, and death in mice. *The Journal of Infectious Diseases* 181(2) 664–70.
- Zhu C, Yu J, Yang Z, Davis K, Rios H, Wang B, Glenn G & Boedeker EC (2008). Protection against Shiga toxin-producing *Escherichia coli* infection by transcutaneous immunization with Shiga toxin subunit B. *Clinical and Vaccine Immunology : CVI* 15(2) 359–66.
- Zhu J, Miller MB, Vance RE, Dziejman M, Bassler BL & Mekalanos JJ (2002). Quorum-sensing regulators control virulence gene expression in *Vibrio cholerae*. *Proceedings of the National Academy of Sciences of the United States of America* 99(5) 3129–34.
- Zoja C, Corna D, Farina C, Sacchi G, Lingwood C, Doyle MP, Padhye VV, Abbate M & Remuzzi G (1992). Verotoxin glycolipid receptors determine the localization of microangiopathic process in rabbits given verotoxin-1. *The Journal of Laboratory and Clinical Medicine* 120(2) 229–38.

Chapter 9: Appendices

9.1 Characterisation of *E. coli* Str^R mutants

The eight spontaneous Str^R mutants of each *E. coli* strain were characterised to ensure that the mutant selected for use in animals was as phenotypically similar to the wild type as possible. The characteristics studied included growth, motility, secretion in MEM media (data not shown) and adherence to Caco-2 cells.

9.1.1 Bacterial growth in LB, MEM and M9 media

Growth of the wild type and mutant strains in LB, MEM and M9 media over 6 hours found that the majority of Str^R mutants displayed a growth curve very similar to that of the wild type, although all Str^R mutants showed slightly slower growth in M9 media (Figure 9-1).

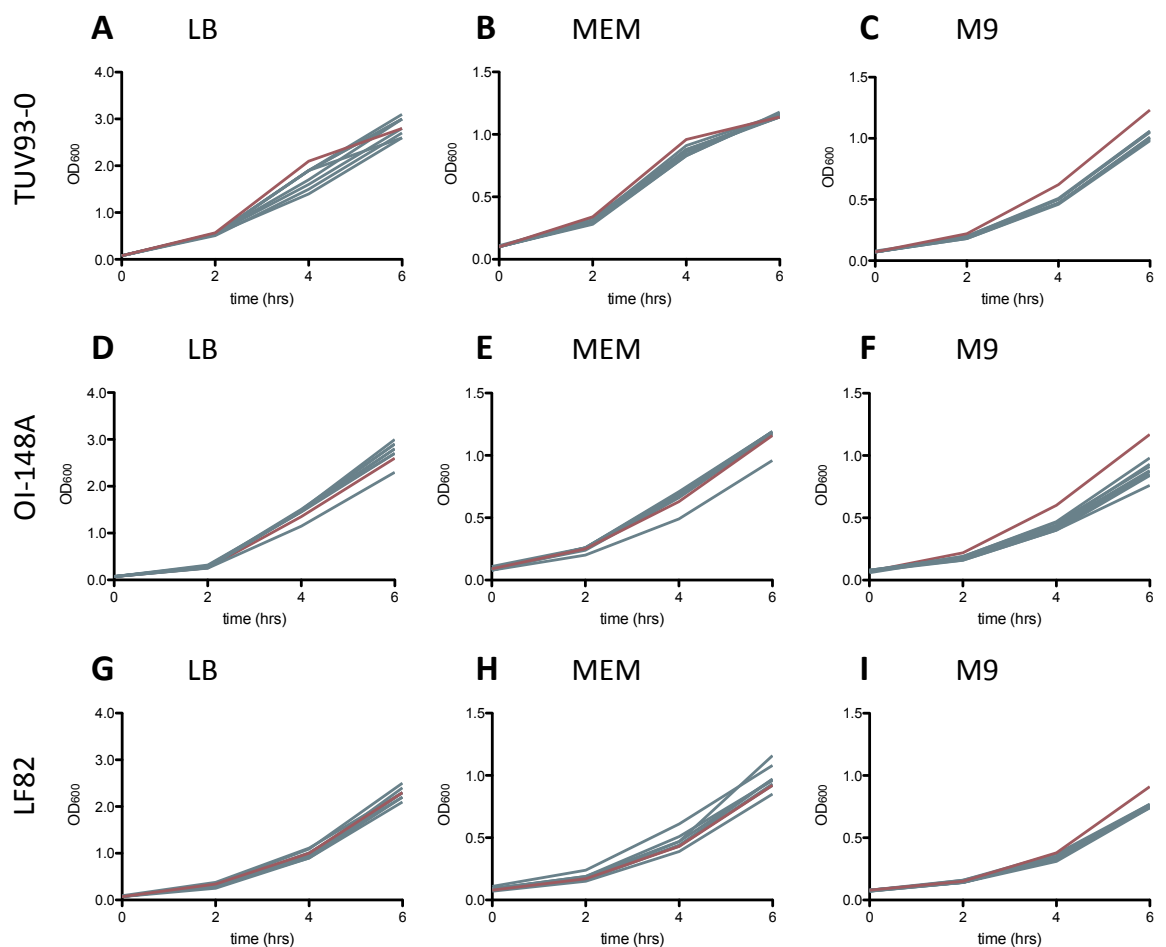


Figure 9-1: Growth curves of *E. coli* Str^R mutants. Bacterial growth of wild type (red) and Str^R (blue) TUV93-0 (A-C), OI-148A (D-F) and LF82 (G-I) in LB, MEM and M9 media. Data shown is from a single experiment.

9.1.2 Bacterial motility

Motility of strains was assessed by measuring the diameter growth of bacteria on 0.25% agar after 24 hours at 30°C (Figure 9-2). Strains with the K42T mutation had similar motility profiles to that of the wild type, and out of the available K24T Str^R mutants we selected those that were most similar to the wild type for use in animal models (TUV93-0: Str^R 1; OI-148A: Str^R 5; LF82: Str^R 6).

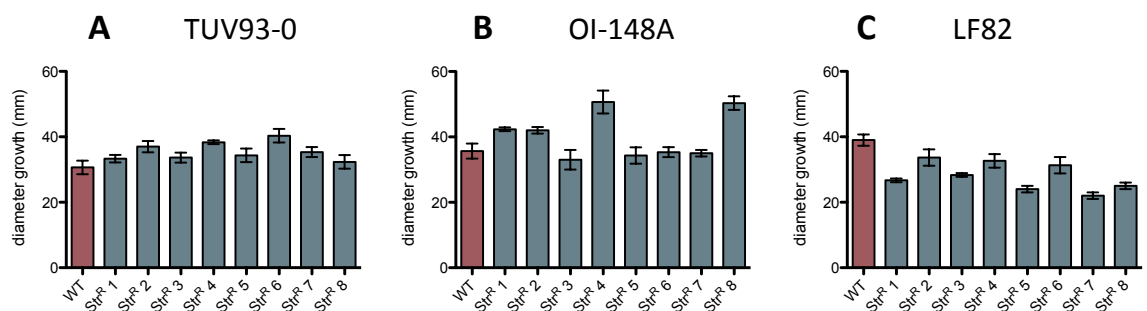


Figure 9-2: Motility of Str^R mutants. WT (red) and Str^R (blue) bacteria were grown on 0.25% agar at 30 °C for 16 hours, and the diameter growth of bacteria measured. Experiments were performed in triplicate and data shown as the average diameter with standard deviation from the mean displayed as error bars.

9.1.3 Bacterial adherence to Caco-2 cells

Adherence of the K42T Str^R *E. coli* strains to Caco-2 cells was determined by incubation of the mutant or the wild type with 90% confluent Caco-2 monolayers for four hours, after which growth media was removed, Caco-2 cells washed, and adhered *E. coli* harvested by a five minute saponin wash. Non-adherent bacteria were collected by pooling the growth media and washes, and pelleting cells by centrifugation. Bacteria were quantified by serial dilution onto LB agar. Comparison of Str^R bacteria in the adhered and non-adhered fractions to those of the corresponding wild type found no significant difference ($p > 0.05$) in either the number of bacteria in the media or attached to cells for all three *E. coli* strains (Figure 9-3).

9. APPENDICES

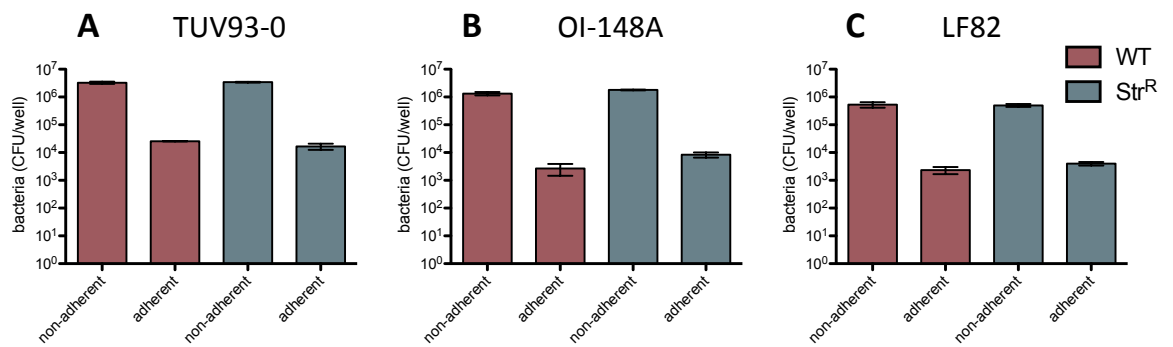


Figure 9-3: Bacterial adherence to Caco-2 cells. Total numbers of WT (red) and K42T Str^R (blue) mutants free in media (non-adherent) or attached to Caco-2 cells (adherent) after incubation in 9.5 cm² wells for 4 hours. Experiments were performed in triplicate and shown as the average count with standard deviation from the mean displayed as error bars.

9.2 The T3SS in O157:H7 colonisation of streptomycin-treated ICR mice

While mouse colonisation studies with Str^R TUV93-0 and OI-148A revealed that the T3SS has no noticeable affect on colonisation of mice, the finding that the K42T *rpsL* mutation conferring streptomycin resistance also decreases production of proteins essential for formation of A/E lesions (Chen *et al.* 2013) raises the consideration that this mutation is responsible for the lack of difference between the two strains we observed. To explore this possibility, colonisation by non-mutant TUV93-0 and OI-148A strains was assessed, using the pGB2 plasmid for streptomycin resistance.

Colonisation of mice by pGB2-transformed *lux*-marked TUV03-0 and OI-148A found that both faecal shedding and luminescence levels of the two were highly similar to that of the K42T *rpsL* mutants. Importantly, no significant difference in shedding or luminescence was shown at any time point (Figure 9-4), implying that the *rpsL* mutation had no discernible influence on colonisation and that the ability of the T3SS-negative OI-148A strain to colonise as effectively as TUV93-0 is due to the T3SS having no detectable influence on colonisation dynamics in the streptomycin-treated mouse model.

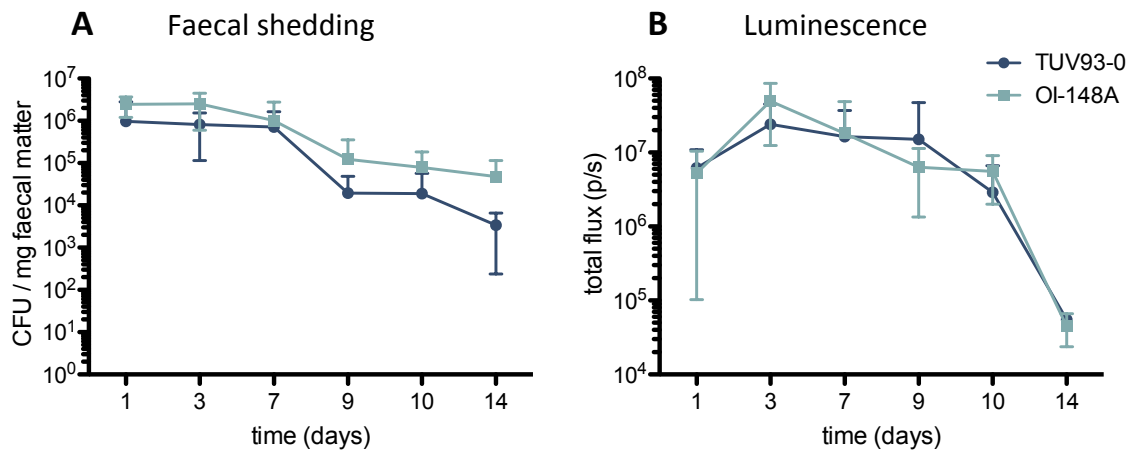


Figure 9-4: Colonisation of pGB2-transformed TUV93-0 and OI-148A. Streptomycin-treated ICR mice were infected with *lux*-marked TUV93-0 or the T3SS-negative OI-148A, both transformed with the streptomycin resistance plasmid pGB2. Drinking water containing 5 g/L streptomycin was provided to both groups until day 10. Colonisation was monitored by faecal shedding (**A**) and live-imaging luminescence (**B**). Each group of mice consisted of 5 animals, with 2 mice from each group culled at day 3, and the remaining 3 mice culled at day 14. Data points shown are the average of each group, and standard deviation from the mean displayed as error bars.

Along with colonisation by faecal shedding and live imaging, luminal and adhered bacterial counts in the intestine of mice infected with pGB2-transformed TUV93-0 and OI-148A was assessed. Two mice from each group were culled 7 days after infection, and the remaining three mice in each group culled 14 days after infection. Similarly to the *rpsL* mutants, both strains were detected in all areas of the intestine with the concentration of bacteria slightly higher in the caecum and large intestine than in the small intestine. No significant difference in numbers of bacteria in either the lumen or tissue between TUV93-0 and OI-148A was observed at any time point (Figure 9-5).

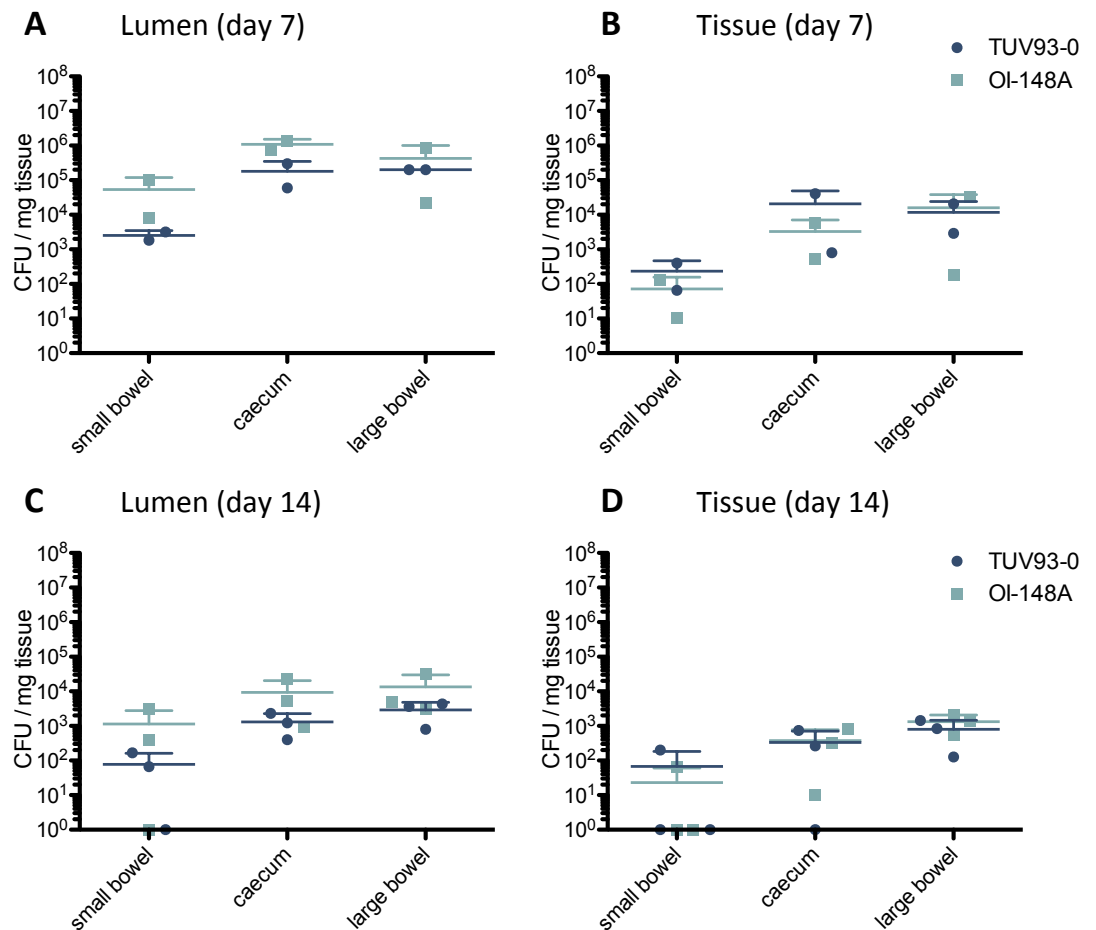


Figure 9-5: Intestinal bacterial recovery of TUV93-0 and OI-148A. Lumen (A, C,) and tissue (B, D,) colonisation of the small bowel, caecum and large bowel of mice infected with *lux*-marked TUV93-0 (dark blue) or OI-148A (light blue), both transformed with the streptomycin resistance pGB2 plasmid. Two mice from each group were culled 7 days after infection (A, B), and the remaining 3 mice in each group culled 14 days after infection (C, D) for intestinal counts. Symbols represent bacterial counts from a single animal. The average bacterial count of each group (long line) and standard deviation from the mean (short line) is also indicated.

9.3 Comparison of pET-21b *eaeH* and *yghJ* to chromosomal sequences

To determine the molecular size of the pET-21b-encoded EaeH and YghJ proteins, the *eaeH* and *yghJ* genes carried by the pET-21b-EaeH and pET-21b-YghJ plasmids were sequenced and compared to TUV93-0 *eaeH* and LF82 *yghJ*. The Eurofins MWG T7 sequencing primer (AATACGACTCACTATAG) was initially used for sequencing both genes, and further primers designed from the end of each ~1000 bp sequenced region. Comparison of the full-length TUV93-0 *eaeH* and LF82 *yghJ* revealed that the pET-21b genes were significantly truncated, with *eaeH* covering approximately 1650 bp (full length *eaeH* = 4254 bp) from ~1780-3430 bp (Figure 9-3), and *yghJ* covering approximately 2700 bp (full length *yghJ* = 4563 bp), from ~100-2800 bp (Figure 9-4).

9. APPENDICES

```

pET-21b eaeH   GGGTGTGACCAGCAAGACGCGGAATACAGTAACAAC TAATGCTGCAGGTATAGCGGACAT
TUV93-0 eaeH   GGGTGTGACCAGCAAGACGCGGAATACAGTAACAAC TAATGCTGCAGGTAAAGCGGACAT 3300
*****

pET-21b eaeH   TGAGCTTATGTCAACGGTTGCGGGAGAACACAATATTTCCGCTTCGGTGAATGGTGTCA
TUV93-0 eaeH   TGAGCTTATGTCAACGGTTGCGGGAGAACACAATATTTCCGCTTCGGTGAATGGTGTCA 3360
*****

pET-21b eaeH   GAAGACGGTCACGGTAAATTC AACGCGGATGCCAGCACCGGT CAGGCAAACCTGCTGGT
TUV93-0 eaeH   GAAGACGGTCACGGTAAATTC AACGCGGATGCCAGCACCGGT CAGGCAAACCTGCTGGT 3420
*****

pET-21b eaeH   AGACGCTCTGCTCAA--GTGA-----AATTATGCA-----
TUV93-0 eaeH   AGACGCTCTGCTCAAAGTGGCAAACGGCAAAGATGCCTTTACGCTGACGGCGAACGT 3480
*****

pET-21b eaeH   -----
TUV93-0 eaeH   TGAGGATAAAAATGGTAACCTGTTCAGGGAGCCTGGTGACCTTTAATCTGCCCGGGG 3540

pET-21b eaeH   -----
TUV93-0 eaeH   TGTCAAGCCGCTTACAGGCGATAATGTC TGGGTGAAAGCCAACGATGAGGGGAAGCAGA 3600

pET-21b eaeH   -----
TUV93-0 eaeH   GTTGACAGTGGTTTCAGTGACTGCCGGAACGTATGAGATCACGGCATCGGCAGGAATAG 3660

pET-21b eaeH   -----
TUV93-0 eaeH   CCAGCCTTCGAATACGCAGACTATAACGTTGTAGCCGATAAGGCTACCGCAACCGTCTC 3720

pET-21b eaeH   -----
TUV93-0 eaeH   CGGTATTGAGGTGATTTGGCAACTATGCACTGGCGGACGGCAATGCCAAACAGACGTATAA 3780

pET-21b eaeH   -----
TUV93-0 eaeH   CAGCCCGCAAATTTAGTCTGACTCCCAATGGGACGGGAAACTAATGAGCAAGGACA 3840

pET-21b eaeH   -----
TUV93-0 eaeH   GGCATTTTTCACCGCCACGACCTGTCGACGCAAATATACACTCACGGCGAAGTGAG 3900

pET-21b eaeH   -----
TUV93-0 eaeH   TCAGGCCGACGGTCAGGAATCGACGAAAAC TGCCGAATCTAAATTCGTCGGGATGATAC 3960

pET-21b eaeH   -----
TUV93-0 eaeH   AAATGCAGTACTACCGCATCATCTGATGTGACTTCTCTGGTGGCGGATGGGATATCGAC 4020

pET-21b eaeH   -----
TUV93-0 eaeH   TGCGAAGCTGGAGGTGACACTGATGTCCGCAAATAACCCGTTGGGGGAATATGTGGGT 4080

pET-21b eaeH   -----
TUV93-0 eaeH   CGACATTAAGACGCGCAGAAGGGGTGACGGAGAAGGATTATCAGTTCCTGCCCTGAAAAA 4140

pET-21b eaeH   -----
TUV93-0 eaeH   TGACCATTTTCGTGAGCGGAAAAATCACGCGTACATTTAGTACCAGCAAGCCTGGTGTCTA 4200

pET-21b eaeH   -----
TUV93-0 eaeH   TACGTTACATTTAACGCCCTGACGTATGGCGGGTACGAAAGGAGCGATGAACTAA 4254

```

Figure 9-6: Comparison of pET-21b-EaeH *eaeH* and TUV93-0 *eaeH*. Sequences were compared using Clustal Omega. An asterisk (*) indicates a conserved base between the two sequences, and a dash (-) indicates a gap in the sequences.

9. APPENDICES

pET-21b yghJ CGCGTACTGCGACTTTCAACCTGCCGTTTATTTTCGCTGGGGCAAGTCGGTGAAGCCAAA 1680
LF82 yghJ CGCGTACTGCGACTTTCAACCTGCCGTTTATTTTCGCTGGGGCAAGTCGGTGAAGCCAAA

pET-21b yghJ CTGATGGTTATCGTTAACCCGCACACAAACAGCATCCTCGCTTGCCTGACCGGTTACAGT 1740
LF82 yghJ *****

pET-21b yghJ TGGGGCGGTGGTGTAAATAGTAAAGGTGAGTGTACGCTCGGCGGTGATCTGATGACATG 1800
LF82 yghJ TGGGGCGGTGGTGTAAATAGTAAAGGTGAGTGTACGCTCGGCGGTGATCTGATGACATG

pET-21b yghJ AAGCACTTTATGCAGAACGTCTCGCTACTTGTCAAATGACATCTGGCAGCCAAATACC 1860
LF82 yghJ AAGCACTTTATGCAGAACGTCTCGCTACTTGTCAAATGACATCTGGCAGCCAAATACC

pET-21b yghJ AAGAGCATCATGACTGTCGGCACCAACCTGGAGAAGCTTTATTTCAAAAAGCGGGCCAG 1920
LF82 yghJ AAGAGCATCATGACTGTCGGCACCAACCTGGAGAAGCTTTATTTCAAAAAGCGGGCCAG

pET-21b yghJ GTAGTGGGAAATAGTGCACCATTGCTTTCCATGAGGATTTCAATGGTATCACAGTTAAA 1980
LF82 yghJ GTATTTGGGAAATAGTGCACCATTGCTTTCCATGAGGATTTCAATGGTATCACAGTTAAA
*** *****

pET-21b yghJ CAGTTGACCAGCTATGGCGATCTGAATCCGGAAGAGATCCGTTGCTGATCCTCAACGGC 2040
LF82 yghJ CAGTTGACCAGCTATGGCGATCTGAATCCGGAAGAGATCCGTTGCTGATCCTCAACGGC

pET-21b yghJ TTTGAATATGTGACTCAGTGGTCTCGCGATCCCTATGCTGTGCCTCTGCGTGCAGATACC 2100
LF82 yghJ TTTGAATATGTGACTCAGTGGTCTCGCGATCCCTATGCTGTGCCTCTGCGTGCAGATACC

pET-21b yghJ AGCAAACCGAAGCTGACTCAGCAGGATGTGACCGATCTGATCGCTTATCTGAACAAGGT 2160
LF82 yghJ AGCAAACCGAAGCTGACTCAGCAGGATGTGACCGATCTGATCGCTTATCTGAACAAGGT

pET-21b yghJ GGCTCGGTGCTGATCATGGAACCGTGTAGAGCAATCTTAAGGAAGAGAGCGCGTCCAGT 2220
LF82 yghJ GGCTCGGTGCTGATCATGGAACCGTGTAGAGCAATCTTAAGGAAGAGAGCGCGTCCAGT

pET-21b yghJ TTTGTGGGTCTGCTGGATGCCCGGATCTGACAATGGCTCTGAACAAATCGGTGGTGAAC 2280
LF82 yghJ TTTGTGGGTCTGCTGGATGCCCGGATCTGACAATGGCTCTGAACAAATCGGTGGTGAAC

pET21b yghJ AACGATCCGCAAGGGTATCCGGATCCGCTTCGTCAGCGTCCGCGGACTGGCATTGGGGTT 2340
LF82 yghJ AACGATCCGCAAGGGTATCCGGATCCGCTTCGTCAGCGTCCGCGGACTGGCATTGGGGTT

pET21b yghJ TATGAACGTTATCCTGCTGCAGACGGCGGCAACCGCCTACACCATCGACCCAAATACA 2400
LF82 yghJ TATGAACGTTATCCTGCTGCAGACGGCGGCAACCGCCTACACCATCGACCCAAATACA

pET21b yghJ GGGGAAGTGACCTGGAATACCAGCAAGACAACAAGCCTGATGACAAGCCGAACTGGAA 2460
LF82 yghJ GGGGAAGTGACCTGGAATACCAGCAAGACAACAAGCCTGATGACAAGCCGAACTGGAA

pET21b yghJ GTTCCGAGCGGGCAGGAGAAAGTTGAGGGCAACAGGTAACCGCTTATGCCTTTATTGAT 2520
LF82 yghJ GTTCCGAGCTGGCAGGAGAAAGTTGAGGGCAACAGGTAACCGCTTATGCCTTTATTGAT

pET21b yghJ GAAGCGGAATACACAACAAGAATCTCTGGAAGCGCAAGGCAAAAATCTGTGAGAAG 2580
LF82 yghJ GAAGCGGAATACACAACAAGAATCTCTGGAAGCGCAAGGCAAAAATCTGTGAGAAG

pET21b yghJ TTTCTGGGTTACAGGAGTGTAAAGACTCGACTTACCATTACGAGATTAACGTTTGGAG 2640
LF82 yghJ TTTCTGGGTTACAGGAGTGTAAAGACTCGACTTACCATTACGAGATTAACGTTTGGAG

pET21b yghJ CGCCGCCAGGCCCGGATGTCCGGTAACAGTGGCATGTATGTTCCGCGCTATACGCAA 2700
LF82 yghJ CGCCGCCAGGCCCGGATGTCCGGTAACAGTGGCATGTATGTTCCGCGCTATACGCAA

pET21b yghJ CTGAATCTTGACCGCGACACCGCAAGCGATAGTGCAGGCGCGGATTTTGGCACCAAC 2760
LF82 yghJ CTGAATCTTGACCGCGACACCGCAAGCGATAGTGCAGGCGCGGATTTTGGCACCAAC

pET21b yghJ ATTCGCGCCTGTATCAGCTTGAGGTTT----CGTCCGA----- 2820
LF82 yghJ ATTCAGCGCCTGTATCAGCATGAGCTTATTTCCGTACCAAAGGCAGTAAGGTGAGCGTA
*** *****

pET21b yghJ ----- 2880
LF82 yghJ CTGAACAGTGTGATCTGGAACGCTCTGTACCAGAACATGTCGGTCTGGCTGTGGAACGAT

pET21b yghJ ----- 2940
LF82 yghJ ACGAAATATCGTTACGAAGAGGGCAAGGAAGATGAGCTGGGCTTTAAAACGTTACCGAG

pET21b yghJ ----- 3000
LF82 yghJ TTCTGAACTGCTACGCCAATGATGCCTATGACGGCGGCAACAGTGTCCGCGATCTG

pET21b yghJ ----- 3060
LF82 yghJ AAAAAATCGTGGTTCGATAACAACATGATCTACGGTACGGTAGCAGCAAAGCGGCATG

pET21b yghJ ----- 3120
LF82 yghJ ATGAACCCAGCTATCCGCTCAACTATATGGAAAAACCGCTGACGCGCTGATGCTGGC

pET21b yghJ ----- 3180
LF82 yghJ CGTTCCTGGTGGATCTGAACATTAAGTTGATGTGAGAAGTACCTGGAGCGGTATCT

pET21b yghJ ----- 3240
LF82 yghJ GTAGGGGGAAGAGGTTACTGAAACCATCAGCCTGTACTCGAATCCGACCAATGGTTT

9. APPENDICES

pET21b yghJ LF82 yghJ	----- GCAGGTAAACATGCAGTCAACTGGCCTGTGGGCACCGGCTCAGAAAAGAGGTCACCATTAAAG	3300
pET21b yghJ LF82 yghJ	----- TCCAATGCGAACGTTCTCTGTGACCGTCACCGTGGCGTGGCTGACGACCTGACCGGACGT	3360
pET21b yghJ LF82 yghJ	----- GAGAAGCATGAAGTTGCGCTGAACCGTCCGCCAAGAGTGACTAAAACGTACTCTCTGGAC	3420
pET21b yghJ LF82 yghJ	----- GCTAGCGGTACGGTGAAGTTCAAGTGCCTTACGGTGGCCTGATTTATATCAAGGGCAAT	3480
pET21b yghJ LF82 yghJ	----- AGCTTACCAATGAATCTGCCAGCTTCACCTTTACTGGCGTGGTAAAAGCACCGTTCTAT	3540
pET21b yghJ LF82 yghJ	----- AAAGACGGGCATGGAAAAACGATCTGAACTCTCTGCCCGCTGGGCGAACTGGAGTCT	3600
pET21b yghJ LF82 yghJ	----- GCGTCGTTCTGTATACCACACCGAAGAAGAACCTGAATGCCAGCAATTACACGGGCGGA	3660
pET21b yghJ LF82 yghJ	----- CTGGATCAATTCGCTAAAGATCTGGATACCTTTGCCAGCTCGATGAATGATTTCTACGGT	3720
pET21b yghJ LF82 yghJ	----- CGTAATGATGAAGACGGTAAAGCACCGGATGTTTACCTATAAAAACTTGACGGGCCACAAG	3780
pET21b yghJ LF82 yghJ	----- CATCGTTTCACAAACGATGTGCAGATCTCCATCGGTGATGCCACTCTGGTTATCCGGTA	3840
pET21b yghJ LF82 yghJ	----- ATGAACAGCAGCTTCTCGACGAACAGCACCGCTGCCGACGACGCGCTGAACGACTGG	3900
pET21b yghJ LF82 yghJ	----- CTGATTTGGCACGAAGTCGGTCATAACGCTGCAGAAACACCGCTGAAACGTACCGGGTGCA	3960
pET21b yghJ LF82 yghJ	----- ACTGAAGTGGCGAACAAACGTGCTGGCGCTGTACATGCAGGATCGCTATCTCGGCAAGATG	4020
pET21b yghJ LF82 yghJ	----- AACCGTGTCTGACGACATTACCGTCCGCGCGAATATCTGGAGGAGAGCAACGGTCAG	4080
pET21b yghJ LF82 yghJ	----- GCATGGGCCCGCGCGGTGCGGGTGACCGTCTGTCTGATGTACGCGCAGCTGAAAGAGTGG	4140
pET21b yghJ LF82 yghJ	----- GCAGAGAAAACTTGATATCAACAGTGGTATCCAGAAGGTGACCTGCCTAAGTTCTAC	4200
pET21b yghJ LF82 yghJ	----- AGCGATCGTAAAGGGATGAAGGGTGAACCTGTTCAGTTGATGCACCGTAAAGCGCGC	4260
pET21b yghJ LF82 yghJ	----- GGCGATGATGTCAGCAATGACAAGTTGGCGGCAGAAATTAAGTGTGCTGAGTCAACCGGT	4320
pET21b yghJ LF82 yghJ	----- AACCGTGTGACACGCTGATGCTGTGTGCATCCTGGGTGCTCAGGCGGATCTTTCGGAA	4380
pET21b yghJ LF82 yghJ	----- TTCTTTAAGAAATGGAATCCGGGCGCAATGCTTACCAGCTTCCGGGGCAAGTGAGATG	4440
pET21b yghJ LF82 yghJ	----- AGCTTCGAAGCGGAGTGAGCCAGTCCGGCTTACAACACGCTCGCTCAGCTCAAGCTGCCG	4500
pET21b yghJ LF82 yghJ	----- AAACCGGAACAGGGCCGGAAACCATTAACAAGGTTACCGAGCATAAGATGTCTGCCGAG	4560
pET21b yghJ LF82 yghJ	--- TAA	4563

Figure 9-7: Comparison of pET-21b-YghJ *yghJ* and LF82 *yghJ*. Sequences were compared using Clustal Omega. An asterisk (*) indicates a conserved base between the two sequences, and a dash (-) indicates a gap in the sequences.